UNIVERSIDADE FEDERAL DO AMAZONAS

PRÓ-REITORIA DE PESQUISA E PÓS-GRADUAÇÃO

INSTITUTO DE CIÊNCIAS BIOLÓGICAS-ICB

PROGRAMA DE PÓS-GRADUAÇÃO EM IMUNOLOGIA BÁSICA E APLICADA

PEDRO VIEIRA DA SILVA NETO

Avaliação do potencial de TREM-1 como biomarcador da Covid-19 e sua correlação com a patogenicidade da doença

Assessment of the TREM-1 potential as a biomarker of Covid-19 and its correlation with the disease pathogenicity

MANAUS

2022

UNIVERSIDADE FEDERAL DO AMAZONAS
PRÓ-REITORIA DE PESQUISA E PÓS-GRADUAÇÃO
INSTITUTO DE CIÊNCIAS BIOLÓGICAS-ICB
PROGRAMA DE PÓS-GRADUAÇÃO EM IMUNOLOGIA BÁSICA E APLICADA

PEDRO VIEIRA DA SILVA NETO

Avaliação do potencial de TREM-1 como biomarcador da Covid-19 e sua correlação com a patogenicidade da doença

Assessment of the TREM-1 potential as a biomarker of Covid-19 and its correlation with the disease pathogenicity

Tese apresentada ao Programa de Pós-Graduação em Imunologia Básica e Aplicada da Universidade Federal do Amazonas para obtenção do título de Doutor em Imunologia **Área de concentração:** Imunologia Básica e Aplicada.

Orientador: Prof. Dr. Carlos Artério Sorgi
Coorientadora: Profa. Dra. Lúcia Helena Faccioli

MANAUS
2022

Ficha Catalográfica

Ficha catalográfica elaborada automaticamente de acordo com os dados fornecidos pelo(a) autor(a).

Nome: da Silva-Neto, Pedro V.

Título: Avaliação do potencial de TREM-1 como biomarcador da Covid-19 e sua correlação com a patogenicidade da doença

> Tese apresentada ao Programa de Pós-Graduação em Imunologia Básica e Aplicada da Universidade Federal do Amazonas para obtenção do título de Doutor em Imunologia
>
> **Área de concentração:** Imunologia Básica e Aplicada.

Aprovado em: **30/11/2022**

BANCA EXAMINADORA

Prof (a). Dr (a): Carlos Artério Sorgi

Instituição: Faculdade de Filosofia, Ciências e Letras de Ribeirão Preto (FFCLRP)

Julgamento:_____

Prof (a). Dr (a): Aya Sadahiro

Instituição: Universidade Federal do Amazonas (UFAM)

Julgamento:_____

Prof (a). Dr (a): Eugenio Damaceno Hottz

Instituição: Universidade Federal de Juiz de Fora (UFJF)

Julgamento:_____

Prof (a). Dr (a): Marco Aurelio Sartim

Instituição: Universidade do Estado do Amazonas (UEA)

Julgamento:_____

Prof (a). Dr (a): Ronaldo Bragança Martins Júnior

Instituição: Faculdade de Ciências Farmacêuticas de Ribeirão Preto (FCFRP)

Julgamento:_____

Dedicatória

Dedico este trabalho,

A todos os educadores e professores que passaram pela minha vida.

Em especial dedico este trabalho a matriarca da família Vieira que sempre me incentivou, apoiou e dedicou seus esforços por nós minha querida mãe **Maria da Paz Oliveira Vieira**.

Aos meus amigos e colegas por todo apoio, companheirismo e incentivo durante esta caminhada.

Agradecimentos

Primeiramente gostaria de agradecer a **DEUS**, pois é nele que deposito toda minha Fé, agradeço a minha família, por me proporcionar a oportunidade de chegar até este momento da minha vida, pois o que conquistei foi através da sua vontade, me guiando, fortalecendo e encorajando-me nos momentos em que fraquejei.

A minha amada mãe **Maria da Paz Oliveira Vieira**, pelo seu amor e carinho, a primeira incentivadora para que eu chegasse até esta etapa da minha vida, é esta mulher que tenho como alicerce e exemplo de vida e que amarei para todo sempre.

Aos meus queridos irmãos que não são poucos, em especial a **Graça Oliveira Vieira** como representante de todos, obrigado pelo apoio e incentivo nos estudos.

Ao meu orientador, o Prof. **Dr. Carlos Artério Sorgi**, por ter me dado a oportunidade de realizar esse projeto e por todo conhecimento adquirido. Agradeço toda compreensão e confiança e principalmente a parceria, apoio e orientação durante a execução, discussão dos resultados e principalmente pelo seu exemplo em ser um pesquisador jovem, determinado e sonhador. Meu muito obrigado.

A minha coorientadora prof. **Dra. Lúcia Helena Faccioli**, por me proporcionar um ambiente de aprendizado e conhecimento em seu laboratório e pelo apoio acadêmico e institucional. Por ter aberto os caminhos para que eu pudesse realizar meu projeto. Agradeço todo incentivo e parceria.

A colaboração da prof. **Raquel Fernanda Gerlach**, responsável pelo laboratório de Proteínas e Histologia da Faculdade de Odontologia de Ribeirão Preto pela orientação nos experimentos que envolviam atividade enzimática de MMPs e proteases, gostaria ainda de agradecer imensamente a colaboração da mestranda **Valéria Beatriz do Valle** e **Patrícia Adriana Basile** pela ajuda nos experimentos.

A colaboração dos professores **Dr. Marcelo Dias Baruffi** e **Dra. Cristina R. B. Cardoso** e **Dr. Eurico de Arruda Neto** pela oportunidade de colaboração e parcerias futuras.

Á **Fabiani Rosseto** e **Thais Fernanda de Campos Fraga da Silva** e **Camila de Oliveira Silva e Souza** pelo auxílio com a aquisição dos dados de citometria, ensinamentos e oportunidade de trabalho.

Epígrafe

"**Um livro, uma caneta, uma criança e um professor podem mudar o mundo**"

Malala Yousafzai

RESUMO

da Silva-Neto, P.V. **Avaliação do potencial de TREM-1 como biomarcador da Covid-19 e sua correlação com a patogenicidade da doença**. 2022. Tese (Doutorado). Universidade Federal do Amazonas - UFAM. Manaus, Amazonas, 2022

Coronavirus 2019 (Covid-19) é uma doença causada pelo coronavírus da síndrome respiratória aguda grave 2 (SARS-CoV-2) que afeta principalmente o sistema respiratório, caracterizada por quadros inflamatórios graves. Nesse contexto, o receptor expresso nas células mieloides-1 (TREM-1) é considerado um amplificador intrínseco de sinais inflamatórios. Assim, para elucidar como esse receptor contribui para a imunopatologia ou desregulação da resposta imune observada na Covid-19, determinamos a expressão de TREM-1 e de seu correspondente solúvel (sTREM-1) durante a gravidade da doença e no microambiente pulmonar, correlacionando estes dados com outros parâmetros clínicos, moleculares e celulares. Com base em escores clínicos, incluímos em nossa coorte pacientes positivos para Covid-19 classificados em grupos específicos de gravidade de sintomas (leve, moderado, grave e crítico). No sangue periférico observamos que a produção de sTREM-1 foi significativamente maior entre os pacientes com doença grave, apresentando correlações positivas com parâmetros inflamatórios, progressão do quadro clínico e mortalidade. Além disso, seus níveis sistêmicos foram correlacionados positivamente com a expressão elevada de MMP-8, sugerindo um mecanismo de liberação de TREM-1 da superfície das células sanguíneas periféricas. No microambiente pulmonar relacionamos a alta diversidade de MMPs à gravidade da Covid-19. Nossos resultados indicaram uma forte atividade enzimática de MMP-2 em amostras de fluido traqueal aspirado (TAF) de pacientes que vieram a óbito. Além disso, observamos um aumento na infiltração de neutrófilos, produção de espécies reativas de oxigênio (ROS) e peroxidação lipídica, em cooperação com a expressão de MMP-8 e MMP-2, também favoráveis para liberação de sHLA-G e sTREM-1 no tecido pulmonar. A análise de redes mostrou que, miRNAs relacionados com a via de TREM-1 podem favorecer processos de regulação durante a gravidade da doença. Em conjunto, sugerimos que TREM-1 pode ser usado como uma ferramenta preditiva para progressão e desfecho da Covid-19, como também participar do mecanismo de patogenicidade aumentando a hiperinflamação na covid-19, por via de ação de endoproteinases e na regulação da resposta imune por miRNA.

Palavras-chaves: Covid-19; sTREM-1; biomarcador; mortalidade, metaloproteinases.

ABSTRACT

da Silva-Neto, P.V. **Assessment of the potential of TREM-1 as a biomarker of Covid-19 and its correlation with the pathogenicity of the disease**.2022. Thesis (Doctorate). University Federal of Amazonas -UFAM. Manaus, Amazonas, 2022

Coronavirus 2019 (Covid-19) is a disease caused by the severe acute respiratory syndrome coronavirus 2 (SARS-CoV-2) that mainly affects the respiratory system, characterized by severe inflammatory conditions. In this context, the receptor expressed in myeloid cells-1 (TREM-1) is considered an intrinsic amplifier of inflammatory signals. Thus, to elucidate how this receptor contributes to the immunopathology or dysregulation of the immune response observed in Covid-19, we determined the expression of TREM-1 and its soluble counterpart (sTREM-1) during disease severity and in the pulmonary microenvironment, correlating these data with other clinical, molecular and cellular parameters. Based on clinical scores, we included Covid-19-positive patients classified into specific symptom severity groups (mild, moderate, severe, and critical) in our cohort. In peripheral blood, we observed that the production of sTREM-1 was significantly higher among patients with severe disease, showing positive correlations with inflammatory parameters, clinical progression and mortality. Furthermore, their systemic levels were positively correlated with elevated MMP-8 expression, suggesting a mechanism for TREM-1 release from the surface of peripheral blood cells. In the lung microenvironment, we related the high diversity of MMPs to the severity of Covid-19. Our results indicated a strong enzymatic activity of MMP-2 in aspirated tracheal fluid (TAF) samples from patients who died. Furthermore, we observed an increase in neutrophil infiltration, production of reactive oxygen species (ROS) and lipid peroxidation, in cooperation with the expression of MMP-8 and MMP-2, also favorable for the release of sHLA-G and sTREM-1 in lung tissue. Network analysis showed that miRNAs related to the TREM-1 pathway may favor regulatory processes during disease severity. Together, we suggest that TREM-1 can be used as a predictive tool for the progression and outcome of Covid-19, as well as participating in the pathogenicity mechanism by increasing hyperinflammation in Covid-19, via the action of endoproteinases and in the regulation of the response. miRNA immune.

Keywords: Covid-19; sTREM-1; biomarker; mortality, metalloproteinases.

LISTA DE FIGURAS

LISTA DE TABELAS

LISTA DE SIGLAS

OMS	Organização mundial da saúde
Covid-19	Coronavírus 19
ACE2	Enzima conversora de angiotensina
AT 1-2	Células alveolares tipo I e II
Calu-3	Células epiteliais pulmonares humanas
CBA	Cytometric bead array
CD	Domínio conector
CDS	Sequência de codificação
CH	Hélice central
CoVs	Coronavírus
COX-2	Ciclooxigenase 2
DAP12	Proteína ativadora de DNAx
DCs	Células dendríticas
DCV	Doença cardiovascular
DPOC	Doença pulmonar obstrutiva crônica
ER	Retículo endoplasmático
EVs	Vesículas extracelulares
G-CSF	Fator estimulador de colônia de granulócitos
GI	Gastrointestinais
HR1-2	Repetição do heptal
ICTV	Comitê internacional de taxonomia de vírus
IKKε	Quinase- ε
IL	Interleucina
ISGs	Ligados a sequência ativada por gama
IκB	Inibidor do fator nuclear κb
kb	Kilo base
LPS	Lipopolissacarídeo
MAVS	Adaptador de proteína de sinalização antiviral mitocondrial
MERS-CoV	Coronavírus da síndrome respiratória do Oriente Médio
miRISC	Complexo de silenciamento induzido por RNA

MPO	Mieloperoxidase
MVB	Corpos multivesiculares
NOD	Receptores do tipo NOD
NTD	Domínio N-terminal
ORF	Região de leitura Aberta
PAMPs	Padrões moleculares associados a patógenos
PCR	Proteína C reativa
PGE	Prostaglandinas
PMN	Polimorfonucleares
PRRs	Receptores de Reconhecimento de Padrões
RBD	Domínio de ligação ao receptor
RdRP	RNA polimerase dependente de RNA
RIG-I	Receptor de ácido retinóico induzível 1
ROS	Espécies reativas de oxigênio
RTC	Complexo de replicação-transcricional
S1	Subunidade de superfície 1
sHLH	Linfo-histiocitose hemofagocítica secundária
ssRNA+	RNA de fita simples de polaridade positiva
sTREM-1	Receptor desencadeador expresso em células mieloides 1 solúvel
TLRs	Receptores do tipo Toll
TMPRSS2	Protease transmembrana serina 2
TRAF3	Receptor do fator de necrose tumoral
TREM-1	Receptor desencadeador expresso em células mieloides 1
Tyk2	Tirosina quinase 2

1.Introdução

Segundo a Organização Mundial de Saúde (OMS) entre dezembro de 2019 e o início de 2020, o número crescente de mortes por pneumonia grave na província de Wuhan, China, levou à identificação de um novo coronavírus, denominado Coronavírus da Síndrome Respiratória Aguda Grave 2 (SARS-CoV-2), como causa da doença do Coronavírus 2019 (Covid-19) (1,2).

Cerca de 80% das pessoas infectados com SARS-CoV-2 desenvolvem uma forma leve de Covid-19, os ~20% restantes desenvolvem formas mais graves da doença e requerem atenção hospitalar acompanhada de cuidados intensivos e ventilação mecânica. Aproximadamente 5% desses pacientes podem evoluir para quadros de sepse em condições clínicas críticas com desfechos desfavoráveis até o óbito, o que pode estar associado à hiperinflamação pulmonar e insuficiência respiratória(3–5).

Os pacientes infectados podem ser caracterizados como assintomático ou sintomático, podendo apresentar sinais clínicos como tosse seca, dor de garganta intensa e febre, acompanhada por cefaleia, diarreia e insuficiência respiratória leve, moderada ou grave (6). A gravidade da Covid-19 está associada à comorbidades que incluem: senescência, obesidade, hipertensão, doenças cardiovasculares, doenças pulmonares crônicas dentre outras (7).

Durante a infecção pelo SARS-CoV-2, a resposta imune inata desregulada induz a liberação acentuada de citocinas inflamatórias (tempestade de citocinas), que favorecerem os sintomas críticos da doença (8,9). Células da imunidade inata desempenham papel importante orquestrando a resposta imune adaptativa, de modo a favorecer os mecanismos efetores contra patógenos. O reconhecimento antigênico através dos receptores de reconhecimento de padrão (PRRs) e a liberação citocinas induzidas no microambiente infeccioso são fundamentais na ativação dos diferentes tipos de respostas que serão desenvolvidas pelo hospedeiro (10)

Os monócitos e macrófagos, são tipos celulares imunes encontrados nos pulmões de pacientes infectados pelo SARS-CoV-2, ao qual desempenham um papel importante na imunopatogênese da Covid-19 (11,12). Uma vez que estas células são os principais componentes da imunidade inata capazes de desenvolver fenótipos distintos através de polarização inflamatória (13).

Estudos de mecanismos imunológicos são fundamentais para avaliação de vias de sinalização celular, tendo como alvo a identificação de agentes imunorregulatórios durante a inflamação. Os miRNAs são reconhecidos como reguladores-chave de muitos processos biológicos e fisiopatológico como proliferação celular, metabolismo e apoptose (14,15). A expressão desregulada destas moléculas tem sido associada ao desenvolvimento de diversas doenças, uma vez que a estimulação de receptores induz a ativação de vias de sinalização, resultando na indução transcricional de múltiplos genes, responsáveis pela regulação da resposta imune (16), polarização de células (17,18) e replicação viral (19)

No contexto de inflamação e dano de órgãos, as metaloproteinases da matriz extracelular (MMPs) agem como as principais enzimas reguladoras da homeostase do tecido. No entanto, durante processos inflamatórios exacerbados, sua atividade é drasticamente elevada, fazendo com que as células aumentem sua expressão e ação de clivagem em substratos relacionados com a resposta imune, como receptores de membranas, citocinas e quimiocinas (20,21)

O TREM-1 (receptor expresso nas células mieloides-1) é um receptor membro da família de imunoglobulinas expresso em células mieloides, principalmente em neutrófilos, monócitos e macrófagos. Após a ativação celular, este receptor pode amplificar a resposta inflamatória em sinergismo com a sinalização de receptores do tipo *Toll* (TLRs) (22,23). A variante solúvel de TREM-1 (sTREM-1) é proveniente da clivagem proteolítica de TREM-1 por MMPs (24) já foi detectado no plasma de camundongos e humanos em condições patológicas inflamatórias (25,26)

Dados publicados anteriormente, reforçam que quantidades elevadas de sTREM-1 plasmático podem representar um indicativo de progressão clínica, sendo um importante marcador de prognóstico em pacientes com choque séptico (27) e outras infecções bacterianas e virais (28–30). Visto que o SARS-CoV-2 induz uma resposta hiperinflamatória, sugerimos que durante a infecção, o vírus poderia desencadear uma ativação e regulação positiva da via de TREM-1, induzindo a liberação da forma solúvel (sTREM-1) de acordo com a gravidade da doença mediante a cooperação pela atividade proteolítica de MMPs e regulação dos sistema imune por microRNAs.

2. Revisão Bibliográfica

2.1. Histórico pandêmico e possível origem do SARS-CoV-2

Os coronavírus (CoVs) têm sido o agente causador de duas pandemias de grande escala nas últimas duas décadas. No final de 2002, o primeiro caso conhecido de Síndrome Respiratória Aguda Grave (SARS), ocorreu na província de Guangdong, China China (31,32), seguidas de novos relatados em Hong Kong (33), Vietnã, Canadá e outros países (34).

Em março de 2003, a Organização Mundial de Saúde (OMS) instituiu esforços para identificar o agente causador da "síndrome respiratória aguda grave" (SARS). No corrente ano, uma rede de laboratórios internacionais levou à identificação e caracterização inicial de um novo coronavirus associados aos casos de SARS (32,35–37). Casos adicionais de SARS, resultantes de transmissão zoonótica, ocorreram em 2003 e 2004 (38), porém nenhum caso humano de SARS foi detectado desde então. No entanto, alguns vírus semelhantes ao SARS-CoV encontrados em morcegos demonstraram capacidade de infectar células humanas sem adaptação prévia (39,40), indicando que a SARS poderia ressurgir (**Figura 1**).
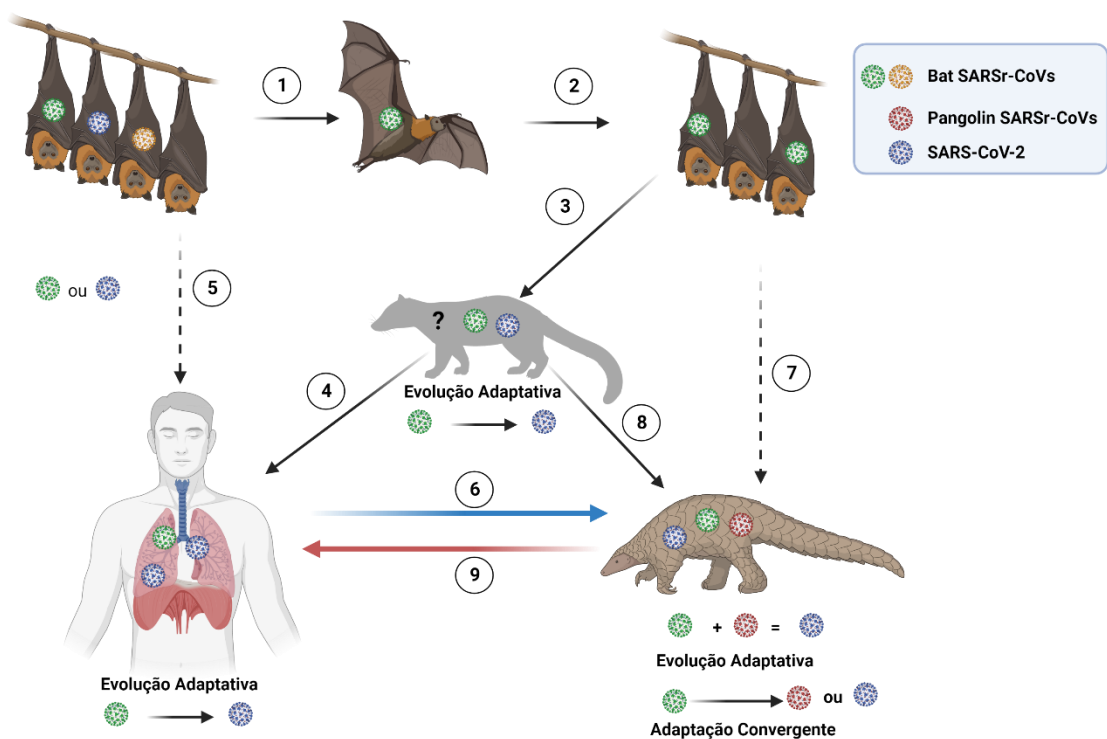
Figura 1.Cenários possíveis para a origem do SARS-CoV-2.
Fonte: Adaptado de Banerjee *et al.,* 2021 (41)

Em 13 junho de 2012, 10 anos após o primeiro surgimento do SARS-CoV, um novo coronavírus, o Coronavírus da Síndrome Respiratória do Oriente Médio (MERS-CoV) foi

isolado de escarro de um homem de 60 anos internado na Arábia Saudita com sintomas de pneumonia aguda, que faleceu por insuficiência respiratória e renal progressiva (42). Após esse relato, casos de doença respiratória grave ocorreram na Jordânia (MERS), Reino Unido e países fora da Península Arábica (43).

Após esses dois eventos pandêmicos, estudos enfatizaram o risco em potencial de ressurgimento de SARS-CoV, uma vez que os CoVs poderiam sofrer recombinação genética e gerar novos genótipos, além da presença de um grande reservatório em morcegos (96%). Outros estudos sugerem possíveis evoluções e combinações adaptativas em pangolins (92,4%) e civetas de palmas (99,8%) com grande similaridade genética ao SARS-CoV com potencial de infectar seres humanos (44,45)

No final de dezembro de 2019, a OMS foi comunicada sobre um surto de pneumonia grave de etiologia desconhecida em Wuhan, província de Hubei na China, (46–48). Em 30 de janeiro de 2020 devido aos números crescentes de casos e óbitos, foi então declarado Estado de Emergência de Saúde Pública de Importância Internacional (ESPII), como o mais alto nível de alerta, conforme previsto no Regulamento Sanitário Internacional (49).

Uma semana depois, em 7 de janeiro de 2020, as autoridades chinesas confirmaram que haviam identificado um novo tipo de coronavírus (2019-nCoV) não identificada antes em seres humanos, sugerindo o β-Coronavírus como o agente etiológico responsável. Em 11 de fevereiro de 2020, foi então nomeado de Coronavírus da Síndrome Respiratória Aguda Grave 2 (SARS-CoV-2) como causador da Doença do Coronavírus 2019 (Covid-19) (50).

2.2. Característica genômica, estrutural e replicação do SARS-CoV-2

Segundo o comitê internacional de taxonomia de vírus (ICTV), os coronavírus (CoVs) são um grupo de vírus envelopados, pertencentes à ordem *Nidovirales*, família *Coronaviridae* e subfamília *Coronavirinae*. Com base em suas sequências de proteínas os membros da subfamília *Coronavirinae* podem ser classificados em quatro gêneros: *Alphacoronavírus*, *Betacoronavírus*, *Deltacoronavírus* e *Gammacoronavírus* (51,52).

Pertencente ao gênero *Betacoronavírus* ((47,53), o SARS-CoV-2 compartilha aproximadamente 80% de similaridade de sequência com o SARS-CoV (2002) e em média 50% com o coronavírus da síndrome respiratória do Oriente Médio (MERS-CoV) (2013) (2). Os CoVs são patógenos zoonóticos originários de animais e podem ser transmitidos a humanos por contato direto. Análises evolutivas de estudos genômicos sugerem a

semelhança do SARS-CoV-2 com o SARS de morcego ou pangolins como o reservatório intermediário (**Figura 1**) (54,55). No entanto, mais estudos estão sendo realizados para definição do principal hospedeiro intermediário.

Como um microrganismo intracelular obrigatório, os coronavírus usam a maquinaria da célula hospedeira para sua própria replicação e disseminação. Composto por uma RNA de fita simples de polaridade positiva (+ssRNA)(~30 kb) com estrutura 5′ e cauda 3′-poli-A (**Figura 2**) (56) Após a liberação do RNA genômico viral no citoplasma da célula-alvo, o RNA é codificado por duas poliproteínas ORF1a, b (pp1a, pp1b) localizadas na extremidade 5', que codificam 16 proteínas não estruturais (NSP1– NSP16) que compõem o complexo replicase (57,58). As NSPs são processadas para formar um complexo de replicação-transcricional (RTC) envolvido na transcrição e replicação do genoma (58).
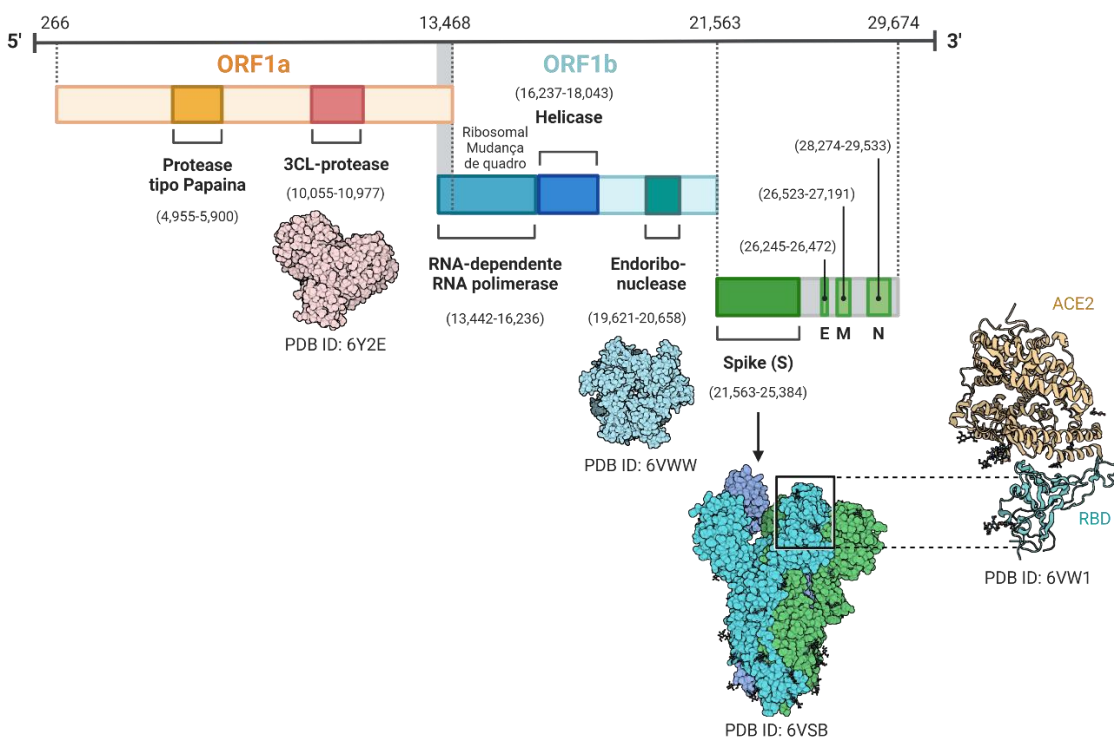
Figura 2. Organização genômica do SARS-CoV-2. Spike (S), envelope (E), membrana (M) e nucleocapsídeo (N), domínio de ligação ao receptor (RBD), fase de leitura aberta (ORF), RNA polimerase dependente de RNA (RdRP). **Fonte.** Adaptado de V'kovski *et al.,* 2021 (59)

O terço restante localizadas na extremidade 3' codifica nove proteínas acessórias (ORF) e quatro proteínas estruturais: glicoproteína de envelope (S), responsável por reconhecer os receptores da célula hospedeira (60). Proteínas de membrana (M),

responsáveis pela formação dos *vírions* (61), como também, proteínas do envelope (E), responsáveis pela montagem e liberação dos *vírions* ((62)).
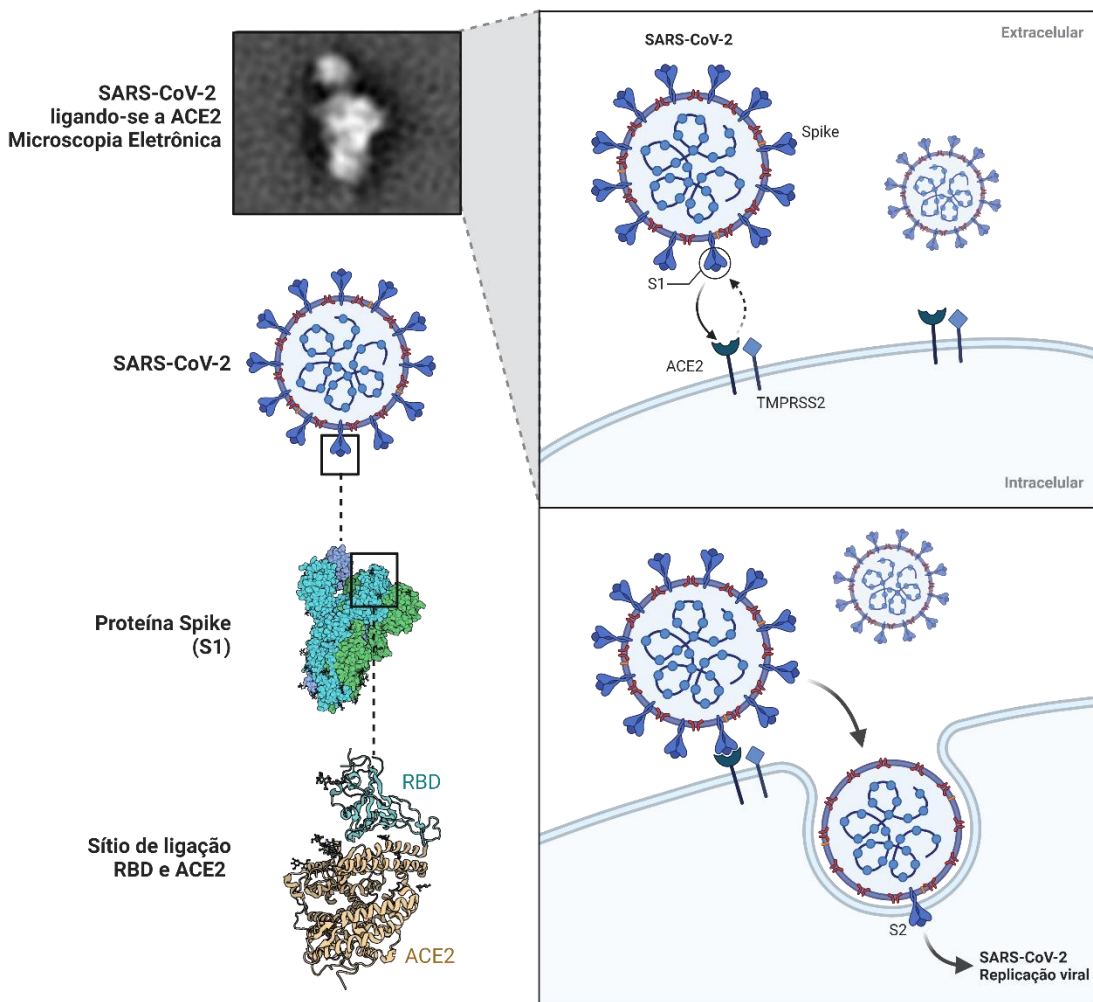
Figura 3. Interação SARS-CoV-2 e ACE2 na infecção celular.
Fonte: Adaptado de Ryan *et al*., 2020 (63).

As proteínas do nucleocapsídeo (N) envolvidas no empacotamento do genoma do RNA e nos vírions desempenham papéis na patogenicidade como um inibidor do interferon (IFN) (64). Além dessas quatro proteínas estruturais principais, diferentes CoVs codificam proteínas estruturais e acessórias especiais, como proteína HE, proteína 3a/b e proteína 4a/b. O gene S do SARS-CoV-2 é altamente variável compartilhando <75% de similaridade com os nucleotídeos do SARS-CoV (2).

A proteína S (Spike) é composta por duas subunidades funcionais: subunidades S1 e S2. A subunidade de superfície S1 contém um domínio N-terminal (NTD) e o domínio de ligação ao receptor (RBD) responsável pela ligação do vírus ao receptor da enzima

conversora de angiotensina 2 (ACE2) na superfície da célula hospedeira (65,66). A subunidade S2 apresenta o peptídeo de fusão (FP), a repetição do heptal 1 (HR1), a hélice central (CH), o domínio conector (CD), a repetição do heptado 2 (HR2), o domínio transmembrana (TM) e a cauda citoplasmática (CT) atuando como proteína de fusão, clivado proteoliticamente pela catepsina L celular e a protease transmembrana serina 2 (TMPRSS2), que por sua vez facilita a entrada do vírus na superfície da membrana plasmática (**Figura 4**) (67,68)

A transmissão ocorre de pessoa para pessoa, sendo o principal modo de propagação. Isso ocorre por meio de gotículas respiratórias liberadas por tosse ou espirro, aerossol e contato da membrana mucosa com fômites (69). A transmissão fecal-oral tem sido especulada uma vez que a detecção de RNA viral nas fezes, sintomas gastrointestinais (GI) e expressão de ACE2 ao longo do trato GI tem sido observada (70,71)
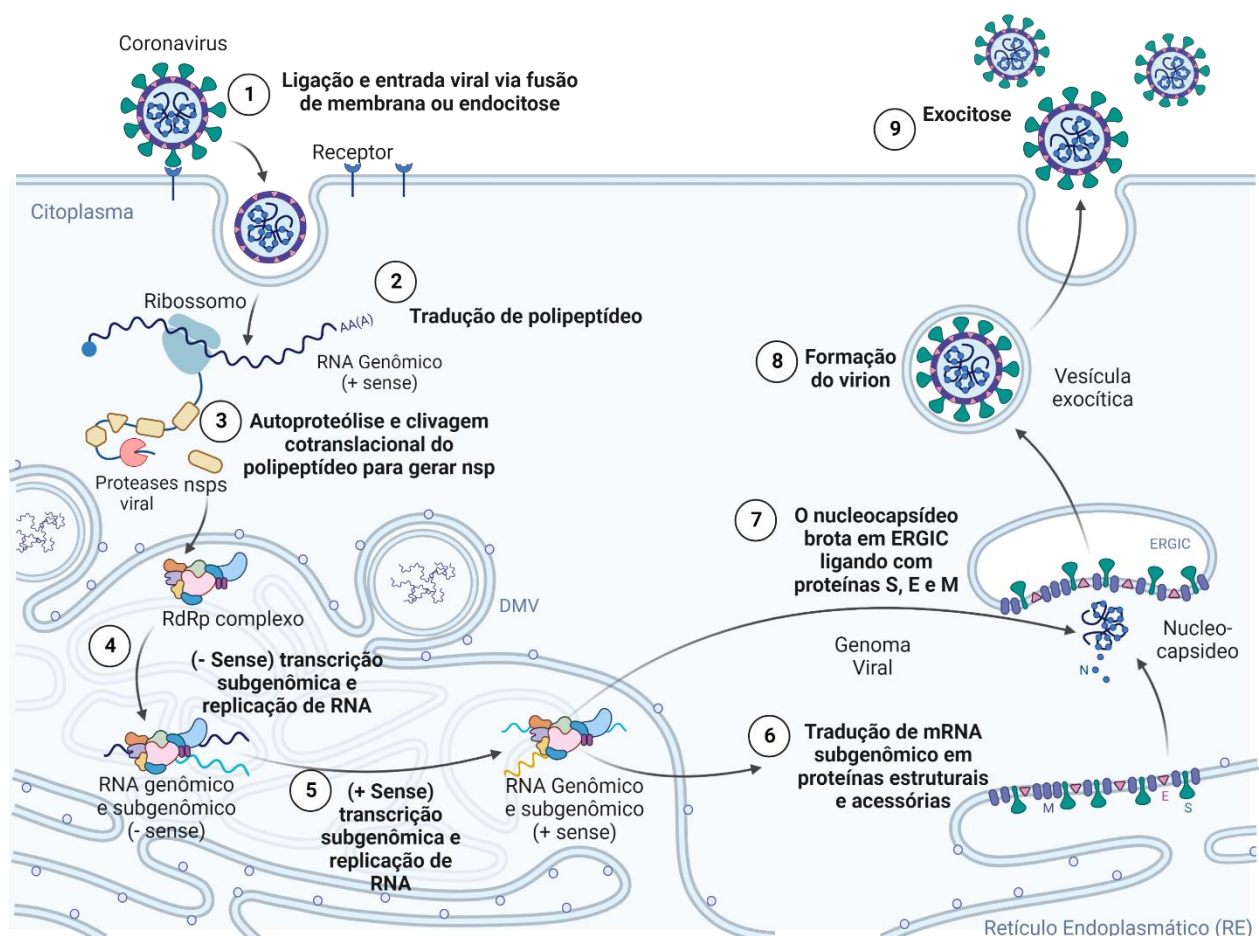
Figura 4. Ciclo de replicação do SARS-CoV-2 nas células hospedeiras.
Fonte: Adaptado de V'kovski *et al.,* 2021 (59)

As células epiteliais do trato respiratório expressam tanto ACE2 quanto TMPRSS2 em sua superfície, e esta via de entrada direta parece ser o modo predominante de acesso do SARS-CoV-2 no tecido respiratório. Alternativamente, o SARS-CoV-2 também pode usar a via endossômica, pela qual o complexo ACE2-vírus é translocado para endossomos e a iniciação da proteína S é realizada pelas proteases de cisteína endossômica catepsina B e catepsina L. Após, o vírus é liberado do endossomo no citoplasma das células epiteliais brônquicas ciliadas e pneumócitos tipo II (72).

Uma vez que o genoma é liberado no citosol da célula, as ORF1a e ORF1b são traduzidas em proteínas replicase viral, que são clivadas em NSPs individuais (via hospedeiro e/ou proteases virais); estes formam a RNA polimerase dependente de RNA (nsp12 derivado de ORF1b) (73). Os componentes da replicase reorganizam o retículo endoplasmático (ER) em vesículas de membrana dupla (DMVs) que facilitam a replicação viral de RNAs genômicos e subgenômicos (sgRNA); os últimos são traduzidos em proteínas estruturais acessórias e virais que facilitam a formação de partículas virais (74).

Assim como outros vírus, o SARS-CoV-2 evolui com o tempo e variações ocorrem através de mudanças de nucleotídeos no genoma viral durante a replicação. Alterações genômicas vantajosas em relação a replicação viral, transmissão e evasão imune, tornam a resposta imune ineficaz devido à sua incapacidade de reconhecer e eliminar o vírus (75). Até o momento sabe-se que o SARS-CoV-2 originou-se da recombinação entre espécies entre coronavírus de morcego e pangolim (41) e é provável que as variantes estejam surgindo como resultado da recombinação (76,77).

A variante α (B.1.1.7) foi detectada pela primeira vez no final de setembro de 2020 e rapidamente se tornou a cepa predominante no Reino Unido (78). A variante β (B.1.351), detectada pela primeira vez em outubro de 2020, tornou-se a cepa dominante resultando na segunda onda na África do Sul (79). Da mesma forma, a variante γ (P.1) foi detectada em quatro indivíduos brasileiros que viajaram ao Japão em janeiro de 2021 (80) e foi responsável pelo ressurgimento de infecções em Manaus (Amazonas, Brasil (81,82). Variante δ (B.1.617.2), detectada em dezembro de 2020, foi responsável pelo aumento maciço de casos, causando uma segunda onda na Índia (83,84) e infecções em vários locais nos Estados Unidos (85).

A variante O (B.1.1.529), a última variante de preocupação anunciada pela OMS, foi detectada pela primeira vez em novembro de 2021 por laboratórios de vigilância genômica de classe mundial na África do Sul e encontrada em outros países ao redor do mundo (86).

O surgimento dessas variantes torna-se preocupante, pois podem afetar a transmissibilidade viral, virulência e quadros de reinfecção por escapar da imunidade natural ou induzida por vacina (87)

2.3. Epidemiologia da infecção pelo SARS-CoV-2

Apesar dos esforços globais em conter a doença, em 11 de março de 2020 a OMS declarou Estado Pandêmico para a Covid-19 (88). Desde sua identificação, o vírus se espalhou rapidamente em escala global, mais de 415 milhões de casos, com mais de 5,84 milhões de mortes decorrentes da doença causando uma pandemia sem precedentes que sobrecarregou muitos sistemas de saúde (89). Em poucos dias a Europa se tornou o epicentro da pandemia (90), seguido dos Estados Unidos e posteriormente países da América Latina, incluindo o Brasil (**Figura 5**) (91).

No Brasil, em 3 de fevereiro de 2020 foi declarado Estado de Emergência em Saúde Pública de Importância Nacional pelo Ministério da Saúde (92). No dia 26 de fevereiro de 2020, foi confirmado o primeiro caso de Covid-19 no estado de São Paulo em um viajante retornando da Itália. Em 17 de março de 2020, a primeira morte relacionada à Covid-19 foi confirmada (93).
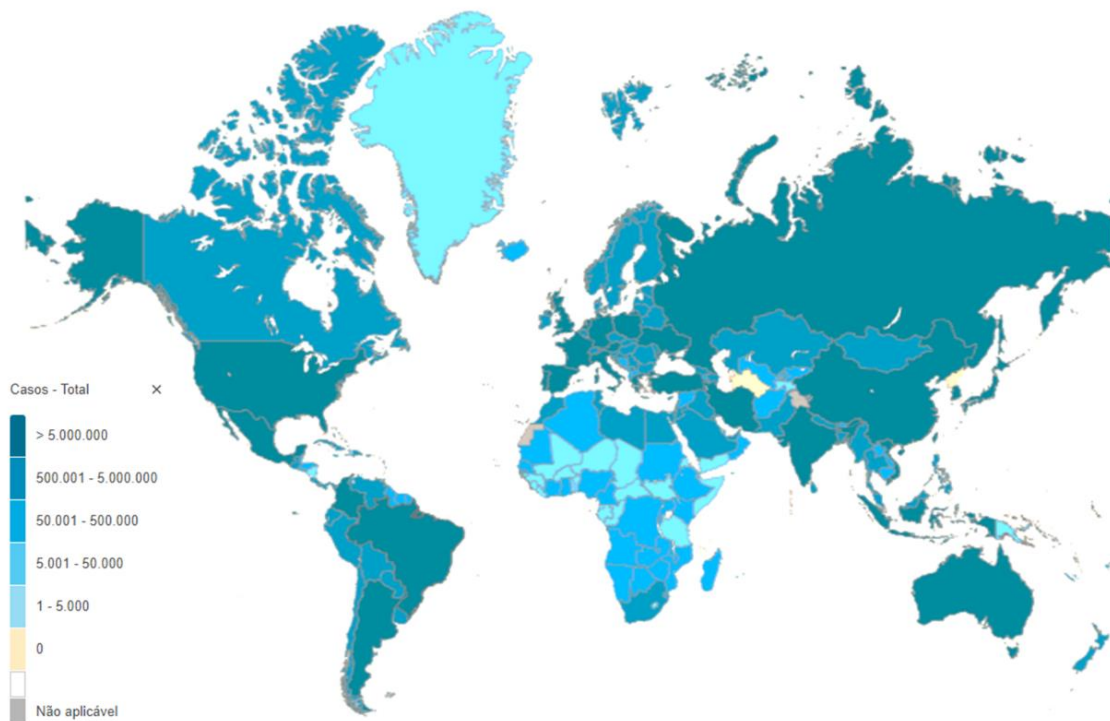
Figura 5. Incidência de casos novos de Covid-19.
Fonte: adaptado da WHO (89)

O governo brasileiro introduziu medidas de restrição para limitar a propagação viral como: isolamento social, fechamento de escolas, universidades e comércios não essenciais, além das medidas de obrigatoriedade, como o uso de máscaras de proteção individual e quarentena (94). As medidas de restrição foram progressivamente flexibilizadas devido os impactos negativos na economia imposta pelo governo atual (95) e as viagens entre os estados brasileiros permaneceram amplamente possíveis possibilitando o surgimento de novas linhagens contagiosas (82,96,97).

No dia 7 de janeiro de 2021, o Brasil registrou o maior número de casos novos (87.843 casos), desta forma, tornando-se o segundo epicentro da pandemia com um total de 21,2 milhões de casos e um número de mortos superior a 591.000 casos até o final de setembro de 2021 (98). Após dois anos de pandemia, até 28 de outubro de 2022, segundo a OMS havia 626.337.158 casos confirmados de Covid-19, incluindo 6.566.610 mortes mundiais. Por outro lado, até 26 de outubro de 2022, um total de 12.830.378.906 doses de vacina foram administradas na população mundial. No Brasil, de 3 de janeiro de 2020 a 28 de outubro de 2022, houve 34.807.075 casos confirmados de Covid-19 com 687.907 óbitos relatados.

Em 17 de janeiro de 2021 a Agência Nacional de Vigilância Sanitária (ANVISA) aprovou o uso emergencial de vacinas contra a Covid-19, e iniciou-se imediatamente a Campanha Nacional de Imunização. O Instituto Butantan (São Paulo) e a fundação Oswaldo Cruz (Fiocruz) (Rio de Janeiro, Brasil), importaram as primeiras 6 milhões de doses de CoronaVac e Astrazeneca em colaboração com a Sinovac Biotech (Pequim, China e Oxford (Inglaterra), até 21 de outubro de 2022, um total de 486.682.379 doses de vacina foram administradas e aproximadamente 71,8% da população brasileira está vacinada com a primeira dose de qualquer uma das vacinas atualmente disponíveis.

2.4. Características clínicas da infecção pelo SARS-CoV-2

O tempo entre a exposição ao SARS-CoV-2 e o momento em que os primeiros sintomas da Covid-19 começam a surgir (período de incubação) são de aproximadamente 5 a 7 dias em média, podendo variar de 1 a 14 dias. Pacientes infectados podem desenvolver a doença com sintomas leves, como febre, tosse seca ou produtiva, mialgia, cefaleia, hemoptise, diarreia, dispneia; como também, em alguns casos, sintomas graves, que evoluem desde síndrome do desconforto respiratório agudo (SDRA), lesão cardíaca aguda, infecções secundárias e falência de múltiplos órgãos (99–102)

Em média 80% dos pacientes que apresentam apenas sintomas leves da doença se recuperam sem precisar de tratamento hospitalar. No entanto, um menor número apresenta uma rápida progressão dos sintomas, evoluindo para quadros críticos. Dentre as manifestações mais graves, evidencia-se a pneumonia e os infiltrado bilaterais que podem ser identificados através de imagens radiográficas do tórax (103).

Segundo Cheng et al., 2020, 17% dos pacientes de Covid-19 são acometidos pela Síndrome do Desconforto Respiratório Agudo (SDRA) e, entre esses, 65% pioraram rapidamente e morreram de falência de múltiplos órgãos (104). O risco heterogêneo para o desenvolvimento de formas grave da doença causada pelo SARS-CoV-2 é um dos aspectos mais relevantes na patogênese e no curso clínico da Covid-19. Neste sentido, alguns preditores clínicos importantes foram identificados em diferentes populações, principalmente abrangendo fatores de risco relacionado ao sexo masculino, idade superior a 60 anos e obesidade (105,106).

A maioria dos casos graves de pacientes com Covid-19, geralmente apresentam comorbidades, como hipertensão arterial (HA), doença cardiovascular (DCV), doença pulmonar obstrutiva crônica (DPOC), obesidade, diabetes tipo II e doença renal e hepática (107,108), sugerindo que estas comorbidades representam um fator de risco adicional para o desenvolvimento de Covid-19 grave, com evoluções para disfunções multiorgânicas, choque séptico e óbito (109,110).

2.5. Imunopatogênese da infecção pelo SARS-CoV-2

O estabelecimento do tropismo viral depende da suscetibilidade e permissividade de uma célula hospedeira específica. O SARS-CoV-2 apresenta tropismo primário pelo pulmão (111), infectando células epiteliais alveolares, células endoteliais vasculares e macrófagos (112,113). Visto que além de estar expresso em células epiteliais alveolares tipo II dos tecidos pulmonares (114), os receptores ACE2 já foram descritos em outros tecidos extrapulmonares, como coração, endotélio, rins e intestinos (115,116). Processos inflamatórios recorrentes que podem ser desencadeados pela presença de comorbidades e pela própria infeção do SARS-CoV-2 desempenham um papel chave na patogênese da Covid-19 e na expressão de ACE2.

A resposta imune é um dos principais determinantes da suscetibilidade e gravidade da doença. O epitélio pulmonar constitui uma barreira de defesa do hospedeiro contra patógenos invasores. Os alvéolos são revestidos pelo epitélio alveolar formado por uma

monocamada de células alveolares tipo I (AT1) e células alveolares tipo II (AT2). Em condições homeostáticas, as AT2 têm a função de secretar líquido surfactante cobrindo todo o epitélio de revestimento interno facilitando a expansão do alvéolo (117). Tem sido descrito que AT1, AT2 e células endoteliais dos capilares sanguíneos encontram-se fortemente conectadas através de junções estreitas, que controlam o fluxo de íons, fluídos e o infiltrado de células inflamatórias no espaço intersticial entre os alvéolos e através do epitélio pulmonar (118).

Adicionalmente, as células AT2 expressam de maneira constitutiva o receptor ACE2, componente do sistema renina-angiotensina (SRA) responsável pelo aumento da atividade simpática, vasoconstrição, inflamação, liberação de aldosterona e vasopressina. Além das células AT2, os macrófagos alveolares residentes são as principais células-alvo da infecção pelo vírus (67). O reconhecimento do vírus pelas células induz ativação de vias de sinalização que levam a liberação de citocinas e quimiocinas, favorecendo o recrutamento de novas células com fenótipos inflamatórios para os alvéolos infectados, gerando uma resposta imunológica exacerbada (119)

A resposta imune inata constitui uma linha de defesa contra infecções virais, desencadeada pelo reconhecimento de padrões moleculares associados a patógenos e danos (PAMPs e DAMPs) em toda superfície celular e pelos PRRs intracelulares (120). A produção de IFN-I é resultante do reconhecimento de ácidos nucleicos virais do SARS-CoV-2 pelas células infectadas. A sinalização induzida por IFN-I converge em fatores de transcrição, o que induz rapidamente a expressão de genes estimulados por esta citocina (121).

O RNA viral pode ser detectado por sensores citosólicos, os quais incluem o gene 1 induzível por ácido retinóico (RIG-I) e o gene 5 associado à diferenciação de melanoma (MDA5) (122,123). Após a ativação, o RIG-I e o MDA5 interagem com o adaptador de proteína de sinalização antiviral mitocondrial (MAVS), favorecendo o recrutamento do fator 3 associado ao receptor do fator de necrose tumoral (TRAF3), além do ativador de NF-κB associado à família TRAF (TANK) cinase 1 de ligação (TBK1), ao inibidor do fator nuclear κB (IκB) e quinase-ε (IKKε), responsáveis pela fosforilação do fator regulador do gene de IFN (IRF) 3 e IRF7 (124) (**Figura 6**).
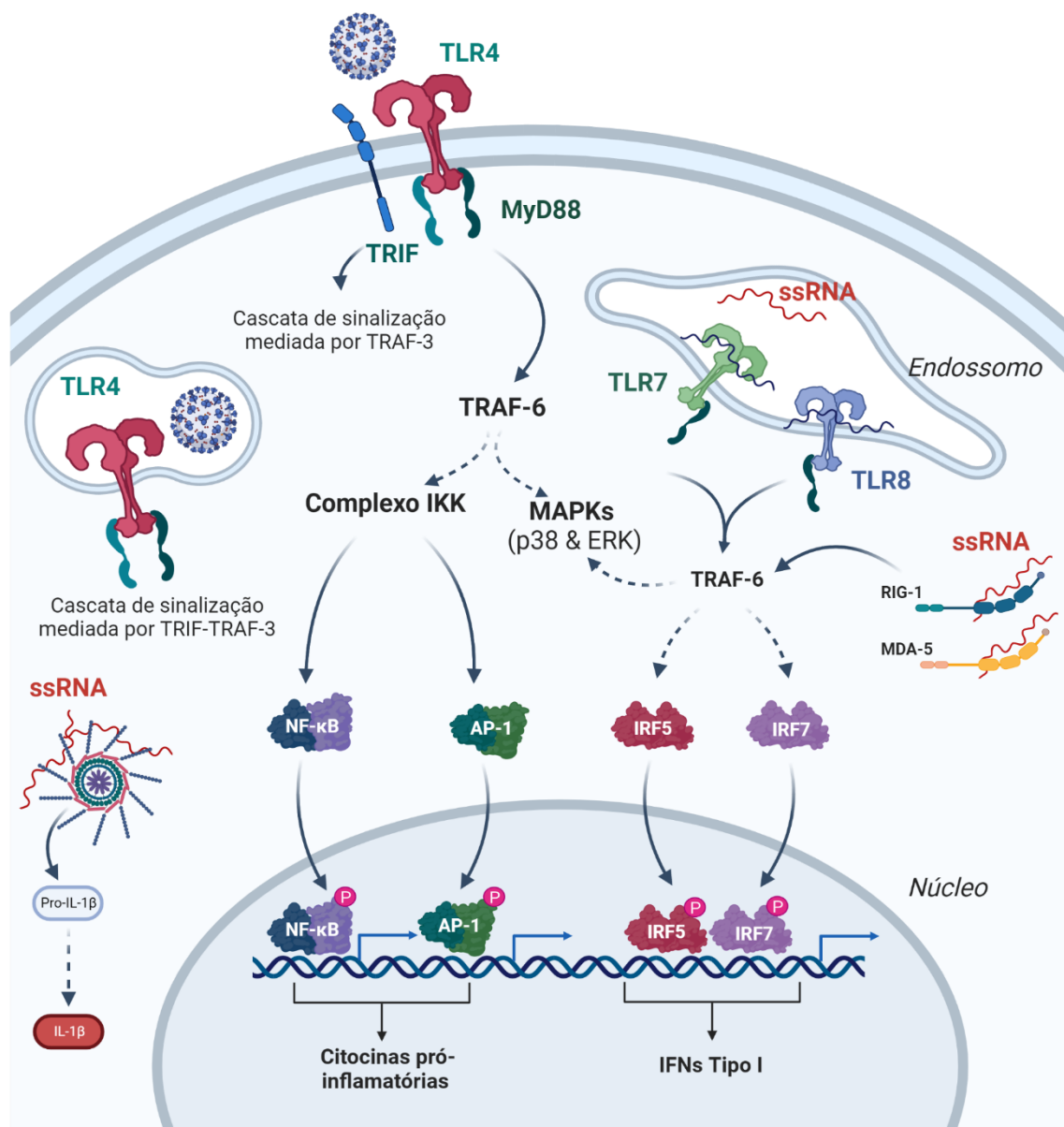
Figura 6. Reconhecimento de SARS-CoV-2 por receptor de reconhecimento de padrões (PRRs) e via de fatores de transcrição. O SARS-CoV-2 apresenta afinidade com TLR-4 (membrana e endossomal), sugerindo que o vírus pode ser reconhecido por este receptor. O ssRNA SARS-CoV-2 é reconhecido principalmente por TLR-7 endossomal e 8, 3) e receptores citoplasmáticos RIG-1 e MDA5. As vias de sinalização ativam NF-KB, AP1 e fatores de transcrição de IRFs levando a produção de citocinas pro-inflamatórias**. Fonte:** Adaptada de Luiz Boechat *et al.* 2020 (119)

Após a fosforilação de IRF3 e IRF7 esses migram para o núcleo, induzindo a expressão de IFN-I ligados a sequência ativada por gama (ISGs) (125). O IFN-I secretado se liga ao receptor do interferon alfa e beta, promovendo à ativação das tirosinas quinase Jak tirosina quinase 2 (Tyk2) e Janus quinase 1 (JAK1), responsáveis por fosforilar o transdutor de sinal e o ativador da transcrição (STAT)1 e STAT2 induzindo assim a expressão de produtos ISG que estabelecem o estado antiviral no local da infecção viral (126).

Segundo a literatura, o SARS-CoV-2 é um indutor fraco da resposta do IFN-I, que além de sua ação antiviral, atuam também na ativação de células residentes e no recrutamento de células imunes para o local da infecção, de modo a torná-las ativadas para que desempenhem suas funções efetoras. A inflamação local persistente leva à ativação de células como NK (*Natural Killer*), monócitos, macrófagos, células dendríticas (DCs) e polimorfonucleares (PMN) (125,127,128).

As células DCs plasmocitoides (pDCs), por sua vez, reconhecem o RNA viral através dos PRRs tais como receptores *Toll-like* receptors (TLRs), receptores para RNA helícase RIG-I e receptores *NOD-like* receptors (NLRs), presentes também em células do sistema imunológico. O TLR-3 expresso na membrana endossomal detecta o dsRNA (double stranded RNA), enquanto ssRNA (single stranded RNA) são detectadas pelo TLR-7 e TLR-8 (10,129) (**Figura 7**).
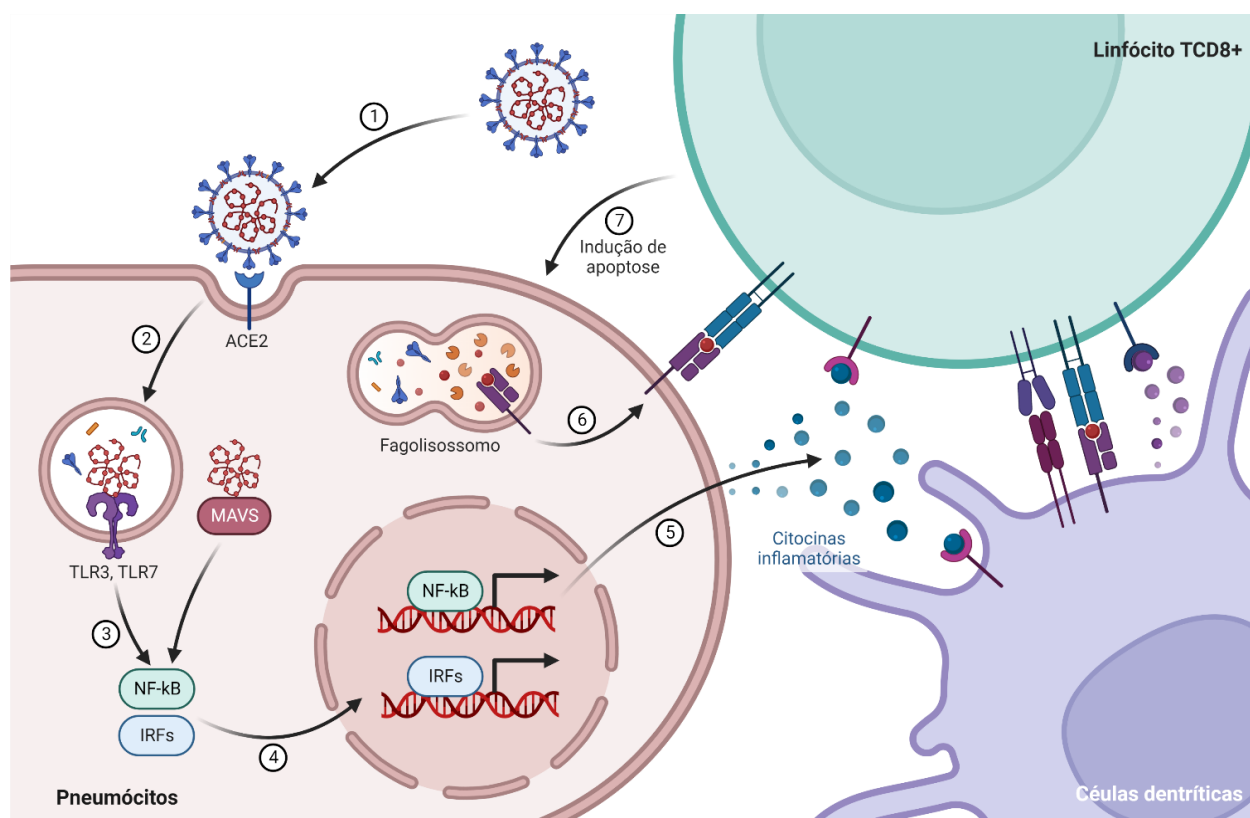
Figura 7. Células de apresentação de antígeno (APC) e interação de células T e imunopatogense da Covid-19 durante a infecção por SARS-CoV-2. Apresentação de antígeno para linfócitos T CD4$^+$ via MHC Classe II e apresentação cruzada para T CD8$^+$ linfócitos via MHC classe I. Fonte: Adaptada de Yang *et al.* 2020 (130)

O reconhecimento desencadeia a ativação de fatores de transcrição, tais como IRFs (IRF3/7) e NF-kB, que convergem para ativação de genes alvo do IFN tipo I (α e β) resultando na inibição da replicação viral e na produção de uma variedade de citocinas pró-

inflamatórias TNF-α, IL-12, IL-1 e IL-6 (131,132). Dessa forma, este reconhecimento leva à ativação de cascatas de sinalização, culminando na liberação de citocinas e quimiocinas, que direcionam o recrutamento de células imunes para o local da infecção; essas células imunes com base em seu estado de ativação, estão envolvidas na eliminação do patógeno por meio de vários mecanismos celulares.

A tempestade de citocinas na circulação e no dano alveolar difuso na pneumonia de pacientes graves com Covid-19 são características compartilhadas com a SDRA (133). A Covid-19 é caracterizada por um aumento sistêmico de inúmeras citocinas, incluindo interleucina (IL)-1α, IL-1β, IL-6, IL-7, IL-10, fator de necrose tumoral (TNF), IFN tipo I e II e as quimiocinas inflamatórias CCL2/MCP-1, CCL3/MIP-1a, CXCL10/IP-10 o que pode ser causado por uma resposta imune disfuncional, levando a tempestade de citocinas periféricas (134,135).

Evidências mostraram que pacientes com Covid-19 apresentam uma desregulação da resposta imune que leva ao desenvolvimento de hiperinflamação periférica e viral (136). Podendo ser uma consequência da linfo-histiocitose hemofagocítica secundária (sHLH), síndrome rara que causa hiperativação imunológica, associada a infecções virais, caracterizada por altos níveis de citocinas, quimiocinas circulantes, redução nos linfócitos TCD8+ e células NK, casos graves de Covid-19 são acompanhados por uma redução em todas as populações de linfócitos: células B, TCD4+, TCD8 +, NK e por neutrofilia (135).

2.6. Metaloproteinases e o processo inflamatório da Covid-19

As MMPs são uma família de 23 membros de endoproteinases secretadas, dependentes de zinco e contendo Ca2+, que clivam um amplo espectro de substratos, que incluem componentes da matriz extracelular (colágenos, fibronectina e elastina), mediadores metabólicos solúveis e fatores de crescimento ancorados na matriz extracelular (137,138).

Além disso, durante o processo inflamatório, as MMPs surgem como potentes enzimas que medeiam a clivagem de receptores, citocinas e quimiocinas; como também participam da remodelação de tecidos, migração celular e apoptose (139). O processamento descontrolado de MMP em componentes da matriz extracelular e citocinas pode ser altamente pró-inflamatório e afetar a fisiologia do pulmão e de outros órgãos (140). Em condições de homeostasia, as MMPs são pouco expressas nos tecidos. No

entanto, após lesão, inflamação, renovação da matriz e reparo, sua expressão é aumentada. Curiosamente, pacientes graves com Covid-19 apresentam ruptura da barreira alveolar em resposta à infecção por SARS-CoV-2, intensificando a permeabilidade a fluidos e o extravasamento de leucócitos (141,142). Estas lesões pulmonares podem ser produzidas diretamente pelo vírus, células inflamatórias, hipóxia e/ou outros fatores moleculares, causando dissociação das junções intracelulares (141)

Em estudo comparativo de pacientes criticamente doentes com Covid-19 e influenza A, demonstrou-se que fatores moleculares observados apenas na Covid-19 envolviam concentrações aumentadas de MMP-1 e -3, sugerindo um possível papel dessas MMPs no dano tecidual associado à infecção grave por SARS-CoV-2 (143). Além disso, é sabido que a expressão epitelial pulmonar de MMP-1 correlaciona-se com a redução na função mitocondrial, aumentando a expressão de HIF-1α, diminuindo a produção de espécies reativas de oxigênio (ROS) e promovendo um fenótipo proliferativo-migratório antiapoptótico em células epiteliais alveolares (**Figura 8**) (144–146).
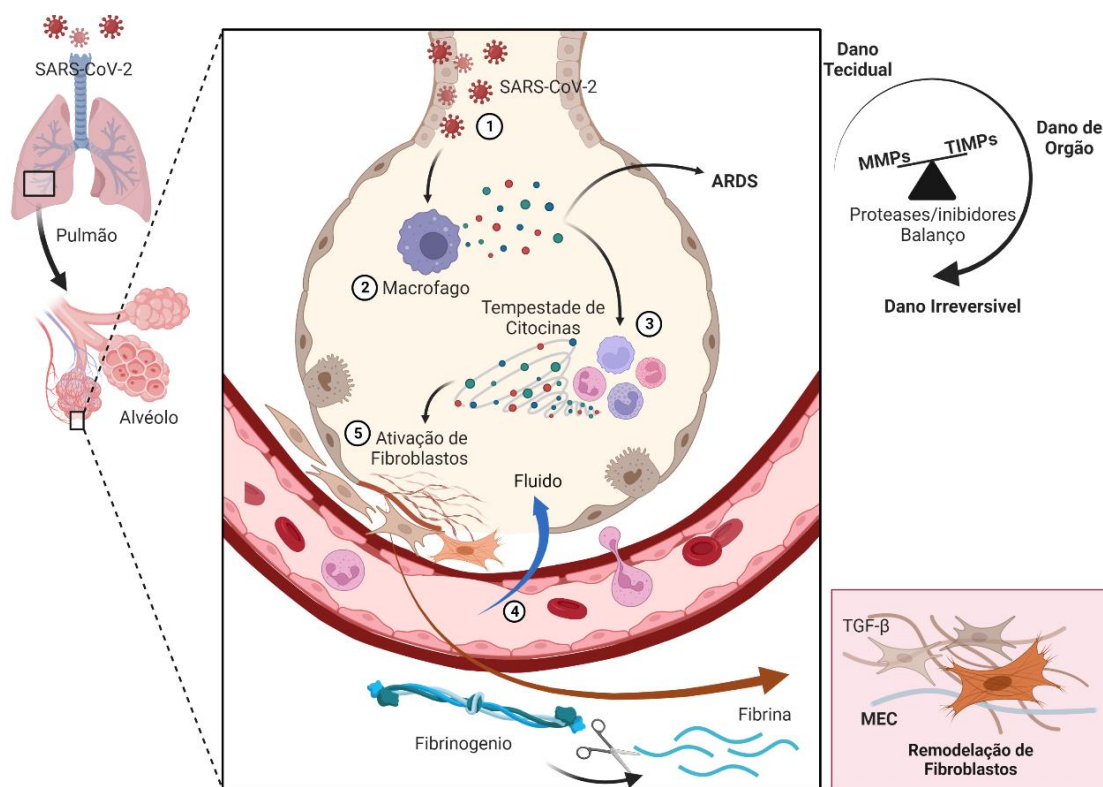
Figura 8. Interação entre mediadores hiperinflamatórios, lesão tecidual e desenvolvimento da fibrose pulmonar. Figura esquemática ilustrando os mecanismos propostos durante a infecção por SARS-CoV-2 e resposta imune desregulada via liberação acentuada de citocinas, quimiocinas, fatores de crescimento e proteases, como metaloproteinases (MMPs) e seus inibidores (TIMPs). Fatores de crescimento, especialmente TGF-β, podem ser ativados por citocinas e MMPs, promovendo proliferação de fibroblastos e diferenciação de miofibroblastos. **Fonte:** Adaptado de Ramírez-Martínez *et al.,* 2022 (147)

Durante a infecção pelo SARS-COV-2 ocorre uma resposta imune desregulada sustentada no pulmão, resultando no recrutamento excessivo de neutrófilos para o sítio de infecção e a consequente liberação exacerbada de proteases, espécies reativas de oxigênio e armadilhas extracelulares de neutrófilos (NETs), que podem acarretar danos teciduais graves aos pacientes, uma vez que a resposta à infecção induz células imunes a liberarem MMPs como estímulos fisiológicos que fazem com que todas as células alterem sua produção e liberem MMPs favoráveis para modular a clivagem de citocinas e quimiocinas (148–150).

O papel de MMPs na patogênese de sequelas graves de infecção por SARS-CoV-2 torna-se de particular interesse, uma vez que favorecem à remodelação da matriz extracelular e danos teciduais evidentes. Pouco se sabe sobre a origem celular e os mecanismos implicados na produção e liberação de MMPs nas configurações da infecção por SARS-CoV-2 (21).

2.7. Correlações do TREM-1 com a regulação da resposta inflamatória e atividade de MMPs.

O sistema imune é constantemente estimulado por agentes inflamatórios infecciosos e não infecciosos. Vários receptores celulares desempenham importantes funções na modulação da respostas imune, sendo responsáveis pelo reconhecimento, adesão e ativação celular, originado o processo inflamatório (151)

O TREM-1 é uma glicoproteína transmembrana de 30kDa, reconhecida como membro da superfamília de imunoglobulinas altamente expresso em células mieloides como neutrófilos, monócitos/macrófagos (152–154). No entanto, a expressão de TREM-1 não é exclusiva de células mieloides, uma vez que já foi descrita sua expressão em células parenquimatosas, epiteliais brônquicas, córneas, gástricas e células endoteliais hepáticas (153–156). Os genes que codificam a família de receptores TREM estão localizados no cromossomo 6p21, composto por TREM-1, TREM-2 e TREM-3 sendo este último descritos apenas em camundongos (152).

Estruturalmente, TREM-1 possui um domínio extracelular tipo imunoglobulina do tipo V, um domínio intramembranas com aminoácidos de lisina carregados positivamente e um domínio intracelular ausente de domínio ITAM (Imunoreceptor motivo de ativação baseado em tirosina). O domínio intracelular de TREM-1 associa-se à proteína de ativação DAP12 (Proteína ativadora de DNAx) necessária para a expressão e sinalização via

domínio intracitoplasmático de ITAM, recrutando um domínio imunorreceptor de tirosina quinase Syk e ativa a sinalização de PI3K, resultando no início da cascata de sinalização e aumento da expressão de citocinas e quimiocina, como IL-6, IL-10, IL-12, TNF-α, GM-CSF, IL-8, MPO, MIP-1 e MCP-1, provenientes de neutrófilos, monócitos/macrófagos (152,157) (**Figura 9**).
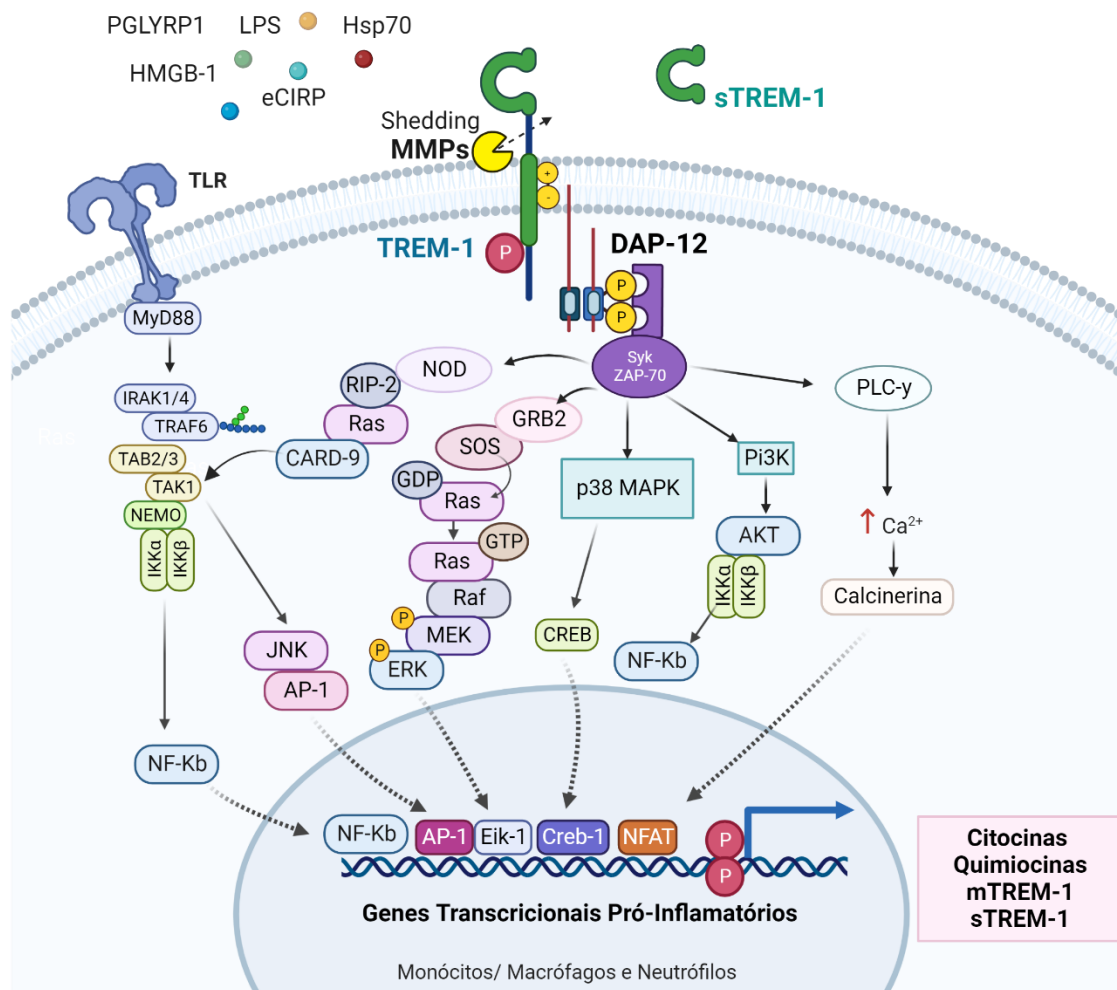
Figura 9. Organização das proteínas transmembranas e complexo de ativação TREM-1/DAP12. Abreviaturas: ITAM = motivo de ativação baseado em tirosina de imunorreceptor; ITIM = motivo inibitório baseado em tirosina do imunorreceptor. **Fonte:** Adaptado de Cao *et al.*, 2017 (158)

Como um importante coativador das vias de sinalização celulares o receptor TREM-1 age em sinergismo com os receptores Toll e NOD, favorecendo a sincronização dos ligantes intracitoplasmáticos do receptor TREM-1, induzindo aumento de fluxo de cálcio intracelular, secreção de citocinas pró-inflamatórias, sobrevivência celular via Bcl-2 e ativação de neutrófilos (23). A inflamação é um importante mecanismo para a eliminação de patógenos, porém, a amplificação mediada pela via de TREM-1 pode causar uma desregulação celular (159).

Durante a infecção pelo SARS-CoV-2, células pulmonares infectadas ativam macrófagos derivados de monócitos por meio da via do receptor *Toll-like* 4 (TLR4) e sinalização celular por TRIF-TRAF6-NF-κB levando a exacerbação da inflamação (160) Portanto, esses sinergismos podem contribuir para a indução da tempestade de citocinas no contexto da Covid-19.

A expressão de TREM-1 na superfície celular é regulada positivamente após estímulos com lipopolissacarídeo (LPS) e outros constituintes microbianos (161,162). A transcrição do gene TREM-1 é regulada pela proteína ativadora 1 (AP-1), cAMP, NF-κB, receptor de vitamina D e elementos de resposta à hipóxia (156,163). Além disso, a expressão do receptor induzido pelo LPS parece ser mediada por prostaglandina $(PG)E_2$ endógena ao qual desencadeia mecanismos dependentes de EP4, como cAMP/PKA, seguidos pela ativação de MAPK p38 e PI3K (164).

Em infecções virais ocasionadas pelo vírus da hepatite C ou B (165,166) a ciclooxigenase 2 (COX-2) está envolvida na síntese de mediadores inflamatórios lipídicos, onde a PGE_2 promove a expressão de TREM-1, enquanto a PGD_2 e PGJ_2 apresentam funções contrárias, suprimindo a expressão deste receptor (167,168).

Outros estudos investigaram a interação molecular da expressão do TREM-1 em monócitos/macrófagos associados com cânceres coloretal, pulmonar e carcinoma hepatocelular. Tais estudos concluíram que a expressão de TREM-1 apresenta um efeito direto na progressão tumoral e está associada com o aumento da recorrência e à baixa sobrevida de pacientes (155,169,170).

Além da forma ligada à membrana, uma variante de TREM-1 solúvel (sTREM-1) foi determinada em soro de camundongos e humanos (25,26). Proveniente da clivagem proteolítica do TREM-1 da superfície de membranas, através da ação de MMPs (24) As quantidades elevadas de sTREM-1 circulantes apresentaram valor prognóstico no plasma de pacientes durante episódios de choque séptico (27) e em outros processos infecciosos (28–30). Assim, evidências sugerem um papel importante de sTREM-1 na evolução de doenças infecciosas e a variação da produção do receptor solúvel pode ser um marcador confiável de inflamação durante sepse e pneumonia (171,172). No entanto, apesar de várias investigações, o ligante de TREM-1 ainda não foi determinado, como também, ainda não foi determinado a validade de sTREM-1 como um biomarcador de gravidade da Covid-19.

2.8. Função dos miRNAs na patogenicidade do SARS-CoV-2

Diferentes classes de RNAs regulatórios já foram identificadas, se diferem em sua biogênese, comprimento e distribuição tecidual. Entre os pequenos RNAs estão os microRNAs (miRNAs) (173,174). Estes são RNAs de fita simples não codificantes com 19–28 nucleotídeos, que regulam a expressão gênica e a síntese de proteínas ao patamar de tradução ou degradação do RNAm alvo, considerados reguladores chave da expressão gênica e proteica (175,176).

Aproximadamente 2.000 miRNAs humanos já foram identificados (miRBase 22), e previstos para regular mais de 60% de todos os genes codificadores de proteínas humanas (177). Os miRNAs maduros são carregados em proteínas argonaute (AGO2) para formar o complexo de silenciamento induzido por RNA (miRISC) que o direciona para o RNAm alvo por meio de pareamento de bases (178). Uma fita do miRNA maduro tem como alvo os mRNAs, responsáveis em promover a degradação ou bloqueio translacional nos corpos de processamento (179).

Como um regulador negativo de mRNA, o silenciamento do gene é realizado por miRNAs que têm como alvo a região 3′ não traduzida (3′-UTR) do mRNA, induzindo a degradação do mRNA ou supressão da tradução. Além disso os miRNAs também podem interagir em outras regiões da sequência de codificação (CDS) de mRNA, como emparelhamento de bases da extremidade 5′ não traduzida (5′-UTR) e promotores de genes (177,180,181). Observa-se que os miRNAS estão envolvidos em processos fisiológicos e estágios fisiopatológicos, como proliferação, metabolismo, diferenciação, apoptose, modulam a imunidade inata e adaptativa (182–184).

Os miRNA apresentam um papel importante em numerosos processos biológicos, o desequilíbrio na expressão destas moléculas tem sido associado a doenças humanas, uma vez que os miRNAs têm papel nas interações vírus-hospedeiro, sendo que os vírus induzem microambientes favoráveis que facilitam o ciclo de vida viral por meio de alterações na expressão do miRNA do hospedeiro, atuando como reguladores críticos da patogênese viral (185–187) Estudos recentes sugerem que os miRNAs são transportados entre diferentes compartimentos subcelulares para controlar a taxa de tradução e transcrição (188). Os miRNAs extracelulares têm sido amplamente relatados como potenciais biomarcadores para uma variedade de doenças e servem como moléculas de sinalização para mediar as comunicações célula-célula através de vesículas extracelulares (189–191)

Exossomos são vesículas extracelulares (EVs), que junto com as microvesículas e corpos apoptóticos, ajudam na remoção de componentes celulares indesejados (192) responsáveis pelo transporte de biomoléculas e outros constituintes celulares (193–195) (**Figura 10**).
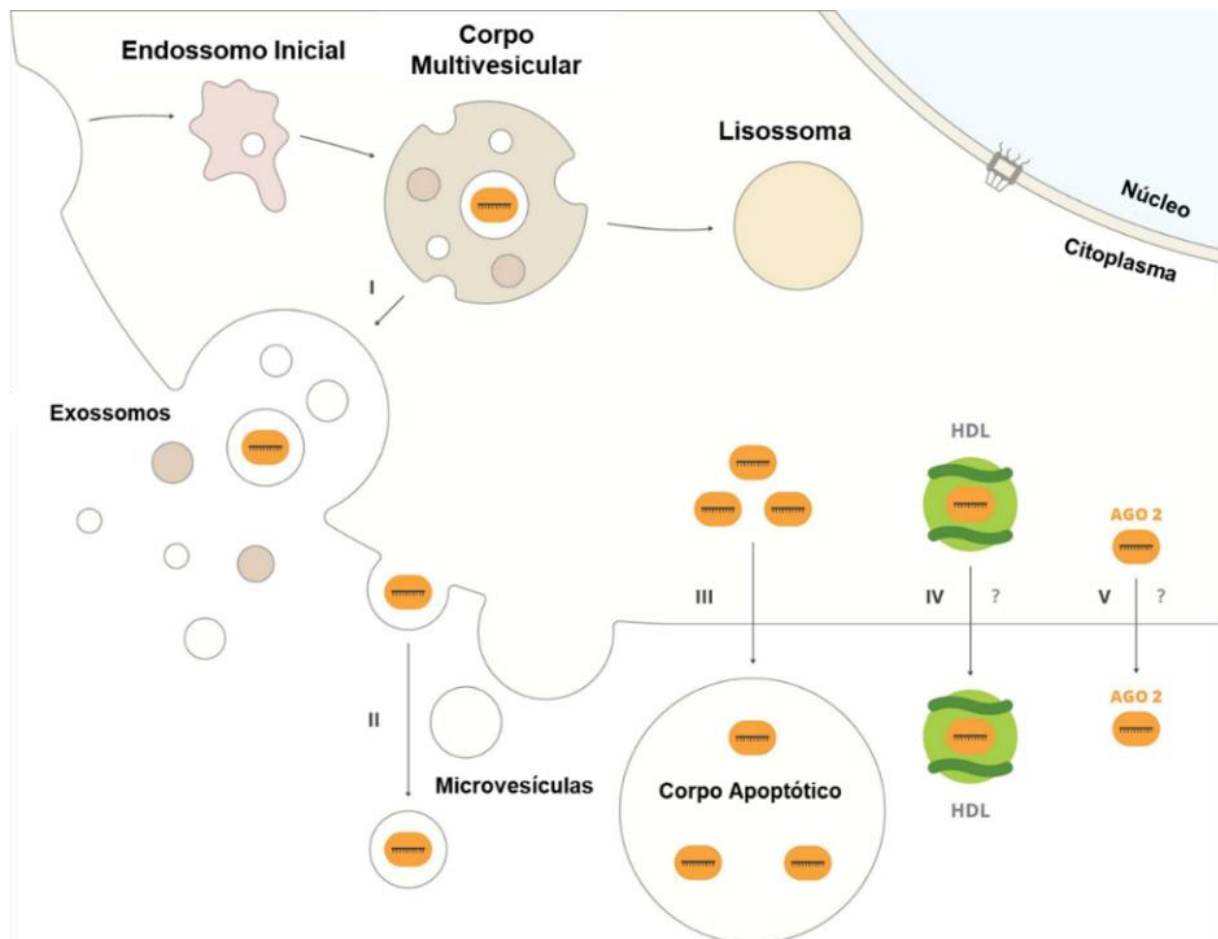
Figura 10. Mecanismos intracelulares de biogênese, secreção de exossomos e miRNA.
Fonte: Adaptado de *Makarova et al*., 2016 (188)

Formados por invaginações de membranas de endossomos e corpos multivesiculares (MVB). Os MVB se fundem com os lisossomos ou com a membrana plasmática promovendo a liberação de exossomos, desencadeando uma série de eventos como sinalização celular, desregulação imune, alteração metabólica e expressão gênica (196–198).

Estudos demonstram que os exossomos são capazes de carregar mRNAs e miRNAs funcionais com capacidade de regular a expressão génica em células receptoras (199–201). Tem sido relatado que exossomos podem ser responsáveis por transferir o receptor ACE2 para células saudáveis facilitando a entrada do vírus e aumentando a disseminação da doença no organismo (202,203). Nas infecções virais, a expressão de miRNAs em células

epiteliais podem ter função na patogênese através da modulação do sistema imunológico (204,205) (**Tabela 1**).

Tabela 1. miRNAs na imunidade Inata

miRNA	Alvos	Efeito
miR-9	NF-κB1	Regulador negativo de sinalização TLR4
miR-19	TLR2	Diminui a inflamação mediada por TLR2
miR-21	PDCD4, IL-12 p35	Regulador negativo de sinalização TLR4
miR-27b	PPAR-γ	Melhora a resposta ao LPS
miR-105	TLR2	Diminui a inflamação mediada por TLR2
miR-106a	IL-10	Diminui IL-10
miR-125b	TNF-α; IRF4	Diminui a inflamação; aumenta a ativação de macrófagos
miR-145	TIRAP	Inibe a sinalização TLR
miR-146a	TRAF6, IRAK1, IRAK2	Regulador negativo de sinalização TLR
miR-155	MyD88; TAB2; Pellino-1; IKKε; NAVIO-1; SOCS1; C / EBP-β	Aumenta a inflamação; regulamento de feedback negativo
miR-223	IKKα; Pknox1	Ativação pró-inflamatória de macrófagos
Let-7i, let-7e	TLR4	Regular baixo a sinalização inflamatória

Fonte: Adaptado de Liu *et al*., 2013 (18)

Até o momento, o papel dos miRNAs na infectividade dos coronavírus não foi examinado em estudos *in vivo*. Sabe-se que células infectadas pelo coronavírus ativam uma cascata de sinalização, resultando no aumento da expressão de miRNA permitindo a tradução de NF-kB e produção de citocinas pró-inflamatórias (206). Um número limitado de estudos *in vitro* realizado no coronavírus OC43, e análises in sílico conduzidas no SARS-CoV e MERS-CoV (207), demonstraram que os miRNAs interagem com mRNAs do coronavírus, influenciando a inibição da replicação viral através da regulação positiva de miR-214, miR-574-5p e miR-17, miR-223, miR-98, miR-146a-5p, miR-21-5p, miR-126-3p, miR-200c, miR-98-5p, miR-32, miR-218-5p, let-7g-5p, miR-506-3p, miR-133b, miR-124-3p, miR-22-3p e miR-133a-3p (205,208). O perfil de miRNAs examinados em transcriptomas mostraram o aumento significativo da expressão do miR-155 em células

infectadas com SARS-CoV-2 gerando um aumento na expressão dos genes da resposta imune estimulado por IFN e citocinas inflamatórias (209).

Assim, os miRNAs tornam-se candidatos promissores como biomarcadores e alvos terapêuticos. Os miRNAs podem regular uma ampla variedade de infecções virais, incluindo os CoVs, uma vez que proteínas virais do SARS-CoV regularam negativamente os miR-223 e miR-98, para modular a diferenciação da célula hospedeira e induzir respostas pró-inflamatórias (210).

Sabe-se que o desenvolvimento e a função das células mieloides fornecem processos bem caracterizados para a regulação de miRNAs, os macrófagos apresentam dois principais miRNAs (miR-155 e miR-146a) que participam da regulação e desenvolvimento destas células (211–213) Macrófagos e células dendríticas induzem fortemente a expressão de miR-155 via NF-κB e proteína ativadora 1 (AP-1) em resposta a uma ampla gama de receptores TLRs e citocinas (211). A ligação ao receptor TLR4, favorece a ativação de macrófagos induzindo a produção de miRNA-155, por sua vez, amplifica a sinalização inflamatória ao diminuir o domínio SH2 contendo inositol 5'-fosfatase 1 (SHIP1) e supressor de sinalização de citocina 1 (SOCS1) (214). O miR-146a também é induzido por NF-κB e regula negativamente a sinalização de TLR ao direcionar TRAF6 e IRAK1 (215).

3. Justificativa

A infecção por SARS-CoV-2 resulta em uma doença leve na maioria dos pacientes. Porém, alguns desenvolvem insuficiência respiratória aguda, levando à internação em Unidade de Terapia Intensiva (UTI) e sem critérios preditivos aceitos para agravamento. As formas graves induzidas na Covid-19 são consequência do estado hiperinflamatório e pró-coagulante (3–5). Sabe-se que além do dano viral, a inflamação descontrolada também contribui para a gravidade da doença (13). Nesse contexto, altas quantidades de marcadores inflamatórios, como citocinas IL-6, IL-8, quimiocinas (216), proteína C reativa (PCR), ferritina, dímero D e proporção de neutrófilos/linfócitos (217,218) foram propostos para fins de estratificação de risco, monitoramento e prognóstico em pacientes com Covid-19 (219). Entretanto, o vírus possui estratégias para evadir da resposta imune, favorecendo o estabelecimento da infecção. Durante processos infecciosos, alterações no perfil de expressão dos miRNAs do hospedeiro podem induzir modulação de mecanismos de defesa do hospedeiro contra o patógeno. TREM-1 é um imunorreceptor que atua como um amplificador da resposta inflamatória. Altamente expresso na superfície de células mielóides como neutrófilos e monócitos/macrófagos. Sua ativação leva ao dano tecidual endotelial e ao estado hiperinflamatório, já associados com a gravidade da Covid-19 (13,220). TREM-1 na sua forma solúvel (sTREM-1) apresenta valor prognóstico durante o choque séptico e outras doenças infecciosas (29,30,221) No contexto da infecção causada pelo vírus SARS-CoV-2, a via do receptor TREM-1 estaria altamente modulada, principalmente na expressão do receptor em monócitos/macrófagos, podendo ter efeito no aumento da expressão de fatores de transcrição, miRNAs, mediadores inflamatórios e liberação da sua forma solúvel em pacientes graves. Com isso, o presente estudo estabelece uma estratégia para avaliar a expressão de TREM-1 como um biomarcador de estratificação de risco, além de identificar a atividade e função de MMPs e miRNAs envolvidos na via de sinalização de TREM-1, evidenciando um novo mecanismo de patogenicidade da Covid-19.

4. Objetivos

4.1 Objetivo Geral

Determinar o potencial de TREM-1 como biomarcador associado a progressão clinica durante a infecção pelo SARS-CoV-2 e a sua correlação com a atividade de metaloproteinases e função de microRNAs na patogenese da doença.

4.2 Objetivos Específicos

- Avaliar a associação plasmática de sTREM-1 e a expressão de mediadores inflamatórios na gravidade da Covid-19;

- Avaliar o valor preditivo de morte em razão da expressão de sTREM-1 em pacientes com Covid-19;

- Identificar a expressão e atividade de MMPs no plasma, tecido pulmonar (biópsias) e fluido do aspirado traqueal de pacientes críticos infectados por SARS-CoV-2;

- Identificar a expressão de microRNAs e fatores de transcrição, utilizando metadados públicos de biópsias de pulmão de pacientes infectados por SARS-CoV-2 e fazer a associação de rede com a via de TREM-1.

- Avaliar a modulação da resposta imune após tratamento com antagonista de TREM-1 em monócitos/macrófagos *in vitro*.

5. Pacientes e Métodos

5.1. Aspectos Éticos

O presente estudo constitui um subprojeto derivado de um consórcio de pesquisa "Avaliação prospectiva de expressão gênica e resposta humoral em Covid-19 grave: busca de potenciais biomarcadores para evolução da doença em pacientes infectados por SARS-CoV-2" (ImunoCovid), realizado em pacientes positivos para Covid-19 na cidade de Ribeirão Preto/SP. O projeto de pesquisa foi registrado no sistema CEP/CONEP sob o número do Certificado de Apresentação de Apreciação Ética (CAAE) 30525920.7.0000.5403. Após verificar a elegibilidade e a aptidão para participar do estudo, todos os voluntários foram convidados a disponibilizarem seu consentimento por escrito de acordo com os regulamentos do Conselho Nacional de Pesquisa em Humanos (CONEP) e do Comitê de Ética Humana da Faculdade de Ciências Farmacêuticas de Ribeirão Preto (CEP-FCFRP-USP). O tamanho da amostra foi determinado pela conveniência da amostragem, disponibilidade em hospitais parceiros, acordo para participação e condições da pandemia.

5.2. Casuística do Estudo

Trata-se de um estudo observacional, analítico e transversal, com coletas em pacientes realizadas entre maio e dezembro de 2020, em pacientes infectados pelo vírus SARS-CoV-2 na cidade de Ribeirão Preto/SP, sem vacinação contra Covid-19. A distribuição geral segundo a idade dos participantes da pesquisa, mostrou-se não-gaussiana, portanto, não paramétrica e não normal, devido a fatores como livre-demanda de amostras, agravamento da doença no grupo de pessoas idosas, em relação aos mais jovens e colapso do sistema de saúde.

5.3. Recrutamento de indivíduos para coorte experimental

Os indivíduos conhecidamente negativos para SARS-CoV-2 foram recrutados no Parque Tecnológico Supera (Supera Parque), onde foram devidamente testados e o resultado negativo confirmado.

Para pacientes positivos para SARS-CoV-2 em isolamento domiciliar, estabilizamos um acordo com a Secretaria Municipal de Saúde de Ribeirão Preto e via formulários eletrônicos, amplamente divulgados em mídias sociais, fizemos o recrutamento ativo dos pacientes que receberam atendimento médico oferecido pelo Sistema Único de Saúde. Estes foram enquadrados na classificação de indivíduos assintomático/leve e moderados da doença, que não necessitavam de internação hospitalar.

Adicionalmente, realizamos acordo de parceria com 2 grandes importantes centros hospitalares da cidade de Ribeirão Preto: Hospital São Paulo de Ribeirão Preto e Hospital da Irmandade da Santa Casa de Misericórdia de Ribeirão Preto, para o recrutamento de pacientes em isolamento Hospitalar em quadros clínicos graves da covid-19.

5.4. Classificação dos pacientes do estudo

Inicialmente, analisamos os pacientes somente com base na presença ou ausência de infecção por SARS-CoV-2, resultando em dois grandes grupos:

- ❖ **Controle**: pacientes saudáveis, ou com doenças de base não predisponentes e controladas, e sabidamente negativos para SARS-CoV-2.
- ❖ **Covid-19**: todos os indivíduos positivos para SARS-CoV-2, independentes da gravidade e local de isolamento.

Ao notarmos agrupamentos de resultados dispersos graficamente, nas mais variadas formas, realizamos outra estratificação dos pacientes para melhor caracterização do grupo, sendo:

- **Domiciliares:** indivíduos positivos para SARS-CoV-2 que não necessitavam de suporte e cuidados hospitalar;
- **Hospitalizados:** indivíduos positivos para SARS-CoV-2 que precisavam de suporte e manejo hospitalar.

Contudo, outras variações foram descritas entre os indivíduos hospitalizados, e para melhor caracterizar estes pacientes, dicotomizamos mais uma vez o grupo, conforme a gravidade da doença, sendo:

- Assintomáticos / Leve;
- Moderado;
- Grave;
- Crítico;

Com essa maior dicotomização dos grupos, tivemos a necessidade de estabelecer mais um grupo controle , que pudesse atender as características de pacientes internados em condições críticas de sintomas. Assim, estabelecemos:

- ❖ **Controle crítico**: pacientes internados em UTI, portadores de doença de base, comprovadamente negativos para SARS-CoV-2, e necessariamente entubados.

5.5. Sinais, sintomas e parâmetros para classificação geral dos participantes

Os participantes foram classificados em seis grupos e foram dicotomizados com base na gravidade da doença, parâmetros clínicos, manejo do paciente e resultados laboratoriais, seguindo as recomendações da OMS (222–224). Além disso, baseamos nossa classificação em vários ensaios clínicos e *pré-prints* (225–230). Estas classificações foram utilizadas para definir a escala da progressão clínica dos pacientes. Os critérios e os grupos podem ser visualizados conforme mostrado na **Tabela 2**.

Tabela 2. Classificação dos participantes do estudo.

Classificação do participante	Sintomas, sinais e parâmetros
Voluntários saudáveis	- Negativo para ácido nucleico SARS-CoV-2 - Sem sinais clínicos
Leve	- Positivo para ácido nucleico SARS-CoV-2 e / ou teste sorológico - Com ou sem os seguintes sintomas: diarreia, tosse, febre, dor de cabeça, perda do paladar (ageusia)/ cheiro (anosmia), mialgia, náusea e vômito - Saturação de oxigênio 94-99% no ar ambiente
Moderado	- Positivo para ácido nucleico SARS-CoV-2 e / ou teste sorológico - Manifestação de sintomas leves de doença, incluindo dispneia - Saturação de oxigênio ≥ 93-99% no ar ambiente - PaO2/FiO2 250-300 mmHg - Não necessidade de ventilação mecânica invasiva; uso de cateter de baixo fluxo (oxigênio 2-4L/min), ou reservatório de oxigênio (4-10L/min)
Grave	- Positivo para ácido nucleico SARS-CoV-2 e / ou teste sorológico - Possível admissão em unidades de terapia intensiva - Desconforto respiratório grave - Saturação de oxigênio <93% em ar ambiente - PaO2/FiO2 <250 mmHg - Não necessidade de ventilação mecânica inva-siva: reservatório

	de oxigênio (4-10L/min); ou máscara/cateter de oxigênio de alto fluxo (10-15L/min).
Crítico	- Positivo para ácido nucleico SARS-CoV-2 e / ou teste sorológico - Admissão (preferencialmente), ou não em UTI - Desconforto respiratório agudo grave - Necessidade de ventilação mecânica - PaO2/FiO2 < 200 mmHg - Com ou sem um ou mais parâmetros adicionais: necessidade de hemodiálise, sepse, choque séptico e disfunção de órgãos múltiplos
Controle crítico	- Negativo para SARS-CoV-2 - Admissão em UTI - Necessidade de ventilação mecânica invasiva - PaO2/FiO2 <200mmHg - Com ou sem parâmetros adicionais: necessidade de hemodiálise, septicemia, choque séptico e disfunção multiórgãos.

Abreviaturas: FiO2, fração inspirada de oxigênio; PaO2, pressão parcial de oxigênio.

Entretanto, para fazer essa classificação dos pacientes conforme seus estágios clínicos, desenvolvemos um sistema de pontuações, onde ponderamos com diferentes valores, as diversas condições clínicas apresentadas pelos pacientes. Deste modo, cada item avaliado recebia um ponto e ao final somava-se os valores para determinar seu escore clínico. A **Tabela 3**, apresenta as pontuações e as respectivas classificações dos pacientes:

Tabela 3. Score clínico para classificação de pacientes no estudo

Pontuação	Classificação
< 2 pontos	Leve
≥ 2 a ≤ 4 pontos	Moderado
≥ 5 a ≤ 9 pontos	Grave
≥ 10 a ≤ 15 pontos	Crítico

A **Tabela 4** apresenta as pontuações e os pesos sobre uma variável clínica avaliada nos pacientes:

Tabela 4. Sistema de pontos para classificação de pacientes

Item avaliado	Pontuação recebida	Observação
Apresenta algum sintoma gripal	1	
Necessidade de UTI	4	Imediatamente já estava incluso no grupo grave caso pontuasse mais algum item.
Dispneia	1	
Sat.O2 ≤93%	1	
$\frac{PaO_2}{FiO_2} = \geq 250mmHg$	1	Pontuação única, ou seja, paciente poderia pontuar somente em uma das 3 relações apresentadas
$\frac{PaO_2}{FiO_2} = \geq 200a \leq 250mmHg$	2	
$\frac{PaO_2}{FiO_2} = <200mmHg$	3	
O₂ ofertado ≥ 2 a ≤ 4 L/min	1	Pontuação única, ou seja, paciente poderia pontuar somente em uma das 3 ofertas de O₂ apresentadas
O₂ ofertado ≥ 5 a ≤ 10 L/min	2	
O₂ ofertado ≥ 11 a ≤ 15 L/min	3	
Necessidade de IOT	5	Somado ao ponto da UTI, imediatamente o paciente já estava no classificado como crítico
Hemodiálise; e/ou choque; e/ou septicemia; e/ou CID; e/ou falência multiórgãos	1	

5.5.1. Critérios de inclusão

Indivíduos de ambos os sexos, idade igual ou superior a 18 anos, com diagnóstico molecular ou sorológico positivo para o SARS-CoV-2, atendidos nas Unidades Básicas de Saúde com quadros leves que foram encaminhados para isolamento domiciliar e acompanhados via Sistema Único de Saúde – SUS, Hospital São Paulo e Hospital Santa Casa de Misericórdia de Ribeirão Preto em Ribeirão Preto/SP.

5.5.2. Critério de exclusão:

Foram excluídas as grávidas, lactantes e menores de idade.

5.6. Procedimentos

5.6.1. Coleta e processamento do sangue periférico

As amostras analisadas neste estudo foram coletadas através de punção venosa dos pacientes em ponto único, apenas uma coleta ou em seguimento. Aproximadamente 20 mL de volume total de sangue periférico foi obtido em sistema de coleta à vácuo, distribuído em tubos Vacutainer® contendo: 1) EDTA (BD Vacutainer® EDTA K2); 2) tubo PPT (Plasma Preparation Tube, Vacuntainer BD); 3) tubos contendo Heparina (BD Vacutainer® PST™).

Os sangues dos participantes controles ou infectados pelo SARS-CoV-2 hospitalizados ou não, foram processadas em uma Instalação de Biossegurança Nível 2 (NB2), localizado no Departamento de Análises Clínicas, Toxicológicas e Bromatológicas da Faculdade de Ciências Farmacêuticas de Ribeirão Preto, Universidade de São Paulo, Ribeirão Preto, São Paulo (DACTB-FCFRP-USP). Os exames laboratoriais de sangue dos participantes saudáveis e pacientes infectados não hospitalizados foram realizados pelo Serviço de Análises Clínicas (SAC) - DACTB-FCFRP-USP, as investigações laboratoriais clínicas incluíram hemograma, testes bioquímicos séricos (incluindo função hepática e renal), enzimas miocárdicas e de fatores de coagulação. Posteriormente, as amostras processadas e separadas em plasma/soro, *buffy coat* de células ou sangue total foram armazenadas em freezers -80ºC. Para pacientes hospitalizados, os exames laboratoriais de sangue foram realizados pelos laboratórios de análises clínicas em seus respectivos hospitais.

5.6.2. Coleta e processamento de Fluido de Aspirado Traqueal

Os fluidos de aspirados traqueais (TAF) foram coletados de pacientes hospitalizados em UTI: 1) positivos para SARS-CoV-2, entubados, nos estágios graves ou críticos da doença (n= 39); 2) pacientes negativos para SARS-CoV-2, entubados, referidos como pacientes Controle Crítico (n= 13).

O TAF foi coletado com o auxílio de um cateter de sucção brônquica endotraqueal de vinila siliconado (Mark Med, Porto Alegre, Rio Grande do Sul, Brasil), instilando no paciente de 10-20 mL de solução fisiológica 0.9% (*m/v*) e recuperando com o auxílio do mesmo cateter em estado de sucção em um sistema Trach Care fechado (Bioteque Corporation, Cirurgic Fernandes LTDA, Santana Parnaíba, São Paulo, Brasil), em um frasco estéril de polipropileno de 120mL (Biomeg-Biotec Hospital Products LTDA, Mairiporã, São Paulo, Brasil) sob condições assépticas. Aproximadamente 5-10 mL de fluido traqueal foi recuperado, com rendimento médio

de 60% após instilação. As amostras de TAF foram colocadas em gelo para transporte, e processadas dentro de no máximo 4h, em Laboratório de Biossegurança Nível 3, (NB3), no Departamento de Bioquímica e Imunologia da Faculdade de Medicina de Ribeirão Preto - FMRP-USP. Os aspirados foram colocados em tubos cônicos de polipropileno de 15 mL e receberam adição de solução salina tamponada com fosfato (PBS) 0,1M (2:1 *v/v*). Após a centrifugação (700 g/10 min/4ºC), os sobrenadantes do TAF foram recuperados e armazenados à -80°C.

Posteriormente, o aspirado restante foi diluído em 10 mL de PBS, gentilmente filtrado em filtro de 100µm (Falcon Cell Strainer, Corning Inc., Corning, Nova York, EUA) usando um êmbolo de seringa. O aspirado de filtragem primária foi submetido a mais uma etapa de purificação de impurezas, desta vez, utilizando um filtro de 0,20 µm (Minisart®, Sartorius Stedim Biotech, Otto-Brenner-Straße, Göttingen, Alemanha) acoplado a uma seringa. O material resultante foi utilizado para quantificação de mediadores inflamatórios e proteínas/enzimas.

O precipitado resultante da centrifugação do TAF foi utilizado para outras análises. Então, os eritrócitos foram lisados usando 1mL de tampão de cloreto de amônio (NH$_4$Cl) 0,16 M durante 5 min. As células restantes foram lavadas com 10 mL de PBS, ressuspendidas em PBS adicionado de 2% de soro fetal de bovino (SFB) inativado por calor, e posteriormente contadas com Azul de Trypan usando um contador automático de células (Condessa, ThermoFisher Scientific, Waltham, MA, EUA). Os números de leucócitos foram ajustados para $1x10^9$ células/L e feitas contagens diferenciais, e $1x10^6$ células/mL foram destinadas para análise por citometria de fluxo. Todos os procedimentos foram realizados em condições de biossegurança NB3.

5.6.3. Citometria de fluxo

Amostras de sangue contendo EDTA (BD Vacutainer® EDTA K2) foram processadas para análise de citometria de fluxo de leucócitos circulantes. O sangue total (1 mL) foi separado e os glóbulos vermelhos foram lisados usando tampão de lise RBC (Roche Diagnostics GmbH, Mannheim, GR). Os leucócitos foram lavados em PBS contendo 5% de SFB (Gibco ™, EUA), centrifugados e ressuspensos em solução salina balanceada de Hank (Sigma-Aldrich, Merck, Darmstadt, DE) contendo 5% de SFB, seguido de coloração com antígeno de superfície. Resumidamente, as células foram coradas com *Fixable Viability Stain 620* (BD Bioscience, 1: 1000) e incubadas com anticorpos monoclonais específicos para CD14 (clone: M5E2, Biolegend, 1: 100), HLA-DR (clone: G46-6, BD Bioscience , 1: 100), CD16 (clone: 3G8, Biolegend, 1:

100) e TREM-1 (clone: CB38, BD Bioscience, 1: 100), por 30 min à 4 ºC. As células coradas foram lavadas e fixadas com BD Cytofix ™ Fixation Buffer (554655, BD Bioscience - San Diego, CA, EUA). A aquisição de dados foi realizada usando um citômetro de fluxo BD LSR-Fortessa ™ (BD Bioscience - San Jose, CA, EUA) e software FACS-Diva (Versão 8.0.1, BD Biosciences, Franklin Lakes, NJ, EUA). Para análise, 300.000 eventos foram adquiridos para cada amostra. Os dados foram avaliados com o software FlowJo®, versão 10.7.0 (Tree Star, Ashland, OR, EUA) para o cálculo da frequência celular, redução da dimensionalidade e Análise de incorporação estocástica de vizinhança distribuída por T (t-SNE). Estratégia feita conforme descrito antes (231)

5.6.4. Dosagem de citocinas por *Cytometric Bead Array* (CBA)

As citocinass IL-6, IL-8, IL-1ß, IL-10 e TNF foram quantificados em plasma heparinizado e TAF usando kit BD *Cytometric Bead Array* (CBA) *Human Inflammatory* (BD Biosciences, San Jose, CA, EUA), de acordo com as especificações do fabricante. Resumidamente, após o processamento da amostra, as citocinas foram determinadas em um citômetro de fluxo através de *beads* (FACS Canto TM II, BD Biosciences, San Diego, CA, EUA) e as análises foram realizadas usando o software FCAP Array 3.0 (BD Biosciences, San Jose, CA), EUA). As concentrações de citocinas foram expressas em pg/mL.

5.6.5. Quantificação de sTREM-1 e MMPs

As amostras de plasma e de TAF foram analisadas em placas de 96 poços. A concentração de sTREM-1 e MMP-2 e -8 foram determinadas utilizando kit de ELISA (DuoSet-Human TREM-1, DuoSet-Human Total MMP-8 e DuoSet-Human Total MMP-2, R&D System, Minneapolis, MN, EUA), de acordo com as especificações do fabricante. As amostras que excederam o limite de quantificação foram devidamente diluídas e após corrigidas pelo fator de diluição.

5.6.6. Quantificação de HLA-G Solúvel

A isoforma solúvel de HLA-G no TAF, foi detectada usando ensaio de ELISA. As moléculas de sHLA-G foram capturadas incubando as amostras de TAF em uma placa de monocamada de anticorpo monoclonal imobilizado (MEM-G/9) (Exbio, Praga, República Tcheca) por 18 h à 4°C. As ligações não específicas foram bloqueadas usando albumina 2% (*m/v*) em PBS por 30 min. Após a lavagem das placas (três vezes com PBS contendo 0,05% de Tween 20), foram incubadas por 1 h com o anticorpo de detecção conjugado com a HRP-anti-b2-microglobulina peroxidase e com o substrato

(orto-fenil-n-diamino-dihidroxi cloreto) (DAKO, Santa Clara, CA). A reação foi interrompida pela adição de H$_2$SO$_4$ (1M). A leitura de absorbância foi realizada imediatamente em 490 nm usando um espectrofotômetro ELISA (AgileReader™ ELISA Plate Readers, Avans Biotechnology, Taipei City, Taiwan). As qauntidades de sHLA-G foram estimadas por uma curva padrão de cinco pontos (12,5 - 200 ng/mL), usando sobrenadante de cultura de linha celular expressando o hibridoma M8-HLA-G5.

5.6.7. Avaliação de estresse oxidativo por formação de peróxido lipídico (MDA).

Os concentrações de peróxido lipídico em amostras de TAF foram determinados pela medida indireta de substâncias reativas ao ácido tiobarbitúrico (TBARS) usando método fluorimétrico descrito anteriormente (232,233). Resumidamente, o malondialdeído (MDA) reage com o ácido tiobarbitúrico (TBA) sob altas temperaturas (90 – 100°C), em condições ácidas, gerando o aduto MDA-TBA. O aduto MDA-TBA é determinado fluorometricamente em um comprimento de onda de excitação 515 nm e emissão em 553 nm, utilizando 1,1,3,3-tetrametoxipropano como padrão para curva de quantificação. Todas as análises foram realizadas usando um leitor de microplacas multimodo Synergy 2 e o software Gen5 (BioTek, Winooski, VT, EUA). As amostras de TAF foram transferidas para um volume igual de 20% (*v/v*) ácido tricloroacético frio em HCl 0,6 M, misturado e centrifugado a 1200 g por 15 min. Em um volume de sobrenadante, um volume de 0,2 volume de ácido tiobarbitúrico 0,12 M/Tris 0,26 M, pH 7,0 foi adicionado e imerso em banho de água fervente por 1 h. As quantidades de peróxido lipídico foram expressas em referência a MDA (nmol/mL).

5.6.8 Quantificação da atividade de MMPs por Zimografia

As atividades de MMP-2 e MMP-9 no TAF foram determinadas por meio de um ensaio de protease de zimograma em gelatina como previamente descrito (234,235). Resumidamente, alíquotas de TAF (15 μL) foram misturadas com um tampão de amostra (0,5 m Tris-HCl, pH = 6,8, glicerol, SDS 10% e azul de bromofenol 0,1%) e carregadas no gel. Em seguida, as amostras preparadas foram submetidas à eletroforese em géis de dodecilsulfato de sódio (SDS) a 10% - poliacrilamida contendo 0,1% de gelatina. Após a eletroforese, os géis foram lavados duas vezes em 2,5% Triton X-100 (Sigma-Aldrich) durante 1 h à temperatura ambiente para remover o SDS. Os géis foram então incubados à 37°C por 15 h em tampão de substrato contendo 50 mmol/L de Tris-HCl e 10 mmol/L de CaCl$_2$ a pH 8,0 e corados com 0,5% de azul de Coomassie R250 em 50% de metanol e 10% ácido acético glacial. Os padrões de proteína (Bio-Rad) foram executados simultaneamente e os pesos moleculares aproximados foram

determinados traçando as mobilidades relativas de proteínas conhecidas. As atividades gelatinolíticas foram detectadas como bandas não coradas contra o fundo da gelatina corada com azul de Coomassie. A atividade da enzima foi avaliada por densitometria usando um Sistema de Análise e Documentação de Eletroforese Kodak (Kodak, Rochester, NY).

5.6.9. Reanálise dos dados de transcriptoma sanguíneo e proteômica de biópsias pulmonares de pacientes com Covid-19

Os dados de expressão de proteínas para biópsias pulmonares de amostras Covid-19 e não-Covid-19, foram obtidos de um estudo proteômico (236). Apenas proteínas com valores de expressão em pelo menos três amostras para cada grupo foram utilizadas na análise estatística. O teste de *Student t* entre os grupos Covid-19 e não-Covid-19 foi realizado para todas as proteínas selecionadas após a transformação dos valores de expressão usando a escala Log2. Os resultados das MMPs foram extraídos de estatísticas usando valores de *p* nominais e ajustados com resultados significativos (p < 0,05). A análise estatística foi realizada em R, e as figuras foram produzidas usando o pacote ggplot2.

Como dado preliminar, realizamos uma nova análise reutilizando um conjunto de dados públicos abertos de transcriptoma (237), depositado no repositório Gene Expression Omnibus (GEO) sob o número de acesso GSE15031619. A estratégia de reanálise do transcriptoma foi implementada de acordo com três etapas consecutivas: (i) análise de co-expressão, (ii) análise de expressão diferencial e (iii) construção da rede biológica. Inicialmente, para o estudo de co-expressão, os dados do transcriptoma normalizado em log2 de leituras por milhão (RPM) foram filtrados excluindo contagens diferentes de zero em pelo menos 20% das amostras. Em seguida, os genes e miRNA selecionados foram explorados na ferramenta de identificação de módulos de co-expressão do pacote R (CEMITool).

5.6.10. Quantificação de RNA viral por qRT-PCR

O RNA total foi extraído de 20 uL de amostras de TAF utilizando o regante Trizol (Thermo, EUA) de acordo com recomendações do fabricante. O ensaio qPCR foi realizado para a região do gene E e região N2 no gene N (238,239). Para quantificação do RNA viral, foi realizado a reação de transcriptase reversa seguida da reação quantitativa em tempo real de polimerização em cadeia (qRT-PCR) utilizando-se o kit *TaqMan® Fast Virus 1-Step Master Mix* (Applied Bossystems, Foster City, CA, EUA), a reação amplifica uma região de 100pb do gene *RdRp* de SARS-CoV-2 (*Foward*: '5–

GTGAAATGGTCATGTGTGGCGG–3'; *Reverse*: '5–CAAATGTTAAAAACACTATTAGCATA–3' and Sonda: '5-FAM–CAGGTGGAACCTCATCAGGAGATGC – BHQ1-3'). com os seguintes parâmetros: 25°C por 2 min, 50°C por 15 min, 95°C por 2 min, seguido de 45 ciclos de 94°C por 5 se 60°C por 30 s. A reação foi realizada em equipamento *StepOnePlus Real-Time PCR system* (Applied Biossystems, EUA). As cargas virais do SARS-CoV-2 foram determinadas usando uma curva padrão preparada com um plasmídeo contendo todos os três alvos para os conjuntos de primers/sondas projetados pelo protocolo do CDC (N1, N2 e N3) (240)

5.6.11. Cultura de células humanas.

Linhagem celular de monócitos de sangue periférico humano (THP-1, BCRJ 0234) ($1x10^5$ células/poço), foram cultivadas em placas de 96 poços e mantidas à 37°C, 5% de CO_2 em DMEM (1 g/L D-glicose, GIBCO) suplementado com 20% de SFB (FBS, Gibco) e 1% de penicilina/estreptomicina (Gibco). As células THP-1 foram diferenciadas em um fenótipo semelhante a macrófagos (TDM, macrófagos derivados de THP-1) usando forbol-12-miristato-13-acetato (PMA, 5 ng/mL) por 24 h e 5 dias para período de descanso em meio livre de PMA, como descrito por Baxter et al. (241).Após este período, os TDM foram estimulados com 100 ng/mL de LPS (Sigma-Aldrich, EUA) por 24h à 37°C, com 5% de CO_2. Células tratadas apenas com DMEM-C foram utilizadas como controle. Em seguida, os sobrenadantes dos tratamentos foram obtidos e armazenados à -20°C, para análise de produção de mediadores inflamatórios.

5.6.12. Peptídeo antagonista de TREM-1

As células THP-1 (TDM) foram tratados com um peptídeo TREM-1 antagonista, LP17 (LQVTDSGLYRCVIYHPP) ou um peptídeo controle de sequência codificada (TDSRCVIGLYHPPLQVY), conforme descrito anteriormente por (242). Os peptídeos foram sintetizados quimicamente (Pepscan Systems, Lelystad, Holanda). As células foram tratadas com 100 ng/mL de peptídeo.

5.6.13. Imunofluorescência e microscopia confocal

As lâminas de monócitos THP-1 (TDM) foram fixados e posteriormente bloqueados com 2% de soro de cabra em tampão PBS por 1 h à temperatura ambiente. Após o bloqueio, as lâminas foram incubadas com anticorpo anti-TREM-1 (HPA005563, Sigma) na diluição de 1:500 durante 18 h à 4°C, após três lavagens em PBS frio, foi adicionado anticorpo secundário (anti-coelho IgG,1:500) durante 1h à

temperatura ambiente. O meio de montagem contendo DAPI (Molecular Probes) foi usado para coloração nuclear.

5.6.14. Análise estatística

Os resultados obtidos foram analisados através do programa GraphPad Prism 9 (Gran Pad Software Inc., San Diego, CA, EUA). Levando em consideração a distribuição não paramétrica dos dados, as análises comparativas entre os grupos foram realizadas por meio dos testes de *Mann-Whitney* ou *Kruskal-Wallis* seguido de *Dunn´s*. Para as comparações entre três ou mais grupos não pareados foram realizadas análises de variância *ANOVA one way* seguido do teste de *Tukey* para múltiplas comparações. Para as correlações, os dados foram analisados pela correlação de *Spearman r*, visto que os dados não obedeceram à distribuição normal. Para as análises e precisões de biomarcadores, utilizamos a área sob a curva (AUC) da característica operacional do receptor (ROC). As AUCs, com intervalos de confiança de 95% e AUC > 0,70 foi considerada clinicamente relevante. A dependência de múltiplas variáveis foi calculada pelo teste de correlação de *Spearman* r, e as diferenças foram consideradas estatisticamente significativas com p<0,05. A matriz de correlação calculada foi apresentada graficamente usando o pacote R qgraph, e a análise de componentes principais (PCA) com PCATools. Um modelo de regressão de *Poisson* multivariado com variância robusta foi aplicado para ajustar a razão da taxa de incidência (IRR) de óbitos para as principais variáveis de risco, realizado por meio do STATA 15 (Stata Corp, College Station, TX, EUA).

6. Resultados

6.1. Capítulo I: *sTREM-1 Predicts Disease Severity and Mortality in Covid-19 Patients: Involvement of Peripheral Blood Leukocytes and MMP-8 Activity*

Pedro V. da Silva-Neto [1,2,†], Jonatan C. S. de Carvalho [1,3,†], Vinícius E. Pimentel [1,4,†], Malena M. Pérez [1,†], Diana M. Toro [1,2,†], Thais F. C. Fraga-Silva [4,†], Carlos A. Fuzo [1,†], Camilla N. S. Oliveira [1,4,†], Lilian C. Rodrigues [1], Jamille G. M. Argolo [5], Ingryd Carmona-Garcia [5], Nicola T. Neto [5], Camila O. S. Souza [1,4], Talita M. Fernandes [5], Victor A. F. Bastos [1], Augusto M. Degiovani [6], Leticia F. Constant [6], Fátima M. Ostini [6], Marley R. Feitosa [7], Rogerio S. Parra [7], Fernando C. Vilar [8], Gilberto G. Gaspar [8], José J. R. da Rocha [7], Omar Feres [7], Fabiani G. Frantz [1], Raquel F. Gerlach [10], Sandra R. Maruyama [9], Elisa M. S. Russo [1], Angelina L. Viana [5], Ana P. M. Fernandes [5], Isabel K. F. M. Santos [4], Vânia L. D. Bonato [4], Antonio L. Boechat [2], Adriana Malheiro [2], Ruxana T. Sadikot [11], Marcelo Dias-Baruffi [1,‡], Cristina R. B. Cardoso [1,‡], Lúcia H. Faccioli [1,*,‡] and Carlos A. Sorgi [2,3,4,*,‡] on behalf of the IMUNOCOVID Study Group [§]

1- Departamento de Análises Clínicas, Toxicológicas e Bromatológicas, Faculdade de Ciências Farmacêuticas de Ribeirão Preto-FCFRP, Universidade de São Paulo-USP, Ribeirão Preto 14040-903, SP, Brazil; 2- Programa de Pós-Graduação em Imunologia Básica e Aplicada-PPGIBA, Instituto de Ciências Biológicas, Universidade Federal do Amazonas-UFAM, Manaus 69080-900, AM, Brazil; 3-Departamento de Química. Faculdade de Filosofia, Ciências e Letras de Ribeirão Preto-FFCLRP, Universidade de São Paulo-USP, Ribeirão Preto 14040-901, SP, Brazil; 4-Departamento de Bioquímica e Imunologia. Faculdade de Medicina de Ribeirão Preto-FMRP, Universidade de São Paulo-USP, Ribeirão Preto, SP, Brazil; 5-Escola de Enfermagem de Ribeirão Preto-EERP, Universidade de São Paulo-USP, Ribeirão Preto 14040-902, SP, Brazil; 6-Hospital Santa Casa de Misericórdia de Ribeirão Preto, Ribeirão Preto 14085-000, SP, Brazil; 7-Departamento de Cirurgia e Anatomia, Faculdade de Medicina de Ribeirão Preto-FMRP, Universidade de São Paulo (USP), Ribeirão Preto, SP, Brazil; 8-Departamento de Clínica Médica, Faculdade de Medicina de Ribeirão Preto—FMRP, Universidade de São Paulo (USP), Ribeirão Preto 14049-900, SP, Brazil; 9-Departamento de Genética e Evolução, Centro de Ciências Biológicas e da Saúde, Universidade Federal de São Carlos (UFSCar), São Carlos 13565-905, SP, Brazil; 10-Departamento de Morfologia, Fisiologia e Patologia básica, Faculdade de Odontologia de Ribeirão Preto, Universidade de São Paulo (USP), Ribeirão Preto 14040-904, SP, Brazil; 11-Department of Internal Medicine, Division of Pulmonary, Critical Care and Sleep, College of Medicine, University of Nebraska Medical Center, Omaha, NE 68198, USA; *

Correspondence: carlos.sorgi@usp.br (C.A.S.); faccioli@fcfrp.usp.br (L.H.F.);

† These authors contributed equally to this work.

‡ Senior authors contributed equally to this work.

§ Members are listed in Appendix A.

Abstract: Uncontrolled inflammatory responses play a critical role in coronavirus disease (Covid-19). In this context, because the triggering-receptor expressed on myeloid cells-1 (TREM-1) is considered an intrinsic amplifier of inflammatory signals, this study investigated the role of soluble TREM-1 (sTREM-1) as a biomarker of the severity and mortality of Covid-19. Based on their clinical scores, we enrolled Covid-19 positive patients ($n = 237$) classified into mild, moderate, severe, and critical groups. Clinical data and patient characteristics were obtained from medical records, and their plasma inflammatory mediator profiles were evaluated with immunoassays. Plasma levels of sTREM-1 were significantly higher among patients with severe disease compared to all other groups. Additionally, levels of sTREM-1 showed a significant positive correlation with other inflammatory parameters, such as IL-6, IL-10, IL-8, and neutrophil counts, and a significant negative correlation was observed with lymphocyte counts. Most interestingly, sTREM-1 was found to be a strong predictive biomarker of the severity of Covid-19 and was related to the worst outcome and death. Systemic levels of sTREM-1 were significantly correlated with the expression of matrix metalloproteinases (MMP)-8, which can release TREM-1 from the surface of peripheral blood cells. Our findings indicated that quantification of sTREM-1 could be used as a predictive tool for disease outcome, thus improving the timing of clinical and pharmacological interventions in patients with Covid-19.

Keywords: Covid-19; sTREM-1; biomarker; inflammation; MMP-8

1. Introduction

Coronavirus disease (Covid-19), which is caused by the severe acute respiratory syndrome coronavirus 2 (SARS-CoV-2), became a global public health problem due to the important frequencies of mortality. Approximately 80% of patients infected with SARS-CoV-2 will exhibit mild symptoms or remain asymptomatic. However, this infection may lead to serious clinical conditions, such as acute respiratory distress syndrome (ARDS), cardiovascular disorders, coagulopathy, and shock, which can result in multiorgan system dysfunction in certain patients [1–3]. Elderly, male, and obese patients, or those with chronic comorbidities, are more likely to develop the worst outcomes [4]. Moreover, patients with Covid-19 were found to exhibit multiple hematological abnormalities, including lymphopenia and thrombocytopenia as the most prominent manifestations, in addition to developing neutrophilia [5].

Similarly to SARS, inflammation plays an important role in the pathophysiology of Covid-19, and patients with severe disease may have high serum concentrations of inflammatory markers such as IL-6, TNF, C-reactive protein (CRP), and D-dimer [6,7]. Triggering receptor expressed on myeloid cells 1 (TREM-1) is a member of the immunoglobulin superfamily expressed on myeloid and epithelial cells. Activation of TREM-1 induces the increased secretion of TNF-α, IL-6, IL-1β, IL-2, and IL-12p40 by monocytes, macrophages, and dendritic cells, which enhances inflammation during infection caused by different pathogens, such as influenza A virus, dengue virus, hepatitis C virus, *Plasmodium falciparum*, *Staphylococcus aureus*, and *Pseudomonas aeruginosa* [8–11]. The immune responses to viral and bacterial infections are modulated by the activation of TREM-1 in macrophages [12]. Furthermore, infection with hepatitis C virus and the human immunodeficiency virus (HIV), or even exposure to the HIV proteins Tat or gp120 without infection [13], induces the expression of TREM-1. The soluble form of TREM-1 (sTREM-1) has been detected in biological samples, such as plasma, during infection and inflammation processes [14,15]. sTREM-1 is a 27 kDa polypeptide consisting of the extracellular domain of TREM-1, which is released from the cell surface by metalloproteinase [16]. Furthermore, sTREM-1 is an important prognostic marker in diseases that also develop severe inflammatory pathways, such as sepsis and AIDS [10,15,17,18]. Recently, our group [19] and other works [20,21] suggested that sTREM-1 levels are related to Covid-19 severity and may serve as early triage tools for patients with adverse outcomes.

Given that SARS-CoV-2 induces a hyper-inflammatory response, we hypothesized that in Covid-19 patients, the virus could trigger activation and up-regulation of TREM-1 in the cell surface and, subsequently, shedding in the soluble form (sTREM-1) by metalloproteinase activity. Therefore, we conducted a prospective study to investigate the usefulness of sTREM-1 as a biomarker that can predict severity and mortality in Covid-19, in addition to confirming its risk stratification performance, thus guiding the development of effective interventions in patients who require intensive care after hospitalization.

2. Materials and Methods

2.1. Study Design and Participants

This prospective study was conducted at the Hospital Santa Casa de Misericórdia of Ribeirão Preto and Hospital São Paulo of Ribeirão Preto, Brazil from June to December of 2020, using stringent and reasonable inclusion and exclusion criteria: adults who tested

positive for Covid-19 and controls (healthy volunteers) who tested negative for Covid-19; and exclusion for children under 18 years of age, and pregnant or lactating women. In total, 50 control subjects were included, along with 237 patients who tested positive for Covid-19, as determined by analyzing nasopharyngeal swabs using a genomic RNA assay with RT-PCR (Biomol OneStep Kit/Covid-19-Instituto de Molecular Biology of Paraná-IBMP Curitiba/PR, Brazil) or using serology-specific IgM and IgG antibodies tests (SARS-CoV-2 antibody test®, Guangzhou Wondfo Biotech Co., Ltd., Guangzhou, China).

2.2. Study Design and Participants

The data were collected from the electronic medical record systems. We included socio-demographic information, comorbidities, medical history, clinical symptoms, routine laboratory tests, immunological tests, chest computed tomography scan results, clinical interventions, and outcomes. Data collection from laboratory results was defined by considering the first examination at admission (within 24 h of admission) with an estimate of 6.1 ± 2.8 (mean $\pm$ SD) days after the onset of the symptom as the primary endpoint and the clinical outcome (death or recovery) as the secondary endpoint.

2.3. Severity Assessment

For assessment of clinical severity, patients with Covid-19 were classified into mild, moderate, severe, and critical groups, based on the modified statement in the Novel Coronavirus Pneumonia Diagnosis and Treatment Guideline (7th ed.) [22,23], shown in Table S1.

2.4. Laboratory Methods

Blood samples were collected by venipuncture in tubes with a vacuum collection system. Two tubes (5 mL capacity) were collected from each patient: one tube containing EDTA anticoagulant (BD Vacutainer® EDTA K2, Franklin Lakes, NJ, USA) to perform hematological tests, and a tube containing heparin anticoagulant (BD SST® Gel Advance®, Franklin Lakes, NJ, USA) to obtain plasma used to quantify levels of circulating protein mediators by flow cytometry or ELISA assay. The samples were stored in a –80 °C freezer.

2.5. Cytokine Measurements

The levels of cytokines IL-1β, IL-6, IL-8, IL-10, IL-12, and TNF were measured using a Cytometric Bead Array kit according to the manufacturer's specifications (BD™ Human Inflammatory Cytokine CBA Kit, Catalog No. 551811, Lot: 9341655). The detection range of each cytokine was 5 to 5000 pg/mL. Data were acquired using a

FACSCanto II flow cytometer and FACSDiva software (BD Biosciences, Franklin Lakes, NJ, USA). Data are presented as mean fluorescence intensity for each serum cytokine.

2.6. Detection of Plasma sTREM-1 and MMP-8

Systemic levels of sTREM-1 and matrix metalloproteinases (MMP)-8 were measured in plasma using an ELISA kit (DuoSet-Human TREM-1 and DuoSet-Human Total MMP-8, R&D System, Minneapolis, MN, USA) according to the manufacturer's specifications.

2.7. Analysis of TREM-1-Positive Cells

Expression of TREM-1 in peripheral blood cells was determined by flow cytometry. Blood (1 mL) was used, and red blood cells were lysed using RBC lysis buffer (Roche Diagnostics GmbH, Mannheim, GR). Leukocytes were washed in PBS containing 5% fetal bovine serum (FBS) (Gibco™, Thermo Fisher Scientific, Waltham, MA, USA), centrifuged, and resuspended in Hank's balanced salt solution (Sigma-Aldrich, Merck, Darmstadt, Germany) containing 5% FBS, followed by surface antigen staining. Briefly, cells were stained with fixable viability stain (1:1000) (BD Biosciences, San Diego, CA, USA) and incubated with monoclonal antibodies specific for CD14 (1:100) (M5E2; Biolegend, San Diego, CA USA), CD16 (1:100) (BV510-3G8; Biolegend, San Diego, CA USA), and TREM-1 (1:100) (FAB1278P; R&D Systems, Minneapolis, MN, USA) for 30 min at 4 °C. The stained cells were washed and fixed with BD Cytofix™ fixation buffer (554655; BD Biosciences, San Diego, CA, USA). Data acquisition was performed using the Fortessa™ LSR flow cytometer (BD Biosciences, San Jose, CA, USA) and the FACS-Diva software (version 8.0.1) (BD Biosciences, Franklin Lakes, NJ, USA). For the analysis, 100,000 events were acquired for each sample. CD14 and CD16 positive cells were gated, and TREM-1 expression analysis was performed using FlowJo® software (version 10.7.0-Tree Star, Ashland, OR, USA) (Figure S1).

2.8. Statistical Analysis

Data are presented in tables and graphs, using GraphPad Prism™ software (version 9) (San Diego, CA, USA). Taking into account the nonparametric distribution of the data, comparative analysis between groups were performed using the Mann–Whitney or Kruskal–Wallis tests, with significance of $p < 0.05$. The accuracy of the predictor was determined by the area under the curve (AUC) of the receiver operating characteristic (ROC). The AUCs, with 95% confidence intervals, were calculated to assess the diagnostic value of sTREM-1; AUC > 0.70 was considered clinically relevant. The dependence on multiple variables was calculated using Spearman's correlation test, and the differences

167 were considered statistically significant with $p < 0.05$. The calculated correlation matrix
168 was presented graphically using the R package qgraph [24], and the principal component
169 analysis (PCA) with PCATools [25]. Correlation coefficients (r) and p-values of the
170 correlation matrix were formatted and tabulated, as seen in Table S2. A ROC curve was
171 applied to select the cutoff value for the sTREM-1 level to the best classification of death
172 as an event. A multivariate Poisson regression model with robust variance was applied to
173 adjust the incidence rate ratio (IRR) of deaths for the main risk variables such as sex, age,
174 comorbidities, disease severity, days of disease, and laboratory markers, performed using
175 STATA 15 (Stata Corp, College Station, TX, USA).

176 *2.9. Ethical Approval*

177   The procedures performed in this study were approved by the institutional ethics
178 board of *Faculdade de Ciências Farmacêuticas de Ribeirão Preto–Universidade de São*
179 *Paulo* and Brazil National Ethics Committee (CAAE: 30525920.7.0000.5403). Written
180 informed consent was obtained from the participants.

181 **3. Results**

182 *3.1. Demographic Data, Clinical and Laboratory Characteristics*

183   In total, 237 patients with laboratory-confirmed Covid-19 were recruited for this
184 study, categorized into residential care (60 subjects) and hospital care (177 subjects), in
185 addition to 50 healthy volunteers (controls). The mean age was 35 years for healthy
186 volunteers and 57 years for Covid-19 patients. The mean age of hospitalized patients was
187 higher than that of domiciliary patients. The number of comorbidities was higher among
188 patients with Covid-19 compared to controls, and among hospitalized patients compared to
189 those with home care (Table 1).

190   The most common initial symptoms in patients were cough, dyspnea, and dysgeusia,
191 followed by diarrhea, fever, muscle soreness, and hyperactive delirium. Moreover, the
192 absolute counts of erythrocytes, hemoglobin, neutrophils, lymphocytes, and monocytes in
193 the Covid-19 patient group were different from those in the control group (Table 1).

194   The median time of hospitalization for Covid-19 patients was 9 days, and almost half
195 of them required intensive care (46.3%). Additionally, these hospitalized patients received
196 the following respiratory support: nasal-cannula oxygen (36.7%), oxygen mask ventilation
197 (16.9%), and invasive mechanical ventilation (39.5%). Oxygen saturation was significantly
198 lower among hospitalized patients compared to residential care patients upon evaluation of
199 our investigations (Table 1). The most common pharmacological treatments for the

200 patients with Covid-19 were glucocorticoid, azithromycin, ceftriaxone, oseltamivir, and

201 colchicine, followed by chloroquine/hydroxychloroquine, anticoagulants, and ivermectin

202 (Table   1)

203   **Table 1.** Clinical and demographic data of Covid-19 patients enrolled in this study.

| Baseline Variable | Healthy Controls N = 50 | All patients N = 237 | Covid-19 care | | *p*-Value |
			Residential N = 60	Hospitalized N = 177	
Demographic characteristics					
Age mean ± SD, (IQR)	35 ± 14.7 (19–80)	57 ± 19 (16–96)	37 ± 12 (16–71)	63 ± 16.4 (20–96)	[a] **<0.0001** [c,d] **<0.0001**
Sex, No. (%)					
Male	22 (44)	84 (35.4)	21 (35)	63 (36)	[d] **0.006**
Female	28 (56)	153 (64.6)	39 (65)	114 (64)	
Comorbidities or coexisting disorders, No. (%)					
Hypertension	7 (14)	116 (48.9)	4 (3.4)	112 (96.6)	[a,c,d] **<0.0001**
Cardiovascular diseases	5 (18.5)	22 (81.5)	8 (36.4)	14 (63.6)	[a] 0.7947 [b] 0.7685 [c] 0.5760 [d] 0.2084
Diabetes mellitus	4 (5.8)	65 (94.2)	5 (7.7)	60 (92.3)	[a] **0.0031** [c] **0.0002** [d] **<0.0001**
History of smoking	3 (10)	27 (90)	6 (22.2)	21 (77.8)	[a] 0.2189 [b] >0.1 [c] 0.1227 [d] 0.0692
History of stroke	-	10 (4.2)	-	10 (5.6)	-
Neurological diseases	-	12 (5.0)	2 (16.7)	10 (83.3)	[d] 0.7353
Cancer	-	7 (2.9)	-	7 (3.9)	-
BMI (kg/m^2)	26.5 ± 5.2	28.4 ± 7.0	27.2 ± 5.6	29.4 ± 7.3	[a] **0.0053**

	(15.4–43.2)	(15.7–65.7)	(17.7–43.8)	(18.4–65.7)	[c] **0.0008**
					[d] **0.0480**
Presenting symptoms, No. (%)					
Dyspnea	-	137 (57.8)	19 (31.6)	118 (66.6)	[a,b,c,d] **<0.0001**
Fever	-	78 (32.9)	1 (1.7)	77 (43.5)	[a,c,d] **<0.0001**
Myalgia	-	52 (21.9)	-	52 (29.4)	-
Diarrhea	-	56 (23.6)	22 (36.7)	34 (19.21)	[d] **0.0082**
Cough	-	161 (67.9)	43 (71.7)	118 (66.7)	[d] **<0.0001**
Hyperactive delirium	-	15 (6.3)	-	15 (8.5)	**-**
Dysgeusia	-	60 (25.3)	40 (66.7)	20 (11.3)	[d] **<0.0001**
Anosmia	-	67 (28.3)	41 (68.3)	26 (14.7)	[d] **<0.0001**
Laboratory findings, mean ± SD, (IQR)					
Erythrocytes $\times 10^9$/L	4.6 ± 0.6 (3.6–5.8)	4.4 ± 0.8 (2.0–5.9)	4.8 ± 0.4 (3.7–5.8)	4.2 ± 0.8 (2.0–5.9)	[a] **0.0078** [c,d] **<0.0001**
Hemoglobin (g/dL)	14.5 ± 1.6 (10.5–17.5)	13.1 ± 2.6 (6.6–18.2)	14.5 ± 1.3 (12.0–17.7)	12.4 ± 2.6 (6.6–18.2)	[a,c,d] **<0.0001**
Leukocytes $\times 10^9$/L	7.5 ± 1.8 (4.1–13.2)	9.0 ± 5.6 (1.6–33)	7.3 ± 2.1 (3.2–13.5)	10.2 ± 6.0 (1.6–33)	[c,d] **<0.0001** [a] **0.0088**
Neutrophils $\times 10^9$/L	4.2 ± 1.4 (2.4–9.8)	7.0 ± 5.0 (1.4–26.1)	4.1 ± 1.9 (1.6–11.0)	8.3 ± 5.0 (1.4–26.1)	[a,c,d] **<0.0001**
Lymphocytes $\times 10^9$/L	1.2 ± 0.7 (1.2–5.0)	1.3 ± 0.9 (0.1–4.2)	2.3 ± 0.6 (1.1–4.3)	1.0 ± 0.7 (0.1–4.1)	[a,c,d] **<0.0001**
RNL	1.8 ± 1.0 (0.9–6.3)	5.6 ± 6.4 (0.1–30.7)	1.7 ± 1.0 (0.5–7.9)	7.3 ± 6.4 (0.2–30.7)	[a,c,d] **<0.0001**
Monocytes $\times 10^9$/L	0.5 ± 0.2 (0.1–1.4)	0.5 ± 0.3 (0.1–1.9)	0.5 ± 0.1 (0.2–0.9)	0.5 ± 0.4 (0.1–1.9)	[a,b,c,d] >0.1
Platelets $\times 10^9$/L	214 ± 51.8 (129–370)	244 ± 98.1 (50–635)	227 ±66.3 (119–474)	245 ± 105.8 (50–635)	[a,b,d] >0.1 [c] 0.0775
Hospital support, No. (%)					

Infirmary	-	95 (40)	-	95 (53.7)	-
Intensive care unit (ICU)	-	82 (34.6)	-	82 (46.3)	-
Hospitalization data, No.					
Hospitalization days, mean (IQR)	-	9 (1–30)	-	9 (1–30)	-
Respiratory support upon assessment (%)					
Nasal-cannula oxygen	-	65 (27.4)	-	65 (36.7)	-
Oxygen masks/noninvasive	-	30 (12.6)	-	30 (16.9)	-
Invasive mechanical ventilation	-	70 (29.5)	-	70 (39.5)	-
Oxygen saturation mean ± SD (IQR)	99 ± 2.4 (89–99)	93 ± 8.7 (54–99)	98 ± 1.8 (92–99)	91 ± 8.9 (54–99)	[a, c,d] **<0.0001**
Medications No. (%)					
Glucocorticoid	-	156 (61.6)	10 (16.7)	146 (82.5)	[d] **<0.0001**
Azithromycin	-	149 (68.6)	18 (30.0)	127 (71.7)	[d] **<0.0001**
Ceftriaxone	-	84 (33.7)	04 (6.7)	80 (45.2)	[d] **<0.0001**
Oseltamivir	-	80 (30.4)	08 (13.3)	72 (40.7)	[d] **<0.0001**
Colchicine	-	05 (2.1)	-	05 (2.8)	-
Chloroquine/hydroxychloroquine	-	18 (7.6)	-	26 (14.7)	-
Anticoagulant	-	34 (14.3)	-	34 (19.2)	-
Ivermectin	-	11 (4.6)	11 (18.3)	-	-

[a]Comparisons between healthy controls and Covid-19 patients; [b] healthy controls versus non-hospitalized Covid-19 patients; [c] healthy controls versus hospitalized Covid-19 patients; [d] non-hospitalized versus hospitalized Covid-19 patients. Patient data were compared using the chi-square test, or Fisher's exact test for categorical variables and one-way analysis of variance (ANOVA). Mann–Whitney, nonparametric t-test was used for continuous variables. $p < 0.05$ was considered statistically significant. Abbreviations: standard deviation (SD); data are median (IQR), n (%), or n/N.

3.2. Significant Association between sTREM-1 Release and Disease Severity

We compared plasma levels of sTREM-1 in control patients and Covid-19, further determining their correlation with the severity of the illness. As shown in Figure 1A, the sTREM-1 levels were higher in patients with Covid-19, especially in hospitalized subjects, with the lowest levels in healthy controls, indicating that this mediator could be a consequence of the infection or be involved in the activation of the inflammatory response against SARS-CoV-2.
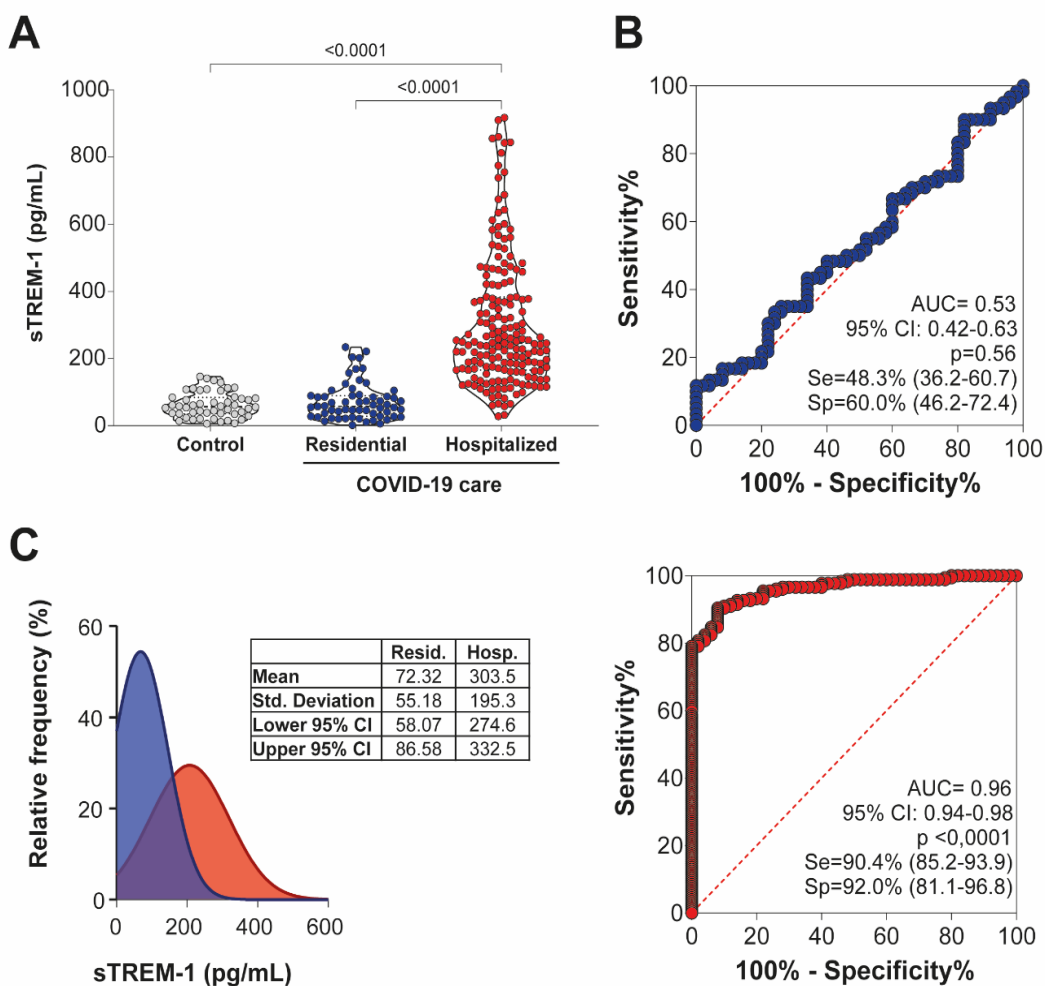
Figure 1. Elevated levels of sTREM-1 in patients with Covid-19. (**A**) The plasma concentration of sTREM-1 in Covid-19 patients under residential care ($n = 60$), hospital care ($n = 177$), or healthy controls ($n = 50$) were analyzed and compared. Data are presented as mean values plus ranges. The Kruskal–Wallis test was used to perform multiple comparisons when the data followed a non-normal distribution. The differences between the groups are indicated by the p-value in the graph above the diagram. (**B**) Receiver operating characteristic (ROC) curves of sTREM-1 concentrations to predict disease among patients with Covid-19 in residential care (blue) and hospital care (red). The area under the curve (AUC) and the p-values for significant differences between patients with Covid-19 and controls are depicted in the graphic. (C) Relative frequency of sTREM-1 between patients under residential care (blue) and hospital care (red) with Covid-19. Mean, standard deviation, lower 95% CI, and upper 95% CI data for each group are presented in the table between graphics.

227

The diagnostic value of sTREM-1 in patients with Covid-19 was evaluated by ROC curves. The AUC for sTREM-1 levels in patients under residential care, which represented mainly the mild form of the disease, was close to the value considered clinically relevant (AUC = 0.53). However, the AUC of sTREM-1 levels in patients under hospital care, who presented the severe form of Covid-19, was higher than the value considered to be clinically relevant (AUC = 0.96), thus distinguishing the disease severity among patients with Covid-19 (Figure 1B).

The plotted relative frequency of patients with sTREM-1 showed a high number of events for low levels of sTREM-1 among patients under residential care (mean = 72.32 pg/mL), and a greater number of events for high sTREM-1 levels among hospitalized patients (mean = 303.5 pg/mL), considering an intersection phase between residential and hospitalized care patients with Covid-19 (Figure 1C). These results demonstrated that sTREM-1 could be considered a potential predictive marker of the severity of Covid-19.

3.3. sTREM-1 Levels Increase with Clinical Disease Severity and Correlate with Comorbidities and the Production of Inflammatory Mediators in Patients with Covid-19

Next, we performed a subgroup analysis of sTREM-1, based on different severities of the disease in admission care. In this case, Sat O2, lymphocyte and neutrophil counts, BMI, hypertension, and IL-1β, IL-6, IL-8, IL-10, IL-12, and TNF production, were identified as independent risk factors or markers of adverse outcomes in patients with Covid-19 (Figure 2A—Heat map). However, when these parameters of inflammation or comorbidities were evaluated in the absence of sTREM-1 values, we were unable to specifically distinguish the subgroups of patients with Covid-19, but we observed a tendency to cluster between patients with critical and severe versus patients with mild and moderate Covid-19, using PCA (Figure 2B—PCA graphic).

252

253
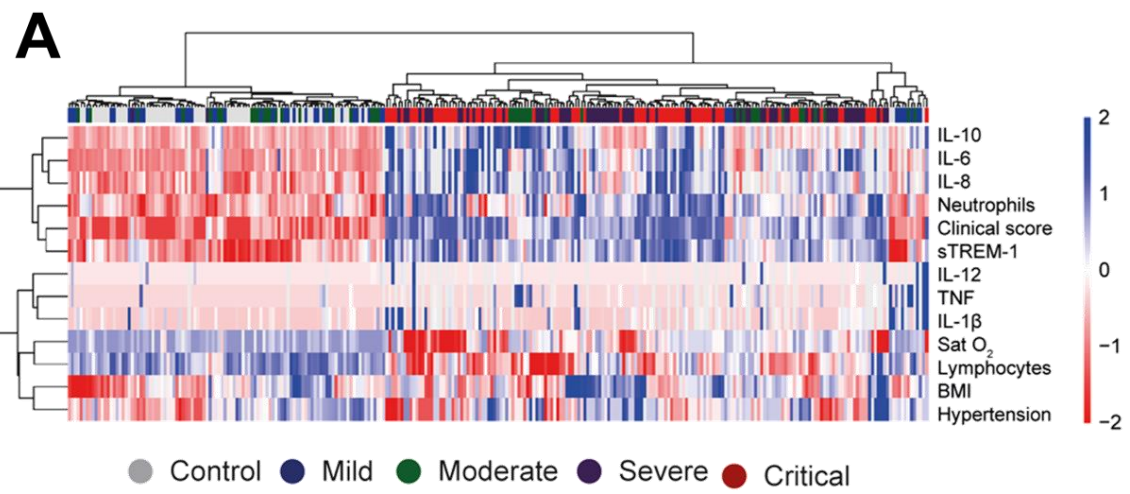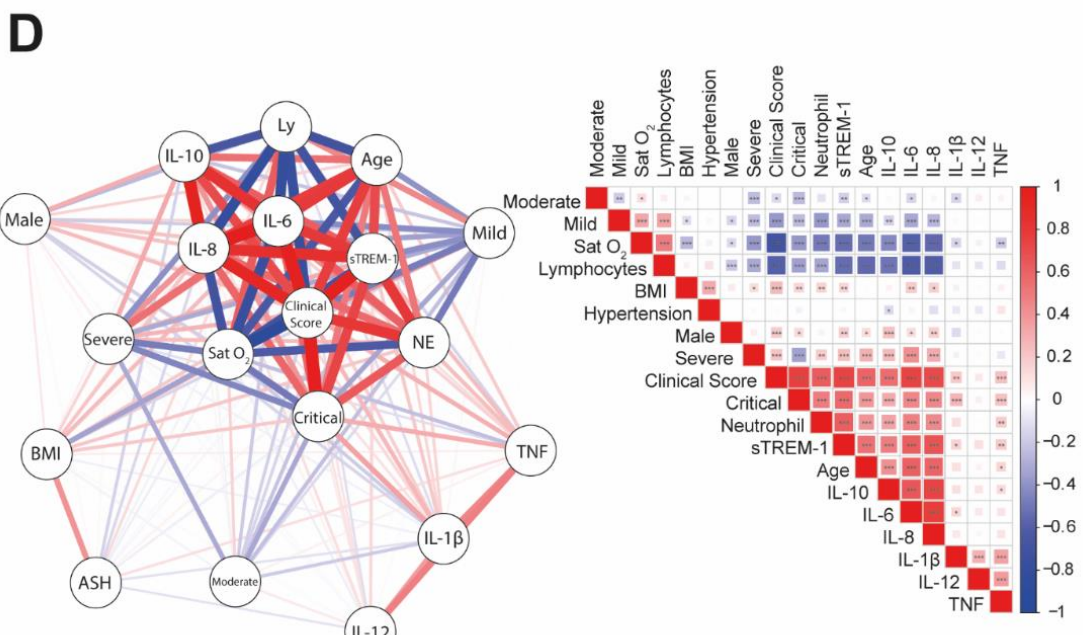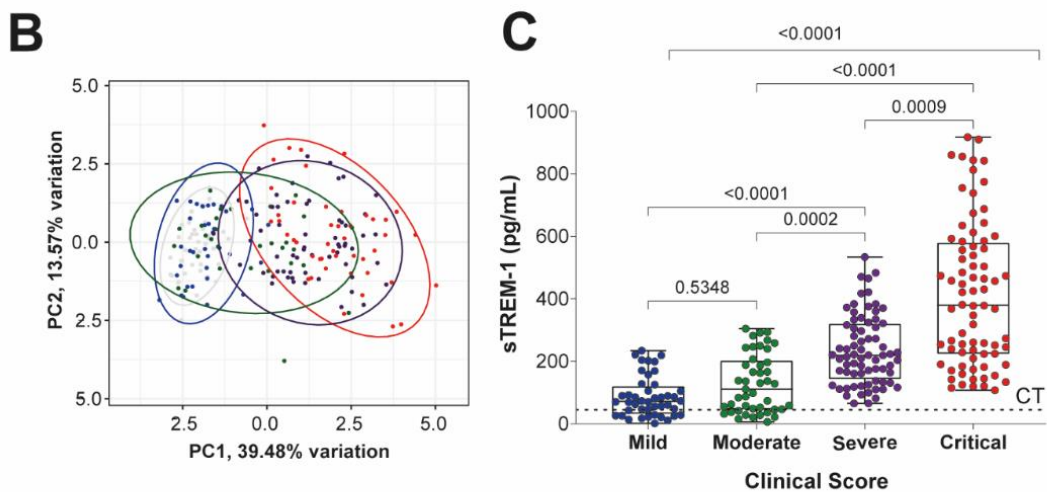
Figure 2. sTREM-1 levels were correlated with inflammatory cytokine production, comorbidities, and clinical severity of Covid-19 patients. (**A**) Unsupervised hierarchical cluster heat map showing the expression of markers and clinical parameters (Sat O_2, lymphocytes (Ly), neutrophil (NE) counts, BMI, hypertension (ASH), sTREM-1, IL-1β, IL-6, IL-8, IL-10, IL-12, and TNF levels) for different groups of patients, according to the disease score (control, mild, moderate, severe, and critical) data are colored by row normalized value for each sample. (**B**) The PCA graphic shows the clusterization of those subgroups of patients (95% confidence interval), including all markers exhibited in the heat map, except for the levels of sTREM-1, performed with the base R functions. The continuous variables were transformed to log2 scale, and in the case of the heat map and PCA, the data used were transformed to z-scores (centered and scaled). (**C**) Levels of sTREM-1 in patients with different severity forms of Covid-19: mild ($n = 44$), moderate ($n = 45$), severe ($n = 72$), and critical ($n = 76$), as well as control (CT line, $n = 50$). Median values are presented with ranges. The Kruskal–Wallis test was used for multiple comparisons in data with non-normal distribution. The differences between each group are indicated by the p-value in the graphic above the diagram. (**D**) The color scale sidebar indicates the correlation coefficients (r), where red represents positive correlation, and blue represents negative correlation. The square size and color intensity are proportional to the correlation coefficients, p values were represented by * <0.05, ** <0.01, and *** <0.001. A network-based on Spearman's correlation ($p < 0.05$) was constructed, analyzed, and graphically represented using the R packages.

As shown in Figure 2C, sTREM-1 levels in Covid-19 patients increased with higher-severity forms of Covid-19 and significantly segregated subgroups of patients, as well as compared to control values.

In Figure 2D, the correlation matrix for Spearman's test showed the significant positive association among sTREM-1 levels with severity and critical form of the disease, neutrophil count, BMI, age, sex male, and levels of IL-1β, IL-6, IL-8, and TNF. However, we also observed a significant negative association between sTREM-1 levels with the mild and moderate form of the disease, Sat O_2, and lymphocyte counts. A network based on these data was constructed, analyzed, and graphically represented (Figure 2D). The complete data on r and p-values of this correlation matrix are available in Table S2.

3.4. Multivariate Regression Analysis for the Prediction of Death and the Incidence Rate Ratio Value of sTREM-1 for the Expectation of Mortality Risk in Covid-19 Patients

To evaluate longitudinal changes, sTREM-1 levels in Covid-19 patients were monitored regularly during hospitalization. A cut-off value for a TREM-1 level of 188.93 pg/mL with the best-case classification rate of death (66.44%), with 0.90 (90%) of sensitivity (95% CI 0.79–0.95) and 0.60 (60%) of specificity (95% CI 0.41–0.63) was calculated (Figure 3A). To better see the overall changes in sTREM-1, plasma concentrations at admission (baseline level), and outcome (death or alive) were compared (Figure 3B).
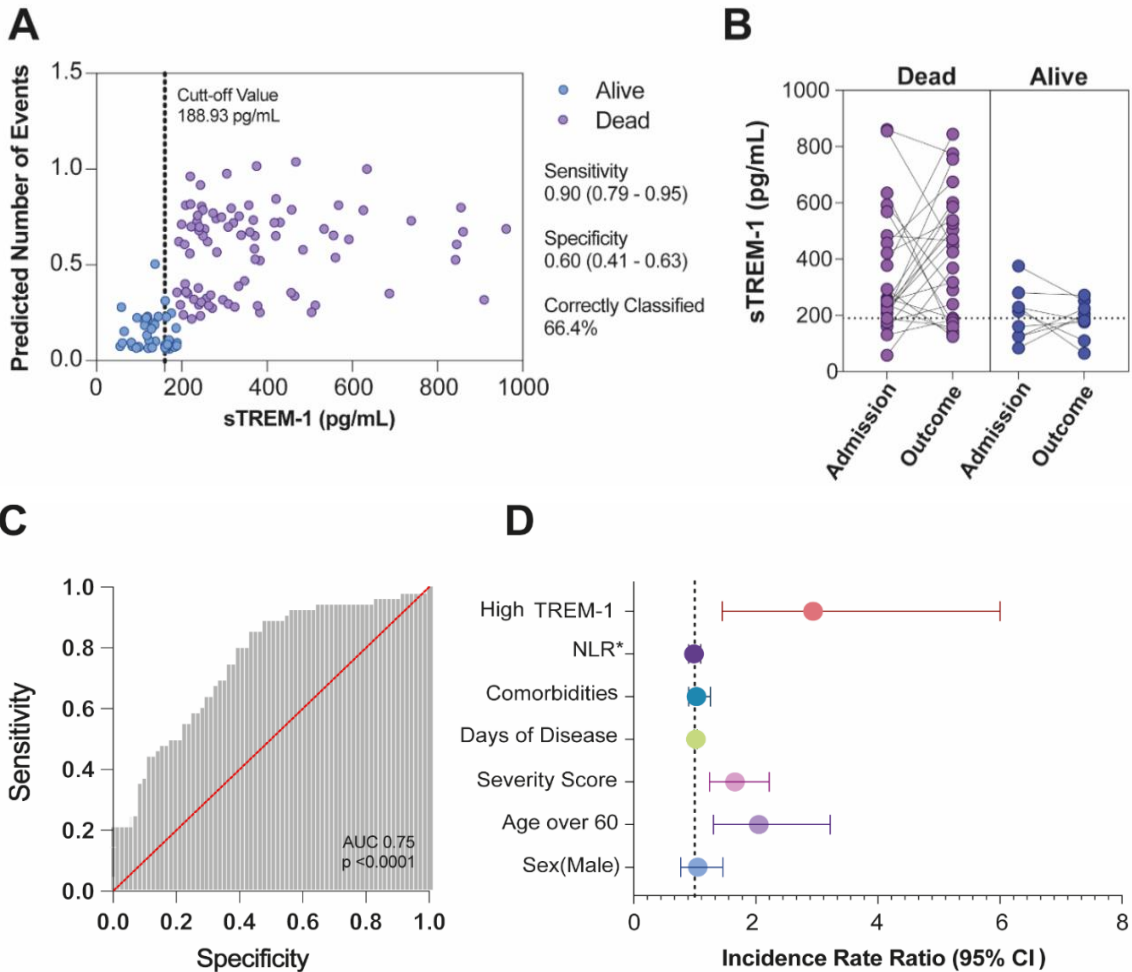
Figure 3. sTREM-1 levels in hospitalized patients with Covid-19 predicted mortality. (**A**) Adjusted predicted number of events for sTREM-1 levels. (**B**) Plasmatic levels of sTREM-1 of severe/critical patients were indicated for each individual on the day of hospital admission and after the outcome (dead or alive). The Mann–Whitney test was used for analyzing data with non-normal distribution, and differences between groups were established. (**C**) ROC and AUC assessing the discrimination capacity of sTREM-1 levels for mortality in hospitalized patients with Covid-19. (**D**) High levels of sTREM-1 and adjusted incidence rate ratio for the predictive variable of deaths.

The calculated area under the curve (AUC = 0.75, 95% CI 0.65–0.82, $p < 0.0001$) from ROC showed that plasma levels of sTREM-1 achieved good discrimination ability for death (Figure 3C). Additionally, the calculated positive likelihood ratio (LR+) was 1.81, and the negative likelihood ratio (LR–) was 0.21. The Poisson multivariate regression model was calculated by classifying patients with high or low serum TREM-1 levels according to the cut-off value (Table S3). High levels of sTREM-1 were the preeminent predictive variable of deaths (IRR 2.94, $p = 0.003$), even after adjusting the model for sex (IRR 1.05, $p = 0.290$), age over 60 years (IRR 2.05, $p = 0.002$), number of comorbidities (IRR 1.11, $p = 0.069$), severity score (IRR 1.65, $p = 0.001$), days of disease (IRR 1.01, $p = 0.174$), and the neutrophil/ lymphocyte ratio (NLR) (IRR 0.99, $p = 0.612$) (Figure 3D).

In Figure S2A, we demonstrated the various pharmacological therapies administered to the cohort of hospitalized Covid-19 patients. Although there are no approved treatments for Covid-19, antibiotics, antivirals, and anti-inflammatory drugs were generally administered to patients under hospital care in Brazil. A Venn diagram represented the combinatorial pharmacological approach for these patients. The changes in oxygen support levels from hospital admission to recovery or death are shown in Figure S2B, and the details of hospital support or supportive therapies for patients with Covid-19 are outlined in Table S4.

3.5. sTREM-1 Was Released from the Surface of Peripheral Blood Leukocytes and Was Correlated with MMP-8 Expression in the Covid-19 Patient

Next, we determined the expression of TREM-1 on the peripheral blood cell surface of patients with Covid-19 [mild ($n = 15$), moderate ($n = 15$), severe ($n = 15$), and critical ($n = 11$)] and healthy controls ($n = 10$). In Figure 4A, we observe the sequential gating of SSC-A versus FSC-A; SSC-A versus CD14 antibody staining patterns; leukocytes gated according to their side scatter; and SSC-A versus CD16 antibody staining patterns. The percentage of $CD14^+$ cells decreased in the blood of Covid-19 patients compared to the control. Furthermore, the percentages of $CD14^+TREM-1^+$ were lower in those Covid-19 patients. Conversely, the percentage of $CD14^-CD16^+$ cells was significantly increased by the Covid-19 severity. The frequency of $CD14^-CD16^+TREM-1^+$ also increased on blood cell surfaces from moderate to critical Covid-19 groups compared to control and mild disease. The amount of TREM-1 expression was obtained by quantification of MFI in both $CD14^+$ and $CD14^-CD16^+$ leukocytes. Interestingly, the total expression of TREM-1 decreased significantly according to the severity of the disease in the population of these cells. For example, these data indicated that the improved release of sTREM-1 matches the reduction in TREM-1 expression on the surface of the membrane of monocytes and polymorphonuclear leukocytes.
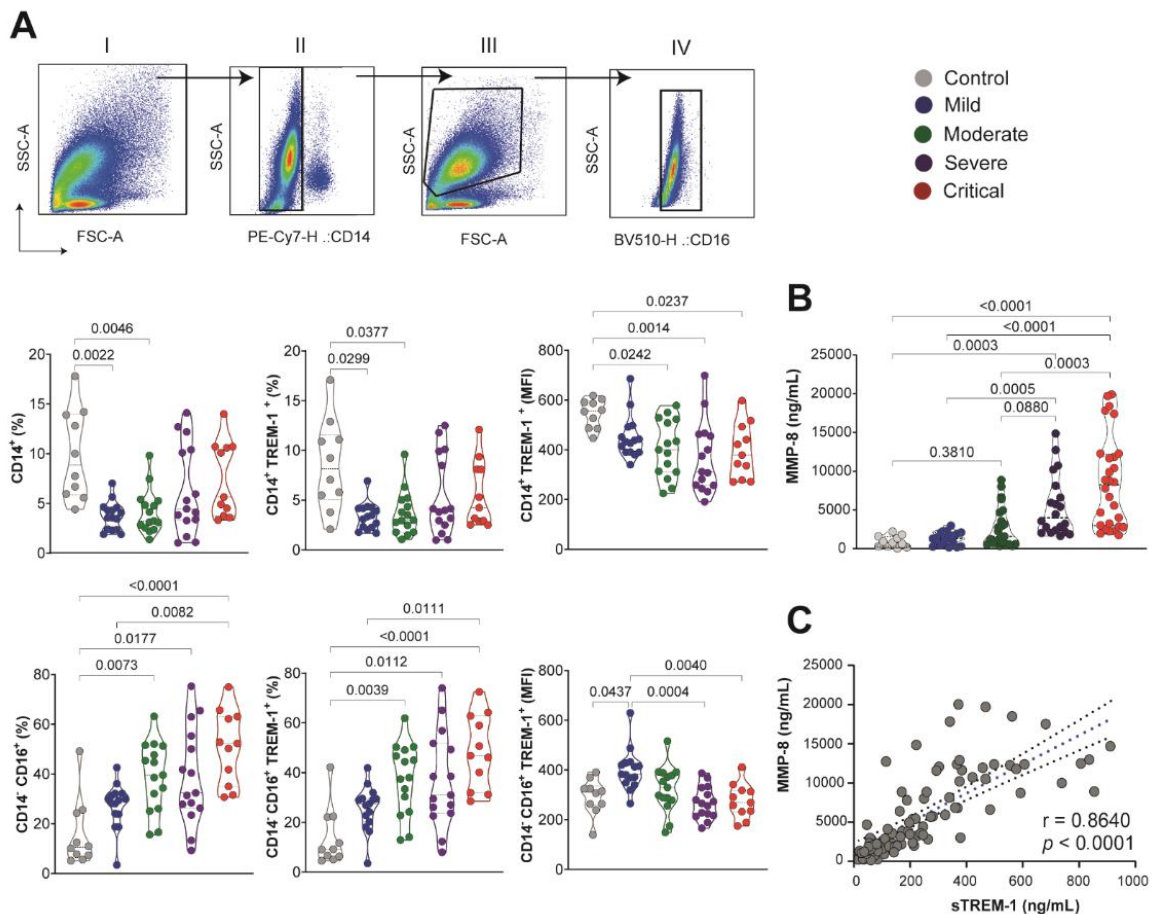
Figure 4. sTREM-1 was released from the surface of the peripheral blood leukocyte membrane, correlated with the expression of MMP-8. (**A**) Sequential gating is shown: (I) SSC-A versus FSC-A; (II) leukocytes gated according to their side scatter and CD14 antibody staining patterns; (III) light scatter flow cytometry profile for cells based on forward scatter (FSC-A) related to size, and side scatters (SSC-A) related to granularity; (IV) gated according to their side scatter and CD16 antibody staining patterns. The percentage of CD14$^+$ and CD14$^-$ CD16$^+$ cells was evaluated for groups of Covid-19 patients, as well as the percentage of CD14$^+$TREM-1$^+$ and CD14$^-$CD16$^+$TREM-1$^+$ in the cell surface. The amount of TREM-1 expression was obtained by quantification of MFI in CD14$^+$ and CD14$^-$CD16$^+$ leukocytes. (**B**) MMP-8 quantification in subgroups of Covid-19 patients. Median values are presented with ranges. The Kruskal–Wallis test was used for multiple comparisons in data with non-normal distribution. Differences between groups are indicated by the p-values in the graphics. (**C**) Spearman test correlation between MMP-8 and sTREM-1 levels. The correlation coefficients (r) and the p-value are indicated in the graphic.

The proteolytic cleavage of TREM-1 anchored to mature membranes could be influenced by metalloproteinase. The expression of MMP-8 in plasma from Covid-19 patients followed the same pattern of sTREM-1 levels with a significant increase in the moderate ($n = 23$), severe ($n = 20$), and critical ($n = 28$) Covid-19 groups, compared to controls ($n = 11$) and mild ($n = 19$) (Figure 4B). The correlation between MMP-8 and sTREM-1 by the Spearman rank test was highly significant ($r = 0.8640, p < 0.0001$; Figure 4C). However, the direct effect of MMP-8 on TREM-1 cleavage is difficult to confirm in

357　our human model. A detailed scheme of a proposed TREM-1 mechanism during Covid-19

358　is shown in Figure 5.
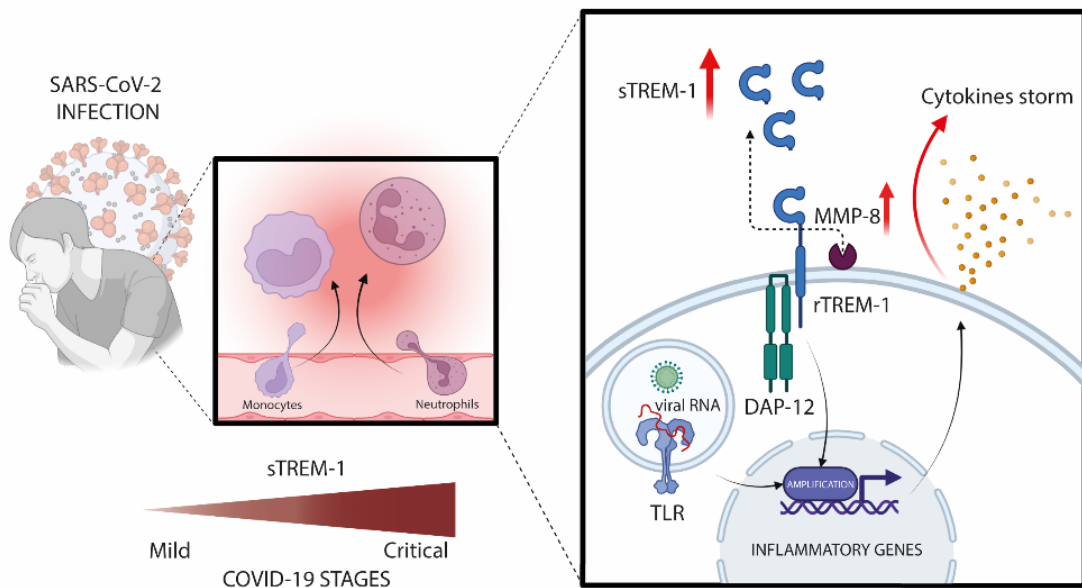
Figure 5. Schematic representation of the TREM-1/sTREM-1 pathway during the severity of Covid-19. SARS-CoV-2 activates innate immune receptors in infected cells and triggers the inflammatory transcription factor into the nucleus, where it induces several pro-inflammatory genes, including up-regulation of TREM-1. After binding to its ligand, TREM-1 associates with the adapter molecule DAP12, leading to a cascade of phosphorylation in a downstream kinase panel that, in turn, activates other transcription factors and amplifies the inflammatory response, as well as production of cytokines. It is speculated that high levels of circulating sTREM-1 were released from the surface of the peripheral blood leukocyte membrane related to MMP-8 activity. Therefore, individuals with high levels of sTREM-1 can indicate a dysregulated immune response (Created with BioRender.com, Agreement number: AZ238AM20F).

4. Discussion

To date, the most significant predictors of Covid-19 disease severity are related to the activation or suppression of host immune response [26,27]. This study reported that plasma sTREM-1 concentration might serve as a predictive factor or biomarker for disease severity and mortality in a population of patients with Covid-19 in Ribeirão Preto, São Paulo State, Brazil. The plasma levels of sTREM-1 gradually increased in patients with mild to moderate, severe, and critical forms of Covid-19. In fact, ROC analysis confirmed that sTREM-1 served as an important predictor of poor disease progression in patients with Covid-19.

TREM-1 amplifies the pro-inflammatory innate immune response, in synergy with Toll-like receptors, which recognize a wide range of bacterial, fungal, and viral components [28]. In addition to expression by neutrophils, monocytes, and macrophages, TREM-1 is also expressed by epithelial and endothelial cells [29]. Elevated sTREM-1

levels are indicative of acute and chronic conditions, including sepsis and pneumonia [30,31]. The enhanced inflammatory response in macrophages has been indicated as a mechanism by which TREM-1 signaling contributes to lung injury; therefore, inhibition of TREM-1 is a potential therapeutic strategy for neutrophil lung inflammation and ARDS [32]. Moreover, the levels in sepsis could reflect an essential immune dysfunction, where excessive cleavage of TREM-1 could contribute to immunosuppression and death during severe infection [33].

Since multiple microorganisms can cause severe infections, the broad prognostic value of sTREM-1 indicates its potential as a severity marker for all-cause febrile disease [34]. However, fever was not the most common sign among patients with Covid-19 in our cohort, especially in cases of mild and moderate disease. While the role of sTREM-1 in patients presenting severe Covid-19 remains unclear, a functional genomic analysis of PBMCs from individuals undergoing infection with enterovirus A71 (EV-A71) determined that activation of TREM-1 was correlated with clinical severity [35]. Interestingly, genetic variants within the gene encoding TREM-1 are associated with different levels of inflammation and with the development of sepsis [36] and severe malaria in which sTREM-1 levels were high [8].

The number of patients with Covid-19 has increased drastically worldwide, mainly due to the prevalence of more infective variants. In this context, the early identification of patients prone to developing severe Covid-19 is essential for the triage and subsequent interventions. Some modeling studies have shown that levels of IL-6 and CRP could be used as independent factors to predict the Covid-19 severity [37]. IL-6 is a multifunctional cytokine that exhibits a strong pro-inflammatory effect [38]. Other studies have suggested that predictive values of IL-10 and IL-6 should be preferentially evaluated for the early diagnosis of patients with severe forms of this disease [39]. IL-10 is highly abundant, especially during the adaptive immune response [40]. However, although certain studies have shown that plasma IL-6 and IL-10 could be used as factors to predict the progression of Covid-19, in our cohort, their values could not be used in isolation to distinguish between patient groups. IL-6 is also elevated in obesity [41] and cannot be specific for Covid-19 patient conditions. Patients with the severe form of Covid-19 also had increased leukocytosis, neutrophilia, lymphopenia, and thrombocytopenia compared to those with non-severe forms of this disease [42]. In this way, we observed a significant correlation

between plasma sTREM-1 and immunological parameters in patients with severe Covid-19.

We also inferred that sTREM-1 could be an independent discriminator of disease severity, in addition to predicting the poor outcome in patients with Covid-19. Therefore, significantly elevated plasma sTREM-1 levels in patients with Covid-19 might be indicative of an excessive inflammatory response and may contribute to severe illness or even death. Furthermore, other authors suggested that plasma sTREM-1 concentrations are related to Covid-19 severity and can discriminate between survivors and non-survivors, and sTREM-1 and IL-6 concentrations can be used as screening tools to decide treatment in patients with Covid-19 [20,21]. Generally, the most common therapeutic options for viral infections are directed at blocking viral replication or modulating immune responses. Dexamethasone exerts broad-spectrum anti-inflammatory effects. Among patients hospitalized with Covid-19, dexamethasone treatment resulted in lower mortality [43]. We evaluated the longitudinal sTREM-1 detection in patient admission and outcome under hospital care. Independent of dexamethasone treatment, sTREM-1 levels increased in most cases after admission and were correlated with the death outcome, but patients treated with dexamethasone, which was more common, tended to stabilize sTREM-1 production. However, this phenomenon did not correlate with better recovery. This represents a point of no return with anti-inflammatory treatment in Covid-19, and sTREM-1 levels could indicate the inflammatory state. Likely, the beneficial effect of glucocorticoids in patients with severe forms of Covid-19 can be dependent on the dosage and time.

In order for sTREM-1 to be a reliable marker of disease, a better understanding of the cells relevant to its release and mechanisms of shedding in Covid-19 are required. Another study reports a matrix metalloproteinase cleavage site within the TREM-1 sequence and demonstrates an in vivo correlation between MMP-9 expression, the appearance of sTREM-1 in airway lavage, and neutrophil recruitment during pulmonary influenza infection [44]. Additionally, it has been suggested that sTREM-1 is generated by cleavage of membrane-bound TREM-1 from the cell surface, and the infection model recruits many neutrophils that express this receptor.

In this case, a decrease in sTREM-1 could reflect a reduction in recruited neutrophils rather than a decrease in sTREM-1 release [16]. We observed that the reduction in the expression of TREM-1 on the cell surface in $CD14^+$ and $CD16^+$ leukocytes from the blood of Covid-19 patients was accompanied by a concomitant increase in plasma levels of

sTREM-1. Indeed, the plasma expression of MMP-8 correlated positively with sTREM-1 levels, specifically in the severe Covid-19 patient group. These findings strongly support the hypothesis that proteolytic cleavage of membrane-anchored TREM-1 by one or several MMP could be responsible for a sTREM-1 generation. CD14 is a lipopolysaccharide (LPS)-binding protein, which functions as an endotoxin receptor [45]. CD14 is strongly positive in monocytes and most tissue macrophages but is weakly expressed or negative in monoblasts, promonocytes, and other granulocytic precursors, but neutrophils and a small proportion of B-lymphocytes may weakly express CD14 [45]. In the blood of Covid-19 patients, we observed a greater association of surface expression of TREM-1 with $CD14^-$ $CD16^+$ than $CD14^+$ cells. In addition, neutrophils have been reported as an important source of sTREM-1 in infectious processes [46], and it has been reported that neutrophils produce several MMP after LPS challenge [47]. However, the role of neutrophils in the TREM-1 pathway during Covid-19 needs further study.

There are certain limitations to our work. First, in some cases, in addition to Covid-19, chronic diseases and secondary infection can contribute to increased plasma levels of sTREM-1; however, to our knowledge, there are no reliable studies relating sTREM-1 with obesity, hypertension, and diabetes, common comorbidities in participants in our study. Second, this study was limited by the sample size. Larger cohort studies are necessary to further confirm the prognostic effect in critically ill patients with Covid-19. Third, some patients with critical illnesses were not admitted to intensive care units, which had a negative impact on the outcomes of these patients.

5. Conclusions

Our results suggest that plasma sTREM-1 levels at hospital admission can be used satisfactorily for evaluating disease severity and predicting adverse outcomes in patients with Covid-19. We suggest the potential role of sTREM-1 in determining the clinical course of Covid-19 and their correlation with other pro-inflammatory parameters. Furthermore, we propose a mechanism for the release of sTREM-1 established by MMP-8 activity on the surface of blood leukocytes. In this way, sTREM-1 has emerged as a potential prognostic biomarker that can be easily detected in plasma samples of Covid-19 patients.

Supplementary Materials:

Supplementary Table 1. Characterization of participants according to signs and symptoms of Covid-19.

Participant's classification	Symptoms, signs, and parameters
Healthy Controls	- Negative for SARS-Cov-2 nucleic acid - No clinical signs
Mild	- Positive for SARS-Cov-2 nucleic acid and/or serological test - With or without the following symptoms: diarrhea, cough, fever, headache, loss of taste (ageusia) / smell (anosmia), myalgia, nausea, and vomiting - Oxygen saturation 94-99 % on room air
Moderate	- Positive for SARS-Cov-2 nucleic acid and/or serological test - Manifestation of mild disease symptoms including dyspnea - Oxygen saturation $\geq$ 93% on room air and PaO_2/FiO_2 250-300 mmHg - Do not need invasive ventilation: nasal catheter (oxygen 2-4 L/min) or oxygen reservoir (oxygen 4-12 L/min)
Severe	- Positive for SARS-Cov-2 nucleic acid and/or serological test - Possible Admission to intensive-care units - Severe respiratory distress - Oxygen saturation < 93 % on room air and $PaO_2/FiO_2 < 250$ mmHg - Need no-invasive ventilation: oxygen reservoir or non-rebreathing face mask (oxygen 10-15 L/min)
Critical	- Positive for SARS-Cov-2 nucleic acid and/or serological test - Admission to intensive-care units - Acute respiratory distress syndrome - Need invasive ventilation - $PaO_2/FiO_2 < 200$ mmHg - With or without one or more additional parameters: need hemodialysis, sepsis, septic shock, and multiorgan dysfunction

480   The participants were classified into five clinical groups, established by the symptoms severity,
481 clinical parameters, patient's management and laboratory findings, following the WHO
482 recommendations [1–8].

483

484   **References**

485   1. Ye, G.; Pan, Z.; Pan, Y.; Deng, Q.; Chen, L.; Li, J.; Li, Y.; Wang, X. Clinical Characteristics
486 of Severe Acute Respiratory Syndrome Coronavirus 2 Reactivation. Journal of Infection 2020, 80,
487 doi:10.1016/j.jinf.2020.03.001.

2. Xu, X.W.; Wu, X.X.; Jiang, X.G.; Xu, K.J.; Ying, L.J.; Ma, C.L.; Li, S.B.; Wang, H.Y.; Zhang, S.; Gao, H.N.; et al. Clinical Findings in a Group of Patients Infected with the 2019 Novel Coronavirus (SARS-Cov-2) Outside of Wuhan, China: Retrospective Case Series. The BMJ 2020, 368, doi:10.1136/bmj.m606.

3. Grasselli, G.; Zangrillo, A.; Zanella, A.; Antonelli, M.; Cabrini, L.; Castelli, A.; Cereda, D.; Coluccello, A.; Foti, G.; Fumagalli, R.; et al. Baseline Characteristics and Outcomes of 1591 Patients Infected with SARS-CoV-2 Admitted to ICUs of the Lombardy Region, Italy. JAMA - Journal of the American Medical Association 2020, 323, 1574–1581, doi:10.1001/jama.2020.5394.

4. Marshall, J.C.; Murthy, S.; Diaz, J.; Adhikari, N.; Angus, D.C.; Arabi, Y.M.; Baillie, K.; Bauer, M.; Berry, S.; Blackwood, B.; et al. A Minimal Common Outcome Measure Set for Covid-19 Clinical Research. The Lancet Infectious Diseases 2020, 20.

5. Office, W.H.O.E.M.R. Updated Clinical Management Guideline for Covid-19. Weekly Epidemiology Monitor 2020, 13.

6. Wei, P.-F. Diagnosis and Treatment Protocol for Novel Coronavirus Pneumonia (Trial Version 7). Chinese Medical Journal 2020, 133, 1087–1095, doi:10.1097/CM9.0000000000000819.

7. Wan, S.; Xiang, Y.; Fang, W.; Zheng, Y.; Li, B.; Hu, Y.; Lang, C.; Huang, D.; Sun, Q.; Xiong, Y.; et al. Clinical Features and Treatment of Covid-19 Patients in Northeast Chongqing. Journal of Medical Virology 2020, 92, 797–806, doi:10.1002/jmv.25783.

8. Hadjadj, J.; Yatim, N.; Barnabei, L.; Corneau, A.; Boussier, J.; Smith, N.; Péré, H.; Charbit, B.; Bondet, V.; Chenevier-Gobeaux, C.; et al. Impaired Type I Interferon Activity and Inflammatory Responses in Severe Covid-19 Patients. Science 2020, 369, doi:10.1126/science.abc6027.

Abbreviations: FiO$_2$ (fraction of inspired oxygen); PaO$_2$ (partial pressure of oxygen).

Supplementary Table 2. Information about r and *p*-values of the correlation matrix shown in Figure 2.

Comparison	Row	Column	Correlation	*P-value*
1	Mild	Moderate	-0.231155018	0.000332594
2	Sat O$_2$	Moderate	0.256343743	7.28466E-05
3	Lymphocyte	Moderate	0.152904628	0.018504855
4	BMI	Moderate	-0.077106244	0.239009016
5	Hypertension	Moderate	-0.004953154	0.940185148
6	Male	Moderate	-0.001387137	0.983052766
7	Severe	Moderate	-0.315407459	7.15624E-07
8	Clinical Score	Moderate	-0.361940265	9.56482E-09
9	Critical	Moderate	-0.328051133	2.37513E-07

10	Neutrophil	Moderate	-0.194937891	0.002577148
11	sTREM-1	Moderate	-0.305649126	1.62032E-06
12	Age	Moderate	-0.232030568	0.00031521
13	IL-10	Moderate	-0.099067545	0.171587141
14	IL-6	Moderate	-0.333358878	2.94361E-06
15	IL-8	Moderate	-0.205944097	0.005412874
16	IL-1B	Moderate	-0.202705785	0.004695755
17	IL-12	Moderate	0.047893541	0.508345685
18	TNF	Moderate	0.001018876	0.988779933
19	Sat O_2	Mild	0.493797962	8.69017E-16
20	Lymphocyte	Mild	0.473795411	1.15153E-14
21	BMI	Mild	-0.176923201	0.00654393
22	Hypertension	Mild	0.034172795	0.604566858
23	Male	Mild	-0.187577951	0.003752779
24	Severe	Mild	-0.319801075	4.90581E-07
25	Clinical Score	Mild	-0.684083102	4.7457E-34
26	Critical	Mild	-0.332620874	1.57451E-07
27	Neutrophil	Mild	-0.486848071	1.65221E-15
28	sTREM-1	Mild	-0.473164064	1.26229E-14
29	Age	Mild	-0.443947281	7.24186E-13
30	IL-10	Mild	-0.329159002	3.1354E-06
31	IL-6	Mild	-0.524005077	1.19155E-14
32	IL-8	Mild	-0.47734009	1.08997E-11
33	IL-1B	Mild	0.003209787	0.964663496
34	IL-12	Mild	-0.033696836	0.641772093
35	TNF	Mild	-0.028596493	0.693008796
36	Lymphocyte	Sat O_2	0.401200145	1.84023E-10
37	BMI	Sat O_2	-0.235201534	0.000301552
38	Hypertension	Sat O_2	-0.064325069	0.33249921
39	Male	Sat O_2	-0.101669422	0.120916986
40	Severe	Sat O_2	-0.306087002	1.82232E-06
41	Clinical Score	Sat O_2	-0.61107148	2.39767E-25
42	Critical	Sat O_2	-0.321999042	4.80411E-07
43	Neutrophil	Sat O_2	-0.423331473	1.36418E-11
44	sTREM-1	Sat O_2	-0.417465281	2.77006E-11
45	Age	Sat O_2	-0.387049158	8.81104E-10
46	IL-10	Sat O_2	-0.2948569	3.81076E-05
47	IL-6	Sat O_2	-0.477628124	6.21986E-12
48	IL-8	Sat O_2	-0.416622922	7.27459E-09
49	IL-1B	Sat O_2	-0.092911818	0.202305851
50	IL-12	Sat O_2	-0.008326473	0.909224231

51	TNF	Sat O$_2$	-0.120279514	0.098329914
52	BMI	Lymphocyte	0.105807313	0.105686046
53	Hypertension	Lymphocyte	0.102924798	0.117960673
54	Male	Lymphocyte	-0.195809682	0.002462766
55	Severe	Lymphocyte	-0.24467198	0.000141946
56	Clinical Score	Lymphocyte	-0.504559851	1.0349E-16
57	Critical	Lymphocyte	-0.284427783	8.67676E-06
58	Neutrophil	Lymphocyte	-0.244465784	0.000143855
59	sTREM-1	Lymphocyte	-0.450771695	2.91027E-13
60	Age	Lymphocyte	-0.510840741	3.72578E-17
61	IL-10	Lymphocyte	-0.4656599	1.00449E-11
62	IL-6	Lymphocyte	-0.570302316	1.30747E-17
63	IL-8	Lymphocyte	-0.55135014	8.75794E-16
64	IL-1B	Lymphocyte	-0.055937205	0.439722695
65	IL-12	Lymphocyte	-0.066996635	0.35458038
66	TNF	Lymphocyte	-0.069797294	0.334778798
67	Hypertension	BMI	0.337632848	1.54209E-07
68	Male	BMI	0.010023149	0.878527219
69	Severe	BMI	0.090491035	0.16677444
70	Clinical Score	BMI	0.199649214	0.002103156
71	Critical	BMI	0.121363246	0.063252208
72	Neutrophil	BMI	0.144400816	0.026867836
73	sTREM-1	BMI	0.080909355	0.216558849
74	Age	BMI	-0.111379628	0.088452531
75	IL-10	BMI	-0.064540076	0.375061815
76	IL-6	BMI	0.10571597	0.149870463
77	IL-8	BMI	0.079989279	0.285789589
78	IL-1B	BMI	-0.048881404	0.500756237
79	IL-12	BMI	-0.049949198	0.491436097
80	TNF	BMI	-0.003880337	0.957399957
81	Male	Hypertension	0.008049538	0.902941275
82	Severe	Hypertension	0.027496362	0.676949976
83	Clinical Score	Hypertension	-0.02087052	0.751844854
84	Critical	Hypertension	-0.052086696	0.429754465
85	Neutrophil	Hypertension	-0.039892941	0.545451521
86	sTREM-1	Hypertension	-0.024131327	0.714644644
87	Age	Hypertension	-0.048797374	0.459490751
88	IL-10	Hypertension	-0.176737196	0.015255029
89	IL-6	Hypertension	-0.076601215	0.301366345
90	IL-8	Hypertension	-0.155970027	0.037078899
91	IL-1B	Hypertension	-0.088646282	0.225133769

92	IL-12	Hypertension	-0.070127011	0.337623046
93	TNF	Hypertension	0.089498929	0.220686885
94	Severe	Male	0.036825251	0.572678206
95	Clinical Score	Male	0.191474889	0.003080732
96	Critical	Male	0.12249276	0.05971684
97	Neutrophil	Male	0.031451675	0.629982399
98	sTREM-1	Male	0.163859007	0.011525823
99	Age	Male	0.104158239	0.109738178
100	IL-10	Male	0.247127239	0.000548883
101	IL-6	Male	0.119514701	0.102335595
102	IL-8	Male	0.173228274	0.019697498
103	IL-1B	Male	-0.140872767	0.050688253
104	IL-12	Male	-0.051524688	0.476695911
105	TNF	Male	-0.075172413	0.29879757
106	Clinical Score	Severe	0.06320037	0.332653938
107	Critical	Severe	-0.453856055	1.9146E-13
108	Neutrophil	Severe	0.091391754	0.160779086
109	sTREM-1	Severe	0.109629133	0.092205835
110	Age	Severe	0.223739234	0.000519861
111	IL-10	Severe	0.133051116	0.065803523
112	IL-6	Severe	0.339610294	1.86137E-06
113	IL-8	Severe	0.18170797	0.014360805
114	IL-1B	Severe	-0.087249961	0.227607984
115	IL-12	Severe	-0.047658186	0.510434151
116	TNF	Severe	-0.166640725	0.020545856
117	Critical	Clinical Score	0.814088698	2.18852E-57
118	Neutrophil	Clinical Score	0.60170919	9.89693E-25
119	sTREM-1	Clinical Score	0.670648205	2.51929E-32
120	Age	Clinical Score	0.527521057	2.22592E-18
121	IL-10	Clinical Score	0.39350729	1.63783E-08
122	IL-6	Clinical Score	0.706591772	9.50877E-30
123	IL-8	Clinical Score	0.611328472	6.24207E-20
124	IL-1B	Clinical Score	0.193142907	0.007119883
125	IL-12	Clinical Score	0.028906508	0.689851391
126	TNF	Clinical Score	0.13516282	0.060909273
127	Neutrophil	Critical	0.48144692	3.72683E-15
128	sTREM-1	Critical	0.544209066	1.13204E-19
129	Age	Critical	0.345890241	4.59209E-08
130	IL-10	Critical	0.247996578	0.000523876
131	IL-6	Critical	0.435159773	4.35884E-10
132	IL-8	Critical	0.418124958	4.71667E-09

133	IL-1B	Critical	0.27583581	0.000103287
134	IL-12	Critical	0.036207063	0.617144789
135	TNF	Critical	0.200079903	0.005273927
136	sTREM-1	Neutrophil	0.594134952	5.25175E-24
137	Age	Neutrophil	0.337763026	9.83417E-08
138	IL-10	Neutrophil	0.251205264	0.000440416
139	IL-6	Neutrophil	0.409908655	5.16878E-09
140	IL-8	Neutrophil	0.374089043	2.1304E-07
141	IL-1B	Neutrophil	0.115544468	0.109569412
142	IL-12	Neutrophil	0.002980357	0.967187816
143	TNF	Neutrophil	0.159421183	0.026791288
144	Age	sTREM-1	0.488857505	1.21629E-15
145	IL-10	sTREM-1	0.347496792	7.87725E-07
146	IL-6	sTREM-1	0.565137436	2.94966E-17
147	IL-8	sTREM-1	0.579913342	1.18423E-17
148	IL-1B	sTREM-1	0.148895405	0.03877017
149	IL-12	sTREM-1	0.070661441	0.328814567
150	TNF	sTREM-1	0.107860689	0.13541786
151	IL-10	Age	0.362968733	2.28949E-07
152	IL-6	Age	0.560872117	5.71432E-17
153	IL-8	Age	0.537764866	5.89503E-15
154	IL-1B	Age	0.111105111	0.123984768
155	IL-12	Age	0.053394695	0.460824155
156	TNF	Age	0.083246073	0.249741408
157	IL-6	IL-10	0.595828669	1.88665E-19
158	IL-8	IL-10	0.691523071	4.45477E-27
159	IL-1B	IL-10	0.084361802	0.244669961
160	IL-12	IL-10	0.066528425	0.359225709
161	TNF	IL-10	0.029557013	0.684031098
162	IL-8	IL-6	0.75569478	2.30662E-34
163	IL-1B	IL-6	0.139639406	0.055973197
164	IL-12	IL-6	0.065061294	0.375043236
165	TNF	IL-6	0.002706864	0.9705909
166	IL-1B	IL-8	0.042398459	0.57090717
167	IL-12	IL-8	0.004694633	0.949987402
168	TNF	IL-8	-0.008794129	0.906467413
169	IL-12	IL-1B	0.268492309	0.000159788
170	TNF	IL-1B	0.328036453	3.20628E-06
171	TNF	IL-12	0.377835832	6.05668E-08

513

Supplementary Table 3. Multivariate Regression Model* for Death in the Study Population.

Variable	IRR** (95% Confidence Interval)	*p*-value
Sex (Male)	1.05 (0.75 – 1.47)	0.771
Age over 60 years	2.05 (1.31 – 3.22)	0.002
Days of Disease	1.01 (0.90 – 1.04)	0.174
Comorbidities	1.11 (0.90 – 1.24)	0.069
Severity Score	1.65 (1.23 – 2.22)	0.001
Neutrophils-Lymphocytes Ratio	0.99 (0.90 – 1.10)	0.612
High TREM-1	1.05 (0.75 – 1.47)	0.003

*Model *p*-value < 0.0001, Deviance Goodness-of-fit 65.35, *p* = 1.00, Pearson Goodness-of-fit 59.65, *p* = 1.00. **Incidence Rate Ratio

Supplementary Table 4. Hospital support, supportive therapies, and medications of patients moderate, severe, and critical infected with SARS-CoV-2.

During hospital stay	Moderate/Severe/critical N=33
Hospital support, No. (%)	
Infirmary	20 (60.6)
Intensive care unit (ICU)	13 (39.4)
Hospitalization data, No.	
Hospitalization days, median (IQR)	11 (3-30)
Number of days since symptom onset (IQR)	6 (3-11)
Respiratory support received (%)	
Nasal-cannula oxygen	13 (39.4)
Oxygen mask	11(33.3)
Invasive mechanical ventilation	9 (27.3)
Oxygen Saturation median (IQR)	89 (54-99)
Medications	
Glucocorticoid	31 (93.9)
Antibiotics	33 (100)
Oseltamivir	19 (57.6)
Chloroquine/Hydroxychloroquine	10 (30.3)
Anticoagulants	11 (33.3)
Death	24 (72.7)

Abbreviation: IQR, interquartile range, Data are median (IQR), n (%), or n/N.

522
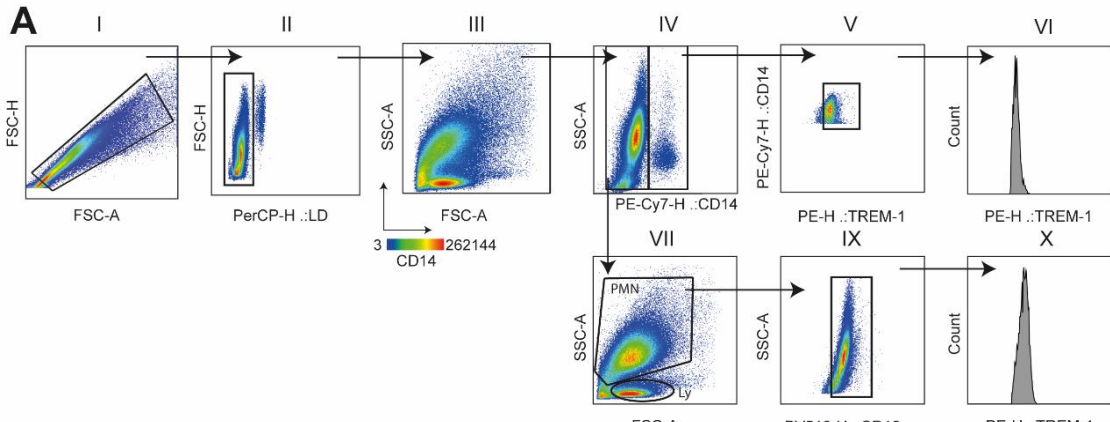
Supplementary Figure 1. Gating strategy used for flow cytometry analysis of peripheral blood leukocytes. Dot plots shown a representative gating strategy for the analysis of (I) singlet gating based FSC-H/FSC-A, (II) FSC-H/FVS-620 (viable cells), (III) SSC-A/FSC-A, followed by (IV) SSC-A/ leukocytes gated according to their side scatter and CD14 (PE-Cy7) antibody staining patterns, (V) CD14 (PE-Cy7) antibody staining patterns versus TREM-1 (PE) antibody staining patterns, with subsequent (VI) TREM-1 (PE) mean fluorescence intensity (MFI); (VII) light scatter flow cytometry profile for cells based on forward scatter (FSC-A) related to size, and side scatters (SSC-A) related to granularity; (IX) gated according to their side scatter and CD16 (BV510) antibody staining patterns, with subsequent (X) TREM-1 mean fluorescence intensity (MFI).

532
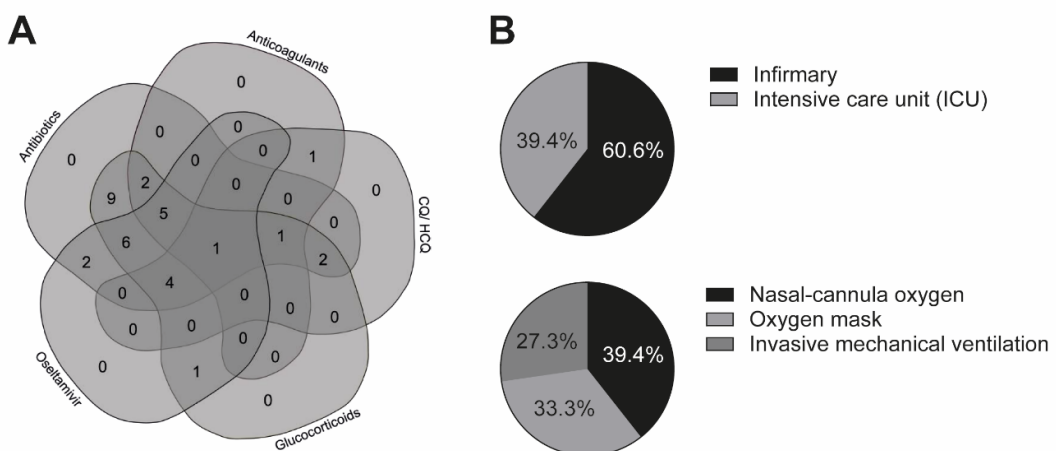
Supplementary Figure 2. Venn diagram of the pharmacological treatment of patients with Covid-19 and hospital/ respiratory support during hospitalization. (A) Venn diagram showed all pharmacological treatment relations between Glucocorticoid, Antibiotics, Oseltamivir, Chloroquine/Hydroxychloroquine and Anticoagulants of different sets of patients with Covid-19 in hospital care. (B) Demonstrative percentages of patients in distinctive hospitals and respiratory support during hospitalization.

Author Contributions: P.V.d.S.-N. and C.A.S., conceptualization of the study. C.A.S., C.R.B.C., E.M.S.R., A.P.M.F., and A.L.V. coordinated the collection of samples and participated with ethical approval. V.E.P., C.N.S.O., P.V.d.S.-N., M.M.P., D.M.T., N.T.N., J.C.S.d.C., I.C.-G., and J.G.M.A. applied the clinical questionnaire by telephone survey, selected patients and volunteers, and organized the database. C.A.S. supervised the

collection of home patients and healthy volunteers. P.V.d.S.-N., J.C.S.d.C., V.E.P., M.M.P., C.O.S.S., V.A.F.B., and D.M.T. performed the main experimental procedure. M.D.-B., C.R.B.C., A.M.D., O.F., and C.A.S. supervised the collection of samples from patients. P.V.D.S.-N., J.C.S.d.C., I.C.-G, J.G.M.A., T.M.F., L.F.C., F.M.O., and F.C.V. helped with sample collection. P.V.d.S.-N., V.E.P., T.F.C.F.-S., J.C.S.D.C., I.C.-G., D.M.T., , C.N.S.O., J.G.M.A., and L.C.R performed sample fractionation, processing, and storage. M.M.P., V.E.P., P.V.D.S.-N., M.D.-B., N.T.N., and D.M.T. collected clinical data, analyzed demographic data, classified participants, and classified patient clinical scores. P.V.d.S.-N., D.M.T., C.N.S.O., I.C.-G, T.F.C.F.-S., L.C.R., RFG, V.A.F.B., and C.R.B.C. performed the experimental cytokine/protein measurement. P.V.d.S.-N., C.O.S.S., T.F.C.F.-S., and C.R.B.C. performed flow cytometry assays. S.R.M. and C.A.F. analyzed the data using the R program. P.V.d.S.-N., D.M.T., M.M.P., V.E.P., A.L.B., and C.A.S. performed statistical analysis of the data and prepared the figures. L.F.C., A.M.D., F.M.O., M.R.F., R.S.P., F.C.V., G.G.G., J.J.R.d.R., and O.F. contributed to the collection of clinical specimens, demographics, helped clinical data management, and clinical characteristics analysis from Covid-19 patients. P.V.d.S.-N., D.M.T., and C.A.S. drafted the manuscript. F.G.F., V.L.D.B., C.R.B.C., R.F.G., and L.H.F. provided study materials, reagents, and other analytical tools and equipment. C.A.S., F.G.F., S.R.M, E.M.S.R., A.L.V., A.P.M.F., I.K.F.M.S., V.L.D.B., C.R.B.C., M.D.-B., A.M., R.T.S., and L.H.F., coordination and idealization of the project; critical revision of the manuscript for the important intellectual concept. L.H.F. and V.L.D.B. provided materials, equipment, and resources. C.A.S. and L.H.F. supervised the project. All authors helped edit the manuscript and agreed with the published version of the manuscript.

Institutional Review Board Statement: The study was conducted according to the guidelines of the Declaration of Helsinki and approved by the Institutional Review Board (or Ethics Committee) of *Faculdade de Ciências Farmacêuticas de Ribeirão Preto– Universidade de São Paulo* and Brazil National Ethics Committee (CONEP), number code: 2020/4.465.002, (CAAE: 30525920.7.0000.5403).

Informed Consent Statement: Informed consent was obtained from all subjects involved in the study.

Data Availability Statement: All data generated or analyzed during this study are included in this published article and its preprint manuscript form: https://doi.org/10.1101/2020.09.22.20199703

Conflicts of Interest: The authors declare no conflicts of interest.

Appendix A. IMUNOCOVID Study Group

Ana C. Xavier, Giovanna da S. Porcel, Isabelle C. Guarneri, Kamila Zaparoli, Caroline T. Garbato, Ângelo A.F. Júnior from Escola de Enfermagem de Ribeirão Preto–EERP-Universidade de São Paulo–USP, Ribeirão Preto, SP, Brazil. Alessandro P. de Amorim, Dayane P. da Silva, Debora C. Nepomuceno, Rafael C. da Silva from Hospital Santa Casa de Misericórdia de Ribeirão Preto, Ribeirão Preto, SP, Brazil. Rita de C.C. Barbieri from Hospital São Paulo, Ribeirão Preto, SP, Brazil. Cristiane M. Milanezi from Departamento de Bioquímica e Imunologia, Faculdade de Medicina de Ribeirão Preto–FMRP, Universidade de São Paulo–USP, Ribeirão Preto, SP, Brazil. Cassia F.S.L. Dias from

609   Departamento de Análises Clínicas, Toxicológicas e Bromatológicas, Faculdade de

610   Ciências Farmacêuticas de Ribeirão Preto–FCFRP, Universidade de São Paulo–USP,

611   Ribeirão Preto, SP, Brazil.

612   6 References

613   1.   Velavan, T.P.; Meyer, C.G. The Covid-19 Epidemic. *Trop. Med. Int. Health* **2020**,

614   *25*, 278–280.

615   2.   Xu, D.; Zhou, F.; Sun, W.; Chen, L.; Lan, L.; Li, H.; Xiao, F.; Li, Y.; Kolachalama,

616   V.B.; Li, Y.; et al. Relationship Between Serum SARS-CoV-2 Nucleic Acid(RNAemia)

617   and Organ Damage in Covid-19 Patients: A Cohort Study. *Clin. Infect. Dis.* **2020**, *73*, 68–

618   75.

619   3.   Becker, R.C. Covid-19 Update: Covid-19-Associated Coagulopathy. *J. Thromb.*

620   *Thrombolysis* **2020**, *50*, 54–67. https://doi.org/10.1007/s11239-020-02134-3.

621   4.   Lighter, J.; Phillips, M.; Hochman, S.; Sterling, S.; Johnson, D.; Francois, F.;

622   Stachel, A. Obesity in Patients Younger than 60 Years Is a Risk Factor for Covid-19

623   Hospital Admission. *Clin. Infect. Dis.* **2020**, *71*, 896–897.

624   5.   Henry, B.M.; de Oliveira, M.H.S.; Benoit, S.; Plebani, M.; Lippi, G. Hematologic,

625   Biochemical and Immune Biomarker Abnormalities Associated with Severe Illness and

626   Mortality in Coronavirus Disease 2019 (Covid-19): A Meta-Analysis. *Clin. Chem. Lab.*

627   *Med.* **2020**, *58*, 1021–1028.

628   6.   Guan, W.; Ni, Z.; Hu, Y.; Liang, W.; Ou, C.; He, J.; Liu, L.; Shan, H.; Lei, C.; Hui,

629   D.S.C.; et al. Clinical Characteristics of Coronavirus Disease 2019 in China. *N. Engl. J.*

630   *Med.* **2020**, *382*, 1708–1720. https://doi.org/10.1056/nejmoa2002032.

631   7.   Yao, Y.; Cao, J.; Wang, Q.; Shi, Q.; Liu, K.; Luo, Z.; Chen, X.; Chen, S.; Yu, K.;

632   Huang, Z.; et al. D-Dimer as a Biomarker for Disease Severity and Mortality in Covid-19

633   Patients: A Case Control Study. *J. Intensive Care* **2020**, *8*, 1–11.

634   https://doi.org/10.1186/s40560-020-00466-z.

635   8.   Adukpo, S.; Gyan, B.A.; Ofori, M.F.; Dodoo, D.; Velavan, T.P.; Meyer, C.G.

636   Triggering Receptor Expressed on Myeloid Cells 1 (TREM-1) and Cytokine Gene Variants

637   in Complicated and Uncomplicated Malaria. *Trop. Med. Int. Health* **2016**, *21*, 1592–1601.

638   https://doi.org/10.1111/tmi.12787.

639   9.   Hommes, T.J.; Dessing, M.C.; Van't Veer, C.; Florquin, S.; Colonna, M.; de Vos,

640   A.F.; van der Poll, T. Role of Triggering Receptor Expressed on Myeloid Cells-1/3 in

Klebsiella-Derived Pneumosepsis. *Am. J. Respir. Cell Mol. Biol.* **2015**, *53*, 647–655. https://doi.org/10.1165/rcmb.2014-0485OC.

10.   de Oliveira Matos, A.; dos Santos Dantas, P.H.; Figueira Marques Silva-Sales, M.; Sales-Campos, H. The Role of the Triggering Receptor Expressed on Myeloid Cells-1 (TREM-1) in Non-Bacterial Infections. *Crit. Rev. Microbiol.* **2020**, *46*, 237–252.

11.   Dantas, P.H. dos S.; Matos, A. de O.; da Silva Filho, E.; Silva-Sales, M.; Sales-Campos, H. Triggering Receptor Expressed on Myeloid Cells-1 (TREM-1) as a Therapeutic Target in Infectious and Noninfectious Disease: A Critical Review. *Int. Rev. Immunol.* **2020**, *39*, 188–202.

12.   Weber, B.; Schuster, S.; Zysset, D.; Rihs, S.; Dickgreber, N.; Schürch, C.; Riether, C.; Siegrist, M.; Schneider, C.; Pawelski, H.; et al. TREM-1 Deficiency Can Attenuate Disease Severity without Affecting Pathogen Clearance. *PLoS Pathog.* **2014**, *10*, e1003900. https://doi.org/10.1371/journal.ppat.1003900.

13.   Yuan, Z.; Fan, X.; Staitieh, B.; Bedi, C.; Spearman, P.; Guidot, D.M.; Sadikot, R.T. HIV-Related Proteins Prolong Macrophage Survival through Induction of Triggering Receptor Expressed on Myeloid Cells-1. *Sci. Rep.* **2017**, *7*, 42028. https://doi.org/10.1038/srep42028.

14.   Tammaro, A.; Derive, M.; Gibot, S.; Leemans, J.C.; Florquin, S.; Dessing, M.C. TREM-1 and Its Potential Ligands in Non-Infectious Diseases: From Biology to Clinical Perspectives. *Pharmacol. Ther.* **2017**, *177*, 81–95.

15.   Cao, C.; Gu, J.; Zhang, J. Soluble Triggering Receptor Expressed on Myeloid Cell-1 (STREM-1): A Potential Biomarker for the Diagnosis of Infectious Diseases. *Front. Med.* **2017**, *11*, 169–177.

16.   Gómez-Piña, V.; Soares-Schanoski, A.; Rodríguez-Rojas, A.; del Fresno, C.; García, F.; Vallejo-Cremades, M.T.; Fernández-Ruiz, I.; Arnalich, F.; Fuentes-Prior, P.; López-Collazo, E. Metalloproteinases Shed TREM-1 Ectodomain from Lipopolysaccharide-Stimulated Human Monocytes. *J. Immunol.* **2007**, *179*, 4065–4073. https://doi.org/10.4049/jimmunol.179.6.4065.

17.   Jedynak, M.; Siemiatkowski, A.; Mroczko, B.; Groblewska, M.; Milewski, R.; Szmitkowski, M. Soluble TREM-1 Serum Level Can Early Predict Mortality of Patients with Sepsis, Severe Sepsis and Septic Shock. *Arch. Immunol. Et Ther. Exp.* **2018**, *66*, 299–306. https://doi.org/10.1007/s00005-017-0499-x.

18.   Huang, C.T.; Lee, L.N.; Ho, C.C.; Shu, C.C.; Ruan, S.Y.; Tsai, Y.J.; Wang, J.Y.; Yu, C.J. High Serum Levels of Procalcitonin and Soluble TREM-1 Correlated with Poor Prognosis in Pulmonary Tuberculosis. *J. Infect.* **2014**, *68*, 440–447. https://doi.org/10.1016/j.jinf.2013.12.012.

19.   Silva-Neto, P. v; S de Carvalho, J.C.; Pimentel, V.E.; Pérez, M.M.; Carmona-Garcia, I.; Neto, N.T.; S Oliveira, C.N.; C Fraga-Silva, T.F.; Milanezi, C.M.; Rodrigues, L.C.; et al. Prognostic Value of STREM-1 in Covid-19 Patients: A Biomarker for Disease Severity and Mortality. *Medrxiv* **2020**, 1, 1-28. https://doi.org/10.1101/2020.09.22.20199703.

20.   Van-Singer, M.; Brahier, T.; Ngai, M.; Wright, J.; Weckman, A.M.; Erice, C.; Meuwly, J.Y.; Hugli, O.; Kain, K.C.; Boillat-Blanco, N. Covid-19 Risk Stratification Algorithms Based on STREM-1 and IL-6 in Emergency Department. *J. Allergy Clin. Immunol.* **2021**, *147*, 99–106.e4. https://doi.org/10.1016/j.jaci.2020.10.001.

21.   Nooijer, A.H.; Grondman, I.; Lambden, S.; Kooistra, E.J.; Janssen, N.A.F.; Kox, M.; Pickkers, P.; Joosten, L.A.B.; van de Veerdonk, F.L.; Derive, M.; et al. Increased STREM-1 Plasma Concentrations Are Associated with Poor Clinical Outcomes in Patients with Covid-19. *Biosci. Rep.* **2021**, *41*, 41. https://doi.org/10.1042/BSR20210940.

22.   Wei, P.-F. Diagnosis and Treatment Protocol for Novel Coronavirus Pneumonia (Trial Version 7). *Chin. Med. J.* **2020**, *133*, 1087–1095. https://doi.org/10.1097/CM9.0000000000000819.

23.   Wan, S.; Xiang, Y.; Fang, W.; Zheng, Y.; Li, B.; Hu, Y.; Lang, C.; Huang, D.; Sun, Q.; Xiong, Y.; et al. Clinical Features and Treatment of Covid-19 Patients in Northeast Chongqing. *J. Med. Virol.* **2020**, *92*, 797–806. https://doi.org/10.1002/jmv.25783.

24.   Epskamp, S.; Cramer, A.O.J.; Waldorp, L.J.; Schmittmann, V.D.; Borsboom, D. Qgraph: Network Visualizations of Relationships in Psychometric Data. *J. Stat. Softw.* **2012**, *48*, 1–18.

25.   Blighe, K.; Lun, A. PCAtools: Everything Principal Components Analysis. 2021. Available   online: https://bioconductor.org/packages/release/bioc/vignettes/PCAtools/inst/doc/PCAtools.html (accessed on 26 November 2021).

26.   Yang, P.; Ding, Y.; Xu, Z. ; Pu, R. ; Li, P. ; Yan, J. ; Liu, J. ; Meng, F. ; Huang, L. ; Shi, L. ; et al. Epidemiological and Clinical Features of Covid-19 Patients with and without

705   Pneumonia in Beijing, China. *Medrxiv* **2020**, 1, 1-31.
706   https://doi.org/10.1101/2020.02.28.20028068.

707   27.   Zumla, A.; Hui, D.S.; Azhar, E.I.; Memish, Z.A.; Maeurer, M. Reducing Mortality
708   from 2019-NCoV: Host-Directed Therapies Should Be an Option. *Lancet* **2020**, *395*, e35–
709   e36.

710   28.   Zheng, H.; Heiderscheidt, C.A.; Joo, M.; Gao, X.; Knezevic, N.; Mehta, D.;
711   Sadikot, R.T. MYD88-Dependent and -Independent Activation of TREM-1 via Specific
712   TLR Ligands. *Eur. J. Immunol.* **2010**, *40*, 162–171. https://doi.org/10.1002/eji.200839156.

713   29.   Chen, L.C.; Laskin, J.D.; Gordon, M.K.; Laskin, D.L. Regulation of TREM
714   Expression in Hepatic Macrophages and Endothelial Cells during Acute Endotoxemia.
715   *Exp. Mol. Pathol.* **2008**, *84*, 145–155. https://doi.org/10.1016/j.yexmp.2007.11.004.

716   30.   Dimopoulou, I.; Pelekanou, A.; Mavrou, I.; Savva, A.; Tzanela, M.; Kotsaki, A.;
717   Kardara, M.; Orfanos, S.E.; Kotanidou, A.; Giamarellos-Bourboulis, E.J. Early Serum
718   Levels of Soluble Triggering Receptor Expressed on Myeloid Cells-1 in Septic Patients:
719   Correlation with Monocyte Gene Expression. *J. Crit. Care* **2012**, *27*, 294–300.
720   https://doi.org/10.1016/j.jcrc.2011.06.013.

721   31.   Gibot, S.; Levy, B.; Bene, M.-C.; Faure, G.; Bollaert, P.-E. Soluble Triggering
722   Receptor Expressed on Myeloid Cells and the Diagnosis of Pneumonia. *N. Engl. J. Med.*
723   **2004**, *350*, 451–458.

724   32.   Yuan, Z.; Syed, M.; Panchal, D.; Joo, M.; Bedi, C.; Lim, S.; Onyuksel, H.;
725   Rubinstein, I.; Colonna, M.; Sadikot, R.T. TREM-1-Accentuated Lung Injury via MiR-155
726   Is Inhibited by LP17 Nanomedicine. *Am. J. Physiol. Lung Cell Mol. Physiol.* **2016**, *310*,
727   426–438. https://doi.org/10.1152/ajplung.00195.2015.-Trig.

728   33.   Hotchkiss, R.S.; Monneret, G.; Payen, D. Immunosuppression in Sepsis: A Novel
729   Understanding of the Disorder and a New Therapeutic Approach. *Lancet Infect. Dis.* **2013**,
730   *13*, 260–268.

731   34.   Richard-Greenblatt, M.; Boillat-Blanco, N.; Zhong, K.; Mbarack, Z.; Samaka, J.;
732   Mlaganile, T.; Kazimoto, T.; D'Acremont, V.; Kain, K.C. Prognostic Accuracy of Soluble
733   Triggering Receptor Expressed on Myeloid Cells (STREM-1)-Based Algorithms in Febrile
734   Adults Presenting to Tanzanian Outpatient Clinics. *Clin. Infect. Dis.* **2020**, *70*, 1304–1312.
735   https://doi.org/10.1093/cid/ciz419.

736   35.   Amrun, S.N.; Tan, J.J.L.; Rickett, N.Y.; Cox, J.A.; Lee, B.; Griffiths, M.J.;
737   Solomon, T.; Perera, D.; Ooi, M.H.; Hiscox, J.A.; et al. TREM-1 Activation Is a Potential

Key Regulator in Driving Severe Pathogenesis of Enterovirus A71 Infection. *Sci. Rep.* **2020**, *10*, 3810–3813. https://doi.org/10.1038/s41598-020-60761-5.

36. Aldasoro Arguinano, A.A.; Dadé, S.; Stathopoulou, M.; Derive, M.; Coumba Ndiaye, N.; Xie, T.; Masson, C.; Gibot, S.; Visvikis-Siest, S. TREM-1 SNP Rs2234246 Regulates TREM-1 Protein and MRNA Levels and Is Associated with Plasma Levels of L-Selectin. *PLoS ONE* **2017**, *12*, e0182226. https://doi.org/10.1371/journal.pone.0182226.

37. Liu, F.; Li, L.; Xu, M. da; Wu, J.; Luo, D.; Zhu, Y.S.; Li, B.X.; Song, X.Y.; Zhou, X. Prognostic Value of Interleukin-6, C-Reactive Protein, and Procalcitonin in Patients with Covid-19. *J. Clin. Virol.* **2020**, *127*, 104370. https://doi.org/10.1016/j.jcv.2020.104370.

38. Taniguchi, K.; Karin, M. IL-6 and Related Cytokines as the Critical Lynchpins between Inflammation and Cancer. *Semin. Immunol.* **2014**, *26*, 54–74.

39. Han, H.; Ma, Q.; Li, C.; Liu, R.; Zhao, L.; Wang, W.; Zhang, P.; Liu, X.; Gao, G.; Liu, F.; et al. Profiling Serum Cytokines in Covid-19 Patients Reveals IL-6 and IL-10 Are Disease Severity Predictors. *Emerg. Microbes Infect.* **2020**, *9*, 1123–1130. https://doi.org/10.1080/22221751.2020.1770129.

40. McKinstry, K.K.; Strutt, T.M.; Buck, A.; Curtis, J.D.; Dibble, J.P.; Huston, G.; Tighe, M.; Hamada, H.; Sell, S.; Dutton, R.W.; et al. IL-10 Deficiency Unleashes an Influenza-Specific Th17 Response and Enhances Survival against High-Dose Challenge. *J. Immunol.* **2009**, *182*, 7353–7363. https://doi.org/10.4049/jimmunol.0900657.

41. Kang, Z.; Luo, S.; Gui, Y.; Zhou, H.; Zhang, Z.; Tian, C.; Zhou, Q.; Wang, Q.; Hu, Y.; Fan, H.; et al. Obesity Is a Potential Risk Factor Contributing to Clinical Manifestations of Covid-19. *Int. J. Obes.* **2020**, *44*, 2479–2485. https://doi.org/10.1038/s41366-020-00677-2.

42. Vardhana, S.A.; Wolchok, J.D. The Many Faces of the Anti-COVID Immune Response. *J. Exp. Med.* **2020**, *217*, e20200678.

43. Horby, P.; Lim, W.S.; Emberson, J.R.; Mafham, M.; Bell, J.L.; Linsell, L.; Sta-plin, N.; Brightling, C.; Ustianowski, A.; Elmahi, E.; et al. Dexamethasone in Hospitalized Patients with Covid-19. *N. Engl. J. Med.* **2021**, *384*, 693–704. https://doi.org/10.1056/NEJMoa2021436.

44. Weiss, G.; Lai, C.; Fife, M.E.; Grabiec, A.M.; Tildy, B.; Snelgrove, R.J.; Xin, G.; Lloyd, C.M.; Hussell, T. Reversal of TREM-1 Ectodomain Shedding and Improved

770 Bacterial Clearance by Intranasal Metalloproteinase Inhibitors. *Mucosal. Immunol.* **2017**,

771 *10*, 1021–1030. https://doi.org/10.1038/mi.2016.104.

772 45.   Heinzelmann, M.; Mercer-Jones, M.; Cheadle, W.G.; Polk, H.C. CD14 Expression

773 in Injured Patients Correlates with Outcome. *Ann. Surg.* **1996**, *224*, 91–96.

774 46.   Klesney-Tait, J.; Turnbull, I.R.; Colonna, M. The TREM Receptor Family and

775 Signal Integration. *Nat. Immunol.* **2006**, *7*, 1266–1273.

776 47.   Shimizu, T.; Kanai, K.-I.; Kyo, Y.; Suzaki, H.; Asano, K.; Hisamitsu, T. Effect of

777 Tranilast on Matrix Metalloproteinase Production from Neutrophils In-Vitro. *J. Pharm.*

778 *Pharmacol.* **2010**, *58*, 91–99. https://doi.org/10.1211/jpp.58.1.0011.

6.2 <u>Capítulo II</u>: *Matrix Metalloproteinases on Severe Covid-19 Lung Pathogenesis: Cooperative Actions of MMP-8/MMP-2 Axis on Immune Response Through HLA-G Shedding and Oxidative Stress*

Pedro V. da Silva-Neto[1,2&], Valéria B. do Valle[3&], Carlos A. Fuzo[1&], Talita M. Fernandes [4&], Diana M. Toro[1,2&], Thais F. C. Fraga-Silva[5], Patrícia A. Basile[3], Jonatan C. S. de Carvalho[1,6], Vinícius E. Pimentel[1,5], Malena M. Pérez[1], Camilla N. S. Oliveira[1,5], Lilian C. Rodrigues[1], Victor A. F. Bastos[1], Sandra O. C. Tella[7], Ronaldo B. Martins[8], Augusto M. Degiovani[9], Fátima M. Ostini[9], Marley R. Feitosa[10], Rogerio S. Parra[10], Fernando C. Vilar[11], Gilberto G. Gaspar[11], José J. R. da Rocha[10], Omar Feres[10], Eurico Arruda[8], Sandra R. Maruyama[12], Elisa M. S. Russo[1], Angelina L. Viana[4], Isabel K. F. M. Santos[5], Vânia L. D. Bonato[5], Cristina R. B. Cardoso[1], Jose E. Tanus-Santos[7], Eduardo A. Donadi[11], Lúcia H. Faccioli[1], Marcelo Dias-Baruffi[1#], Ana P. M. Fernandes[4#], Raquel F. Gerlach[3#*] and Carlos A. Sorgi[2,5,6#*] on behalf of the IMUNOCOVID study group.

1-Departamento de Análises Clínicas, Toxicológicas e Bromatológicas, Faculdade de CiênciasFarmacêuticas de Ribeirão Preto-FCFRP, Universidade de São Paulo-USP, Ribeirão Preto 14040-903, SP, Brazil; 2-Programa de Pós-Graduação em Imunologia Básica e Aplicada-PPGIBA, Instituto de Ciências Biológicas, Universidade Federal do Amazonas-UFAM, Manaus 69080-900, AM, Brazil. 3-Departamento de Biologia Básica e Oral, Faculdade de Odontologia de Ribeirão Preto, Universidade de São Paulo-USP, Ribeirão Preto 14040-904, SP, Brazil. 4-Departamento de Enfermagem Geral e Especializada, Escola de Enfermagem de Ribeirão Preto-EERP, Universidade de São Paulo-USP, Ribeirão Preto 14040-902, SP, Brazil; 5-Departamento de Bioquímica e Imunologia, Faculdade de Medicina de Ribeirão Preto-FMRP, Universidade de São Paulo-USP, Ribeirão Preto 14040-900 , SP, Brazil; 6-Departamento de Química, Faculdade de Filosofia, Ciências e Letras de Ribeirão Preto-FFCLRP, Universidade de São Paulo-USP, Ribeirão Preto 14040-901, SP, Brazil; 7-Departamento de Farmacologia, Faculdade de Medicina de Ribeirão Preto-FMRP, Universidade de São Paulo-USP, Ribeirão Preto 14049-900, SP, Brazil; 8-Departamento de Biologia Celular e Molecular e Bioagentes Patogênicos, Faculdade de Medicina de Ribeirão Preto-FMRP, Universidade de São Paulo-USP, Ribeirão Preto 14049-900, SP, Brazil; 9-Hospital Santa Casa de Misericórdia de Ribeirão Preto, Ribeirão Preto 14085-000, SP, Brazil; 10-Departamento de Cirurgia e Anatomia, Faculdade de Medicina de Ribeirão Preto-FMRP, Universidade de São Paulo-USP, Ribeirão Preto 14048-900, SP, Brazil; 11-Departamento de Clínica Médica, Faculdade de Medicina de Ribeirão Preto-FMRP, Universidade de São Paulo-USP, Ribeirão Preto 14049-900, SP, Brazil; 12-Departamento de Genética e Evolução, Centro de Ciências Biológicas e da Saúde, Universidade Federal de São Carlos-UFSCar, São Carlos 13565-905, SP, Brazil;

* Correspondence: rfgerlach@forp.usp.br (R.F.G.); carlos.sorgi@usp.br (C.A.S.);

† These authors contributed equally to this work.

‡ Senior authors contributed equally to this work.

Abstract: Patients with Covid-19 predominantly have a respiratory tract infection and acute lung failure is the most severe complication. While the molecular basis of SARS-CoV-2 immunopathology is still unknown, it is well established that lung infection is associated with hyper-inflammation and tissue damage. Matrix metalloproteinases (MMPs) contribute to tissue destruction in many pathological situations, and the activity of MMPs in the lung leads to the release of bioactive mediators with inflammatory properties. We sought to characterize a scenario in which MMPs could influence the lung pathogenesis of Covid-19. Although we observed high diversity of MMPs in lung tissue from Covid-19 patients by proteomics, we specified the expression and enzyme activity of MMP-2 in tracheal-aspirate fluid (TAF) samples from intubated Covid-19 and non-Covid-19 patients. Moreover, the expression of MMP-8 was positively correlated with MMP-2 levels and possible shedding of the immunosuppression mediator sHLA-G and sTREM-1. Together, overexpression of the MMP-2/MMP-8 axis, in addition to neutrophil infiltration and products, such as reactive oxygen species (ROS), increased lipid peroxidation that could promote intensive destruction of lung tissue in severe Covid-19. Thus, the inhibition of MMPs can be a novel target and promising treatment strategy in severe Covid-19.

Keywords: Metalloproteinases, sHLA-G, sTREM-1, lipid peroxidation, Covid-19.

1. Introduction

Severe acute respiratory syndrome coronavirus 2 (SARS-CoV-2) is the infectious agent that causes Covid-19. So far, a massive number of people worldwide have died from severe forms of Covid-19, and vaccination was associated with a significant reduction in Covid-19 infection as well as a reduction in mortality [1]. The severe forms of Covid-19 screening a systemic inflammatory response, thromboembolic complications, and multi-organ failure [2]. Often, the lung becomes non-functional, with potentially fatal consequences [3]. This disease, still today, is a challenge for intensive care physicians, which treat the severe forms of this disease with supportive treatment only [4].

Overall, the pathological mechanisms that lead to death in severe forms of Covid-19 remain unclear. Nonetheless, an important point of this analysis is the fact that the severity of Covid-19 is exacerbated by pre-existing comorbidities, such as hypertension, heart disease, obesity, diabetes, cancer, and a compromised immune system [5,6]. Among comorbidities, all of them, except the last one, are known to show increased levels of gelatinases in plasma [7]. Therefore, it is tempting to hypothesize that the pre-infection

level of plasma matrix metalloproteinases (MMPs) or the potential of the host cells to secrete these proteases (depending on age and genetic polymorphisms) and the activation of those in the host would result in a worsening of the Covid-19 disease course. Therefore, it is tempting to hypothesize that the pre-infection level of plasma matrix metalloproteinases (MMPs) or the potential of the host cells to secrete these proteases (depending on age and genetic polymorphisms) and the activation of those in the host would result in a worsening of the Covid-19 disease course. In many scenarios, excessive proteolysis also involves the activation of several other proteinases, such as coagulation or complement protease cascades [8].

MMPs are believed to be contributing factors to injurious processes in lung pathologies [9], and recent clinical data suggest an increase in plasma MMPs levels in patients with Covid-19 [10]. MMPs represent a family of proteolytic enzymes that contain a zinc ion at the active site of catalysis [11,12] and can cleave a wide variety of substrates, including extracellular matrix (ECM) components (collagens, fibronectin, and elastin), secreted and ECM-anchored growth factors, chemokines, and cytokines [13]. In this regard, some evidence denotes that the soluble form of the human leukocyte antigen-G (HLA-G), a key membrane molecule in pregnancy immune regulation and inflammation control [14], and the Triggering receptor expressed on myeloid cells 1 (TREM-1), a member of the immunoglobulin superfamily expressed on myeloid and epithelial cells [15] is generated through the shedding by MMPs pathways [15–18].

The hyper-inflammatory responses to Covid-19 are characterized by cytokine release syndrome (also called "cytokine storm"), leading to acute respiratory distress syndrome (ARDS), increased pulmonary edema, fibrosis, and hypoxia [19,20]. In addition, excessive neutrophil recruitment into the alveolar space can cause lung injury, as neutrophils release large amounts of proteases, reactive oxygen species (ROS), and extracellular neutrophil extracellular traps (NETs), which are detrimental to host tissues [21]. Autopsy tissue examination of critically ill patients with Covid-19 shows a high degree of diffuse alveolar damage, perivascular inflammatory cell infiltration [22], extensive damage to the vascular lining [23,24], and enhanced remodeling of the fibrosis and extracellular matrix (ECM) in the lung [25].

Inflammatory and parenchymal cells perform some of their functions by releasing MMPs into the lung [26]. The "imbalanced" or excessive proteolytic activity characteristic of the time when active MMPs appear in tissues or plasma is generally found in

102   exacerbated inflammatory responses and results in excessive destruction of structure [27].

103   Therefore, MMPs are crucial components of the processes leading to the state of Covid-19

104   pneumonia. To better define the role of MMPs in severe Covid-19 lungs, we investigate

105   the expression of MMPs in the lung parenchyma and the association between the

106   bronchoalveolar-tracheal levels and activity of MMP-2 and MMP-8 to the immune

107   response

108   associated with sHLA-G and sTREM-1 release, in addition to tissue damage by oxidative

109   stress in Covid-19 outcomes.

110   **2. Materials and Methods**

111   *2.1. Ethical approval*

112   All participants or legal tutors gave their written consent through the informed

113   consent form, in accordance with the regulations and human ethics guidelines of the

114   National Council on Human Research (CONEP) and the Research Ethics Committee from

115   Faculdade de Ciências Farmacêuticas de Ribeirão Preto da Universidade de São Paulo

116   (CEP-FCFRP-USP). The research protocol was approved and received the Certificate of

117   Ethics Presentation and Appreciation (CAAE: 30525920.7.0000.5403). The sample size

118   was determined by the convenience of collection, availability in partner hospitals,

119   participation agreement, and pandemic conditions within the local community.

120   *2.2. Study design and participants*

121   This observational, analytical, and prospective study was conducted at the Hospital

122   Santa Casa de Misericordia of Ribeirão Preto and Hospital São Paulo of Ribeirão Preto-

123   Brazil from June 2020 to January 2021, using stringent and reasonable inclusion and

124   exclusion criteria: adults who tested positive for Covid-19 and controls who tested negative

125   for Covid-19; exclusion for children under 18 years of age and pregnant or lactating

126   women. In total, non-Covid-19 subjects (n = 13), who were hospitalized and intubated due

127   to different clinical primary conditions (Supplementary Table S1) and negative for SARS-

128   CoV-2 infection, along with patients in severe/critical illness (n = 39), intubated and

129   hospitalized in intensive care unit (ICU) who tested positive for SARS-CoV-2 infection, as

130   determined by analyzing nasopharyngeal swabs using a genomic RNA assay with RT-PCR

131   (Biomol OneStep Kit/Covid-19-Instituto de Molecular Biology of Paraná-IBMP

132   Curitiba/PR-Brazil). Peripheral blood samples were collected by venipuncture on first

133   admission and/or during hospitalization for clinical analysis.

134   *2.3. Data collection*

The data were collected from the electronic medical record systems of each patient and carefully revised. We included socio-demographic information, comorbidities, medical history, clinical symptoms, routine laboratory tests, clinical interventions, and outcomes. Data collection from laboratory results was defined by considering the first examination at admission (within 24 h of admission) as the primary endpoint. Blood exams of hospitalized patients were performed at clinical analysis laboratories in their respective hospitals.

2.4. Tracheal aspirate fluid (TAF) collection and processing

TAF samples were collected from hospitalized patients with severe Covid-19 and non-Covid-19 (control), as previously described [28], using a catheter (Mark Med, Porto Alegre, Brazil) with a Trach Care closed endotracheal suction system (Bioteque Corporation, Chirurgic Fernandes Ltd., Santana Parnaíba, Brazil), and sterile polypropylene vials (Biomeg-Biotec Hospital Products Ltd., Mairiporã, Brazil), under aseptic conditions. Approximately 5–10 mL of sterile isotonic saline was instilled into the endotracheal tube; the individual was manually ventilated for 3 breaths, and the trachea was suctioned twice, each time for 5 s; and the TAF samples were collected, placed on ice, and processed within 4 h. In a Biosafety Level 3 facility at Departamento de Bioquímica e Imunologia, Faculdade de Medicina de Ribeirão Preto, Universidade de São Paulo, the TAF samples were placed in 15 mL tubes and diluted with 0.1 M phosphate buffered saline (PBS) (2:1, *v/v*). After centrifugation (700× g/10 min), the sample supernatants were recovered and stored at −80 ◦C and further used for inflammatory mediators and MMPs analysis. Red blood cells in the centrifuged pellet were lysed with 1 mL of NH4Cl buffer (0.16 M) for 5 min. The remaining cells were washed with 10 mL of PBS and suspended in 2% heat-inactivated fetal bovine serum (FBS) in PBS. Cell suspension aliquots were diluted with Trypan blue and counted in an automated cell counter (Countess, Thermo Fisher Scientific, Waltham, MA, USA).

The leukocyte numbers were adjusted to 1×10^9 cells/L for differential counts. Subsequently, differential leukocyte counts (mononuclear cells, neutrophils, and eosinophils) were performed by adding 100 μL of the TAF cell sample to cytospin and stained with Fast Panoptic dye (Laborclin-Laboratory Products Ltd., Pinhais, Brazil). An average of 200 cells were examined and morphologically characterized under an optical microscope (Zeiss EM109; Carl Zeiss AG, Oberkochen, Germany) equipped with a 100× objective (immersion oil) attached to a digital camera (Olympus Soft Imaging Solutions Gmbh, Germany) and analyzed with ImageJ software (1.45 s) (National Institutes of

168   Health, Rockville, MD, USA).

169   *2.5. Soluble TREM-1 and MMPs quantification*

170   The levels of sTREM-1, MMP-2 and MMP-8 were measured in TAF samples using

171   an ELISA kit (DuoSet-Human TREM-1, DuoSet-Human Total MMP-2 and DuoSet-

172   Human Total MMP-8, R&D System, Minneapolis, USA) according to the manufacturer's

173   specifications.

174   *2.6. Quantification of active MMPs levels by zymography*

175   The active MMP-2 and MMP-9 forms were measured in TAF samples by gelatin

176   zymography as previously described [29]. Briefly, the samples were diluted (1:5 *v/v*) with

177   extraction buffer containing 10 mM CaCl2, 50 mM Tris-HCl pH 7.4 The protein content

178   was measured using the Bradford method [30]. Protein concentration varied from 3 to 40

179   µg/µL. Other aliquots with the same protein concentration were then used for total protein

180   analysis in conventional SDS-PAGE and zymography gels. 10 µg of protein from each

181   sample was mixed with non-reducing sample buffer (see below) and used for conventional

182   gel electrophoresis (the gel did not contain gelatin), followed by silver staining. The

183   samples were then further diluted to run 1 µg of protein/lane for the zymograms. Samples

184   were always kept on ice and gels were run on ice. Prior to running, samples in non-

185   reducing sample buffer (2% SDS, 125 mM Tris-HCl, pH 6.8, 10% glycerol, and 0.001%

186   bromophenol blue) were kept 5 min. at 60 ◦C in a bath to reduce dymers. SDS-PAGE gels

187   (12%) co-polymerized or not with 1% gelatin and casein were used for this study. Casein

188   and gelatin gels were used in the initial tests, and the results are shown in the supplemental

189   material (Supplementary Figure S1).

190   After the electrophoresis was complete, the gels were incubated twice for 30 min at

191   room temperature in 2% Triton X-100 solution, followed by incubation at 37 ◦C for 18 h in

192   Tris-HCl buffer, pH 7.4, containing 10 mM CaCl2. The gels were stained with 0.05%

193   Coomassie brilliant blue G-250 for 18 h and unstained with 30% methanol and 10% acetic

194   acid. Gelatinolytic activities were detected as unstained bands against the background of

195   Coomassie blue-stained gelatin. Enzyme activity was assayed by densitometry using an

196   electrophoresis documentation system (ChemiDoc MP Imaging System, BioRad, Hercules,

197   CA, USA). Enzyme activities were normalized against an internal standard (fetal bovine

198   serum, FBS) run in all gels, to allow inter-gel analyses and comparisons. The molecular

199   weight for pro-MMP-2/MMP-2 (72–64 kDa) and pro-MMP-9/MMP-9 (92–86 kDa),

200   respectively, by the relation of logMr to the relative mobility of the SDS-PAGE protein

201 ladder (BlUeye Prestained Protein Ladder-Sigma, Saint Louis, MO, USA). The results

202 were then scanned at 400 dpi and analyzed with ImageJ software (1.45 s) (National

203 Institutes of Health, Rockville, MD, USA).

2.7. Soluble HLA-G Quantification

205 sHLA-G levels in TAF samples were measured using a sandwich ELISA with mAb anti-

206 HLA-G (MEM-G/9-Exbio, Czech Republic) and anti-β2-microglobulin (Dako, Brooklyn,

207 NY, USA) as capture and detection antibodies, respectively [31]. Briefly, microtitration

208 plates were coated with MEM-G/9 (10 µg/mL) at 4 ∘C for 18 h. After blocking unspecific

209 ligands in the wells with 300 µL of diluent (Dako, Brooklyn, NY, USA) for 2 h, two-fold

210 diluted TAF samples (50 µL) were added and incubated for 2 h. The wells were then

211 incubated with rabbit-anti-human β2-microglobulin detection antibody (Dako, Brooklyn,

212 NY, USA) for an additional hour. 100 µL of horseradish peroxidase enhancer (Dako,

213 Brooklyn, NY, USA) was then added and incubated for 1 h. All incubation steps were

214 performed at room temperature. Each step was followed by 4 washes using a specific

215 washing buffer containing PBS and 0.1% Tween (Sigma, Saint Louis, MO, USA). Finally,

216 the wells were incubated with substrate (tetramethylbenzidine-TMB) in the dark for 30

217 min. After the addition of 1 NHCl, optical densities were measured using microplate reader

218 (SpectraMax Plus 384, Molecular Devices, San Jose, CA, USA), applying an absorbance

219 filter of 450 nm. All samples were assayed in duplicate, and the total levels of sHLA-G

220 were determined from a standard curve of five points, using calibrated HLA-G5 dilutions

221 as a standard. Results were expressed as ng/mL.

2.8. Assessment of lipid peroxide levels (MDA)

223 Lipid peroxide levels in TAF samples were determined by measuring thiobarbituric

224 acid-reactive substances (TBARS) using a fluorimetric method described previously

225 [32,33]. In this method, malondialdehyde (MDA) reacts with thiobarbituric acid (TBA)

226 under high temperatures (90–100 ∘C) and acidic conditions, generating the MDATBA

227 adduct. The MDA-TBA adduct was determined fluorometrically at an excitation

228 wavelength at 515 nm and emission at 553 nm and uses 1,1,3,3-tetramethoxypropane as

229 standard for curve. All the measurements were performed using the Synergy 2 multi-mode

230 microplate reader and Gen5 Software (BioTek, Winooski, VT, USA). Briefly, TAF

231 samples were transferred to an equal volume of 20% (v/v) cold trichloroacetic acid in 0.6

232 M HCl, mixed and centrifuged at 1200× g for 15 min. In a volume of clear supernatant, a

233 0.2 volume of 0.12 M thiobarbituric acid/0.26 M Tris, pH 7.0 was added, and immersed in

234 a boiling water bath for 1 h. The lipid peroxide levels were expressed in terms of MDA

235 (nmol/mL).

236 *2.9. Detection of SARS-CoV-2 RNA.*

237   Total RNA was extracted from 20 uL of TAF samples with TRIzol reagent according

238 to the manufacturer's instructions. The qPCR assay was performed for the E gene region

239 and N2 region in the N gene [34,35]. Real-time RT-PCR was performed using TaqPath 1-

240 Step qRT-PCR Master Mix (Applied Biosystems, Foster City, CA, USA) on a StepOne

241 Plus real-time PCR system (Applied Biosytems, Foster City, CA, USA) with the following

242 parameters: 25 °C for 2 min, 50 °C for 15 min, 95 °C for 2 min, followed by 45 cycles of

243 94 °C for 5 s and 60 °C for 30 s. SARS-CoV-2 viral loads were determined using a

244 standard curve prepared with a plasmid containing all three targets for the sets of

245 primers/probes designed by the CDC protocol (N1, N2 and N3) [36].

246 *2.10. Statistical analysis*

247   Data are presented in tables and graphs, using GraphPad PrismTM software, version

248 9 (San Diego, CA, USA). Taking into account the nonparametric distribution of the data,

249 comparative analyzes between groups were performed using the Mann-Whitney or

250 Kruskal-Wallis tests, with $p < 0.05$ significant. The dependence on multiple variables was

251 calculated using Spearman's correlation test, and the differences were considered

252 statistically significant with $p < 0.05$.

253 *2.11. Re-analysis of proteomics data*

254   Protein expression data for lung biopsies from Covid-19 and non-Covid-19 samples

255 were obtained from the supplementary tables of an original proteomic study [37]. Only

256 proteins with expression values in at least three samples for each group were used in the

257 statistical analysis. Student's test between the Covid-19 and non-Covid-19 groups was

258 carried out for all selected proteins after transforming expression values using the Log2

259 scale, and the false discovery rate was controlled using the Benjamini and Hockberg

260 correction [38]. The results of MMPs were extracted from the whole statistics using both

261 nominal and adjusted p-values with significant results ($p < 0.05$) (Supplementary Table

262 S2). Statistical analysis was performed in R [39], and figures were produced using the

263 package ggplot2 [40].

264 **3. Results**

265 *3.1. Participants demographic data and clinical characteristics*

266   In total, 39 patients with laboratory-confirmed Covid-19 were enrolled in this study,

267   classified as severe/critical ill with oxygen support, intubated in ICU hospital care, in

268   addition to 13 critical volunteers, negative for Covid-19 (non-Covid-19) but hospitalized

269   and intubated due to different primary clinical conditions (Supplementary Table S1). The

270   median age and BMI were not significantly different between non-Covid-19 volunteers

271   and patients with Covid-19. The percentage of men was higher among patients with Covid-

272   19 than in non-Covid-19, as well as the percentage of comorbidities especially

273   hypertension with significant consideration (Table 1). The most common symptoms in the

274   patients were dyspnea, cough, fever, and myalgia followed by diarrhea, anosmia, and

275   dysgeusia; in non-Covid-19, only dyspnea was observed (Table 1). Moreover, the absolute

276   blood counts of erythrocytes and hemoglobin concentration in the Covid-19 patient group

277   were different from those in the non-Covid-19 group, while the counts of leukocytes,

278   neutrophils, lymphocytes, neutrophil/lymphocytes ratio (NLR), monocytes and platelets

279   were not significantly different between those groups (Table 1).

280   The median time of hospitalization for Covid-19 patients was 6.5 days and 23 days

281   for non-Covid-19. Additionally, all those hospitalized patients received respiratory support

282   by invasive mechanical ventilation, but the oxygen saturation was significantly lower

283   among Covid-19 patients (91%) as compared to the non-Covid-19 group (94%) (Table 1).

284   The percentage of death outcomes was 84.6% for Covid-19 patients and 61.5% for non-

285   Covid-19 individuals (Table 1).

286

287   **Table 1.** Participants clinical and demographic data enrolled in this study

Baseline Variable	Non-Covid-19 N= 13	Covid-19 N= 39	Covid-19 Survival N= 6	Covid-19 Non-Survival N= 33	*p Value*
Demographic characteristics (median ± SD)					
Age median ± SD	61±17.8	66±16.0	61±24.1	66±14.3	0.5200 [a] 0.5488 [b]
BMI (kg/m^2)	26.8±6.5	29.4±7.0	27.4±6.7	29.5±7.1	0.1528 [a] 0.3915 [b]
Sex, No. (%)					
Male	4 (30.8)	21 (55.2)	1 (16.7)	17 (51.5)	-
Female	9 (69.2)	18 (44.7)	5 (83.3)	16 (48.5)	-
Comorbidities or coexisting disorders, No. (%)					
Hypertension	3 (23.1)	23(59)	3 (50)	20 (60.6)	**0.0250 [a]** 0.6271 [b]
Dyslipidemia	-	2 (5.1)	-	2 (6.0)	-
Diabetes *mellitus*	2 (15.4)	15 (38.4)	1 (16.7)	14 (42.4)	0.1245 [a] 0.2329 [b]
Obesity	3 (23.1)	17 (43.6)	1 (16.7)	16 (48.5)	0.1880 [a] 0.1482 [b]
Neurological Disease	2 (15.4)	3 (7.7)	-	3 (9.1)	0.4152 [a]
Respiratory Disorders	1 (16.7)	5 (12.8)	-	5 (21.7)	0.6162 [a]
Presenting symptoms, No. (%)					
Dyspnea	4 (30.7)	27 (69.2)	4 (66.7)	23 (69.7)	**0.0144 [a]** 0.8824 [b]
Fever	-	12 (30.8)	2 (33.3)	10 (30.3)	0.8824 [b]
Myalgia	-	17 (43.6)	1 (16.7)	16 (48.5)	**0.0037 [a]** 0.1482 [b]

Diarrhea	-	7 (18)	-	7 (21.2)	-
Cough	-	13 (33.3)	4 (66.7)	9 (27.3)	0.0597 [b]
Anosmia	-	4 (10.3)	1 (16.7)	3 (9.1)	0.5737 [b]
Dysgeusia	-	3 (7.7)	-	3 (9.1)	-
Laboratory findings, median ± SD					
Erythrocytes x 10^9/L	2.7±0.9	3.7±0.8	3.0±0.7	3.9±0.7	**0.0037 [a]** **0.0136 [b]**
Hemoglobin (g/dL)	8.7±2.9	10.7±2.2	9.4±1.3	10.9±1.9	**0.0090 [a]** **0.0115 [b]**
Leukocytes x 10^9/L	11.5±15.4	15.1±16.7	11.2±4.2	16.2±18.0	0.5318 [a] 0.1850 [b]
Neutrophils x 10^9/L	8.7±11.1	12.8±5.5	7.6±4.1	13.4±5.5	0.8028 [a] 0.1327 [b]
Lymphocytes x 10^9/L	1.1±1.1	0.9±0.5	1.4±0.8	0.9±0.5	0.5117 [a] 0.5820 [b]
NLR	7.0 ±21.1	12.3±10.5	5.0±10.0	12.8±10.6	0.1879 [a] 0.3311 [b]
Monocytes x 10^9/L	0.48±0.4	0.52±0.5	0.6±0.4	0.5±0.5	0.7854 [a] 0.6482 [b]
Platelets x 10^9/L	250±165.8	229±9.15	286±80.7	228±92.3	0.3112 [a] 0.6693 [b]
Hospital support, No. (%)					
Intensive care unit (ICU)	13 (100)	39 (100)	6 (100)	33 (100)	-
Hospitalization data, No.					
Hospitalization days, median ± SD	23±19.6	6.5±2.6	23.5±8.2	17 ±8.4	**<0.0001 [a]** **0.0374 [b]**
Respiratory support received (%)					
Invasive mechanical ventilation	13 (100)	39 (100)	6 (100)	33 (100)	-
Oxygen Saturation median ± SD	94 ±6.3	91±10.7	91.5±4.2	91±11.3	**0.0125 [a]** 0.3240 [b]
PaO$_2$/FiO$_2$, ratio median ± SD	156.3±58.3	140.3±94.8	106.4±165	140.3±76.4	0.9335 [a]

					0.9245 [b]
Denouement, No (%)					
Survival	5 (38.5)	6 (15.4)	-	-	-
Non-survival	8 (61.5)	33 (84.6)	-	-	-
Viral charge					
ΔCT	-	57.8±3402	30.2±3899	52.6±10455	0.3706 [b]

[a] Comparisons between non-Covid-19 and Covid-19 patients; [b] Covid-19 survival versus Covid-19 non-survival patients. Patient data were compared using the chi-square test, or Fisher's exact test for categorical variables and one-way analysis of variance (ANOVA) Mann-Whitney; nonparametric t-test was used for continuous variables. $p < 0.05$ was considered statistically significant. Abbreviations: Standard deviation (SD); percentage (%).

3.2. Elevated Expression of MMPs on Lung-Tissue and MMP-2 Active form on TAF Samples from Covid-19 Patients

Initially, we reanalyzed proteomics data from lung biopsy samples of Covid-19 patients (n = 30) and non-Covid-19 individuals (n = 6) [37]. Comparative analysis was performed using the log2 target of MMP protein expression: MMP-1, MMP-2, MMP-7, MMP-8, MMP-9, MMP-10, MMP-12, MMP-14, MMP-15, MMP-19, MMP-28, MMP-23B, and MMP-24OS (Figure 1A). This target proteomics approach indicated that MMP-2, MMP-7, MMP-8, and MMP-14 figured out the Covid-19 perturbation with a significant increase compared to non-Covid-19 individuals. However, the expression of the MMP-15 protein in Covid-19 was lower than in non-Covid-19 lung tissue. Therefore, we hypothesize that MMPs were strongly associated with lung Covid-19 severity.

To verify the importance of MMPs in Covid-19 lung disease pathogenesis, we performed a protease screening on TAF samples from our cohort. For this, we focused on the classical protease cleavage of substrates in gels (zymograms), including gelatin and casein as substrates co-polymerized in SDS-PAGE gels. Results indicated a strong gelatinolytic activity and a much lower caseinolytic activity when the same amount of TAF–Covid-19 protein was used in the gels (Supplementary Figure S1A-gelatin zymogram and Supplementary Figure S1B-casein zymogram).

Next, the gelatinolytic activity in zymograms was observed after the gels had been incubated overnight in the presence of protease inhibitors. The control gel was not incubated with proteinase inhibitors (Supplementary Figure S2A), while other gels were incubated with the inhibitors of the most common classes of protease found in eucariotic cells, namely: serine-, metallo-, and cysteine-proteinases. The gelatin-containing zymograms had been prepared and run in the same way and contained the same samples as the gel presented in Supplementary Figure S2A. Supplementary Figure S2B shows the gel incubated with 1 mM 1-10-Phenanthroline, a preferential zinc-chelator, and a potent metalloproteinase inhibitor. Supplementary Figure S2C shows the gel incubated with 1 mM Phenylmethylsulphonylfluoride (PMSF), a serine-proteinase inhibitor (PMSF-gel). The gel incubated with N-ethyl-maleimide, a cysteine-protease inhibitor, is not shown. No significant activity was observed. When considering that 1 µg of total TAF protein was loaded onto the lanes containing the higher masses, it can be easily realized that a huge concentration of gelatinases is present in the TAF samples (at this point, the samples were selected at random, since these experiments were part of the initial characterization steps).

Regarding the use of inhibitors, strong gelatinolytic activity was observed in the control gel, with a similar result for gels incubated with PMSF and NEM, but without detected gelatinolytic activity in gel incubated with 1-10-Phenanthroline. Interestingly, neither serine nor cysteine proteinases were detected in our TAF samples in significant amounts, even using very high amounts of protein (considering that zymograms regularly detect nanograms of gelatinases and therefore the usual amounts of load used for Western Blots (usually 30 µg), for example, cannot be applied to zymograms. Moreover, it became clear that metalloproteinases were the most active proteases in our TAF samples, and second protein quantification was performed, to ensure that no problems in comparison of samples would come from the serial dilution of samples, that was necessary to apply 0.1 µg of total protein per sample/lane. This was necessary since quantification of gelatinolytic bands should only be done when the gelatinotic bands are found in a range where the total activity was still not reached (for plasma, we used 0.2 to 1 µL to obtain gelatinolytic bands that were adequate for quantification and comparison between patients).
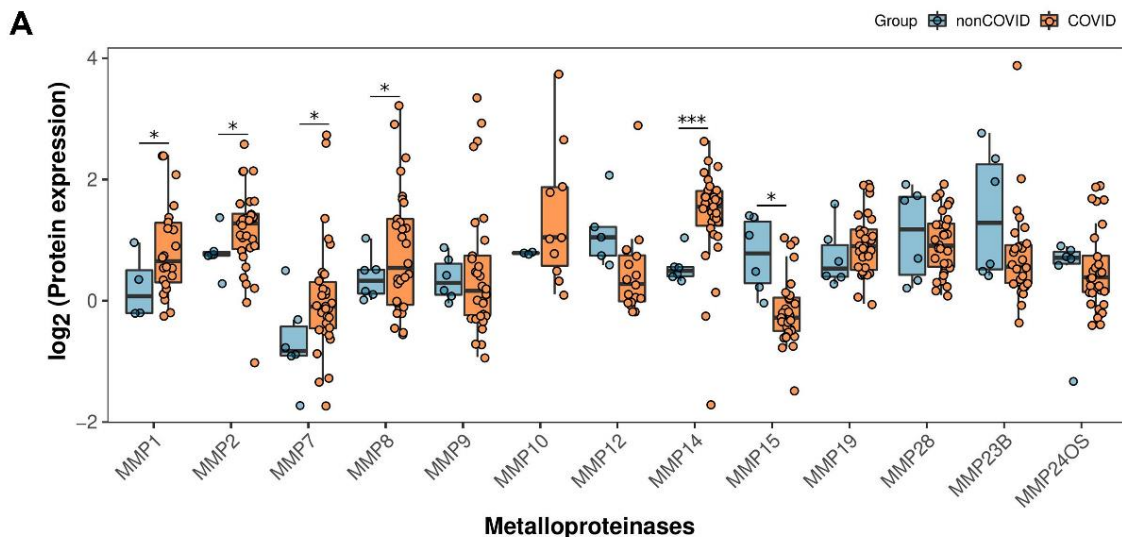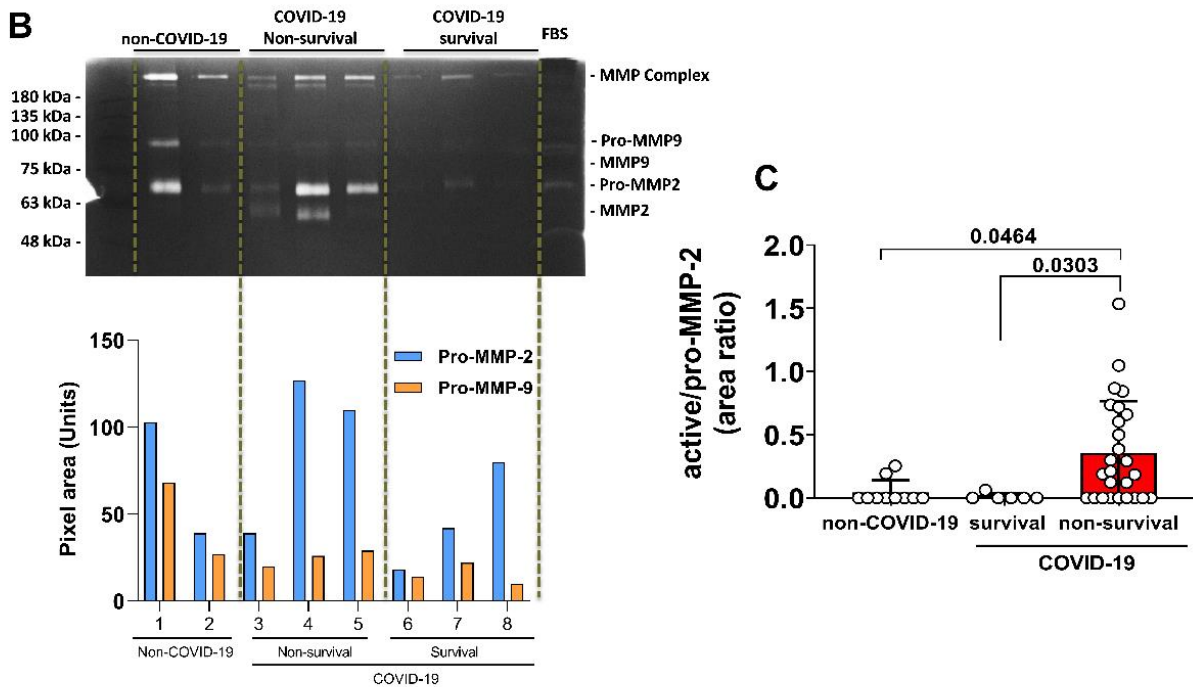
Figure 1. The expression of matrix metalloproteinase and active-MMP-2 form increased in Covid-19 lung. (A) Protein expression data obtained from literature [37] was reanalyzed aiming to evaluate MMPs expression changes. Significant changes are indicated by nominal p-values (* p < 0.05 and *** p < 0.001). Only MMP-14 presented significant difference with adjusted p-value equal to 0.000508. (B) Expression and different molecular weight forms of MMP-2, cleavage of pro-MMP-2 to active MMP-2, and MMP-9 analyzed by gelatin zymography. Representative gel from non-Covid-19 (n = 13), survival (n = 6) and non-survival (n = 33) Covid-19 patients is shown. Positions of proMMP-9, pro-MMP-2 and active MMP-2 with sizes in kDa are indicated. (C) Quantification of active-MMP-2 represented by area ratio to pro-MMP-2. Statistical analyzes were performed using the Kruskal-Wallis multiple comparison test, followed by the Dunns post-test to compare pairs. Data are expressed as median with 95% confidence intervals. Statistical differences between groups are considered by p < 0.05 and represented directly in the graphic figure.

As demonstrated in Figure 1B-panel and Supplementary Figure S3, the zymogram showed the presence of complex, pro- and active forms of MMPs. Indeed, pro-MMP-2 and pro-MMP-9 were present in all TAF samples from non-Covid-19 and Covid-19 patients. However, activated MMP-2 was prominent on Covid-19 samples only, while activated MMP-9 was not found, neither in Covid-19 or non-Covid-19 samples. Regarding stratifying the Covid-19 patients based on the outcome (survival and non-survival), we observed that the ratio of active-/pro-MMP-2 levels was significantly increased in the group of non-survival patients (Figure 1B-graphic). MMP-9 levels were not associated with Covid-19 lung pathology and did not show a correlation with mechanical ventilation in non-Covid-19 subjects.

3.3. MMP-2 and MMP-8 Expression Increased in Lung from Patients with Non-Survival Covid-19 and Was Correlated with the Release of sTREM-1 and sHLA-G

Considering the total protein form by ELISA, MMP-2 and MMP-8 were significantly higher in TAF from patients with Covid-19 compared to non-Covid-19 (Figure 2A). Furthermore, comparing non-survival with survival Covid-19 patients, we observed a significant increase in MMP-2 and MMP-8 levels in the non-survival group, compared to the survival group and the non-Covid-19 group. There was no statistical difference between the Covid-19 survival patients to non-Covid-19 (Figure 2A).
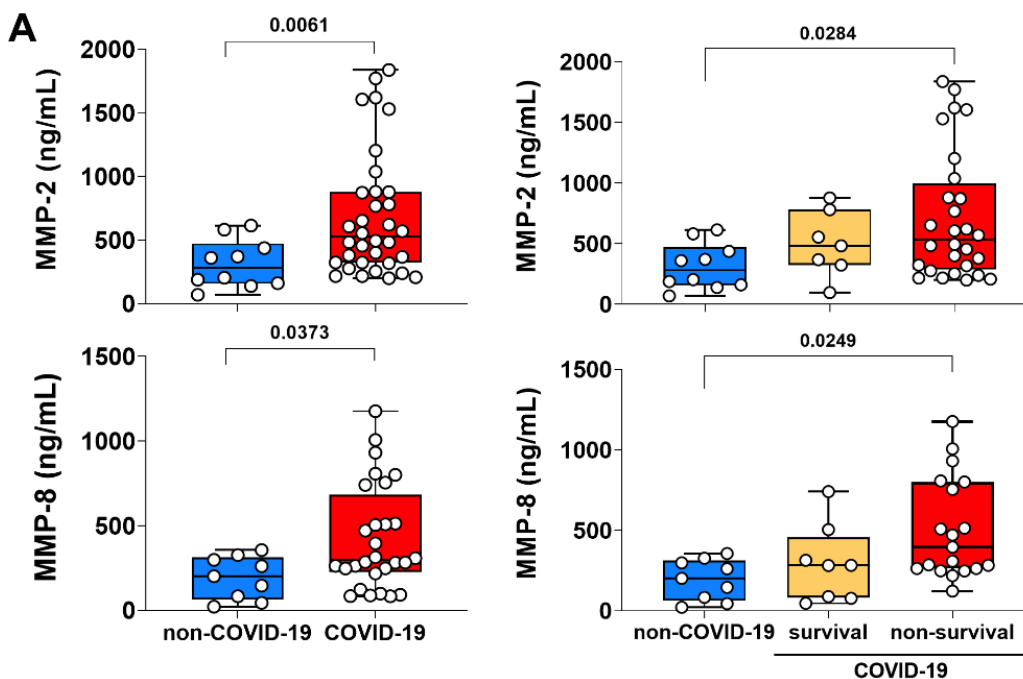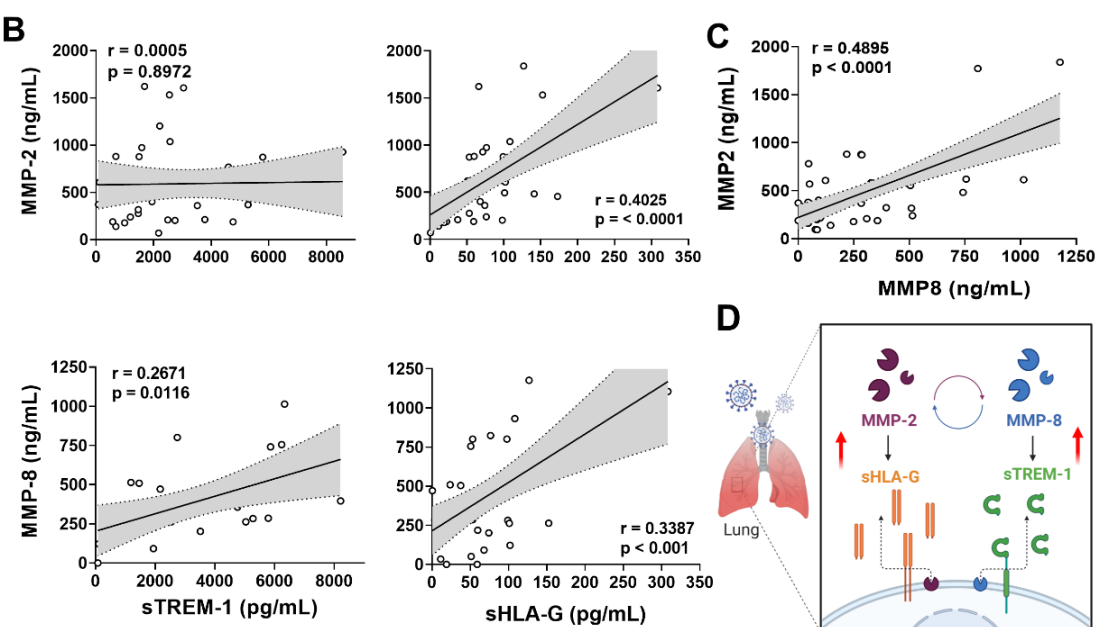
Figure 2. Increased levels of MMP-2 and MMP-8 in TAF samples correlated with non-survival Covid-19 and shed of sHLA-G and sTREM-1. (A) Quantification of MMP-2 and MMP-8 in TAF samples from non-Covid-19 (n = 13) and Covid-19 patients (survival n = 6, non-survival n = 33). Statistical analyzes were performed using the Kruskal–Wallis multiple comparison test, followed by the Dunns post-test to compare pairs. Data are expressed as median with 95% confidence intervals. Statistical differences between groups are considered by p < 0.05 and represented directly in the graphic figure. (B) Correlations between MMP-2 and MMP-8 levels and soluble immune factors sHLA-G and sTREM-1 in total TAF samples from non-Covid-19 and Covid-19 patients at hospital admission. (C) Correlations between MMP-2 and MMP-8 levels in total TAF samples from non-Covid-19 and Covid-19 patients at hospital admission. Spearman correlation analysis, r and p value indicated in each panel. (D) Schematic representation of the MMP-2 and MMP-8 positive looping inducing the release of sHLA-G and sTREM-1 in lung from severe Covid-19. (Created with BioRender.com, Agreement number: IZ23RHRAES).

MMP-2 and MMP-8 were unambiguously elevated proteinases in the lung of patients with Covid-19. To date, those MMPs have been only analyzed in systemic Covid-19 studies [10,41]. On the other hand, there are some key proteins for the immune response that can be generated through proteolytic cleavage, which is known to be mediated by MMPs, such as sHLA-G [18] and sTREM-1 [15]. Taken together, our data demonstrated that both sHLA-G and sTREM-1 levels on TAF samples were elevated in Covid-19 patients and sTREM-1 positively correlated with MMP-8, while sHLA-G levels positively correlated with both MMP-2 and MMP-8 expression (Figure 2B). However, some evidence suggested that TREM-1 site cleavage to release sTREM-1 was specific for MMP-8 activity [15] and HLA-G site cleavage to release sHLA-G was specific for MMP-2 activity [42]. In fact, we confirmed the MMP-8 specific axis to sTREM-1, but there was an ambiguity about MMPs and sHLA-G release in our data. For this, we analyzed a Spearman test correlation between MMP-2 and MMP-8 levels and showed a positive and significant result on TAF samples (Figure 2C). These data suggested that MMP-8 could perform to generate active-MMP-2, and MMP-2 was involved in sHLA-G release (Figure 2D).

3.4. Relationship of MMP-2 Levels and Oxidative Stress in the Lung of Non-Survival Covid-19 Patients

Reactive oxygen species (ROS) disrupt lipids, proteins, and DNA, potentially resulting in tissue damage and cell death [43]. The interaction of ROS with cell membranes leads to the generation of lipid peroxides, which can be quantified using thiobarbituric reactive substances (TBARS) and could represent oxidative stress [32]. Although nonspecific, TBARS are considered a stable marker of free radical damage and oxidative stress due to their rapid generation and excretion. We showed in Figure 3A that the level of lipid peroxidation (MDA) was significantly increased in TAF samples of Covid-19 compared to non-Covid-19. Additionally, when we stratified the Covid-19 patients in the

412 survival and non-survival group, we observed that this high level of lipid peroxidation was
413 significantly related to the non-survival patients, compared to survival patients and non-
414 Covid-19 (Figure 3A).

415   As previously demonstrated, neutrophils were the main cells whose increases in the
416 blood of count patients with severe Covid-19 [44], and this phenomenon can be associated
417 with hyper-inflammatory response and "cytokine storm" [45]. In fact, neutrophilia is an
418 indicator of severe respiratory symptoms and an unfavorable outcome in Covid-19 [46].
419 We next determined the cell infiltration in TAF samples (Supplementary Figure S4), and
420 we detected a significant increase only in neutrophil counts from patients with Covid-19
421 compared with non-Covid-19. In this context, in Figure 3B we demonstrated that the
422 neutrophils count in non-survival Covid-19 patients was significantly higher compared to
423 non-Covid-19. The regression approach revealed a positive association of lipid
424 peroxidation levels (MDA) and neutrophil counts in TAF samples, suggesting that ROS
425 species production and consequently oxidative stress could be related to these immune
426 cells in the lung microenvironment of SARS-CoV-2 infection (Figure 3B).

427   Interestingly, we showed a positive and significant correlation between lipid
428 peroxidation (MDA) levels and MMP-2 expression on TAF samples (Figure 3C). We
429 emphasized a relative looping in our data when ROS formation by oxidative stress,
430 probably due to neutrophils activity, could trigger MMP-2 activation and MMP-2 function
431 could increase ROS formation in the lung of Covid-19 patients (Figure 3D).

432
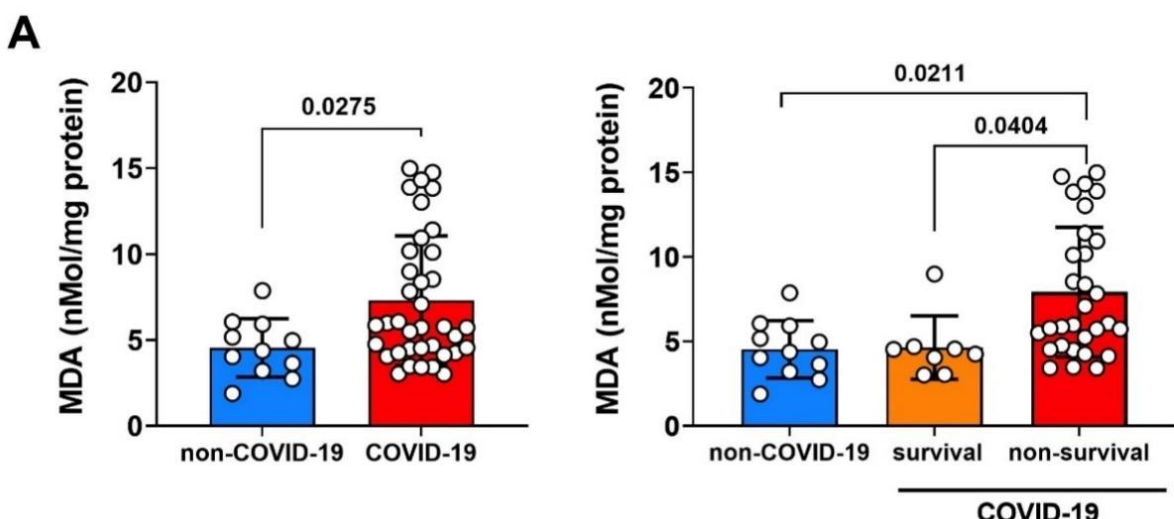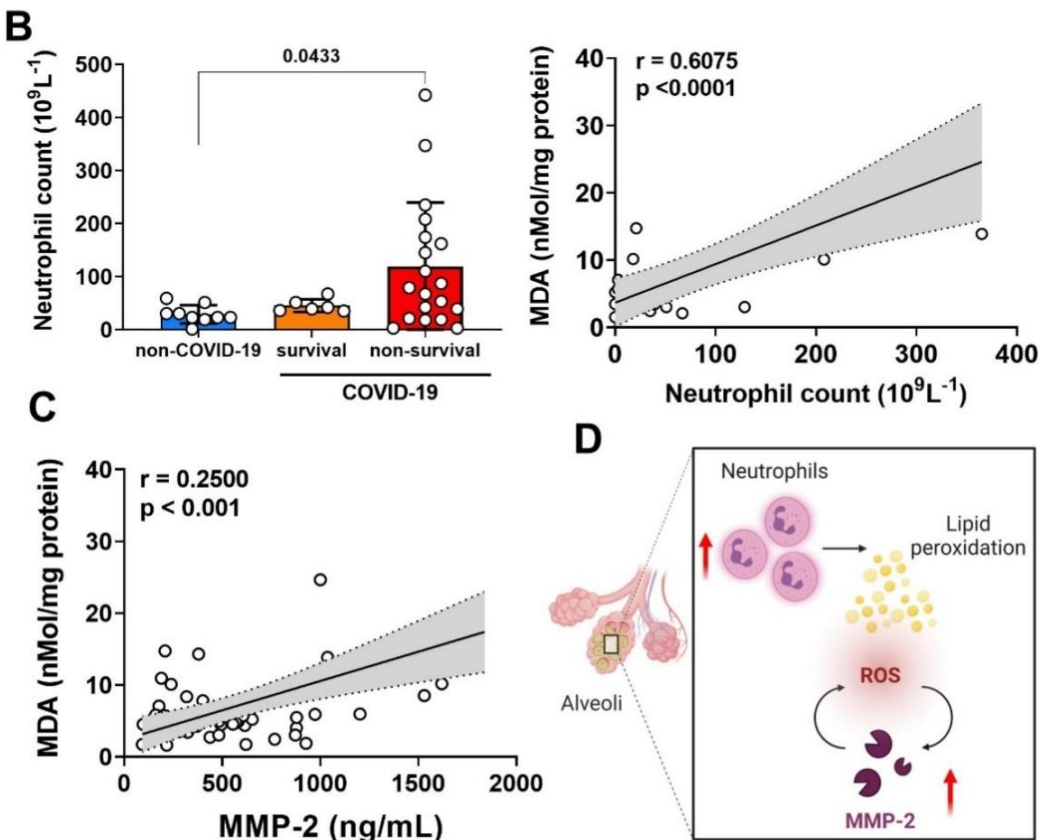
Figure 3. Oxidative stress and neutrophil infiltration into the lung of patients with severe Covid-19. (A) Representative lipid peroxidation levels by concentrations of thiobarbituric acidreactive species expressed in terms of MDA in TAF samples from non-Covid-19 (n = 13) and Covid-19 patients (survival n = 6, non-survival n = 33). (B) Absolute neutrophil counts in TAF samples from non-Covid-19 and Covid-19 patients (survival, non-survival), and correlation between the quantification of MDA and the number of neutrophils in total TAF samples from non-Covid-19 and Covid-19 patients at hospital admission. (C) Correlation between MDA quantification and MMP-2 levels in total TAF samples from non-Covid-19 and Covid-19 patients at hospital admission. Spearman correlation analysis, r and p value indicated in each panel. Statistical analyzes were performed using the Kruskal–Wallis multiple comparison test, followed by the Dunns post-test to compare pairs. Data are expressed as median with 95% confidence intervals. Statistical differences between groups are considered by p < 0.05 and represented direct in the graphic figure. (D) Schematic representation of the lung neutrophil infiltration and ROS production trigger a positive looping of MMP-2 and ROS production in lung from severe Covid-19. (Created with BioRender.com, Agreement number: CG23RHR5O1).

4. Discussion

Survival of Covid-19 patients with severe symptoms depends on the extension of lung injury, damage to other organs, comorbidities of the infected patient, and appropriate viral immune response [47]. Even though MMPs play a key role in lung immunity by facilitating the influx of inflammatory cells and modulating the activities of inflammatory mediators and defensins [9], the unbalanced levels of a variety of MMPs have been predictable in many lung disorders [9]. In this context, cytokines, inflammatory mediators and MMPs levels could define an immune-based biomarker system of Covid-19. However,

no enzyme activity of MMPs has been studied in the lungs of patients with Covid-19 and correlation to tissue pathology. We demonstrated, for the first time, that the enzymatic activity and levels of MMP-2 and MMP-8 increased significantly in the lung microenvironment of intubated patients with Covid-19, and this MMP-axis was associated with infiltration of lung neutrophils, oxidative stress and release of sTREM-1 and sHLA-G, important mediators for the regulation of immune response.

As in all tissues, the expression of MMPs in the lung is a highly regulated process [48,49]. Moreover, MMPs degrade the ECM of the interstitium leading to an increase in alveolar permeability that is observed in destructive lung diseases, including ARDS, COPD, tuberculosis, sarcoidosis, and idiopathic pulmonary fibrosis (IPF) [50,51]. Although small amounts of MMP-2 and MMP-14 are present in the lung lining fluid under normal conditions, other MMPs, such as MMP-7, MMP-8, MMP-9, and MMP-12, are up-regulated under many pathological conditions [48,52,53]. Indeed, epithelial cells from bronchoalveolar lavage fluid (BALF) on severe Covid-19 showed elevated frequencies of MMP-7+ and MMP-9+ and a tendency to increase portions of MMP-2+ and MMP-13+ compared to mild cases [54]. It appears partly reasonable with our results from proteomics reanalysis, which showed a significant increase in detection of MMP-2, MMP-7, MMP-8, and MMP-14, but not the expression of the MMP-9 protein, in lung tissue from Covid-19 compared to non-Covid-19 subjects.

MMPs are initially synthesized in a latent pro-form as zymogens. The basic structure of the catalytic portion of proteases consists of a catalytic domain with three histidine residues related to a zinc atom ($Zn2+$) and a pro-domain containing a cysteine [55]. For enzymatic activation, proteolytic cleavage of the pro-domain and exposition of the catalytic site are required [56]. MMP-2 was synthesized by a wide variety of cells, including fibroblasts, endothelial cells, and alveolar epithelial cells and plays role in lung inflammatory
diseases [57,58]. In fact, the absence of MMP-2 was protective in allotransplant models reducing cellular infiltration and fibrosis; in contrast, deficiency in MMP-2 increased the susceptibility of mice to lethal asphyxiation in an asthma model [59,60]. We observed that TAF samples from Covid-19 and non-Covid-19 individuals expressed high levels of pro-MMP-9 and pro-MMP-2 by zymogram. However, only the active form of MMP-2 was extremely associated with non-survival Covid-19 patients. Post-translational modification of MMPs in the lung could be a crucial step in regulating the action of MMPs in vivo.

Several MMPs have soluble and cell surface forms, providing another level of regulation through compartmentalization/localization [61]. In addition, endogenous families of inhibitory proteins, TIMP1-4 and α2-macroglobulin, are known to regulate MMPs at the post-translational level [62]. Uncontrolled MMP-2-activity can be highly pro-inflammatory and affect lung physiology with severe Covid-19.

Apparently, no single MMP is a fundamental mediator of any specific pulmonary pathology, as each MMP plays an individual role in specific periods and potential functional redundancy, based on the numerous overlapping substrate molecules that exist at the site of activity of MMPs [9]. Indeed, the TAF samples of Covid-19 patients presented a high amount of MMP-8, such as high levels of MMP-2. The expression of both MMP was a significant contributor to non-survival Covid-19 patients. Compartmentalization of MMPs in inflammatory cells is another mechanism of regulation; for instance, pro-MMP-8, pro-MMP-9, and pro-MMP-25 are packaged into peroxidase-negative granules within neutrophils to be released upon leukocyte activation [63]. Likewise, neutrophils exposed to pro-inflammatory cytokines increase the expression of active MMP-8 on the cell surface, and its localization on the cell surface confers resistance to inhibition with TIMP [61]. In accordance with our work, it was characterized by immunoblotting MMP-2, -8, and -9 and TIMP-2 in TAF samples from preterm infants with respiratory distress during the first postnatal days, suggesting that in preterm infants, increased pulmonary MMP-8 levels participate in the acute inflammatory injury [64].

In response to SARS-CoV-2 infection, the host's immune system and target cells are likely to release MMPs [10,65,66]. MMP activity normally governs the release of substrates that are anchored either at the extracellular matrix or cell membrane, such as growth factors and cell membrane receptors [67,68]. HLA-G is a non-classical HLA class I antigen, which is pondered as an immune inhibitory mediator and can be up-regulated by several viral infections, including SARS-CoV-2, which can render comprehensive immunosuppressive roles in favoring virus immune evasion and subsequent disease progression [69,70]. Soluble HLA-G proteins can be generated through proteolytic release; for example, there is an effective link between MMP-2 and the shedding of HLA-G, but not for MMP-9 in this process [42]. TREM-1, another membrane receptor, amplifies the pro-inflammatory response in synergism to Toll-like receptors, which recognize a wide range of bacterial, fungal, and viral components [71]. Another study reported an MMPs cleavage site within the TREM-1 sequence and demonstrate a correlation to MMP-9

activity [72]. However, our group demonstrated that plasma expression of MMP-8 was positively correlated with sTREM-1 levels, specifically in the group of patients with severe Covid-19 [41]. As expected, in our TAF samples, the MMP-8 expression correlated positively with sTREM-1 production. However, the release of sHLA-G was positively correlated with both MMP-2 and MMP-8 levels.

Classically, MMP-2 activation on the cell surface is critically dependent on the binding of pro-MMP-2 to MMP-14 and TIMP-2. This complex allows a second active MMP-14 to cleave the pro-domain and release the active-MMP-2 [73]. On the other hand, MMP-7 was able to activate pro-MMP-8, and the accumulation of pro-MMP-8 in the absence of MMP-7 was accompanied by a decrease in pro-MMP-13 levels, suggesting the interaction between MMP-7, MMP-8, and MMP-13 to regulate collagen turnover [74]. However, in TAF samples, we observed a positive and significant correlation between MMP-2 and MMP-8 levels. Since we had evidence of increased expression of MMP-14 and MMP-7 in Covid-19 lung tissue by proteomics reanalysis, both described activation pathways that could be effective in TAF samples to produce active-MMP-2 and active-MMP-8. On the other hand, we could have a new activation positive looping intricate MMP-8 and MMP-2, and this phenomenon could justify the effective action of MMP-2 on HLA-G shedding and indicated that the positive correlation of MMP-8 expression to sHLA-G levels was an indirect axis linked to MMP-2 activation.

Increased inflammatory mediators activate neutrophils and alveolar macrophages, which liberate MMPs and oxygen radicals, thus producing more lung damage, increasing vascular leakage and cell apoptosis [75]. Oxidative stress results from the overproduction or inhibited inactivation of reactive oxygen species (ROS), causing alterations in the redox state of proteins and lipids [76]. Increased ROS formation triggers protein oxidation and activation of a cascade of cell signaling events, resulting in endothelial dysfunction and MMPs activation [77,78]. It has been shown that changes in the tissue concentrations of O^{2-}, H_2O_2, and $ONOO^-$ affect MMP-2 activity [77,79]. However, the increased MMP-2 activity in the vascular system could directly activate pro-oxidant pathways, for example, MMP-2 cleaved pro-heparin binding epidermal growth factor (HB-EGF) and the soluble HBEGF bind the EGF receptor (EGFR), downstream NADPH oxidase, which increased ROS formation [80]. Regarding this, the activation of MMP-2 and MMP-9 was directly involved in the vascular remodeling observed in hypertension [81]. We observed an increased lipid peroxidation levels (MDA quantification) on TAF samples from Covid-19

patients compared to non-Covid-19, and this oxidative stress was significantly more prominent in no-survival than survival patients. In this context, neutrophil counts were higher in samples from Covid-19 patients, indicating a positive correlation between neutrophil infiltration and lipid peroxidation levels (also, ROS production). Moreover, MMP-2 levels were positive and significantly correlated with lipid peroxidation concentration, suggesting another positive looping of neutrophils producing ROS species; ROS triggers MMP-2 activation and MMP-2 enhanced oxidative stress in the Covid-19 lung.

Thus, despite the fact that great efforts have been made toward the development of inhibitors of MMPs, it is not clear whether MMP inhibition is beneficial or harmful in diseases. Covid-19 patients with severe symptoms exhibit impaired endothelial and microcirculatory functions, neutrophilia, and other complications associated with dysregulation of myeloid responses, especially in the lung [82–84]. Epithelial damage is the initial event and hallmark of acute lung injury that initiates a cascade of processes that lead to diffuse lung parenchymal damage [85,86]. We contemplated a scenario for Covid-19 lung immunopathology in which focal airway inflammation produces an elevation of proinflammatory mediators. These mediators activate alveolar macrophages and neutrophils, which release ROS and MMPs, producing additional lung tissue damage. The functional significance of the interactions between MMPs and their immunological substrates in the lung is a novel concept that is currently being explored. In particular, we suggested that excessive cleavage of TREM-1 by MMP-8 could contribute to immunosuppression, as demonstrated during other severe infections [87]. Additionally, the action of MMP-2 on sHLA-G release could induce immune impairment and exhaustion [88]. Furthermore, HLA-G expression induced by SARS-CoV2 infection may be associated with increased morbidity and mortality and, as described, predict a worse outcome [89].

This study had undergone several limitations. First, the patients were not monitored for the level of MMPs from admission until recovery. Second, the profile of pro- and antiinflammatory cytokines was not determined. Third, viral load was not taken into account in the analysis. Fourth, patients with asymptomatic, mild, and moderate Covid-19 were not investigated. Fifth, the small sample size of Covid-19 patients and non-Covid-19 critical controls was another important limitation and may reflect in the statistical significance; and finally, the lack of healthy non-Covid-19 individuals (health control),

588 which could have allowed us to identify a baseline of clinical and inflammatory variables.

5. Conclusions

590   Uncontrolled protease activity and improper expression of several MMPs were
591 correlated to lung disease in severe Covid-19. Although considered plasma prognostic
592 biomarkers, the MMP-2 and MMP-8 pathways in the lung could become the target of
593 specific therapies, including those proposed to diminish cell infiltration, viral
594 immunosuppression response, oxidative stress, and tissue damage during Covid-19.
595 Conversely, MMPs are emerging as an important component of Covid-19
596 immunopathogenesis.
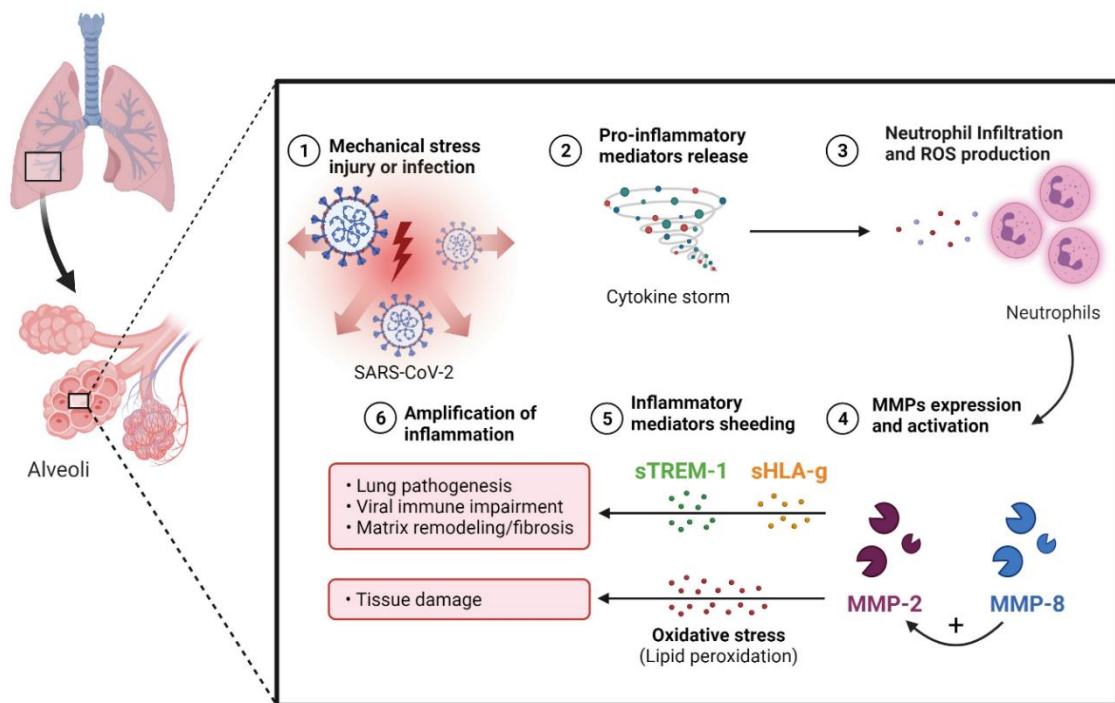
597

598   **Supplementary Materials:** The following are available online at
599 https://www.mdpi.com/article/ 10.3390/biom12050604/s1.

600   **Supplementary Figure 1 - Initial Screening of TAF (tracheal aspirate fluid) in**
601 **zymograms.** Three different protein masses of 3 patients chosen at random were applied
602 per lane in gelatin (A) and casein (B) zymograms.

Suppl. Fig. 1

gelatin-zym

casein-zym
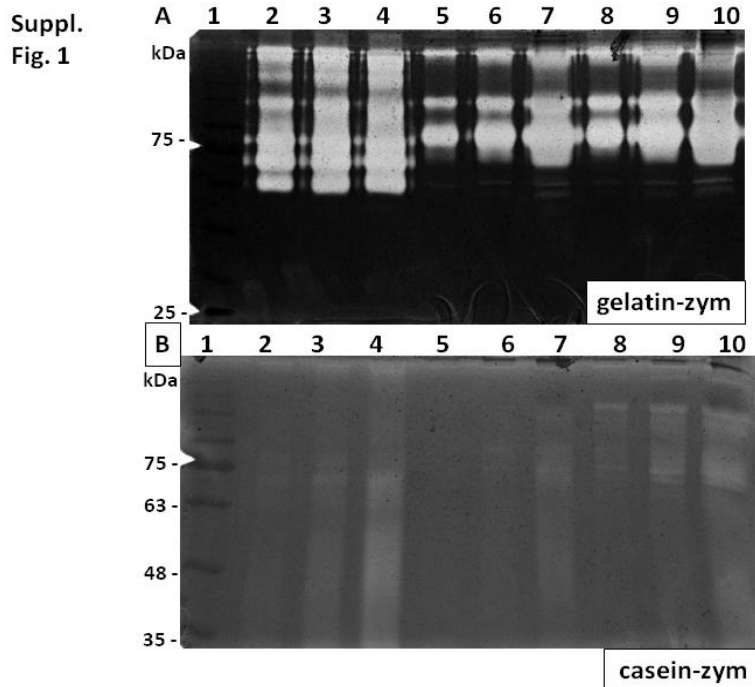
603

604 **A:** Twelve percent gelatin zymogram stained with Coomassie Brilliant Blue.
605 Lane 1: Prestained BluEye Protein Ladder (Sigma), with 75- and 25-kDa
606 markers indicated based on cuts made on the gel prior to staining with
607 Coomassie Brilliant Blue. Lanes 2-4: (non-Covid-19), Lanes 5-7: patient
608 Survival, Lanes 8-10: patient Non-survival (0.1; 0.3; 0.5 ug of protein),
609 respectively. **B:** Twelve percent casein zymogram stained with Coomassie
610 Brilliant Blue. The staining is fainter than the zymogram in A, as casein
611 usually stains less. Exactly the same amounts of total protein from TAF from
612 the same patients loaded in the same lanes of gel A were applied.

613 **Supplementary Figure 2 - Initial Screening of TAF (tracheal aspirate fluid) in**

614 **zymograms regarding the main class of protease present in the patient samples.** Two

615 different protein masses of 3 patients were applied per lane in gelatin zymograms.

616 Zymogram shown in A was incubated with the regular Tris-HCl/CaCl$_2$ buffer (the

617 zymogram buffer), while gels B and C were incubated overnight with 1 mM

618 Phenanthroline and 1mM PMSF, respectively.

619
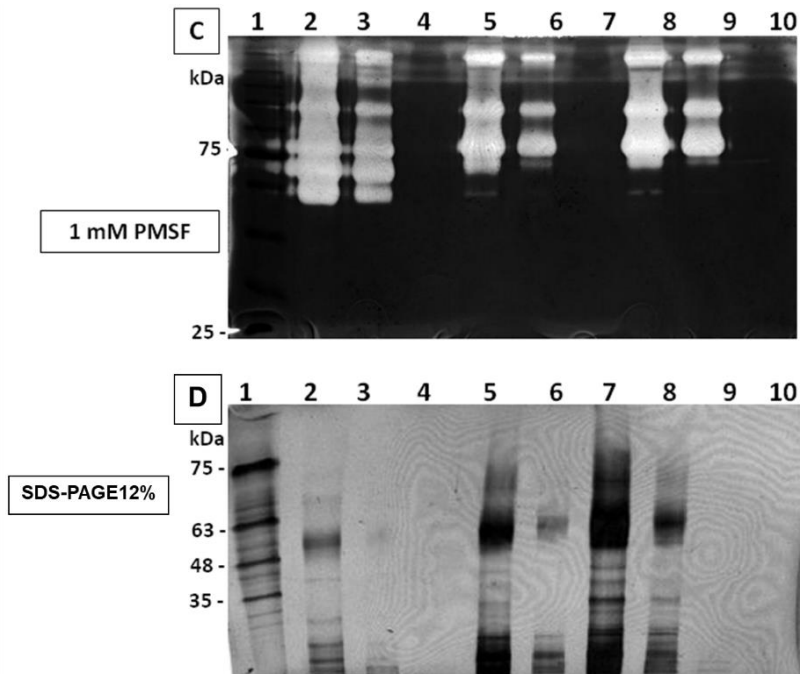
A: Twelve percent gelatin zymogram stained with Coomassie Brilliant Blue after overnight incubation in Tris-HCl/CaCl$_2$ buffer (the zymogram buffer). Lane 1: Prestained BluEye Protein Ladder (Sigma), with 75- and 25-kDa markers indicated based on cuts made on the gel prior to staining with Coomassie Brilliant Blue. Lanes 2-3: (0.05 ug; 0.15 ug of protein) non-Covid-19, Lanes 5-6: (0.05 ug; 0.15 ug of protein) patient Survival, Lanes 8-9: patient Non-survival (0.05; 0.15; ug of protein), Lanes 4, 7,10 empty respectively. **B:** Twelve percent gelatin zymogram stained with Coomassie Brilliant Blue. The whole gel was incubated overnight in the zymogram buffer containing 1 mM Phenanthroline. The samples and protein masses loaded are equal to gel A.**C:** Twelve percent gelatin zymogram stained with Coomassie Brilliant Blue. The whole gel was incubated overnight in the zymogram buffer containing 1 mM Phenyl-methyl-sulphonylfluoride (PMSF) at 1 mM. The samples and protein masses loaded are equal to gel A. **D**: Twelve percent SDS-PAGE gel stained with silver nitrate. Lanes 2-3: non-Covid-19, Lanes 5-6: patient Survival, Lanes 7-8: patient Non-survival (10 ug of protein), Lanes 4, 9,10 empty respectively.

Supplementary Figure 3. Representative gelatin zymogram gels of TAF (tracheal aspirate fluid) samples of COVID patients and controls.

Supple. Fig. 3
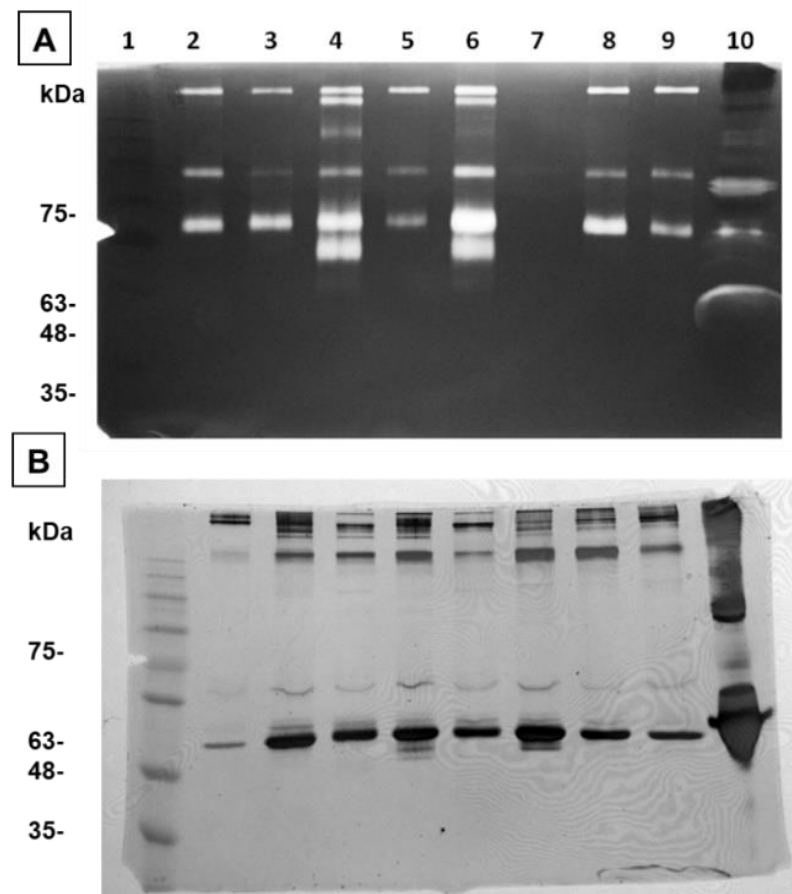
A: Twelve percent SDS-PAGE gel stained with Coomassie Brilliant Blue. Lane 1: Prestained BluEye Protein Ladder (Sigma). Lanes 2 and 3: two control patients (non-Covid-19) that were in the same hospital, but were negative for COVID19. Lanes 4-7: samples from 4 critical SARS-COV-2-infected patients that died (Survival). Lanes 8-9: 2 samples from 2 critical SARS-COV-2-infected patients that non-survived (0.5 ug of protein). Lane 10: Fetal Bovine Serum. B: Twelve percent SDS-PAGE gel stained with silver nitrate. Lanes 2 and 3: two control patients (non-Covid-19) that were in the same hospital but were negative for COVID19. Lanes 4-7: samples from 4 critical SARS-COV2-infected patients that died (Survival). Lanes 8-9: 2 samples from 2 critical SARS-COV2-infected patients that non-survived (10 ug of protein). Lane 10: Fetal Bovine Serum.

Supplementary Table 1. Information about p-value of proteomics reanalyses.

Uniprot ID	Gene name	t	df	pvalue	p.adj
A0A0U1RRL7	MMP24OS	-0,346208644	7,628149286	0,738540407	0,846135094
O75900	MMP23B	1,451850712	6,237048395	0,194919826	0,373242517
P03956	MMP1	-2,049951361	6,608866347	0,081918071	0,215555977
P08253	MMP2	-2,124596412	15,76382051	0,049799151	0,158060835

P09237	MMP7	-2,229832893	13,83080463	0,042860756	0,142757009
P09238	MMP10	-1,75417077	9,010757184	0,113257492	0,26319364
P14780	MMP9	-0,978116457	30,19615568	0,335788517	0,524411715
P22894	MMP8	-2,077762291	26,05263093	0,047724825	0,153479323
P39900	MMP12	1,817928401	7,998976205	0,106594355	0,253771147
P50281	MMP14	-5,382421924	26,68595537	1,13231E-05	0,00050751
P51511	MMP15	3,089793801	6,098825536	0,020946559	0,090643843
Q99542	MMP19	-0,959149878	7,441432919	0,367604031	0,554444983
Q9H239	MMP28	0,519408714	5,91404534	0,622333043	0,767059358

652

683 **Institutional Review Board Statement:** The study was carried out according to the

684 guidelines of the Declaration of Helsinki, and was approved by the Institutional Review

685 Board (or Ethics Committee) of Faculdade de CiênciasFarmacêuticas de Ribeirão Preto-

686 Universidade de São Paulo and Brazil National Ethics Committee (CONEP), CAAE:

687 30525920.7.0000.5403.

688 **Informed Consent Statement:** Informed consent was obtained from all subjects involved

689 in the study.

690 **Data Availability Statement:** All data generated or analyzed during this study are

691 included in this published article and its preprint manuscript form:

692 https://doi.org/10.1016/j.cell.2021.01.004.

702 **Conflicts of Interest:** The authors declare no conflict of interest.

703 **Appendix A. IMMUNOCOVID Study Group**

704 Jamille G. M. Argolo, Ingryd Carmona-Garcia, Nicola T. Neto, Ana C. Xavier, Gio-vanna
705 da S. Porcel, Isabelle C. Guarneri, Kamila Zaparoli, Caroline T. Garbato, Ângelo A. F.
706 Júnior from Escola de Enfermagem de Ribeirão Preto-EERP-Universidade de São Pau-lo-
707 USP, Ribeirão Preto/SP, Brazil. Leticia F. Constant, Alessandro P. de Amorim, Dayane P.
708 da Silva, Debora C. Nepomuceno, Rafael C. da Silva from Hospital Santa Casa de Miseri-
709 córdia de Ribeirão Preto, Ribeirão Preto/SP, Brazil. Rita de C. C. Barbieri from Hospital
710 São Paulo, Ribeirão Preto/SP, Brazil. Cristiane M. Milanezi from Departamento de
711 Bioquímica e Imunologia, Faculdade de Medicina de Ribeirão Preto-FMRP, Universidade
712 de São Pau-lo-USP, Ribeirão Preto/SP, Brazil. Cassia F. S. L. Dias from Departamento de
713 AnálisesClí-nicas, Toxicológicas e Bromatológicas, Faculdade de CiênciasFramacêuticas
714 de Ribeirão Preto-FCFRP, Universidade de São Paulo-USP, Ribeirão Preto/SP, Brazil.

715 **6. References**

716 1. Victora, C.G.; Castro, M.C.; Gurzenda, S.; Medeiros, A.C.; França, G.V.A.; Barros,
717 A.J.D. Estimating the Early Impact of Vaccination against Covid-19 on Deaths among
718 Elderly People in Brazil: Analyses of Routinely-Collected Data on Vaccine Coverage and
719 Mortality. *eClinicalMedicine***2021**, *38*, 101036.
720 https://doi.org/10.1016/j.eclinm.2021.101036.
721 2. Berlin, D.A.; Gulick, R.M.; Martinez, F.J. Severe Covid-19. *N. Engl. J. Med.* **2020**,
722 *383*, 2451–2460. https://doi.org/10.1056/nejmcp2009575.
723 3. CDC Covid-19 Response Team. Severe Outcomes Among Patients with
724 Coronavirus Disease 2019 (Covid-19)—United States, 12 February–16 March 2020.
725 *MMWR Morb. Mortal. Wkly. Rep.***2020**, *69*, 343–346.
726 https://doi.org/10.15585/Mmwr.Mm6912e2.
727 4. Bhatraju, P.K.; Ghassemieh, B.J.; Nichols, M.; Kim, R.; Jerome, K.R.; Nalla, A.K.;
728 Greninger, A.L.; Pipavath, S.; Wurfel, M.M.; Evans, L.; et al. Covid-19 in Critically Ill
729 Patients in the Seattle Region—Case Series. *N. Engl. J. Med.* **2020**, *382*, 2012–2022.
730 https://doi.org/10.1056/nejmoa2004500.
731 5. Guan, W.; Ni, Z.; Hu, Y.; Liang, W.; Ou, C.; He, J.; Liu, L.; Shan, H.; Lei, C.; Hui,
732 D.S.C.; et al. Clinical Characteristics of Coronavirus Disease 2019 in China. *N. Engl. J.
733 Med.* **2020**, *382*, 1708–1720. https://doi.org/10.1056/nejmoa2002032.
734 6. Xie, J.; Wu, W.; Li, S.; Hu, Y.; Hu, M.; Li, J.; Yang, Y.; Huang, T.; Zheng, K.;
735 Wang, Y.; et al. Clinical Characteristics and Outcomes of Critically Ill Patients with Novel

Coronavirus Infectious Disease (Covid-19) in China: A Retrospective Multicenter Study. *Intensive Care Med.* **2020**, *46*, 1863–1872. https://doi.org/10.1007/s00134-020-06211-2.

7.   Malemud, C.J. Matrix Metalloproteinases (MMPs) in Health and Disease: An Overview. *Front. Biosci.* **2006**, *11*, 1696–1701.

8.   Fernandez-Patron, C.; Martinez-Cuesta, M.A.; Salas, E.; Sawicki, G.; Wozniak, M.; Radomski, M.W.; Davidge, S.T. Differential Regulation of Platelet Aggregation by Matrix Metalloproteinases-9 and -2. *Thromb. Haemost.* **1999**, *82*, 1730–1735. https://doi.org/10.1055/s-0037-1614906.

9.   Greenlee, K.J.; Werb, Z.; Kheradmand, F. Matrix Metalloproteinases in Lung: Multiple, Multifarious, and Multifaceted. *Physiol. Rev.* **2007**, *87*, 69–98.

10.   D'Avila-Mesquita, C.; Couto, A.E.S.; Campos, L.C.B.; Vasconcelos, T.F.; Michelon-Barbosa, J.; Corsi, C.A.C.; Mestriner, F.; Petroski-Moraes, B.C.; Garbellini-Diab, M.J.; Couto, D.M.S.; et al. MMP-2 and MMP-9 Levels in Plasma Are Altered and Associated with Mortality in Covid-19 Patients. *Biomed. Pharmacother.* **2021**, *142*, 112067. https://doi.org/10.1016/j.biopha.2021.112067.

11.   Nagaset, H.; Woessner, J.F. Matrix Metalloproteinases. *J. Biol. Chem.* **1999**, *274*, 21491–21494.

12.   Johnson, L.L.; Dyer, R.; Hupe, D.J. Matrix Metalloproteinases. *Curr. Opin. Chem. Biol.* **1998**, *2*, 466–471. https://doi.org/10.1016/S1367-5931(98)80122-1.

13.   Fernandez-Patron, C.; Kassiri, Z.; Leung, D. Modulation of Systemic Metabolism by MMP-2: From MMP-2 Deficiency in Mice to MMP-2 Deficiency in Patients. *Compr. Physiol.* **2016**, *6*, 1935–1949. https://doi.org/10.1002/cphy.c160010.

14.   Baricordi, O.; Stignani, M.; Melchiorri, L.; Rizzo, R. HLA-G and Inflammatory Diseases. *Inflamm. Allergy Drug Targets* **2008**, *7*, 67–74.

15.   Gómez-Piña, V.; Soares-Schanoski, A.; Rodríguez-Rojas, A.; del Fresno, C.; García, F.; Vallejo-Cremades, M.T.; Fernández-Ruiz, I.; Arnalich, F.; Fuentes-Prior, P.; López-Collazo, E. Metalloproteinases Shed TREM-1 Ectodomain from Lipopolysaccharide-Stimulated Human Monocytes. *J. Immunol.* **2007**, *179*, 4065–4073. https://doi.org/10.4049/jimmunol.179.6.4065.

16.   Demaria, S.; Schwab, R.; Gottesman, S.R.S.; Bushkin, Y. Soluble B2-Microglobulin-Free Class I Heavy Chains Are Released from the Surface of Activated and Leukemia Cells by a Metalloprotease. *J. Biol. Chem.* **1994**, *269*, 6689–6694. https://doi.org/10.1016/s0021-9258(17)37430-6.

769 17. Zidi, I.; Guillard, C.; Marcou, C.; Krawice-Radanne, I.; Sangrouber, D.; Rouas-
770 Freiss, N.; Carosella, E.D.; Moreau, P. Increase in *63*, 2669–2681. https://doi.org/10HLA-
771 G1 Proteolytic Shedding by Tumor Cells: A Regulatory Pathway Controlled by NF-KB
772 Inducers. *Cell. Mol. Life Sci.* **2006**, .1007/s00018-006-6341-y.

773 18. Dong, Y.; Lieskovska, J.; Kedrin, D.; Porcelli, S.; Mandelboim, O.; Bushkin, Y.
774 Soluble Nonclassical HLA Generated by the Metalloproteinase Pathway. *Hum. Immunol.*
775 **2003**, *64*, 802–810. https://doi.org/10.1016/S0198-8859(03)00093-4.

776 19. Bonam, S.R.; Kotla, N.G.; Bohara, R.A.; Rochev, Y.; Webster, T.J.; Bayry, J.
777 Potential Immuno-Nanomedicine Strategies to Fight Covid-19 like Pulmonary Infections.
778 *Nano Today* **2021**, *36*, 101051.

779 20. Chen, N.; Zhou, M.; Dong, X.; Qu, J.; Gong, F.; Han, Y.; Qiu, Y.; Wang, J.; Liu,
780 Y.; Wei, Y.; et al. Epidemiological and Clinical Characteristics of 99 Cases of 2019 Novel
781 Coronavirus Pneumonia in Wuhan, China: A Descriptive Study. *Lancet* **2020**, *395*, 507–
782 513. https://doi.org/10.1016/S0140-6736(20)30211-7.

783 21. Narasaraju, T.; Tang, B.M.; Herrmann, M.; Muller, S.; Chow, V.T.K.; Radic, M.
784 Neutrophilia and NETopathy as Key Pathologic Drivers of Progressive Lung Impairment
785 in Patients With Covid-19. *Front. Pharmacol.* **2020**, *11*, 11.
786 https://doi.org/10.3389/fphar.2020.00870.

787 22. Menter, T.; Haslbauer, J.D.; Nienhold, R.; Savic, S.; Hopfer, H.; Deigendesch, N.;
788 Frank, S.; Turek, D.; Willi, N.; Pargger, H.; et al. Postmortem Examination of Covid-19
789 Patients Reveals Diffuse Alveolar Damage with Severe Capillary Congestion and
790 Variegated Findings in Lungs and Other Organs Suggesting Vascular Dysfunction.
791 *Histopathology* **2020**, *77*, 198–209. https://doi.org/10.1111/his.14134.

792 23. Wichmann, D.; Sperhake, J.P.; Lütgehetmann, M.; Steurer, S.; Edler, C.;
793 Heinemann, A.; Heinrich, F.; Mushumba, H.; Kniep, I.; Schröder, A.S.; et al. Autopsy
794 Findings and Venous Thromboembolism in Patients with Covid-19: A Prospective Cohort
795 Study. *Ann. Intern. Med.* **2020**, *173*, 268–277. https://doi.org/10.7326/M20-2003.

796 24. Varga, Z.; Flammer, A.J.; Steiger, P.; Haberecker, M.; Andermatt, R.; Zinkernagel,
797 A.S.; Mehra, M.R.; Schuepbach, R.A.; Ruschitzka, F.; Moch, H. Endothelial Cell Infection
798 and Endotheliitis in Covid-19. *Lancet* **2020**, *395*, 1417–1418.

799 25. George, P.M.; Wells, A.U.; Jenkins, R.G. Pulmonary Fibrosis and Covid-19: The
800 Potential Role for Antifibrotic Therapy. *Lancet Respir. Med.* **2020**, *8*, 807–815.

801   26.   Legrand, C.; Gilles, C.; Zahm, J.M.; Polette, M.; Buisson, A.C.; Kaplan, H.;
802 Birembaut, P.; Tournier, J.M. Airway Epithelial Cell Migration Dynamics: MMP-9 Role in
803 Cell- Extracellular Matrix Remodeling. *J. Cell Biol.* **1999**, *146*, 517–529.
804 https://doi.org/10.1083/jcb.146.2.517.

805   27.   Tetley, T.D. Proteinase Imbalance: Its Role in Lung Disease. *Thorax* **1993**, *48*, 560–
806 565.

807   28.   Shields, M.D.; Riedler, J. Bronchoalveolar Lavage and Tracheal Aspirate for
808 Assessing Airway Inflammation in Children. *Am. J. Respir. Crit. Care Med.* **2000**, *162*,
809 S15–S17.

810   29.   Gerlach, R.F.; Uzuelli, J.A.; Souza-Tarla, C.D.; Tanus-Santos, J.E. Effect of
811 Anticoagulants on the Determination of Plasma Matrix Metalloproteinase (MMP)-2 and
812 MMP-9 Activities. *Anal. Biochem.* **2005**, *344*, 147–149.
813 https://doi.org/10.1016/j.ab.2005.04.038.

814   30.   Bradford, M.M. A Rapid and Sensitive Method for the Quantitation of Microgram
815 Quantities of Protein Utilizing the Principle of Protein-Dye Binding. *Anal. Biochem.* **1976**,
816 *72*, 248–254. https://doi.org/10.1016/0003-2697(76)90527-3.

817   31.   Martelli-Palomino, G.; Pancotto, J.A.; Muniz, Y.C.; Mendes-Junior, C.T.; Castelli,
818 E.C.; Massaro, J.D.; Krawice-Radanne, I.; Poras, I.; Rebmann, V.; Carosella, E.D.; et al.
819 Polymorphic Sites at the 3′ Untranslated Region of the HLA-G Gene Are Associated with
820 Differential Hla-g Soluble Levels in the Brazilian and French Population. *PLoS ONE* **2013**,
821 *8*, e71742. https://doi.org/10.1371/journal.pone.0071742.

822   32.   Tsikas, D. Assessment of Lipid Peroxidation by Measuring Malondialdehyde
823 (MDA) and Relatives in Biological Samples: Analytical and Biological Challenges. *Anal.*
824 *Biochem.* **2017**, *524*, 13–30. https://doi.org/10.1016/j.ab.2016.10.021.

825   33.   Montenegro, M.F.; Pessa, L.R.; Gomes, V.A.; Desta, Z.; Flockhart, D.A.; Tanus-
826 Santos, J.E. Assessment of Vascular Effects of Tamoxifen and Its Metabolites on the Rat
827 Perfused Hindquarter Vascular Bed. *Basic Clin. Pharmacol. Toxicol.* **2009**, *104*, 400–407.
828 https://doi.org/10.1111/j.1742-7843.2009.00377.x.

829   34.   Corman, V.M.; Landt, O.; Kaiser, M.; Molenkamp, R.; Meijer, A.; Chu, D.K.W.;
830 Bleicker, T.; Brünink, S.; Schneider, J.; Schmidt, M.L.; et al. Detection of 2019 Novel
831 Coronavirus (2019-NCoV) by Real-Time RT-PCR. *Eurosurveillance* **2020**, *25*, 2000045.
832 https://doi.org/10.2807/1560-7917.ES.2020.25.3.2000045.

833   35.   *CDC 2019-Novel Coronavirus (2019-NCoV) Real-Time RT-PCR Diagnostic Panel*
834   *For Emergency Use Only Instructions for Use*; Centers for Disease Control and
835   Prevention: Atlanta, GA, USA, 2021.

836   36.   Pontelli, M.C.; Castro, I.A.; Martins, R.B.; Veras, F.P.; la Serra, L.; Nascimento,
837   D.C.; Cardoso, R.S.; Rosales, R.; Lima, T.M.; Souza, J.P.; et al. Infection of Human
838   Lymphomononuclear   Cells   by   SARS-CoV-2.   *bioRxiv***2020**.
839   https://doi.org/10.1101/2020.07.28.225912.

840   37.   Nie, X.; Qian, L.; Sun, R.; Huang, B.; Dong, X.; Xiao, Q.; Zhang, Q.; Lu, T.; Yue,
841   L.; Chen, S.; et al. Multi-Organ Proteomic Landscape of Covid-19 Autopsies. *Cell***2021**,
842   *184*, 775–791.e14. https://doi.org/10.1016/j.cell.2021.01.004.

843   38.   Benjamini, Y.; Hochberg, Y. Controlling the False Discovery Rate—a Practical and
844   Powerful Approach to Multiple Testing. Journal of the Royal Statistical Society Series B-
845   Methodological 1995.Pdf. *J. R. Stat. Soc. Ser. B* **1995**, *57*, 289–300.

846   39.   R Development Core Team. *R a Language and Environment for Statistical*
847   *Computing : Reference Index*; R Foundation for Statistical Computing: City, Counrtry,
848   2010; ISBN 3900051070.

849   40.   Wickham, H. *Ggplot2: Elegant Graphics for Data Analysis*; Springer: New York,
850   NY, USA, 2016.

851   41.   da Silva-Neto, P.v.; de Carvalho, J.C.S.; Pimentel, V.E.; Pérez, M.M.; Toro, D.M.;
852   Fraga-Silva, T.F.C.; Fuzo, C.A.; Oliveira, C.N.S.; Rodrigues, L.C.; Argolo, J.G.M.; et al.
853   sTREM-1 Predicts Disease Severity and Mortality in Covid-19 Patients: Involvement of
854   Peripheral   Blood   Leukocytes   and   MMP-8   Activity.   *Viruses***2021**,   *13*,   2521.
855   https://doi.org/10.3390/v13122521.

856   42.   Rizzo, R.; Trentini, A.; Bortolotti, D.; Manfrinato, M.C.; Rotola, A.; Castellazzi,
857   M.; Melchiorri, L.; di Luca, D.; Dallocchio, F.; Fainardi, E.; et al. Matrix
858   Metalloproteinase-2 (MMP-2) Generates Soluble HLA-G1 by Cell Surface Proteolytic
859   Shedding. *Mol. Cell. Biochem.* **2013**, *381*, 243–255. https://doi.org/10.1007/s11010-013-
860   1708-5.

861   43.   Mittal, M.; Siddiqui, M.R.; Tran, K.; Reddy, S.P.; Malik, A.B. Reactive Oxygen
862   Species in Inflammation and Tissue Injury. *Antioxid. Redox Signal.* **2014**, *20*, 1126–1167.

863   44.   Liu, J.; Liu, Y.; Xiang, P.; Pu, L.; Xiong, H.; Li, C.; Zhang, M.; Tan, J.; Xu, Y.;
864   Song, R.; et al. Neutrophil-to-Lymphocyte Ratio Predicts Critical Illness Patients with

865 2019 Coronavirus Disease in the Early Stage. *J. Transl. Med.* **2020**, *18*, 206.

866 https://doi.org/10.1186/s12967-020-02374-0.

867 45. Ragab, D.; Eldin, H.S.; Taeimah, M.; Khattab, R.; Salem, R. The Covid-19

868 Cytokine Storm; What We Know So Far. *Front. Immunol.* **2020**, *11*, 1446.

869 46. Singh, K.; Mittal, S.; Gollapudi, S.; Butzmann, A.; Kumar, J.; Ohgami, R.S. A

870 Meta-Analysis of SARS-CoV-2 Patients Identifies the Combinatorial Significance of D-

871 Dimer, C-Reactive Protein, Lymphocyte, and Neutrophil Values as a Predictor of Disease

872 Severity. *Int. J. Lab. Hematol.* **2021**, *43*, 324–328. https://doi.org/10.1111/ijlh.13354.

873 47. Matthay, M.A.; Wick, K.D. Corticosteroids, Covid-19 Pneumonia, and Acute

874 Respiratory Distress Syndrome. *J. Clin. Investig.* **2020**, *130*, 6218–6221.

875 48. Parks, W.C.; Shapiro, S.D. Matrix Metalloproteinases in Lung Biology. *Respir.*

876 *Res.* **2001**, *2*, 3–9.

877 49. Kheradmand, F.; Rishi, K. The Role of Proteases in Airway Remodeling. In

878 *Therapeutic Targets in Airway Inflammation*; CRC Press: Boca Raton, FL, USA, 2003; pp.

879 18–19. https://doi.org/10.3109/9780203911471-39/role-proteases-airway-remodeling-

880 farrah-kheradmand-kirtee-rishi.

881 50. McKeown, S.; Richter, A.G.; O'Kane, C.; McAuley, D.F.; Thickett, D.R. MMP

882 Expression and Abnormal Lung Permeability Are Important Determinants of Outcome in

883 IPF. *Eur. Respir. J.* **2009**, *33*, 77–84. https://doi.org/10.1183/09031936.00060708.

884 51. Elkington, P.T.G.; Friedland, J.S. Matrix Metalloproteinases in Destructive

885 Pulmonary Pathology. *Thorax* **2006**, *61*, 259–266.

886 52. Pugin, J.; Verghese, G.; Widmer, M.C.; Matthay, M.A. The Alveolar Space Is the

887 Site of Intense Inflammatory and Profibrotic Reactions in the Early Phase of Acute

888 Respiratory Distress Syndrome. *Crit. Care Med.* **1999**, *27*, 304–312.

889 https://doi.org/10.1097/00003246-199902000-00036.

890 53. Atkinson, J.J.; Senior, R.M. Matrix Metalloproteinase-9 in Lung Remodeling. *Am.*

891 *J. Respir. Cell Mol. Biol.* **2003**, *28*, 12–24.

892 54. Wu, D.; Yang, X.O. Dysregulation of Pulmonary Responses in Severe Covid-19.

893 *Viruses* **2021**, *13*, 957. https://doi.org/10.3390/v13060957.

894 55. van Wart, H.E.; Birkedal-Hansen, H. The Cysteine Switch: A Principle of

895 Regulation of Metalloproteinase Activity with Potential Applicability to the Entire Matrix

896 Metalloproteinase Gene Family. *Proc. Natl. Acad. Sci. USA* **1990**, *87*, 5578–5582.

897 https://doi.org/10.1073/pnas.87.14.5578.

898 56.   Page-McCaw, A.; Ewald, A.J.; Werb, Z. Matrix Metalloproteinases and the
899 Regulation of Tissue Remodelling. *Nat. Rev. Mol. Cell Biol.* **2007**, *8*, 221–233.

900 57.   Yao, P.M.; Maitre, B.; Delacourt, G.; Buhler, J.M.; Harf, A.; Lafuma, C. Divergent
901 Regulation of 92-KDa Gelatinase and TIMP-1 by HBECs in Response to IL-1β and TNF-
902 α. *Am. J. Physiol. Lung Cell. Mol. Physiol.* **1997**, *273*, L866–L874.
903 https://doi.org/10.1152/ajplung.1997.273.4.l866.

904 58.   Schnaper, H.W.; Grant, D.S.; Stetler-Stevenson, W.G.; Fridman, R.; D'Orazi, G.;
905 Murphy, A.N.; Bird, R.E.; Hoythya, M.; Fuerst, T.R.; French, D.L.; et al. Type IV
906 Collagenase(s) and TIMPs Modulate Endothelial Cell Morphogenesis in Vitro. *J. Cell.*
907 *Physiol.* **1993**, *156*, 235–246. https://doi.org/10.1002/jcp.1041560204.

908 59.   Corry, D.B.; Rishi, K.; Kanellis, J.; Kiss, A.; Song, L.-Z.; Xu, J.; Werb, Z.;
909 Kheradmand, F. Decreased Allergic Lung Inflammatory Cell Egression and Increased
910 Susceptibility to Asphyxiation in MMP2-Deficiency. *Nat. Immunol.* **2002**, *3*, 347–353.
911 https://doi.org/10.1038/ni773.

912 60.   Campbell, L.G.; Ramachandran, S.; Liu, W.; Shipley, M.M.; Itohara, S.; Rogers,
913 J.G.; Moazami, N.; Senior, R.M.; Jaramillo, A. Different Roles for Matrix
914 Metalloproteinase-2 and Matrix Metalloproteinase-9 in the Pathogenesis of Cardiac
915 Allograft Rejection. *Am. J. Transplant.* **2005**, *5*, 517–528. https://doi.org/10.1111/j.1600-
916 6143.2005.00744.x.

917 61.   Owen, C.A.; Hu, Z.; Lopez-Otin, C.; Shapiro, S.D. Membrane-Bound Matrix
918 Metalloproteinase-8 on Activated Polymorphonuclear Cells Is a Potent, Tissue Inhibitor of
919 Metalloproteinase-Resistant Collagenase and Serpinase. *J. Immunol.* **2004**, *172*, 7791–
920 7803. https://doi.org/10.4049/jimmunol.172.12.7791.

921 62.   Parks, W.C.; Wilson, C.L.; López-Boado, Y.S. Matrix Metalloproteinases as
922 Modulators of Inflammation and Innate Immunity. *Nat. Rev. Immunol.* **2004**, *4*, 617–629.

923 63.   Faurschou, M.; Borregaard, N. Neutrophil Granules and Secretory Vesicles in
924 Inflammation. *Microbes Infect.* **2003**, *5*, 1317–1327.

925 64.   Cederqvist, K.; Sorsa, T.; Tervahartiala, T.; Maisi, P.; Reunanen, K.; Lassus, P.;
926 Andersson, S. Matrix Metalloproteinases-2, -8, and -9 and TIMP-2 in Tracheal Aspirates
927 from Preterm Infants with Respiratory Distress. *Pediatrics***2001**, *108*, 686–692.
928 https://doi.org/10.1542/peds.108.3.686.

929 65.   Kadry, R.; Newsome, A.S.; Somanath, P.R. Pharmacological Inhibition of MMP3
930 as a Potential Therapeutic Option for Covid-19 Associated Acute Respiratory Distress

931 Syndrome. *Infect. Disord. Drug Targets* **2020**, *21*, e170721187996.
932 https://doi.org/10.2174/1871526520666201116100310.

933 66. Gelzo, M.; Cacciapuoti, S.; Pinchera, B.; de Rosa, A.; Cernera, G.; Scialò, F.;
934 Comegna, M.; Mormile, M.; Fabbrocini, G.; Parrella, R.; et al. Matrix Metalloproteinases
935 (MMP) 3 and 9 as Biomarkers of Severity in Covid-19 Patients. *Sci. Rep.* **2022**, *12*, 1212.
936 https://doi.org/10.1038/s41598-021-04677-8.

937 67. van Lint, P.; Libert, C. Chemokine and Cytokine Processing by Matrix
938 Metalloproteinases and Its Effect on Leukocyte Migration and Inflammation. *J. Leukoc.*
939 *Biol.* **2007**, *82*, 1375–1381. https://doi.org/10.1189/jlb.0607338.

940 68. Rodríguez, D.; Morrison, C.J.; Overall, C.M. Matrix Metalloproteinases: What Do
941 They Not Do? New Substrates and Biological Roles Identified by Murine Models and
942 Proteomics. *Biochim. Et Biophys. Acta Mol. Cell Res.* **2010**, *1803*, 39–54.

943 69. Morandi, F.; Rizzo, R.; Fainardi, E.; Rouas-Freiss, N.; Pistoia, V. Recent Advances
944 in Our Understanding of HLA-G Biology: Lessons from a Wide Spectrum of Human
945 Diseases. *J. Immunol. Res.* **2016**, *2016*, 4326495.

946 70. Al-Bayatee, N.T.; Ad'hiah, A.H. Soluble HLA-G Is Upregulated in Serum of
947 Patients with Severe Covid-19. *Hum. Immunol.* **2021**, *82*, 726–732.
948 https://doi.org/10.1016/j.humimm.2021.07.007.

949 71. Zheng, H.; Heiderscheidt, C.A.; Joo, M.; Gao, X.; Knezevic, N.; Mehta, D.;
950 Sadikot, R.T. MYD88-Dependent and -Independent Activation of TREM-1 via Specific
951 TLR Ligands. *Eur. J. Immunol.* **2010**, *40*, 162–171. https://doi.org/10.1002/eji.200839156.

952 72. Weiss, G.; Lai, C.; Fife, M.E.; Grabiec, A.M.; Tildy, B.; Snelgrove, R.J.; Xin, G.;
953 Lloyd, C.M.; Hussell, T. Reversal of TREM-1 Ectodomain Shedding and Improved
954 Bacterial Clearance by Intranasal Metalloproteinase Inhibitors. *Mucosal Immunol.* **2017**,
955 *10*, 1021–1030. https://doi.org/10.1038/mi.2016.104.

956 73. Strongin, A.Y.; Collier, I.; Bannikov, G.; Marmer, B.L.; Grant, G.A.; Goldberg,
957 G.I. Mechanism of Cell Surface Activation of 72-KDa Type IV Collagenase. *J. Biol.*
958 *Chem.* **1995**, *270*, 5331–5338. https://doi.org/10.1074/jbc.270.10.5331.

959 74. Dozier, S.; Escobar, G.; Lindsey, M. Matrix Metalloproteinase (MMP)-7 Activates
960 MMP-8 But Not MMP-13. *Med. Chem.* **2006**, *2*, 523–526.
961 https://doi.org/10.2174/157340606778250261.

962 75. Solun, B.; Shoenfeld, Y. Inhibition of Metalloproteinases in Therapy for Severe

963 Lung Injury Due to Covid-19. *Med. Drug Discov.* **2020**, *7*, 100052.

964 https://doi.org/10.1016/j.medidd.2020.100052.

965 76. Touyz, R.M.; Rios, F.J.; Alves-Lopes, R.; Neves, K.B.; Camargo, L.L.; Montezano,

966 A.C. Oxidative Stress: A Unifying Paradigm in Hypertension. *Can. J. Cardiol.* **2020**, *36*,

967 659–670.

968 77. Rajagopalan, S.; Meng, X.P.; Ramasamy, S.; Harrison, D.G.; Galis, Z.S. Reactive

969 Oxygen Species Produced by Macrophage-Derived Foam Cells Regulate the Activity of

970 Vascular Matrix Metalloproteinases in Vitro: Implications for Atherosclerotic Plaque

971 Stability. *J. Clin. Investig.* **1996**, *98*, 2572–2579. https://doi.org/10.1172/JCI119076.

972 78. Migita, K.; Maeda, Y.; Abiru, S.; Komori, A.; Yokoyama, T.; Takii, Y.; Nakamura,

973 M.; Yatsuhashi, H.; Eguchi, K.; Ishibashi, H. Peroxynitrite-Mediated Matrix

974 Metalloproteinase-2 Activation in Human Hepatic Stellate Cells. *FEBS Lett.* **2005**, *579*,

975 3119–3125. https://doi.org/10.1016/j.febslet.2005.04.071.

976 79. Viappiani, S.; Nicolescu, A.C.; Holt, A.; Sawicki, G.; Crawford, B.D.; León, H.;

977 van Mulligen, T.; Schulz, R. Activation and Modulation of 72 KDa Matrix

978 Metalloproteinase-2 by Peroxynitrite and Glutathione. *Biochem. Pharmacol.* **2009**, *77*,

979 826–834. https://doi.org/10.1016/j.bcp.2008.11.004.

980 80. Prado, A.F.; Pernomian, L.; Azevedo, A.; Costa, R.A.P.; Rizzi, E.; Ramos, J.; Paes

981 Leme, A.F.; Bendhack, L.M.; Tanus-Santos, J.E.; Gerlach, R.F. Matrix Metalloproteinase-

982 2-Induced Epidermal Growth Factor Receptor Transactivation Impairs Redox Balance in

983 Vascular Smooth Muscle Cells and Facilitates Vascular Contraction. *Redox Biol.* **2018**, *18*,

984 181–190. https://doi.org/10.1016/j.redox.2018.07.005.

985 81. Galis, Z.S.; Khatri, J.J. Matrix Metalloproteinases in Vascular Remodeling and

986 Atherogenesis: The Good, the Bad, and the Ugly. *Circ. Res.* **2002**, *90*, 251–262.

987 82. Stephenson, E.; Reynolds, G.; Botting, R.A.; Calero-Nieto, F.J.; Morgan, M.D.;

988 Tuong, Z.K.; Bach, K.; Sungnak, W.; Worlock, K.B.; Yoshida, M.; et al. Single-Cell

989 Multi-Omics Analysis of the Immune Response in Covid-19. *Nat. Med.* **2021**, *27*, 904–

990 916. https://doi.org/10.1038/s41591-021-01329-2.

991 83. Ren, X.; Wen, W.; Fan, X.; Hou, W.; Su, B.; Cai, P.; Li, J.; Liu, Y.; Tang, F.;

992 Zhang, F.; et al. Covid-19 Immune Features Revealed by a Large-Scale Single-Cell

993 Transcriptome Atlas. *Cell***2021**, *184*, 1895–1913.e19.

994 https://doi.org/10.1016/j.cell.2021.01.053.

995   84.   Huang, C.; Wang, Y.; Li, X.; Ren, L.; Zhao, J.; Hu, Y.; Zhang, L.; Fan, G.; Xu, J.;
996   Gu, X.; et al. Clinical Features of Patients Infected with 2019 Novel Coronavirus in
997   Wuhan. *Lancet* **2020**, *395*, 497–506. https://doi.org/10.1016/S0140-6736(20)30183-5.

998   85.   Kuwano, K. Epithelial Cell Apoptosis and Lung Remodeling. *Cell. Mol. Immunol.*
999   **2007**, *4*, 419–429.

1000 86.   Gropper, M.A.; Wiener-Kronish, J. The Epithelium in Acute Lung Injury/Acute
1001 Respiratory Distress Syndrome. *Curr. Opin. Crit. Care* **2008**, *14*, 11–15.

1002 87.   Hotchkiss, R.S.; Monneret, G.; Payen, D. Immunosuppression in Sepsis: A Novel
1003 Understanding of the Disorder and a New Therapeutic Approach. *Lancet Infect. Dis.* **2013**,
1004 *13*, 260–268.

1005 88.   Amodio, G.; de Albuquerque, R.S.; Gregori, S. New Insights into HLA-G Mediated
1006 Tolerance. *Tissue Antigens* **2014**, *84*, 255–263.

1007 89.   Fraga-Silva, T.F.d.C.; Maruyama, S.R.; Sorgi, C.A.; Russo, E.M.d.S.; Fernandes,
1008 A.P.M.; de Barros Cardoso, C.R.; Faccioli, L.H.; Dias-Baruffi, M.; Bonato, V.L.D. Covid-
1009 19: Integrating the Complexity of Systemic and Pulmonary Immunopathology to Identify
1010 Biomarkers for Different Outcomes. *Front. Immunol.* **2021**, *11*, 599736.

6.3. Capítulo III- Expressão de miRNAs relacionados com a via de TREM-1 durante a infecção pelo SARS-CoV-2.

Sabendo que os miRNAs são moléculas de RNA de tamanho pequeno, que estão envolvidas na regulação fina da expressão gênica, principalmente através da ligação de transcritos alvos. Assim como, durante a infecção pelo SARS-CoV-2 ocorre um aumento nos níveis séricos de sTREM-1 posteriormente correlacionado com o comprometimento da função pulmonar. Levantamos a hipótese de que os miRNAs poderiam desempenhar um papel significativo na regulação de TREM-1 e envolvidos na patogênese da Covid-19, pois o mecanismo relacionado a esta via ainda não está claro e requer mais pesquisas.

Realizamos uma análise em conjuntos de dados de transcriptoma de RNA (RNA-seq) dos pacientes em diferentes gravidades. O diagrama demonstrando no heatmap (**Figura 11 A**) mostra a análise da expressão diferencial classificados de acordo com a ordem de agrupamento. Podemos verificar que os fatores como, RFX-4, HOXB3, GATA-4, AIRE, SUMO-2, MYBL-2, IRF4, XBP-1, MEIS-1, HOXD8, CUX-1, SPI-1, ARID3A, START-5A, ERG e o miRNA650 estavam regulados positivamente e estiveram relacionados com a doença grave. Além disso, os genes ATF-2, BRD-4, GATA-1, STAG-1, GATA-2, TCF-7, MYC, ETS-1, KLF-12, EGR-1 e FOS apresentaram regulações negativas em relação a gravidade.

A
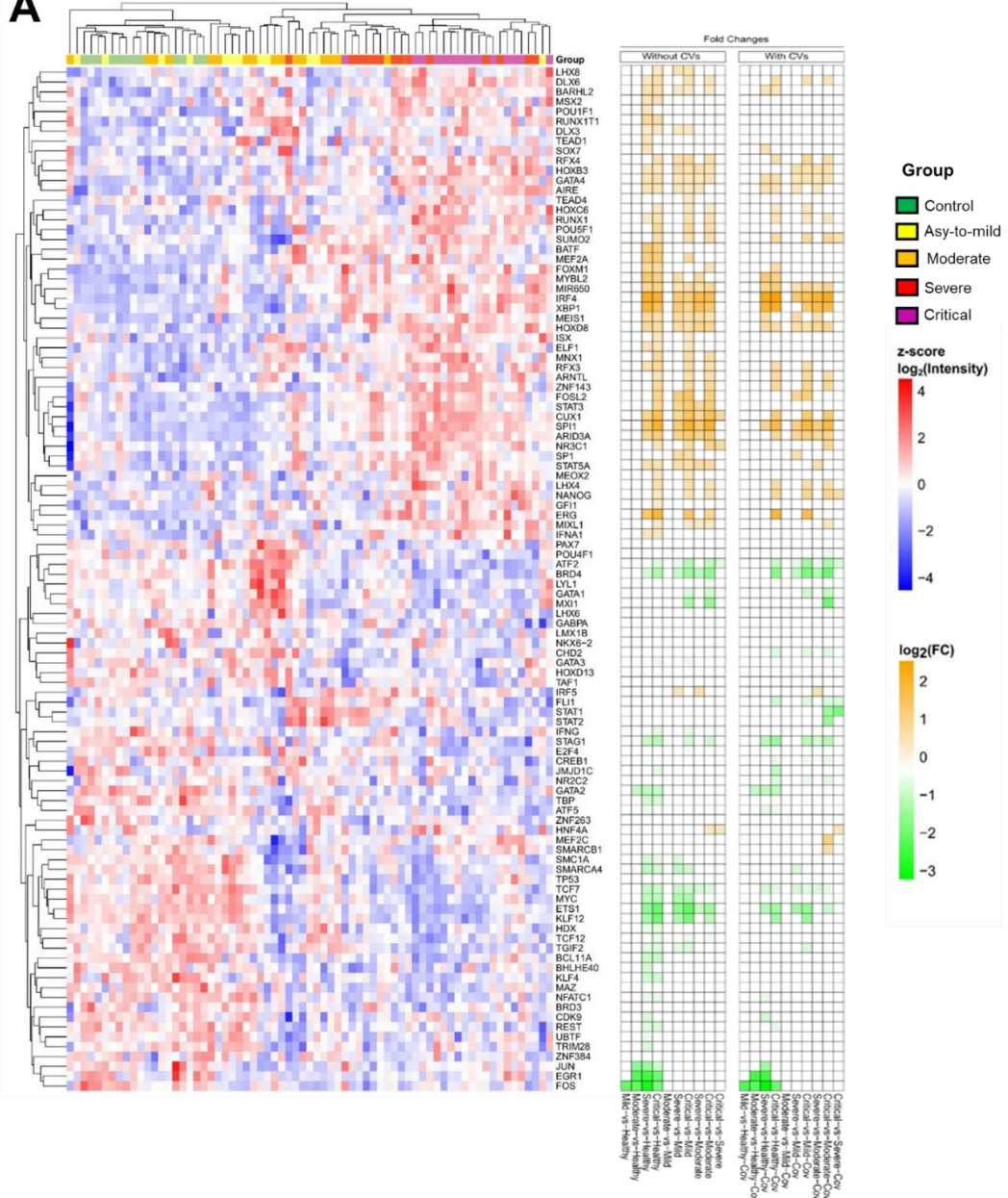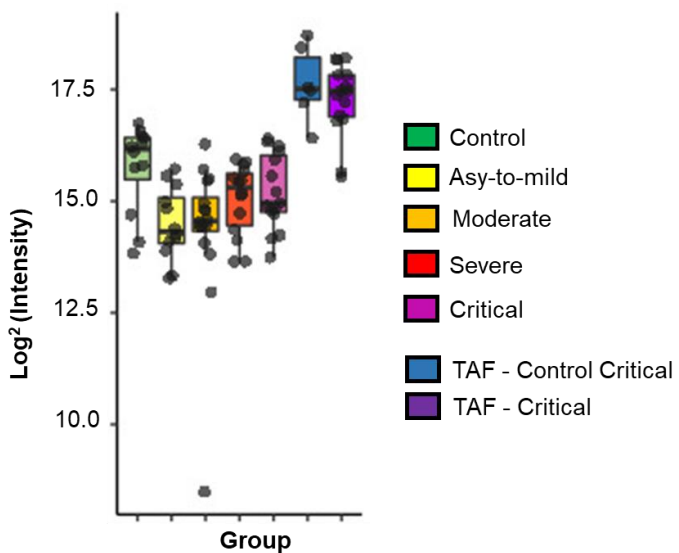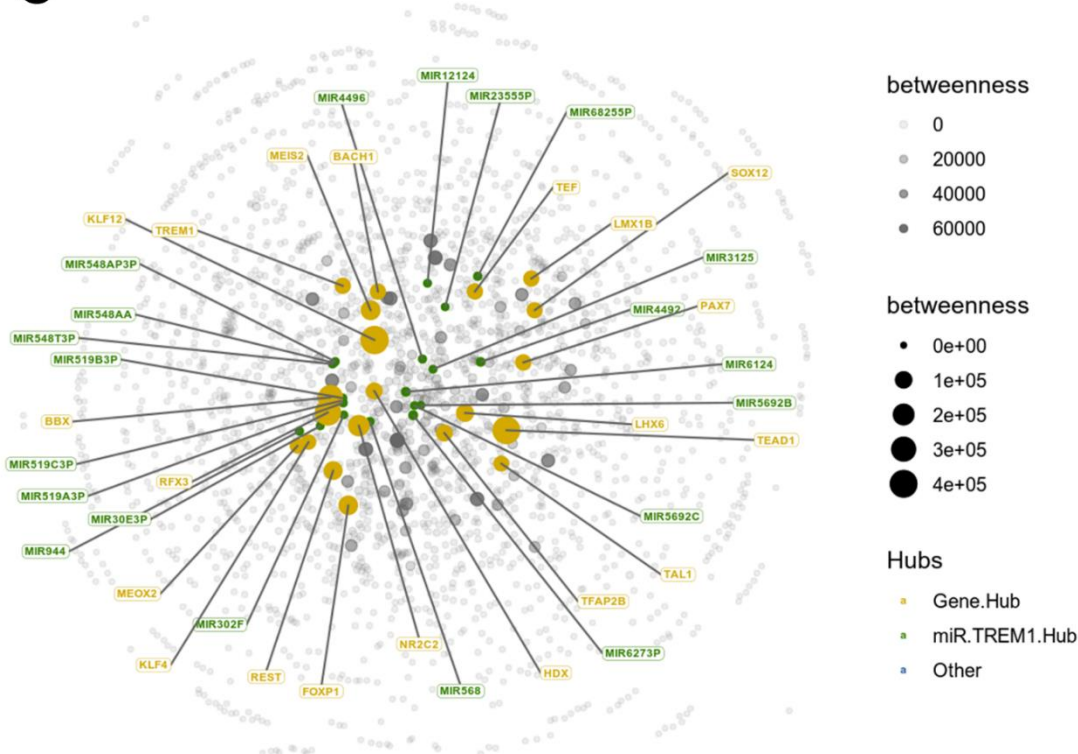
Figura 11. Perfil transcricional e rede biológica específica de miRNAs e genes em pacientes com Covid-19, correlacionados com o receptor TREM-1. (A) Perfil de expressão dos principais DEGs com base nos maiores valores de interação do gene de TREM-1. O diagrama do heatmap mostra o Log2 (*Fold Change*) obtido a partir da análise da expressão diferencial. Os valores Log2 (Fold Change) dos genes foram classificados de acordo com a ordem de agrupamento. A escala de cores do Log2 (*Fold Change*) foi limitada a um intervalo de -2 a +2. (B) A expressão de TREM-1 é expressa em Log_2 por *boxplot*. (C) Análise de rede biológica de co-expressão de genes de miRNAs interagindo com a via de TREM-1. Análise da representação

de Gene Hub e miRNAs, a intensidade da cor e tamanho da esfera ao nível de interação genes relacionados a via de TREM-1. Os círculos verdes representam os miRNA regulado e os amarelos os genes presentes como reguladores, respectivamente.

No que diz respeito ao gene de TREM-1 expresso diferencialmente nos grupos de gravidade, observamos uma tendência elevada em pacientes graves e críticos, assim como sua expressão no pulmão (**Figura 11B**). Após a análise de combinação identificamos aproximadamente 2.367 genes diferencialmente expressos presentes em amostras pulmão, selecionamos os primeiros 15 (**Tabela 5)** genes de fatores de transcrição e miRNAS que interagem com a via de TREM-1 (TREM1+TFs+miRNAs), presentes na rede biológica específica de miRNAs e co-expressão de genes em pacientes com Covid-19 relacionados a interação com o receptor TREM-1 (**Figura 11 C**).

Tabela 5. Reanálise dos dados de transcriptoma e as alterações de expressão nos genes relacionados a miRNAS presentes na via de TREM-1.

Genes	Relação	Grau	Interação	miRNAs	Relação
KLF12	TF for TREM1	533	423591.7879	miRNA-429	TREM1
TEAD1	TF for TREM1	510	402690.5547	miRNA-6793-5p	TREM1
RFX3	TF for TREM1	478	347209.6754	miRNA-642a-5p	TREM1
BBX	TF for TREM1	444	298841.258	miRNA-7-5p	TREM1
NR2C2	TF for TREM1	343	194519.3467	miRNA-1229-3p	TREM1
MEIS2	TF for TREM1	262	152231.2392	miRNA-4471	TREM1
FOXP1	TF for TREM1	275	147346.2116	miRNA-200c-3p	TREM1
REST	TF for TREM1	271	129809.8151	miRNA-200b-3p	TREM1
LHX6	TF for TREM1	233	112956.534	miRNA-4704-3P	TREM1
HDX	TF for	215	90520.71481	miRNA-4700-3p	TREM1

	TREM1				
TFAP2B	TF for TREM1	204	89759.09229	miRNA-944	TREM1
PAX7	TF for TREM1	185	81820.12888	miRNA-3923	TREM1
TEF	TF for TREM1	176	80714.46137	miRNA-548u	TREM1
TREM1	TREM1	171	79841.31036	miRNA-4639-5p	TREM1
BACH1	TF for TREM1	167	78899.63238	miRNA-4865p	TREM1

Descrito como um novo fator de transcrição expresso preferencialmente em células NK, o fator 12 semelhante a kruppel (KLF12) funciona com um repressor ou ativador transcricional, regulando a proliferação celular (243). Sua elevada expressão em células de câncer de pulmão e endométrio correlacionou-se com a diminuição de apoptose, aumento proliferativo e crescimento tumoral (244).

As células NK do pulmão exibem um fenótipo diferenciado, com alta capacidade de responder a infecções virais. No entanto, durante a infecção pelo SARS-CoV-2 foram observados números baixos de células NK no sangue periférico (127,245) e um número crescente destas células no lavado bronco alveolar de pacientes com Covid-19 grave (246), sugerindo que ao migrar para o tecido pulmonar, as células NK induzem processos de lise celular por meio de degranulação citotóxica de perforinas e granzima B e eliminação indireta pela produção de IFN-γ e TNF-α na células-alvo infectadas. Além de expressar o receptor TREM-1 que encontra-se associado à citotoxicidade das células NK (247).

Segundo outros trabalhos, a expressão aumentada de TEAD, RFX3, NR2C2, MEIS2 e TFAP2B, demonstra funções importantes durante os processos de regulação celular. Além disso, observamos suas ações durante episódios de estresse, hipóxia (248) diferenciação de células endócrinas pancreáticas (249), artrite (250), proliferação, diferenciação, migração e invasão de células cancerígenas, associados a um pior prognóstico dos pacientes (251–254)

Considerando a importância dos miRNAs, torna-se imprescindível identificar os miRNAs que regulam a patogênese da Covid-19 e vias inflamatórias que possam estar altamente expressas. Dentre os miRNAs encontrados, observamos a expressão dos

miRNA-429, miRNA-6793-5p, miRNA-642a-5p, miRNA-7-5p, miRNA-1229-3p, miRNA-4471, miRNA-200c-3p, miRNA-200b-3p, miRNA-4704-3p, miRNA-4700-3p, miRNA-944, miRNA-3923, miRNA-548u, miRNA-4639-5p, miRNA-4865p associados ao receptor TREM-1.

O miRNA429, miRNA7-5P, miRNA-944, foram descritos por atuarem com miRNAs supressores de tumor (255) responsável pela inibição da proliferação e migração celular de células cancerosas (256). Além disso, suprimem a diferenciação de células-tronco (257–259). Precursores plasmáticos circulantes de miRNA-944 são descritos como marcadores de precisão diagnóstica para detecção em câncer de pulmão de células não pequenas (260).

O hsa-miR-4639-5p apresenta um importante papel como indutor de estresse oxidativo grave e morte neuronal, estando associado como um biomarcador de diagnóstico periférico (261). A superexpressão do miRNA-486-5p pode estar associado a progressão da doença pulmonar obstrutiva crônica (DPOC), responsável por regular a resposta inflamatória desencadeada por TLR4 de macrófagos alveolares (262), e seus níveis plasmáticos elevados podem servir como um marcador de diagnóstico em câncer cervical (263) e carcinoma hepatocelular (264).

Observamos que miR-200c-3p também interage com o receptor TREM-1 durante a infecção pelo SARS-CoV-2. Durante a infecção pelo vírus H5N1, a expressão de miR-200c-3p foi regulada positivamente pela proteína NS1 e o RNA viral, tendo como alvo a região 3' UTR, induzindo a diminuição da expressão de ACE2 (265). Níveis plasmáticos e expressão aumentada de miR-200c-3p também foram encontrados no fígado de pacientes com carcinoma hepatocelular induzidos pelo vírus da hepatite B e C (266,267), sendo associados com a progressão da doença. No entanto, os mecanismos exatos requerem mais estudos. O perfil de expressão de miRNA no mesmo conjunto de amostras controle nos permitiu investigar a complexidade da desregulação gênica no contexto desta doença. Investigar essas relações pode fornecer mais informações sobre os mecanismos da Covid-19 e sua relação com a via de TREM-1.

6.3.1 Expressão do receptor TREM-1 e inibição da produção de citocina em macrófagos THP-1

O ajuste da resposta imune é fundamental na prevenção de inflamação excessiva e danos nos tecidos. Os receptores TREM-1 podem atuar como amplificadores da resposta inflamatória e produção de citocinas por monócitos e neutrófilos. Portanto, modular a

expressão de TREM-1 pode ajudar a atenuar as respostas imunes para beneficiar o hospedeiro.

Pouco se sabe sobre a regulação da expressão de TREM-1 na resposta a infecções virais, como resultados preliminares avaliamos a expressão de TREM-1 e produção de citocinas pró-inflamatória em monócitos THP-1 após exposição ao LPS, como modelo inflamatório clássico. Primeiramente testamos o envolvimento da via TREM-1 na produção de citocinas pró-inflamatórias usando o peptídeo sintético LP17 (LQVTDSGLYRCVIYHPP), que tem homologia com o domínio extracelular altamente conservado de TREM-1 e que pode estar envolvido na ligação de TREM-1; e um segundo peptídeo, com os mesmos aminoácidos, mas em uma sequência primária diferente (peptídeo de controle LP17s; TDSRCVIGLYHPPLQVY) (**Figura 12 A**). As células THP-1 foram tratadas com 100 ng/mL de LPS (**Figura 12 B**). Alguns poços também foram tratados com peptídeo de controle LP17 ou LP17 em uma concentração de 100 ng/ml, após incubação das células por 24 h, as concentrações de IL-1β no sobrenadante foram quantificados usando a técnica de ELISA (**Figura 12 C**).

Alterações na expressão de superfície de TREM-1 foram observadas, após 24 horas de exposição de células THP-1 (TDM), o que resultou em aumento da expressão superficial de TREM-1 e na liberação da citocina pró-inflamatória IL-1β. Assim, a liberação dessa citocina inflamatória foi reduzida quando as células THP-1 foram incubadas com o peptídeo LP-17 inibidor de TREM-1.
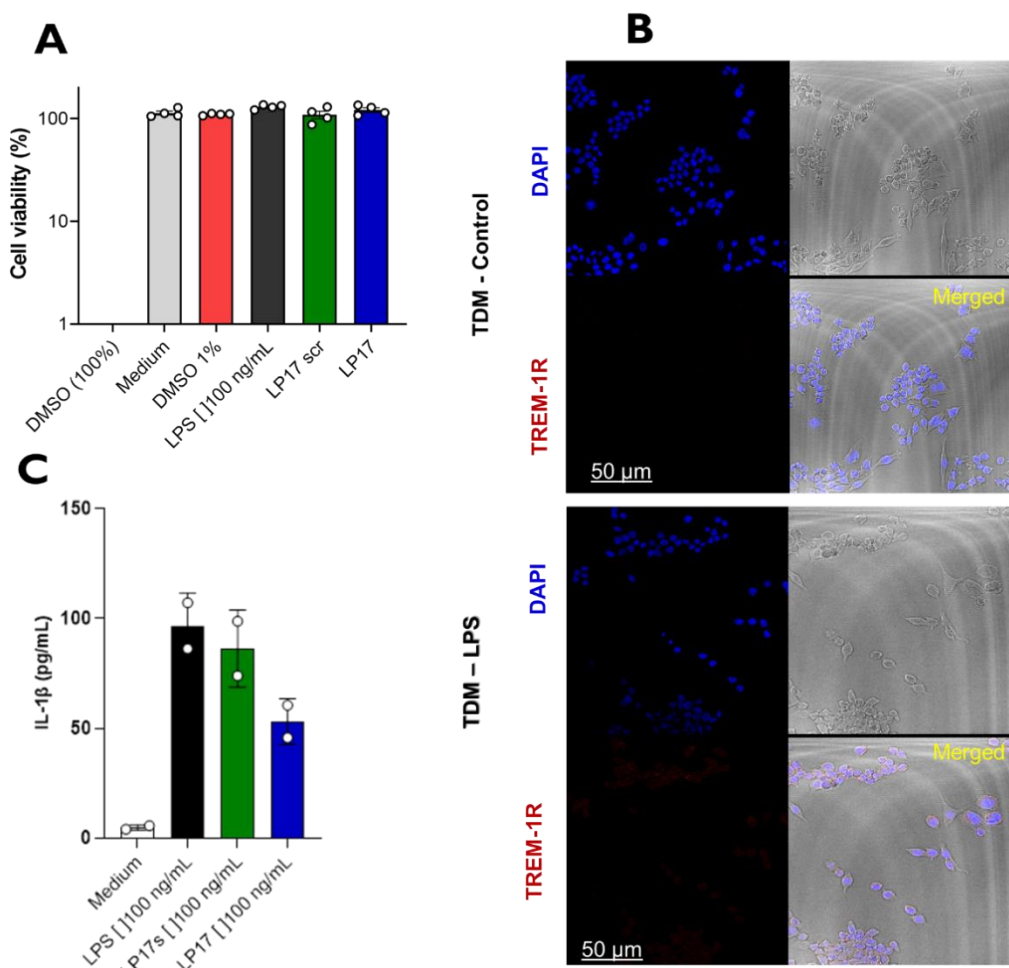
Figura 12. Expressão de TREM-1 em células THP-1 tratadas com inibidor LP17. Imagem imunofluorescência representativa demonstrando a expressão de TREM-1 em monócitos THP-1 em estado estacionário (sem tratamento) e após 24 horas de diferenciação com PMA. (**A**) Os monócitos foram estimulados com LPS e inibidor LP17 e LP17scr por 24 horas, (**B**) Microscopia confocal marcador específico de TREM-1 confirmou que as células que expressam TREM-1. Os núcleos foram corados com DAPI (azul escuro) **e** TREM-1R (vermelho). Barra de escala representados em ampliação de 50 µm. Representante de três imagens por condição. (**C**) Inibição da produção de IL1-β após a inibição com LP-17.

Evidências crescentes sugerem que o TREM-1 desempenha um papel essencial na modulação da resposta imune durante a inflamação aguda e crônica, uma vez o aumento de citocinas é consistente com relatos anteriores de que a estimulação de TREM-1 pode resultar em regulação sinérgica da sinalização iniciada por outros receptores de reconhecimento de padrões, como os TLRs (159,268,269)

O bloqueio da ativação do TREM-1 por análogos sintéticos reduz a síntese e liberação de citocinas pró-inflamatórias como a IL-1β induzida por LPS em monócitos humanos(270,271). Além disso, o efeito inibitório do peptídeo LP-17 suporta a noção de que ele compete com TREM-1 pela ligação do ligante disponível, inibindo assim a via

TREM-1e possibilitando a sobrevida em vários modelos de infecções graves, reduzindo a liberação de citocinas pró-inflamatórias, ativação da piroptose e diminuindo o acúmulo de ROS durante a lesão pulmonar aguda (272)

No entanto, parece que os agentes bloqueadores do TREM-1 fornecem achados controversos em distúrbios inflamatórios estéreis. Uma vez que o tratamento com o inibidor de TREM-1 não anulou completamente a produção de citocinas, tais efeitos já foram descritos em outros estudos observados anteriormente em infecções (273,274) Tomados em conjunto, esses experimentos questionam a possibilidade de TREM-1 como um alvo em potencial para terapias futuras no controle da inflamação.

7. Conclusão

- ❖ sTREM-1 apresenta papel importante na determinação do quadro clínico grave de pacientes com Covid-19, correlacionando com outros parâmetros pró-inflamatórios, desfechos desfavoravel (óbito) e atividade de MMP-8 na superfície de leucócitos sanguíneos.

- ❖ A alta diversidade enzimática das MMPs no microambiente pulmonar está correlacionada positivamente com a infiltração de neutrófilos, liberação de espécies reativas de oxigênio (ROS), aumento da peroxidação lipídica e superexpressão do eixo MMP-2/MMP-8 no pulmão, favoráveis para clivagem proteolítica de sHLA-G, sTREM-1.

- ❖ A expressão miRNAs e fatores de transcrições são favoráveis para um possível perfil de regulação celular, concomitante com a expressão do gene de TREM-1 durante a gravidade clínica da covid-19.

- ❖ A inibição do TREM-1 induz uma diminuição no eixo pro-inflamatório. Portanto, o bloqueio da expressão ou atividade de TREM-1 fornece perspectivas eficazes para novos alvos terapêuticos na inflamação exacerbada.

8. Apêndice

8.1. Apêndice 1: Termo de aprovação do comitê de ética em Pesquisa -CEP- CAAE) 30525920.7.0000.5403

UNIVERSIDADE DE SÃO PAULO
Faculdade de Ciências Farmacêuticas de Ribeirão Preto
Comitê de Ética em Pesquisa / Research Ethics Committee

Ribeirão Preto, January 3, 2021.

Subject: Approval by the Research Ethics Committee

To
Prof. Dr. Cristina Cardoso Ribeiro de Barros
School of Pharmaceutical Sciences of Ribeirão Preto, University of São Paulo (FCFRP-USP)
Department of Clinical Analyses, Toxicology and Food Sciences

Dear Professor,

We inform that the research project entitled **"Prospective evaluation of gene expression and humoral response in severe COVID-19: search for potential biomarkers for disease evolution in patients infected with SARS-COV2"**, was approved by the Research Ethics Committee (CEP) of the FCFRP-USP and the National Research Ethics Commission (CONEP), which constitute the Brazilian body for ethical supervision in research involving human beings (CEP / CONEP system), according to Resolution No. 466/2012 of the National Health Council, Ministry of Health, Brazil. Resolution 466/2012 provides the guidelines and regulatory standards for research involving human beings in Brazil, which is based on the main documents that constitute the pillars of recognition and affirmation of the dignity, freedom and autonomy of human beings, such as Helsinki Declaration of 1964 and its updates; the 2004 Universal Declaration on Bioethics and Human Rights; and the Federal Constitution of the Federative Republic of Brazil, whose objectives are consistent with international documents on ethics, human rights and development.

The present research protocol is registered in the CEP / CONEP system under the number of Certificate of Presentation of Ethical Appreciation (CAAE) 30525920.7.0000.5403. The experimental design / current methods of this research protocol approved by the CEP / CONEP system are described below. Then, the history of the ethical analysis since the first submission of the research protocol and its respective amendments is presented.

"Design/Methods: This study aims to investigate factors of susceptibility and resistance, as well as biomarkers of the disease caused by the SARS-COV2 virus, called COVID-19. For that, healthy participants from the USP community (Campus Ribeirão Preto), individuals with a positive molecular test for SARS-COV2 performed via Basic Health Units in the city of Ribeirão Preto and who are asymptomatic or have mild symptoms, as well as convalescents and patients will be selected from private hospitals (Hospital São Paulo and Hospital Unimed Ribeirão Preto) or another philanthropic hospital (Hospital Santa Casa de Misericórdia de Ribeirão Preto), in the same city, which will be evaluated clinically and laboratory, for the diagnosis of the disease, by the doctors responsible for the care. Men and women will be included, classified into control and sick groups, according to laboratory diagnosis and severity of COVID-19. After this categorization, the volunteers (100 per group) will be divided into healthy individuals with negative molecular

UNIVERSIDADE DE SÃO PAULO
Faculdade de Ciências Farmacêuticas de Ribeirão Preto
Comitê de Ética em Pesquisa / Research Ethics Committee

diagnosis for SARS-COV2 (group 1 - G1), asymptomatic or oligosymptomatic with positive test for the virus (group 2 - G2), hospitalized with moderate symptoms, positive diagnosis (group 3 - G3) and severe hospitalized symptoms, also with positive molecular test for SARS-COV2 (group 4 - G4), severe hospitalized symptoms, with negative molecular test for SARS-COV2 (group 6 - G6). In addition to convalescents, previously tested and confirmed positive for the virus, however in the current absence of signs or symptoms of COVID-19 (group 5 - G5). After the consent and signature of the Informed Consent Form (ICF) by the patients or guardians themselves, samples of venous blood, saliva or pulmonary fluid aspirate will be collected for laboratory processing related to this research project (some control participants will also have collection nasopharyngeal swap for molecular diagnosis of virus infection). Samples from participants in groups G1, G2 and G5 will be collected only once, for research. Patients in groups G3 and G4, will have blood, saliva (only G3) and / or pulmonary fluid aspirate (G4 and G6) collected at the time of admission to the hospital and after 48 hours, repeating the collection once every 7 days, until the end of the hospitalization period. The blood samples will be centrifuged to obtain plasma and leukocytes (buffy coat). The obtained cells will be immediately frozen in Trizol, for subsequent RNA extraction and transcriptomic analysis of gene expression of receptors, transcription factors, steroidogenic enzymes, cytokines, and other mediators related to the immune response. In plasma, cytokines will be quantified by multiplex assay, in addition to eicosanoids, steroid hormones, sphingolipids and ceramides, by mass spectrometry. In addition, the profiles of N-glycans in the Fcs of IgGs and anti-carbohydrate antibodies will be evaluated, to ascertain their correlation with the clinical outcomes of SARS-COV2 infections. New biotechnological tools that allow the study of the relationships between the virus, its cellular targets and antibodies will be produced. With these results together, it is expected to understand more deeply the pathophysiology of COVID-19, as well as to establish markers of disease evolution and morbidity".

History of the approval ethical by CEP / CONEP system:

First approval: - CEP, April 6, 2020 - consubstanced opinion number 3,956,413; and CONEP, April 30, 2020 - consubstanced opinion number. 3,999,280;

Amendment 1 - approval: CEP, June, 8, 2020 - consubstanced opinion number 4,076,158; and CONEP, June 23,2020 - consubstanced opinion number 4,104,192;

Amendment 2 - approval: CEP, July 7, 2020 - consubstanced opinion number 4,134,068; and CONEP, July 28, 2020 – 4,176,358;

Amendment 3 - approval: CEP, November 19, 2020 - consubstanced opinion number 4,409,566; and CONEP, December 02, 2020 – 4,432,873;

Amendment 4 - approval: CEP, December 10, 2020 - consubstanced opinion number 4,454,975; and CONEP, December 15, 2020 - consubstanced opinion number 4,465,002.

UNIVERSIDADE DE SÃO PAULO
Faculdade de Ciências Farmacêuticas de Ribeirão Preto
Comitê de Ética em Pesquisa / Research Ethics Committee

The requirements for the ethical approval of this research protocol also included declarations of agreement from all health institutions (hospitals and basic health units), where the research participants will be recruited. The consultation of the patient's medical record is explained in the Informed Consent Form.

It is the responsibility of the researchers, according to Resolution 466/2012, item IV.5, letter d, to consider that the Informed Consent Form must be presented in two original documents, initialed in all its pages, and signed, at the end, by the research participant, or by his / her legal representative, as well as by the responsible researcher, or by the person (s) delegated by him / her, and the signature pages must be on the same sheet. The addresses and telephone or other contact, of those responsible for the research and of this Ethics Committee must be included.

The final report of the research must be sent to the CEP of the FCFRP-USP in its own form, as well as any changes, complications or interruptions, such as adverse events and eventual modifications to the protocol or team members, through the interposition of amendments on the Brazil Platform, which is the national and unified base of research records involving human beings for the entire CEP / CONEP system.

Prof. Dr. Cleni Mara Marzocchi Machado
Coordinator of the Research Ethics Committee of FCFRP-USP

8.2. Lista de Publicações: Artigos publicados durante o doutorado relacionados à tese

1. sTREM-1 Predicts Disease Severity and Mortality in Covid-19 Patients: Involvement of Peripheral Blood Leukocytes and MMP-8 Activity. **Viruses**. 2021 Dec 15;13(12):2521. doi: 10.3390/v13122521. PMID: 34960790; PMCID: PMC8708887.

2. Matrix Metalloproteinases on Severe Covid-19 Lung Disease Pathogenesis: Cooperative Actions of MMP-8/MMP-2 Axis on Immune Response through HLA-G Shedding and Oxidative Stress. **Biomolecules** 2022, 12, 604. https://doi.org/10.3390/biom12050604

8.3. Artigos publicados durante o doutorado não relacionados à tese

1. The IgG glycome of SARS-CoV-2 infected individuals reflects disease course and severity. **Frontiers in Immunology**., 18 October 2022.Sec. Viral Immunology https://doi.org/10.3389/fimmu.2022.993354.

2. Acetylcholine, Fatty Acids, and Lipid Mediators Are Linked to Covid-19 Severity. **Journal of Immunology**. Fator de Impacto(2021 JCR): 5,4260, v.209, p.250 - 261, 2022.

3. Caloric restriction overcomes pre-diabetes and hypertension induced by a high fat diet and renal artery stenosis. **Molecular Biology Reports**. Fator de Impacto (2021 JCR): 2,7420, v.1, p.1-18 - , 2022.

4. The Severity of Covid-19 Affects the Plasma Soluble Levels of the Immune Checkpoint HLA-G Molecule. **International Journal of Molecular Sciences**. Fator de Impacto (2011 JCR): 2,5980, v.23, p.9736 - , 2022.

5. Changes in heme levels during acute vaso-occlusive crisis in sickle cell anemia. **Hematology/Oncology and Stem Cell Therapy**. v.21, p.1658-3876 - , 2021.

6. Inflammasome genes polymorphisms may influence the development of hepatitis C in the Amazonas, Brazil. **PLoS One**. Fator de Impacto(2021 JCR): 3,7520, v.16, p.e0253470 - , 2021.

7. Combination of genetic polymorphisms in TLR influence cytokine profile in HCV patients treated with DAAs in the State of Amazonas. **Cytokine**. Fator de Impacto (2021 JCR): 3,9260, v.130, p.155052 - , 2020.

8. Neutrophil extracellular trap regulators in sickle cell disease: Modulation of gene expression of PADI4, neutrophil elastase, and myeloperoxidase during vaso-occlusive crisis. **Research and Practice in Thrombosis and Haemostasis**. Fator de Impacto (2021 JCR): 5,9530, v.5, p.204 - 210, 2020.

9. Immunological Dynamics Associated with Direct-Acting Antiviral Therapies in Naive and Experimented HCV Chronic-Infected Patients. **Mediators of Inflammation**. Fator de Impacto (2021 JCR): 4,5290, v.2019, p.1 - 11, 2019.

10. Up-Regulation of the mRNA Expression and Plasma Activity of PADI4in Sickle Cell Anemia during Acute Crisis. **Blood**. Fator de Impacto (2021 JCR): 25,4760, v.134, p.2257 - 2257, 2019.

8.4. Links de entrevistas e publicações em jornais locais e nacionais relacionados à tese.

1. https://www.ppgiba.ufam.edu.br/ultimas-noticias/166-excesso-de-enzimas-pode-agravar-casos-de-covid-descobrem-pesquisadores-da-usp.html
2. https://globoplay.globo.com/v/10647177/
3. https://www.eurekalert.org/news-releases/952539
4. https://medicinasa.com.br/usp-fapesp-teste-covid/
5. https://www.uol.com.br/vivabem/noticias/redacao/2020/10/01/proteina-no-sangue-de-paciente-com-Covid-19-pode-indicar-evolucao-da-doenca.htm
6. https://limhc.fm.usp.br/portal/proteina-no-sangue-de-pacientes-com-Covid-19-pode-indicar-evolucao-e-gravidade-da-doenca/

9. Referencial Bibliográfico

1. Zhou P, Yang X Lou, Wang XG, Hu B, Zhang L, Zhang W, et al. A pneumonia outbreak associated with a new coronavirus of probable bat origin. Nature. 2020;579(7798):270–273.

2. Lu R, Zhao X, Li J, Niu P, Yang B, Wu H, et al. Genomic characterisation and epidemiology of 2019 novel coronavirus: implications for virus origins and receptor binding. The Lancet. 2020;

3. Wu Z, McGoogan JM. Characteristics of and Important Lessons From the Coronavirus Disease 2019 (COVID-19) Outbreak in China. JAMA. 2020;323(13):1239–42.

4. Cao X. COVID-19: immunopathology and its implications for therapy. Nature Reviews Immunology. 2020.

5. Dorward DA, Russell MBChB CD, Hwa Um I, Elshani M, Armstrong SD, Penrice-Randal R, et al. Tissue-specific tolerance in fatal Covid-19. medRxiv. 2020;

6. Practice BB. Coronavirus disease 2019Practice, B.B., 2020. Coronavirus disease 2019. World Heal. Organ. 2019, 2633. https://doi.org/10.1001/jama.2020.2633. World Health Organization. 2020;

7. Wu C, Chen X, Cai Y, Xia J, Zhou X, Xu S, et al. Risk Factors Associated with Acute Respiratory Distress Syndrome and Death in Patients with Coronavirus Disease 2019 Pneumonia in Wuhan, China. JAMA Intern Med. 2020;

8. Tay MZ, Poh CM, Rénia L, MacAry PA, Ng LFP. The trinity of COVID-19: immunity, inflammation and intervention. Nat Rev Immunol. 2020;20(6):363–74.

9. Blanco-Melo D, Nilsson-Payant BE, Liu WC, Uhl S, Hoagland D, Møller R, et al. Imbalanced Host Response to SARS-CoV-2 Drives Development of COVID-19. Cell. 2020;

10. Akira S, Akira S, Uematsu S, Uematsu S, Takeuchi O, Takeuchi O. Pathogen recognition and innate immunity. Cell. 2006;124(4):783–801.

11. Codo AC, Davanzo GG, Monteiro L de B, de Souza GF, Muraro SP, Virgilio-da-Silva JV, et al. Elevated Glucose Levels Favor SARS-CoV-2 Infection and Monocyte Response through a HIF-1α/Glycolysis-Dependent Axis. Cell Metab. 2020 set;32(3).

12. Bost P, Giladi A, Liu Y, Bendjelal Y, Xu G, David E, et al. Host-Viral Infection Maps Reveal Signatures of Severe COVID-19 Patients. Cell. 2020;181(7).

13. Merad M, Martin JC. Pathological inflammation in patients with COVID-19: a key role for monocytes and macrophages. Nat Rev Immunol. 2020 jun 6;20(6).

14. Deiuliis JA. MicroRNAs as regulators of metabolic disease: pathophysiologic significance and emerging role as biomarkers and therapeutics. Int J Obes. 2016 jan 27;40(1).

15. Lee YS, Dutta A. MicroRNAs in Cancer. Annual Review of Pathology: Mechanisms of Disease. 2009 fev;4(1).

16. Gantier MP, Sadler AJ, Williams BRG. Fine-tuning of the innate immune response by microRNAs. Immunol Cell Biol. 2007 ago 10;85(6).

17. Vishnoi A, Rani S. MiRNA Biogenesis and Regulation of Diseases: An Overview. Em 2017.

18. Liu G, Abraham E. MicroRNAs in Immune Response and Macrophage Polarization. Arterioscler Thromb Vasc Biol. 2013 fev;33(2).

19. Jopling CL. Modulation of Hepatitis C Virus RNA Abundance by a Liver-Specific MicroRNA. Science (1979). 2005 set 2;309(5740).

20. Loffek S, Schilling O, Franzke CW. Biological role of matrix metalloproteinases: a critical balance. European Respiratory Journal. 2011;38(1).

21. Ueland T, Holter JC, Holten AR, Müller KE, Lind A, Bekken GK, et al. Distinct and early increase in circulating MMP-9 in COVID-19 patients with respiratory failure: MMP-9 and respiratory failure in COVID-19. Vol. 81, Journal of Infection. 2020.

22. Arts R, Joosten L, van der Meer J, Netea M. TREM-1: intracellular signaling pathways and interaction with pattern recognition receptors. J Leukoc Biol. 2013;93(2):209–15.

23. Tammaro A, Derive M, Gibot S, Leemans JC, Florquin S, Dessing MC. TREM-1 and its potential ligands in non-infectious diseases: from biology to clinical perspectives. Pharmacol Ther. 2017;

24. Gómez-Piña V, Soares-Schanoski A, Rodríguez-Rojas A, del Fresno C, García F, Vallejo-Cremades MT, et al. Metalloproteinases Shed TREM-1 Ectodomain from Lipopolysaccharide-Stimulated Human Monocytes. The Journal of Immunology. 2007 set 15;179(6).

25. Gibot S, Cravoisy A, Kolopp-Sarda MN, Béné MC, Faure G, Bollaert PE, et al. Time-course of sTREM (soluble triggering receptor expressed on myeloid cells)-1, procalcitonin, and C-reactive protein plasma concentrations during sepsis. Crit Care Med. 2005 abr;33(4).

26. Determann RM, Millo JL, Gibot S, Korevaar JC, Vroom MB, van der Poll T, et al. Serial changes in soluble triggering receptor expressed on myeloid cells in the lung during development of ventilator-associated pneumonia. Intensive Care Med. 2005 nov 30;31(11).

27. Gibot S, Cravoisy A. Soluble Form of the Triggering Receptor Expressed on Myeloid Cells-1 as a Marker of Microbial Infection. Clin Med Res. 2004 ago 1;2(3).

28. Richard-Greenblatt M, Boillat-Blanco N, Zhong K, Mbarack Z, Samaka J, Mlaganile T, et al. Prognostic Accuracy of Soluble Triggering Receptor Expressed on Myeloid Cells (sTREM-1)-based Algorithms in Febrile Adults Presenting to Tanzanian Outpatient Clinics. Clinical Infectious Diseases. 2020;70(7):1304–1312.

29. Brenner T, Uhle F, Fleming T, Wieland M, Schmoch T, Schmitt F, et al. Soluble TREM-1 as a diagnostic and prognostic biomarker in patients with septic shock: an observational clinical study. Biomarkers. 2017 jan 2;22(1).

30. Wright SW, Lovelace-Macon L, Hantrakun V, Rudd KE, Teparrukkul P, Kosamo S, et al. sTREM-1 predicts mortality in hospitalized patients with infection in a tropical, middle-income country. BMC Med. 2020 dez 1;18(1).

31. Zhong NS, Zheng BJ, Li YM, Poon LLM, Xie ZH, Chan KH, et al. Epidemiology and cause of severe acute respiratory syndrome (SARS) in Guangdong, People's Republic of China, in February, 2003. The Lancet. 2003 out 25;362(9393):1353–8.

32. Thomas G Ksiazek DECSGSRZTPSESTCU. A Novel Coronavirus Associated with Severe Acute Respiratory Syndrome. N Engl J Med [Internet]. 2003;10:1953–66. Available from: http://www.nejm.org

33. Lee N, Hui D, Wu A, Chan P, Cameron P, Joynt GM, et al. A Major Outbreak of Severe Acute Respiratory Syndrome in Hong Kong. https://doi.org/101056/NEJMoa030685. 2003 maio 15;348(20):1986–94.

34. Guan Y, Peiris JSM, Zheng B, Poon LLM, Chan KH, Zeng FY, et al. Molecular epidemiology of the novel coronavirus that causes severe acute respiratory syndrome. The Lancet. 2004 jan 10;363(9403):99–104.

35. Peiris JSM, Lai ST, Poon LLM, Guan Y, Yam LYC, Lim W, et al. Coronavirus as a possible cause of severe acute respiratory syndrome. Lancet. 2003;361(9366).

36. Drosten C, Günther S, Preiser W, van der Werf S, Brodt HR, Becker S, et al. Identification of a Novel Coronavirus in Patients with Severe Acute Respiratory Syndrome. New England Journal of Medicine. 2003;348(20).

37. World Health Organization (WHO). Emergencies preparedness, response Summary of probable SARS cases with onset of illness from 1 November 2002 to 31 July 2003. Vol. 9, Online 2004. 2020.

38. Wang M, Yan M, Xu H, Liang W, Kan B, Zheng B, et al. SARS-CoV infection in a restaurant from palm civet. Emerg Infect Dis. 2005;11(12):1860–5.

39. Ge XY, Li JL, Yang X Lou, Chmura AA, Zhu G, Epstein JH, et al. Isolation and characterization of a bat SARS-like coronavirus that uses the ACE2 receptor. Nature. 2013;503(7477):535–8.

40. Menachery VD, Yount BL, Debbink K, Agnihothram S, Gralinski LE, Plante JA, et al. A SARS-like cluster of circulating bat coronaviruses shows potential for human emergence. Nat Med. 2015 dez 1;21(12):1508–13.

41. Banerjee A, Doxey AC, Mossman K, Irving AT. Unraveling the Zoonotic Origin and Transmission of SARS-CoV-2. Vol. 36, Trends in Ecology and Evolution. 2021.

42. Zaki AM, van Boheemen S, Bestebroer TM, Osterhaus ADME, Fouchier RAM. Isolation of a Novel Coronavirus from a Man with Pneumonia in Saudi Arabia. New England Journal of Medicine. 2012;367(19).

43. Wise J. Patient with new strain of coronavirus is treated in intensive care at London hospital. BMJ. 2012;345.

44. Menachery VD, Yount BL, Debbink K, Agnihothram S, Gralinski LE, Plante JA, et al. A SARS-like cluster of circulating bat coronaviruses shows potential for human emergence. Nat Med. 2015;21(12).

45. Ge XY, Li JL, Yang X lou, Chmura AA, Zhu G, Epstein JH, et al. Isolation and characterization of a bat SARS-like coronavirus that uses the ACE2 receptor. Nature. 2013;503(7477).

46. Zhu N, Zhang D, Wang W, Li X, Yang B, Song J, et al. A Novel Coronavirus from Patients with Pneumonia in China, 2019. New England Journal of Medicine. 2020;

47. Huang C, Wang Y, Li X, Ren L, Zhao J, Hu Y, et al. Clinical features of patients infected with 2019 novel coronavirus in Wuhan, China. The Lancet. 2020;395(10223):497–506.

48. Li Q, Guan X, Wu P, Wang X, Zhou L, Tong Y, et al. Early Transmission Dynamics in Wuhan, China, of Novel Coronavirus–Infected Pneumonia. New England Journal of Medicine. 2020;

49. WHO. Novel Coronavirus(2019-nCoV) Situation Report - 11. 2020.

50. Hu B. Characteristics of SARS-CoV-2 and COVID-19. Nat Rev Microbiol [Internet]. 2019;(December). Available from: http://dx.doi.org/10.1038/s41579-020-00459-7

51. Harrison AG, Lin T, Wang P. Mechanisms of SARS-CoV-2 Transmission and Pathogenesis. Trends Immunol. 2020;41(12):1100–15.

52. Wu A, Peng Y, Huang B, Ding X, Wang X, Niu P, et al. Genome Composition and Divergence of the Novel Coronavirus (2019-nCoV) Originating in China. Cell Host Microbe. 2020;

53. Zhou P, Yang XL, Wang XG, Hu B, Zhang L, Zhang W, et al. A pneumonia outbreak associated with a new coronavirus of probable bat origin. Nature. 2020 mar 12;579(7798).

54. Zhou F, Yu T, Du R, Fan G, Liu Y, Liu Z, et al. Clinical course and risk factors for mortality of adult inpatients with COVID-19 in Wuhan, China: a retrospective cohort study. The Lancet. 2020 mar;395(10229).

55. Zhang T, Wu Q, Zhang Z. Probable Pangolin Origin of SARS-CoV-2 Associated with the COVID-19 Outbreak. Current Biology. 2020 abr;30(7).

56. Wu F, Zhao S, Yu B, Chen YM, Wang W, Song ZG, et al. A new coronavirus associated with human respiratory disease in China. Nature. 2020;

57. Naqvi AAT, Fatima K, Mohammad T, Fatima U, Singh IK, Singh A, et al. Insights into SARS-CoV-2 genome, structure, evolution, pathogenesis and

therapies: Structural genomics approach. Biochimica et Biophysica Acta - Molecular Basis of Disease. 2020.

58. Masters PS. The Molecular Biology of Coronaviruses. Vol. 65, Advances in Virus Research. 2006.

59. V'kovski P, Kratzel A, Steiner S, Stalder H, Thiel V. Coronavirus biology and replication: implications for SARS-CoV-2. Vol. 19, Nature Reviews Microbiology. 2021.

60. Demogines A, Farzan M, Sawyer SL. Evidence for ACE2-Utilizing Coronaviruses (CoVs) Related to Severe Acute Respiratory Syndrome CoV in Bats. J Virol. 2012;86(11).

61. Neuman BW, Kiss G, Kunding AH, Bhella D, Baksh MF, Connelly S, et al. A structural analysis of M protein in coronavirus assembly and morphology. J Struct Biol. 2011;174(1).

62. DeDiego ML, Álvarez E, Almazán F, Rejas MT, Lamirande E, Roberts A, et al. A Severe Acute Respiratory Syndrome Coronavirus That Lacks the E Gene Is Attenuated In Vitro and In Vivo. J Virol. 2007 fev 15;81(4).

63. Ryan PMD, Caplice N. COVID-19 and relative angiotensin-converting enzyme 2 deficiency: Role in disease severity and therapeutic response. Vol. 7, Open Heart. 2020.

64. Cui L, Wang H, Ji Y, Yang J, Xu S, Huang X, et al. The Nucleocapsid Protein of Coronaviruses Acts as a Viral Suppressor of RNA Silencing in Mammalian Cells. J Virol. 2015 set 1;89(17).

65. Zhang H, Penninger JM, Li Y, Zhong N, Slutsky AS. Angiotensin-converting enzyme 2 (ACE2) as a SARS-CoV-2 receptor: molecular mechanisms and potential therapeutic target. Intensive Care Med. 2020;

66. Li W, Moore MJ, Vasilieva N, Sui J, Wong SK, Berne MA, et al. Angiotensin-converting enzyme 2 is a functional receptor for the SARS coronavirus. Nature. 2003 nov;426(6965).

67. Hoffmann M, Kleine-Weber H, Schroeder S, Krüger N, Herrler T, Erichsen S, et al. SARS-CoV-2 Cell Entry Depends on ACE2 and TMPRSS2 and Is Blocked by a Clinically Proven Protease Inhibitor. Cell. 2020;

68. Qian Z, Travanty EA, Oko L, Edeen K, Berglund A, Wang J, et al. Innate Immune Response of Human Alveolar Type II Cells Infected with Severe Acute Respiratory Syndrome–Coronavirus. Am J Respir Cell Mol Biol. 2013 jun;48(6).

69. Rothan HA, Byrareddy SN. The epidemiology and pathogenesis of coronavirus disease (COVID-19) outbreak. J Autoimmun. 2020 maio;109.

70. Yeo C, Kaushal S, Yeo D. Enteric involvement of coronaviruses: is faecal–oral transmission of SARS-CoV-2 possible? Lancet Gastroenterol Hepatol. 2020 abr;5(4).

71. Zhang H, Kang Z, Gong H, Xu D, Wang J, Li Z, et al. Digestive system is a potential route of COVID-19: an analysis of single-cell coexpression pattern of key proteins in viral entry process. Gut. 2020 jun;69(6).

72. Li W. Delving deep into the structural aspects of a furin cleavage site inserted into the spike protein of SARS-CoV-2: A structural biophysical perspective. Biophys Chem. 2020;

73. Perlman S, Netland J. Coronaviruses post-SARS: update on replication and pathogenesis. Nat Rev Microbiol. 2009 jun 11;7(6).

74. Wu HY, Brian DA. Subgenomic messenger RNA amplification in coronaviruses. Proceedings of the National Academy of Sciences. 2010 jul 6;107(27).

75. Karlsson EK, Kwiatkowski DP, Sabeti PC. Natural selection and infectious disease in human populations. Vol. 15, Nature Reviews Genetics. 2014.

76. Ignatieva A, Hein J, Jenkins PA. Ongoing Recombination in SARS-CoV-2 Revealed through Genealogical Reconstruction. Mol Biol Evol. 2022 fev 3;39(2).

77. Jackson B, Boni MF, Bull MJ, Colleran A, Colquhoun RM, Darby AC, et al. Generation and transmission of interlineage recombinants in the SARS-CoV-2 pandemic. Cell. 2021 set 30;184(20):5179-5188.e8.

78. Volz E, Mishra S, Chand M, Barrett JC, Johnson R, Geidelberg L, et al. Assessing transmissibility of SARS-CoV-2 lineage B.1.1.7 in England. Nature 2021 593:7858. 2021 mar 25;593(7858):266–9.

79. Tegally H, Wilkinson E, Giovanetti M, Iranzadeh A, Fonseca V, Giandhari J, et al. Detection of a SARS-CoV-2 variant of concern in South Africa. Nature 2021 592:7854. 2021 mar 9;592(7854):438–43.

80. Fujino T, Nomoto H, Kutsuna S, Ujiie M, Suzuki T, Sato R, et al. Novel SARS-CoV-2 Variant in Travelers from Brazil to Japan - Volume 27, Number 4—April 2021 - Emerging Infectious Diseases journal - CDC. Emerg Infect Dis. 2021 abr 1;27(4):1243–5.

81. Faria NR, Mellan TA, Whittaker C, Claro IM, Candido DDS, Mishra S, et al. Genomics and epidemiology of the P.1 SARS-CoV-2 lineage in Manaus, Brazil. Science (1979). 2021 maio 21;372(6544).

82. Naveca FG, Nascimento V, de Souza VC, Corado A de L, Nascimento F, Silva G, et al. COVID-19 in Amazonas, Brazil, was driven by the persistence of endemic lineages and P.1 emergence. Nat Med. 2021;27(7).

83. Mlcochova P, Kemp S, Dhar MS, Papa G, Meng B, Mishra S, et al. SARS-CoV-2 B.1.617.2 Delta variant replication, sensitivity to neutralising antibodies and vaccine breakthrough. bioRxiv. 2021 ago 6;2021.05.08.443253.

84. Cherian S, Potdar V, Jadhav S, Yadav P, Gupta N, Das M, et al. SARS-CoV-2 Spike Mutations, L452R, T478K, E484Q and P681R, in the Second Wave of COVID-19 in Maharashtra, India. Microorganisms 2021, Vol 9, Page 1542. 2021 jul 20;9(7):1542.

85. Brown CM, Vostok J, Johnson H, Burns M, Gharpure R, Sami S, et al. Outbreak of SARS-CoV-2 Infections, Including COVID-19 Vaccine Breakthrough Infections, Associated with Large Public Gatherings —

Barnstable County, Massachusetts, July 2021. MMWR Morb Mortal Wkly Rep. 2021 ago 6;70(31):1059–62.

86. WHO. Classification of Omicron (B.1.1.529): SARS-CoV-2 Variant of Concern [Internet]. 2021 [citado 2022 jul 1]. Available from: https://www.who.int/news/item/26-11-2021-classification-of-omicron-(b.1.1.529)-sars-cov-2-variant-of-concern

87. Mistry P, Barmania F, Mellet J, Peta K, Strydom A, Viljoen IM, et al. SARS-CoV-2 Variants, Vaccines, and Host Immunity. Vol. 12, Frontiers in Immunology. 2022.

88. WOH. WHO Director-General's opening remarks at the media briefing on COVID-19 - 11 March 2020. 2020.

89. WHO. Dasbor WHO Coronavirus Disease (COVID-19). World Health Organization. 2021;(January).

90. WHO. Coronavirus disease 2019 (COVID-19) Situation Report – 78. 2020;2019(April).

91. WHO. Coronavirus disease 2019 (COVID-19) Situation Report – 78. 2020;2019(April).

92. Brasil Ministerio da saúde. PORTARIA Nº 188, DE 3 DE FEVEREIRO DE 2020. 2020.

93. Candido DS, Claro IM, de Jesus JG, Souza WM, Moreira FRR, Dellicour S, et al. Evolution and epidemic spread of SARS-CoV-2 in Brazil. Science (1979). 2020;369(6508).

94. Pinto Neto O, Kennedy DM, Reis JC, Wang Y, Brizzi ACB, Zambrano GJ, et al. Mathematical model of COVID-19 intervention scenarios for São Paulo—Brazil. Nat Commun. 2021;12(1).

95. da S. Candido D, Watts A, Abade L, Kraemer MUG, Pybus OG, Croda J, et al. Routes for COVID-19 importation in Brazil. J Travel Med. 2020;27(3).

96. Resende PC, Delatorre E, Gräf T, Mir D, Motta FC, Appolinario LR, et al. Evolutionary Dynamics and Dissemination Pattern of the SARS-CoV-2 Lineage B.1.1.33 During the Early Pandemic Phase in Brazil. Front Microbiol. 2021;11.

97. Giovanetti M, Slavov SN, Fonseca V, Wilkinson E, Tegally H, Patané JSL, et al. Genomic epidemiology reveals how restriction measures shaped the SARS-CoV-2 epidemic in Brazil. medRxiv. 2021;

98. World Health Organization. Covid-19 Situation Report. World Health Organization. 2020;31(2).

99. Huang C, Wang Y, Li X, Ren L, Zhao J, Hu Y, et al. Clinical features of patients infected with 2019 novel coronavirus in Wuhan, China. The Lancet. 2020 fev;395(10223).

100. Zaim S, Chong JH, Sankaranarayanan V, Harky A. COVID-19 and Multiorgan Response. Curr Probl Cardiol. 2020 ago;45(8).

101. Chen N, Zhou M, Dong X, Qu J, Gong F, Han Y, et al. Epidemiological and clinical characteristics of 99 cases of 2019 novel coronavirus

pneumonia in Wuhan, China: a descriptive study. The Lancet. 2020 fev;395(10223).

102. Pan F, Ye T, Sun P, Gui S, Liang B, Li L, et al. Time Course of Lung Changes at Chest CT during Recovery from Coronavirus Disease 2019 (COVID-19). Radiology. 2020 jun;295(3).

103. Wang D, Hu B, Hu C, Zhu F, Liu X, Zhang J, et al. Clinical Characteristics of 138 Hospitalized Patients with 2019 Novel Coronavirus-Infected Pneumonia in Wuhan, China. JAMA - Journal of the American Medical Association. 2020;

104. Chen J, Qi T, Liu L, Ling Y, Qian Z, Li T, et al. Clinical progression of patients with COVID-19 in Shanghai, China. Journal of Infection. 2020 maio;80(5).

105. Bialek S, Boundy E, Bowen V, Chow N, Cohn A, Dowling N, et al. Severe Outcomes Among Patients with Coronavirus Disease 2019 (COVID-19) — United States, February 12–March 16, 2020. MMWR Morb Mortal Wkly Rep. 2020 mar 27;69(12).

106. Onder G, Rezza G, Brusaferro S. Case-Fatality Rate and Characteristics of Patients Dying in Relation to COVID-19 in Italy. JAMA. 2020 mar 23;

107. Pinto BGG, Oliveira AER, Singh Y, Jimenez L, Gonçalves ANA, Ogava RLT, et al. ACE2 Expression Is Increased in the Lungs of Patients With Comorbidities Associated With Severe COVID-19. J Infect Dis. 2020 jul 23;222(4).

108. Wu C, Chen X, Cai Y, Xia J, Zhou X, Xu S, et al. Risk Factors Associated With Acute Respiratory Distress Syndrome and Death in Patients With Coronavirus Disease 2019 Pneumonia in Wuhan, China. JAMA Intern Med. 2020 jul 1;180(7).

109. Guan W jie, Ni Z yi, Hu Y, Liang W hua, Ou C quan, He J xing, et al. Clinical Characteristics of Coronavirus Disease 2019 in China. New England Journal of Medicine. 2020 abr 30;382(18).

110. Huang C, Wang Y, Li X, Ren L, Zhao J, Hu Y, et al. Clinical features of patients infected with 2019 novel coronavirus in Wuhan, China. The Lancet. 2020 fev;395(10223).

111. Peiris J, Chu C, Cheng V, Chan K, Hung I, Poon L, et al. Clinical progression and viral load in a community outbreak of coronavirus-associated SARS pneumonia: a prospective study. The Lancet. 2003 maio;361(9371).

112. Ziegler CGK, Allon SJ, Nyquist SK, Mbano IM, Miao VN, Tzouanas CN, et al. SARS-CoV-2 Receptor ACE2 Is an Interferon-Stimulated Gene in Human Airway Epithelial Cells and Is Detected in Specific Cell Subsets across Tissues. Cell. 2020 maio;181(5).

113. Kuba K, Imai Y, Rao S, Gao H, Guo F, Guan B, et al. A crucial role of angiotensin converting enzyme 2 (ACE2) in SARS coronavirus–induced lung injury. Nat Med. 2005 ago 10;11(8).

114. Zhao Y, Zhao Z, Wang Y, Zhou Y, Ma Y, Zuo W. Single-Cell RNA Expression Profiling of ACE2, the Receptor of SARS-CoV-2. Am J Respir Crit Care Med. 2020 set 1;202(5).

115. Ding Y, He L, Zhang Q, Huang Z, Che X, Hou J, et al. Organ distribution of severe acute respiratory syndrome(SARS) associated coronavirus(SARS-CoV) in SARS patients: implications for pathogenesis and virus transmission pathways. J Pathol. 2004 jun;203(2).

116. Zaim S, Chong JH, Sankaranarayanan V, Harky A. COVID-19 and Multiorgan Response. Vol. 45, Current Problems in Cardiology. 2020.

117. Gillich A, Zhang F, Farmer CG, Travaglini KJ, Tan SY, Gu M, et al. Capillary cell-type specialization in the alveolus. Nature. 2020;

118. Al-Khawaga S, Abdelalim EM. Potential application of mesenchymal stem cells and their exosomes in lung injury: an emerging therapeutic option for COVID-19 patients. Stem Cell Res Ther. 2020;11(1).

119. Luiz Boechat A, Mella Soares Pessoa B, Eduardo Colares Soares C, Barroso T, José Conceição Vila D, Maria Lima Barbosa E, et al. SARS-CoV-2 and Covid-19 Immunopathogenesis. 2020; Available from: www.preprints.org

120. Streicher F, Jouvenet N. Stimulation of Innate Immunity by Host and Viral RNAs. Trends in Immunology. 2019.

121. Schoggins JW. Interferon-Stimulated Genes: What Do They All Do? Annu Rev Virol. 2019;

122. Li J, Liu Y, Zhang X. Murine Coronavirus Induces Type I Interferon in Oligodendrocytes through Recognition by RIG-I and MDA5. J Virol. 2010;

123. Chow KT, Gale M, Loo YM. RIG-I and Other RNA Sensors in Antiviral Immunity. Annual Review of Immunology. 2018.

124. Gatti P, Ilamathi HS, Todkar K, Germain M. Mitochondria Targeted Viral Replication and Survival Strategies—Prospective on SARS-CoV-2. Front Pharmacol. 2020 ago 28;11.

125. Lee JS, Shin EC. The type I interferon response in COVID-19: implications for treatment. Nat Rev Immunol. 2020 out 12;20(10).

126. Schindler C, Levy DE, Decker T. JAK-STAT signaling: From interferons to cytokines. Journal of Biological Chemistry. 2007.

127. van Eeden C, Khan L, Osman MS, Cohen Tervaert JW. Natural Killer Cell Dysfunction and Its Role in COVID-19. Int J Mol Sci. 2020 set 1;21(17).

128. Gustine JN, Jones D. Immunopathology of Hyperinflammation in COVID-19. Am J Pathol. 2021 jan;191(1).

129. Yoneyama M, Fujita T, ., . Function of RIG-I-like receptors in antiviral innate immunity. Journal of Biological Chemistry. 2007;282(21):15315–8.

130. Yang L, Liu S, Liu J, Zhang Z, Wan X, Huang B, et al. COVID-19: immunopathogenesis and Immunotherapeutics. Vol. 5, Signal Transduction and Targeted Therapy. 2020.

131. Buonaguro L, Petrizzo A, Tornesello M, Buonaguro F. Innate immunity and hepatitis C virus infection: a microarray's view. Infect Agent Cancer. 2012;7(1):7.

132. Eksioglu E, Zhu H, Bayouth L, Bess J, Liu H, Nelson D, et al. Characterization of HCV interactions with Toll-like receptors and RIG-I in liver cells. PLoS One. 2011;6(6).

133. Wang C, Xie J, Zhao L, Fei X, Zhang H, Tan Y, et al. Alveolar macrophage dysfunction and cytokine storm in the pathogenesis of two severe COVID-19 patients. EBioMedicine. 2020 jul;57.

134. Han H, Ma Q, Li C, Liu R, Zhao L, Wang W, et al. Profiling serum cytokines in COVID-19 patients reveals IL-6 and IL-10 are disease severity predictors. Emerg Microbes Infect. 2020;9(1):1123–30.

135. Mehta P, McAuley DF, Brown M, Sanchez E, Tattersall RS, Manson JJ. COVID-19: consider cytokine storm syndromes and immunosuppression. The Lancet. 2020.

136. Lagunas-Rangel FA. Neutrophil-to-lymphocyte ratio and lymphocyte-to-C-reactive protein ratio in patients with severe coronavirus disease 2019 (COVID-19): A meta-analysis. J Med Virol. 2020 out 1;92(10):1733–4.

137. Lagente V, Manoury B, Nénan S, le Quément C, Martin-Chouly C, Boichot E. Role of matrix metalloproteinases in the development of airway inflammation and remodeling. Vol. 38, Brazilian Journal of Medical and Biological Research. 2005.

138. Fernandez-Patron C, Kassiri Z, Leung D. Modulation of systemic metabolism by MMP-2: From MMP-2 deficiency in mice to MMP-2 deficiency in patients. Compr Physiol. 2016;6(4).

139. Karamanos NK, Theocharis AD, Neill T, Iozzo R v. Matrix modeling and remodeling: A biological interplay regulating tissue homeostasis and diseases. Vols. 75–76, Matrix Biology. 2019.

140. Alon R, Sportiello M, Kozlovski S, Kumar A, Reilly EC, Zarbock A, et al. Leukocyte trafficking to the lungs and beyond: lessons from influenza for COVID-19. Vol. 21, Nature Reviews Immunology. 2021.

141. Matthay MA, Zemans RL, Zimmerman GA, Arabi YM, Beitler JR, Mercat A, et al. Acute respiratory distress syndrome. Nat Rev Dis Primers. 2018;5(1).

142. Hardy E, Fernandez-Patron C. Targeting mmp-regulation of inflammation to increase metabolic tolerance to covid-19 pathologies: A hypothesis. Biomolecules. 2021;11(3).

143. Choreño-Parra JA, Jiménez-Álvarez LA, Cruz-Lagunas A, Rodríguez-Reyna TS, Ramírez-Martínez G, Sandoval-Vega M, et al. Clinical and Immunological Factors That Distinguish COVID-19 From Pandemic Influenza A(H1N1). Front Immunol. 2021;12.

144. Laronha H, Caldeira J. Structure and Function of Human Matrix Metalloproteinases. Vol. 9, Cells. 2020.

145. Fernandez-Patron C, Kassiri Z, Leung D. Modulation of systemic metabolism by MMP-2: From MMP-2 deficiency in mice to MMP-2 deficiency in patients. Compr Physiol. 2016;6(4).

146. Nangia-Makker P, Raz T, Tait L, Hogan V, Fridman R, Raz A. Galectin-3 cleavage: A novel surrogate marker for matrix metalloproteinase activity in growing breast cancers. Cancer Res. 2007;67(24).

147. Ramírez-Martínez G, Jiménez-Álvarez LA, Cruz-Lagunas A, Ignacio-Cortés S, Gómez-García IA, Rodríguez-Reyna TS, et al. Possible Role of Matrix Metalloproteinases and TGF-β in COVID-19 Severity and Sequelae. Journal of Interferon & Cytokine Research [Internet]. 2022 maio 31;42(8):352–68. Available from: https://doi.org/10.1089/jir.2021.0222

148. Narasaraju T, Tang BM, Herrmann M, Muller S, Chow VTK, Radic M. Neutrophilia and NETopathy as Key Pathologic Drivers of Progressive Lung Impairment in Patients With COVID-19. Front Pharmacol. 2020;11.

149. Menter T, Haslbauer JD, Nienhold R, Savic S, Hopfer H, Deigendesch N, et al. Postmortem examination of COVID-19 patients reveals diffuse alveolar damage with severe capillary congestion and variegated findings in lungs and other organs suggesting vascular dysfunction. Histopathology. 2020;77(2).

150. Varga Z, Flammer AJ, Steiger P, Haberecker M, Andermatt R, Zinkernagel AS, et al. Endothelial cell infection and endotheliitis in COVID-19. Vol. 395, The Lancet. 2020.

151. Takeuchi O, Akira S. Pattern Recognition Receptors and Inflammation. Vol. 140, Cell. 2010.

152. Bouchon A, Dietrich J, Colonna M, . Cutting Edge: Inflammatory Responses Can Be Triggered by TREM-1, a Novel Receptor Expressed on Neutrophils and Monocytes. The Journal of Immunology. 2000;

153. Nguyen-Lefebvre AT, Ajith A, Portik-Dobos V, Horuzsko DD, Arbab AS, Dzutsev A, et al. The innate immune receptor TREM-1 promotes liver injury and fibrosis. J Clin Invest. 2018;

154. Chen LC, Laskin JD, Gordon MK, Laskin DL. Regulation of TREM expression in hepatic macrophages and endothelial cells during acute endotoxemia. Exp Mol Pathol. 2008;

155. Liao R, Sun TW, Yi Y, Wu H, Li YW, Wang JX, et al. Expression of TREM-1 in hepatic stellate cells and prognostic value in hepatitis B-related hepatocellular carcinoma. Cancer Sci. 2012;

156. Rigo I, McMahon L, Dhawan P, Christakos S, Yim S, Ryan LK, et al. Induction of triggering receptor expressed on myeloid cells (TREM-1) in airway epithelial cells by 1,25(OH) 2 vitamin D 3. Innate Immun. 2012;

157. Colonna M. Trems in the immune system and beyond. Nat Rev Immunol. 2003;

158. Cao C, Gu J, Zhang J, . Soluble triggering receptor expressed on myeloid cell-1 (sTREM-1): a potential biomarker for the diagnosis of infectious diseases. Front Med. 2017;11(2):169–77.

159. Arts RJW, Joosten LAB, van der Meer JWM, Netea MG. TREM-1: intracellular signaling pathways and interaction with pattern recognition receptors. J Leukoc Biol. 2013;93(2).

160. Merad M, Martin JC. Pathological inflammation in patients with COVID-19: a key role for monocytes and macrophages. Nat Rev Immunol. 2020 jun 6;20(6).

161. Bouchon A, Dietrich J, Colonna M. Cutting Edge: Inflammatory Responses Can Be Triggered by TREM-1, a Novel Receptor Expressed on Neutrophils and Monocytes. The Journal of Immunology. 2000 maio 15;164(10).

162. Knapp S, Gibot S, de Vos A, Versteeg HH, Colonna M, van der Poll T. Cutting Edge: Expression Patterns of Surface and Soluble Triggering Receptor Expressed on Myeloid Cells-1 in Human Endotoxemia. The Journal of Immunology. 2004 dez 15;173(12).

163. Bosco MC, Pierobon D, Blengio F, Raggi F, Vanni C, Gattorno M, et al. Hypoxia modulates the gene expression profile of immunoregulatory receptors in human mature dendritic cells: identification of TREM-1 as a novel hypoxic marker in vitro and in vivo. Blood. 2011 mar 3;117(9).

164. Murakami Y, Kohsaka H, Kitasato H, Akahoshi T. Lipopolysaccharide-Induced Up-Regulation of Triggering Receptor Expressed on Myeloid Cells-1 Expression on Macrophages Is Regulated by Endogenous Prostaglandin E $_2$. The Journal of Immunology. 2007 jan 15;178(2).

165. Rahman MA, Dhar DK, Yamaguchi E, Maruyama S, Sato T, Hayashi H, et al. Coexpression of inducible nitric oxide synthase and COX-2 in hepatocellular carcinoma and surrounding liver: Possible involvement of COX-2 in the angiogenesis of hepatitis C virus-positive cases. Clinical Cancer Research. 2001;

166. Cheng ASL, Chan HLY, To KF, Leung WK, Chan KK, Liew CT, et al. Cyclooxygenase-2 pathway correlates with vascular endothelial growth factor expression and tumor angiogenesis in hepatitis B virus-associated hepatocellular carcinoma. Int J Oncol. 2004;

167. Murakami Y, Kohsaka H, Kitasato H, Akahoshi T. Lipopolysaccharide-Induced Up-Regulation of Triggering Receptor Expressed on Myeloid Cells-1 Expression on Macrophages Is Regulated by Endogenous Prostaglandin E2. The Journal of Immunology. 2007;

168. Syed MA, Joo M, Abbas Z, Rodger D, Christman JW, Mehta D, et al. Expression of TREM-1 is inhibited by PGD2 and PGJ2 in macrophages. Exp Cell Res. 2010;

169. Ho CC, Liao WY, Wang CY, Lu YH, Huang HY, Chen HY, et al. TREM-1 expression in tumor-associated macrophages and clinical outcome in lung cancer. Am J Respir Crit Care Med. 2008;

170. Duan M, Wang ZC, Wang XY, Shi JY, Yang LX, Ding ZB, et al. TREM-1, an Inflammatory Modulator, is Expressed in Hepatocellular Carcinoma

Cells and Significantly Promotes Tumor Progression. Ann Surg Oncol. 2015;

171. Liu CL, Hsieh WY, Wu CL, Kuo HT, Lu YT. Triggering receptor expressed on myeloid cells-1 in pleural effusions: A marker of inflammatory disease. Respir Med. 2007 maio;101(5).

172. How CK, Chern CH, Wu MF, Wang LM, Huang CI, Lee CH, et al. Expression of the triggering receptor expressed on myeloid cells-1 mRNA in a heterogeneous infected population. Int J Clin Pract. 2009 jan;63(1).

173. Ghildiyal M, Zamore PD. Small silencing RNAs: an expanding universe. Nat Rev Genet. 2009 fev;10(2).

174. Kim VN, Han J, Siomi MC. Biogenesis of small RNAs in animals. Nat Rev Mol Cell Biol. 2009 fev;10(2).

175. He L, Hannon GJ. MicroRNAs: Small RNAs with a big role in gene regulation. Nature Reviews Genetics. 2004.

176. Zhang J, Li S, Li L, Li M, Guo C, Yao J, et al. Exosome and exosomal microRNA: Trafficking, sorting, and function. Genomics, Proteomics and Bioinformatics. 2015.

177. Friedman RC, Farh KKH, Burge CB, Bartel DP. Most mammalian mRNAs are conserved targets of microRNAs. Genome Res. 2008 out 29;19(1).

178. Ha M, Kim VN. Regulation of microRNA biogenesis. Nat Rev Mol Cell Biol. 2014 ago 16;15(8).

179. Kulkarni M, Ozgur S, Stoecklin G. On track with P-bodies. Biochem Soc Trans. 2010 fev 1;38(1).

180. Pasquinelli AE. MicroRNAs and their targets: recognition, regulation and an emerging reciprocal relationship. Nat Rev Genet. 2012 abr 13;13(4).

181. Lu TX, Rothenberg ME. MicroRNA. Journal of Allergy and Clinical Immunology. 2018 abr;141(4).

182. Song L, Tuan RS. MicroRNAs and cell differentiation in mammalian development. Birth Defects Res C Embryo Today. 2006 jun;78(2).

183. Rodrigues DVS, Monteiro VVS, Navegantes-Lima KC, Oliveira AL, Gaspar SL, Quadros LBG, et al. MicroRNAs in cell cycle progression and proliferation: molecular mechanisms and pathways. Noncoding RNA Investig. 2018;2.

184. Sayed D, Abdellatif M. MicroRNAs in Development and Disease. Physiol Rev. 2011 jul;91(3).

185. Singaravelu R, Chen R, Lyn RK, Jones DM, O'Hara S, Rouleau Y, et al. Hepatitis C virus induced up-regulation of microRNA-27: A novel mechanism for hepatic steatosis. Hepatology. 2014 jan;59(1).

186. Singaravelu R, O'Hara S, Jones DM, Chen R, Taylor NG, Srinivasan P, et al. MicroRNAs regulate the immunometabolic response to viral infection in the liver. Nat Chem Biol. 2015 dez 19;11(12).

187. Motsch N, Pfuhl T, Mrazek J, Barth S, Grässer FA. Epstein-Barr Virus-Encoded Latent Membrane Protein 1 (LMP1) Induces the Expression of the Cellular MicroRNA miR-146a. RNA Biol. 2007 jul 27;4(3).

188. Makarova JA, Shkurnikov MU, Wicklein D, Lange T, Samatov TR, Turchinovich AA, et al. Intracellular and extracellular microRNA: An update on localization and biological role. Prog Histochem Cytochem. 2016 nov;51(3–4).

189. Hayes J, Peruzzi PP, Lawler S. MicroRNAs in cancer: biomarkers, functions and therapy. Trends Mol Med. 2014 ago;20(8).

190. Huang W. MicroRNAs: Biomarkers, Diagnostics, and Therapeutics. Em 2017.

191. Wang J, Chen J, Sen S. MicroRNA as Biomarkers and Diagnostics. J Cell Physiol. 2016 jan;231(1).

192. Pan BT, Teng K, Wu C, Adam M, Johnstone RM. Electron microscopic evidence for externalization of the transferrin receptor in vesicular form in sheep reticulocytes. Journal of Cell Biology. 1985;

193. Patil AA, Rhee WJ. Exosomes: Biogenesis, Composition, Functions, and Their Role in Pre-metastatic Niche Formation. Biotechnology and Bioprocess Engineering. 2019.

194. Kowal J, Tkach M, Théry C. Biogenesis and secretion of exosomes. Current Opinion in Cell Biology. 2014.

195. Jabbari N, Karimipour M, Khaksar M, Akbariazar E, Heidarzadeh M, Mojarad B, et al. Tumor-derived extracellular vesicles: insights into bystander effects of exosomes after irradiation. Lasers in Medical Science. 2020.

196. Barnes PJ. Inflammatory mechanisms in patients with chronic obstructive pulmonary disease. Journal of Allergy and Clinical Immunology. 2016.

197. Bourdonnay E, Zasłona Z, Penke LRK, Speth JM, Schneider DJ, Przybranowski S, et al. Transcellular delivery of vesicular SOCS proteins from macrophages to epithelial cells blunts inflammatory signaling. Journal of Experimental Medicine. 2015;

198. Colombo M, Raposo G, Théry C. Biogenesis, Secretion, and Intercellular Interactions of Exosomes and Other Extracellular Vesicles. Annu Rev Cell Dev Biol. 2014 out 11;30(1).

199. Bhome R, del Vecchio F, Lee GH, Bullock MD, Primrose JN, Sayan AE, et al. Exosomal microRNAs (exomiRs): Small molecules with a big role in cancer. Cancer Letters. 2018.

200. Yu X, Odenthal M, Fries JWU. Exosomes as miRNA carriers: Formation-function-future. International Journal of Molecular Sciences. 2016.

201. Kwon Y, Nukala SB, Srivastava S, Miyamoto H, Ismail NI, Ong SB, et al. Exosomes Facilitate Transmission of SARS-CoV-2 Genome into Human Induced Pluripotent Stem Cell-Derived Cardiomyocytes. bioRxiv. 2020;

202. Elrashdy F, Aljaddawi AA, Redwan EM, Uversky VN. On the potential role of exosomes in the COVID-19 reinfection/reactivation opportunity. J Biomol Struct Dyn. 2020;

203. Wang J, Chen S, Bihl J. Exosome-Mediated Transfer of ACE2 (Angiotensin-Converting Enzyme 2) from Endothelial Progenitor Cells Promotes Survival and Function of Endothelial Cell. Oxid Med Cell Longev. 2020;2020.

204. Yuana Y, Sturk A, Nieuwland R. Extracellular vesicles in physiological and pathological conditions. Blood Rev. 2013;

205. Mirzaei R, Mahdavi F, Badrzadeh F, Hosseini-Fard SR, Heidary M, Jeda AS, et al. The emerging role of microRNAs in the severe acute respiratory syndrome coronavirus 2 (SARS-CoV-2) infection. Int Immunopharmacol. 2021;90(October 2020).

206. Lai FW, Stephenson KB, Mahony J, Lichty BD. Human Coronavirus OC43 Nucleocapsid Protein Binds MicroRNA 9 and Potentiates NF- B Activation. J Virol. 2014;

207. Tahamtan A, Inchley CS, Marzban M, Tavakoli-Yaraki M, Teymoori-Rad M, Nakstad B, et al. The role of microRNAs in respiratory viral infection: friend or foe? Reviews in Medical Virology. 2016.

208. Ahmed SSSJ, Paramasivam P, Raj K, Kumar V, Murugesan R, Ramakrishnan. Interplay of host regulatory network on SARS-CoV-2 binding and replication machinery. bioRxiv. 2020.

209. Wyler E, Mösbauer K, Franke V, Diag A, Gottula LT, Arsie R, et al. Bulk and single-cell gene expression profiling of SARS-CoV-2 infected human cell lines identifies molecular targets for therapeutic intervention. bioRxiv. 2020.

210. Arisan ED, Dart A, Grant GH, Arisan S, Cuhadaroglu S, Lange S, et al. The Prediction of miRNAs in SARS-CoV-2 Genomes: hsa-miR Databases Identify 7 Key miRs Linked to Host Responses and Virus Pathogenicity-Related KEGG Pathways Significant for Comorbidities. Viruses. 2020 jun 4;12(6).

211. O'Connell RM, Taganov KD, Boldin MP, Cheng G, Baltimore D. MicroRNA-155 is induced during the macrophage inflammatory response. Proceedings of the National Academy of Sciences. 2007 jan 30;104(5).

212. Curtis AM, Fagundes CT, Yang G, Palsson-McDermott EM, Wochal P, McGettrick AF, et al. Circadian control of innate immunity in macrophages by miR-155 targeting *Bmal1*. Proceedings of the National Academy of Sciences. 2015 jun 9;112(23).

213. Wang L, Zhang H, Rodriguez S, Cao L, Parish J, Mumaw C, et al. Notch-Dependent Repression of miR-155 in the Bone Marrow Niche Regulates Hematopoiesis in an NF-κB-Dependent Manner. Cell Stem Cell. 2014 jul;15(1).

214. O'Connell RM, Chaudhuri AA, Rao DS, Baltimore D. Inositol phosphatase SHIP1 is a primary target of miR-155. Proceedings of the National Academy of Sciences. 2009 abr 28;106(17).

215. Taganov KD, Boldin MP, Chang KJ, Baltimore D. NF- B-dependent induction of microRNA miR-146, an inhibitor targeted to signaling proteins of innate immune responses. Proceedings of the National Academy of Sciences. 2006 ago 15;103(33).

216. Yang Y, Shen C, Li J, Yuan J, Yang M, Wang F, et al. Exuberant elevation of IP-10, MCP-3 and IL-1ra during SARS-CoV-2 infection is associated with disease severity and fatal outcome. medRxiv. medRxiv; 2020.

217. Herold T, Jurinovic V, Arnreich C, Lipworth BJ, Hellmuth JC, von Bergwelt-Baildon M, et al. Elevated levels of IL-6 and CRP predict the need for mechanical ventilation in COVID-19. Journal of Allergy and Clinical Immunology. 2020 jul;146(1).

218. Wu C, Chen X, Cai Y, Xia J, Zhou X, Xu S, et al. Risk Factors Associated With Acute Respiratory Distress Syndrome and Death in Patients With Coronavirus Disease 2019 Pneumonia in Wuhan, China. JAMA Intern Med. 2020 jul 1;180(7).

219. Yan Q, Li P, Ye X, Huang X, Mo X, Wang Q, et al. Longitudinal peripheral blood transcriptional analysis of COVID-19 patients captures disease progression and reveals potential biomarkers. medRxiv. medRxiv; 2020.

220. Gómez-piña V, Soares-schanoski A, Rodríguez-rojas A, Fresno C, García F, Vallejo-cremades MT, et al. Metalloproteinases Shed TREM-1 Ectodomain from Lipopolysaccharide-stimulated Human Monocytes. The Journal of Immunology. 2007;179:4065–73.

221. Richard-Greenblatt M, Boillat-Blanco N, Zhong K, Mbarack Z, Samaka J, Mlaganile T, et al. Prognostic Accuracy of Soluble Triggering Receptor Expressed on Myeloid Cells (sTREM-1)-based Algorithms in Febrile Adults Presenting to Tanzanian Outpatient Clinics. Clinical Infectious Diseases. 2019 maio 18;

222. World Health Organization. Strategic Preparedness and Response Plan. World Health Organisation (WHO). 2020.

223. World Health Organization. Infection prevention and control during health care when novel coronavirus (nCoV) infection is suspected. New York; 2020 mar.

224. World Health Organization. Laboratory testing strategy recommendations for COVID-19: interim guidance. New York; 2020 mar.

225. Hadjadj J, Yatim N, Barnabei L, Corneau A, Boussier J, Smith N, et al. Impaired type I interferon activity and inflammatory responses in severe COVID-19 patients. Science (1979). 2020 ago 7;369(6504).

226. Ye G, Pan Z, Pan Y, Deng Q, Chen L, Li J, et al. Clinical characteristics of severe acute respiratory syndrome coronavirus 2 reactivation. Journal of Infection. 2020 maio;80(5).

227. Xu XW, Wu XX, Jiang XG, Xu KJ, Ying LJ, Ma CL, et al. Clinical findings in a group of patients infected with the 2019 novel coronavirus (SARS-Cov-2) outside of Wuhan, China: retrospective case series. BMJ. 2020 fev 19;

228. Grasselli G, Zangrillo A, Zanella A, Antonelli M, Cabrini L, Castelli A, et al. Baseline Characteristics and Outcomes of 1591 Patients Infected With SARS-CoV-2 Admitted to ICUs of the Lombardy Region, Italy. JAMA. 2020 abr 28;323(16).

229. Marshall JC, Murthy S, Diaz J, Adhikari N, Angus DC, Arabi YM, et al. A minimal common outcome measure set for COVID-19 clinical research. The Lancet Infectious Diseases. 2020.

230. Office WHOEMR. Updated clinical management guideline for COVID-19. Weekly Epidemiology Monitor. 2020.

231. Kuri-Cervantes L, Pampena MB, Meng W, Rosenfeld AM, Ittner CAG, Weisman AR, et al. Comprehensive mapping of immune perturbations associated with severe COVID-19. Sci Immunol. 2020;

232. Tsikas D. Assessment of lipid peroxidation by measuring malondialdehyde (MDA) and relatives in biological samples: Analytical and biological challenges. Anal Biochem. 2017;524.

233. Montenegro MF, Pessa LR, Gomes VA, Desta Z, Flockhart DA, Tanus-Santos JE. Assessment of vascular effects of tamoxifen and its metabolites on the rat perfused hindquarter vascular bed. Basic Clin Pharmacol Toxicol. 2009;104(5).

234. Gerlach RF, Meschiari CA, Marcaccini AM, Palei ACT, Sandrim VC, Cavalli RC, et al. Positive correlations between serum and plasma matrix metalloproteinase (MMP)-2 or MMP-9 levels in disease conditions. Clin Chem Lab Med. 2009 jan 1;47(7).

235. Cancemi P, Aiello A, Accardi G, Caldarella R, Candore G, Caruso C, et al. The Role of Matrix Metalloproteinases (MMP-2 and MMP-9) in Ageing and Longevity: Focus on Sicilian Long-Living Individuals (LLIs). Mediators Inflamm. 2020 maio 5;2020.

236. Nie X, Qian L, Sun R, Huang B, Dong X, Xiao Q, et al. Multi-organ proteomic landscape of COVID-19 autopsies. Cell. 2021 fev 4;184(3):775-791.e14.

237. Desai N, Neyaz A, Szabolcs A, Shih AR, Chen JH, Thapar V, et al. Temporal and spatial heterogeneity of host response to SARS-CoV-2 pulmonary infection. Nat Commun. 2020 dez 9;11(1).

238. Corman VM, Landt O, Kaiser M, Molenkamp R, Meijer A, Chu DKW, et al. Detection of 2019 novel coronavirus (2019-nCoV) by real-time RT-PCR. Eurosurveillance. 2020;25(3).

239. CDC 2019-Novel Coronavirus (2019-nCoV) Real-Time RT-PCR Diagnostic Panel For Emergency Use Only Instructions for Use.

240. Pontelli MC, Castro IA, Martins RB, Veras FP, Serra L la, Nascimento DC, et al. Infection of human lymphomononuclear cells by SARS-CoV-2. bioRxiv. 2020;

241. Baxter EW, Graham AE, Re NA, Carr IM, Robinson JI, Mackie SL, et al. Standardized protocols for differentiation of THP-1 cells to macrophages with distinct M(IFNγ+LPS), M(IL-4) and M(IL-10) phenotypes. J Immunol Methods. 2020;478.

242. Gibot S, Kolopp-Sarda MN, Béné MC, Bollaert PE, Lozniewski A, Mory F, et al. A soluble form of the triggering receptor expressed on myeloid cells-1 modulates the inflammatory response in murine sepsis. Journal of Experimental Medicine. 2004;200(11).

243. Lam VC, Folkersen L, Aguilar OA, Lanier LL. KLF12 Regulates Mouse NK Cell Proliferation. The Journal of Immunology. 2019 ago 15;203(4).

244. Ding L, Ding Y, Kong X, Wu J, Fu J, Yan G, et al. Dysregulation of Krüppel-like factor 12 in the development of endometrial cancer. Gynecol Oncol. 2019 jan;152(1).

245. Giamarellos-Bourboulis EJ, Netea MG, Rovina N, Akinosoglou K, Antoniadou A, Antonakos N, et al. Complex Immune Dysregulation in COVID-19 Patients with Severe Respiratory Failure. Cell Host Microbe. 2020;

246. Liao M, Liu Y, Yuan J, Wen Y, Xu G, Zhao J, et al. Single-cell landscape of bronchoalveolar immune cells in patients with COVID-19. Nat Med [Internet]. 2020; Available from: http://dx.doi.org/10.1038/s41591-020-0901-9

247. Lee YS, Yeo IJ, Kim KC, Han SB, Hong JT. Inhibition of Lung Tumor Development in ApoE Knockout Mice via Enhancement of TREM-1 Dependent NK Cell Cytotoxicity. Front Immunol. 2019 jun 18;10.

248. Meng Z, Moroishi T, Guan KL. Mechanisms of Hippo pathway regulation. Genes Dev. 2016 jan 1;30(1).

249. Ait-Lounis A, Baas D, Barras E, Benadiba C, Charollais A, Nlend RN, et al. Novel function of the ciliogenic transcription factor RFX3 in development of the endocrine pancreas. Diabetes. 2007;56(4).

250. Li C, Li Z, Liu S, Wang C, Han L, Cui L, et al. Genome-wide association analysis identifies three new risk loci for gout arthritis in Han Chinese. Nat Commun. 2015 nov 13;6(1).

251. Fan Z, Zheng J, Xue Y, Liu X, Wang D, Yang C, et al. NR2C2-uORF targeting UCA1-miR-627-5p-NR2C2 feedback loop to regulate the malignant behaviors of glioma cells. Cell Death Dis. 2018 dez 5;9(12).

252. Wan Z, Chai R, Yuan H, Chen B, Dong Q, Zheng B, et al. MEIS2 promotes cell migration and invasion in colorectal cancer. Oncol Rep. 2019 maio 15;

253. Zha Y, Xia Y, Ding J, Choi JH, Yang L, Dong Z, et al. MEIS2 is essential for neuroblastoma cell survival and proliferation by transcriptional control of M-phase progression. Cell Death Dis. 2014 set 11;5(9).

254. Wu H, Zhang J. Decreased expression of TFAP2B in endometrial cancer predicts poor prognosis: A study based on TCGA data. Gynecol Oncol. 2018 jun;149(3).

255. Huang D, Wang F, Wu W, Lian C, Liu E. MicroRNA-429 inhibits cancer cell proliferation and migration by targeting the AKT1 in melanoma. Cancer Biomarkers. 2019 set 5;26(1).

256. Su Z, Jiang G, Chen J, Liu X, Zhao H, Fang Z, et al. MicroRNA-429 inhibits cancer cell proliferation and migration by targeting AKT1 in renal cell carcinoma. Mol Clin Oncol. 2019 out 25;

257. Lan C, Long L, Xie K, Liu J, Zhou L, Pan S, et al. miRNA-429 suppresses osteogenic differentiation of human adipose-derived mesenchymal stem cells under oxidative stress via targeting SCD-1. Exp Ther Med. 2019 nov 26;

258. Giles KM, Brown RAM, Epis MR, Kalinowski FC, Leedman PJ. miRNA-7-5p inhibits melanoma cell migration and invasion. Biochem Biophys Res Commun. 2013 jan;430(2).

259. Powrózek T, Mlak R, Dziedzic M, Małecka-Massalska T, Sagan D. Investigation of relationship between precursor of miRNA-944 and its mature form in lung squamous-cell carcinoma - the diagnostic value. Pathol Res Pract. 2018 mar;214(3).

260. Powrózek T, Kuźnar-Kamińska B, Dziedzic M, Mlak R, Batura-Gabryel H, Sagan D, et al. The diagnostic role of plasma circulating precursors of miRNA-944 and miRNA-3662 for non-small cell lung cancer detection. Pathol Res Pract. 2017 nov;213(11).

261. Chen Y, Gao C, Sun Q, Pan H, Huang P, Ding J, et al. MicroRNA-4639 Is a Regulator of DJ-1 Expression and a Potential Early Diagnostic Marker for Parkinson's Disease. Front Aging Neurosci. 2017 jul 21;9.

262. Zhang J, Xu Z, Kong L, Gao H, Zhang Y, Zheng Y, et al. <p>miRNA-486-5p Promotes COPD Progression by Targeting HAT1 to Regulate the TLR4-Triggered Inflammatory Response of Alveolar Macrophages</p>. Int J Chron Obstruct Pulmon Dis. 2020 nov;Volume 15.

263. Li C, Zheng X, Li W, Bai F, Lyu J, Meng QH. Serum miR-486-5p as a diagnostic marker in cervical cancer: with investigation of potential mechanisms. BMC Cancer. 2018 dez 9;18(1).

264. Weis A, Marquart L, Calvopina D, Genz B, Ramm G, Skoien R. Serum MicroRNAs as Biomarkers in Hepatitis C: Preliminary Evidence of a MicroRNA Panel for the Diagnosis of Hepatocellular Carcinoma. Int J Mol Sci. 2019 fev 17;20(4).

265. Liu Q, Du J, Yu X, Xu J, Huang F, Li X, et al. miRNA-200c-3p is crucial in acute respiratory distress syndrome. Cell Discov. 2017 dez 27;3(1).

266. Ladeiro Y, Couchy G, Balabaud C, Bioulac-Sage P, Pelletier L, Rebouissou S, et al. MicroRNA profiling in hepatocellular tumors is associated with clinical features and oncogene/tumor suppressor gene mutations. Hepatology. 2008 jun;47(6).

267. Mutlu M, Raza U, Saatci Ö, Eyüpoğlu E, Yurdusev E, Şahin Ö. miR-200c: a versatile watchdog in cancer progression, EMT, and drug resistance. J Mol Med. 2016 jun 20;94(6).

268. Arts RJW, Joosten LAB, Dinarello CA, Kullberg BJ, van der Meer JWM, Netea MG. TREM-1 interaction with the LPS/TLR4 receptor complex. Eur Cytokine Netw. 2011;22(1).

269. Prüfer S, Weber M, Sasca D, Teschner D, Wölfel C, Stein P, et al. Distinct signaling cascades of TREM-1, TLR and NLR in neutrophils and monocytic cells. J Innate Immun. 2014;6(3).

270. Dower K, Ellis DK, Saraf K, Jelinsky SA, Lin LL. Innate Immune Responses to TREM-1 Activation: Overlap, Divergence, and Positive and Negative Cross-Talk with Bacterial Lipopolysaccharide. The Journal of Immunology. 2008;180(5).

271. Klesney-Tait J, Turnbull IR, Colonna M. The TREM receptor family and signal integration. Vol. 7, Nature Immunology. 2006. p. 1266–73.

272. Liu T, Zhou Y, Li P, Duan JX, Liu YP, Sun GY, et al. Blocking triggering receptor expressed on myeloid cells-1 attenuates lipopolysaccharide-induced acute lung injury via inhibiting NLRP3 inflammasome activation. Sci Rep. 2016;6.

273. Hu LT, Du ZD, Zhao GQ, Jiang N, Lin J, Wang Q, et al. Role of TREM-1 in response to Aspergillus fumigatus infection in corneal epithelial cells. Int Immunopharmacol. 2014;23(1).

274. Bostanci N, Thurnheer T, Belibasakis GN. Involvement of the TREM-1/DAP12 pathway in the innate immune responses to Porphyromonas gingivalis. Mol Immunol. 2011;49(1–2).